

**SEISMIC ASSESSMENT OF PRE-1970S
REINFORCED CONCRETE STRUCTURE**

A thesis
submitted in partial fulfilment
of the requirements for the Degree
of
Master of Engineering
in the
University of Canterbury
by
Eric Hertanto

University of Canterbury
Christchurch, New Zealand

2005

ABSTRACT

Reinforced concrete structures designed in pre-1970s are vulnerable under earthquakes due to lack of seismic detailing to provide adequate ductility. Typical deficiencies of pre-1970s reinforced concrete structures are (a) use of plain bars as longitudinal reinforcement, (b) inadequate anchorage of beam longitudinal reinforcement in the column (particularly exterior column), (c) lack of joint transverse reinforcement if any, (d) lapped splices located just above joint, and (e) low concrete strength. Furthermore, the use of infill walls is a controversial issue because it can help to provide additional stiffness to the structure on the positive side and on the negative side it can increase the possibility of soft-storey mechanisms if it is distributed irregularly. Experimental research to investigate the possible seismic behaviour of pre-1970s reinforced concrete structures have been carried out in the past. However, there is still an absence of experimental tests on the 3-D response of existing beam-column joints under bi-directional cyclic loading, such as corner joints.

As part of the research work herein presented, a series of experimental tests on beam-column subassemblies with typical detailing of pre-1970s buildings has been carried out to investigate the behaviour of existing reinforced concrete structures. Six two-third scale plane frame exterior beam-column joint subassemblies were constructed and tested under quasi-static cyclic loading in the Structural Laboratory of the University of Canterbury. The reinforcement detailing and beam dimension were varied to investigate their effect on the seismic behaviour. Four specimens were conventional deep beam-column joint, with two of them using deformed longitudinal bars and beam bars bent in to the joint and the two others using plain round longitudinal bars and beam bars with end hooks. The other two specimens were shallow beam-column joint, one with deformed longitudinal bars and beam bars bent in to the joint, the other with plain round longitudinal bars and beam bars with end hooks. All units had one transverse reinforcement in the joint. The results of the experimental tests indicated that conventional exterior beam-column joint with typical detailing of pre-1970s building would experience serious diagonal tension cracking in the joint panel under earthquake. The use of plain round bars with end hooks for beam longitudinal reinforcement results in more severe damage in the joint core when

compared to the use of deformed bars for beam longitudinal reinforcement bent in to the joint, due to the combination of bar slips and concrete crushing. One interesting outcome is that the use of shallow beam in the exterior beam-column joint could avoid the joint cracking due to the beam size although the strength provided lower when compared with the use of deep beam with equal moment capacity. Therefore, taking into account the low strength and stiffness, shallow beam can be reintroduced as an alternative solution in design process. In addition, the presence of single transverse reinforcement in the joint core can provide additional confinement after the first crack occurred, thus delaying the strength degradation of the structure.

Three two-third scale space frame corner beam-column joint subassemblies were also constructed to investigate the biaxial loading effect. Two specimens were deep-deep beam-corner column joint specimens and the other one was deep-shallow beam-corner column joint specimen. One deep-deep beam-corner column joint specimen was not using any transverse reinforcement in the joint core while the two other specimens were using one transverse reinforcement in the joint core. Plain round longitudinal bars were used for all units with hook anchorage for the beam bars. Results from the tests confirmed the evidences from earthquake damage observations with the exterior 3-D (corner) beam-column joint subjected to biaxial loading would have less strength and suffer higher damage in the joint area under earthquake. Furthermore, the joint shear relation in the two directions is calibrated from the results to provide better analysis.

An analytical model was used to simulate the seismic behaviour of the joints with the help of Ruaumoko software. Alternative strength degradation curves corresponding to different reinforcement detailing of beam-column joint unit were proposed based on the test results.

ACKNOWLEDGEMENTS

The research work reported in this thesis was carried out in the Department of Civil Engineering, University of Canterbury, New Zealand.

I wish to express my deepest gratitude to Dr. Stefano Pampanin and Dr. Athol J. Carr, supervisors of this project, for their invaluable advice, encouragement and patience.

Thanks are extended to the technical staff of the Civil Engineering Department under the management of Mr. D. MacPherson, for their assistance and advice in the experimental program. Particularly to Mr. G. Harvey for his valuable contributions to the experimental work and friendship. Thanks are also given to Mr. C. Bliss, Mr. J. Maley and Mr. R. Newton for their preparation of the test frames, test specimens and instrumentations.

I also wish to thank my fellow postgraduate students, in particular, T. H. Chen, Liu Cong, A. Amaris, R. Laffont for their friendship during this research. Also thanks are due to Mr. B. Zaghlool and Dr. U. Sruma for their constructive discussions and invaluable suggestions of the test program.

The research funding provided by the Foundation for Research Science and Technology of New Zealand is gratefully acknowledged.

Finally, I would like to thank my family for their understanding, encouragement and support during the past years.

TABLE OF CONTENTS

ABSTRACT.....	i
ACKNOWLEDGEMENTS.....	iii
TABLE OF CONTENTS.....	iv
NOTATION.....	x
LIST OF FIGURES.....	xii
LIST OF TABLES.....	xviii
CHAPTER 1 INTRODUCTION.....	1
1.1 SEISMIC ASSESSMENT OF EXISTING REINFORCED CONCRETE STRUCTURES.....	1
1.2 BACKGROUND OF THIS RESEARCH PROJECT.....	3
1.3 OBJECTIVES OF THIS RESEARCH PROJECT.....	7
1.4 ORGANIZATION OF THE THESIS.....	8
CHAPTER 2 REVIEW OF STRUCTURAL DEFICIENCIES IN PRE-1970S REINFORCED CONCRETE BUILDINGS AND PREVIOUS INVESTIGATIONS ON BEAM-COLUMN JOINT.....	10
2.1 INTRODUCTION.....	10
2.2 TYPICAL DESIGN APPROACH AND STRUCTURAL DETAILING IN PRE-1970S REINFORCED CONCRETE BUILDINGS.....	12
2.2.1 Introduction.....	12
2.2.2 Development of Design Codes.....	14
2.2.3 Typical Detailing of Pre-1970s Reinforced Concrete	

Structures.....	16
2.2.4 Shallow or Wide Beams.....	21
2.3 RELEVANT PLANE FRAME BEAM-COLUMN JOINT	
RESEARCH PROJECTS.....	21
2.3.1 Research by Aycardi et al. (1994).....	21
2.3.2 Research by Hakuto et al. (1995).....	24
2.3.3 Research by Beres et al. (1996).....	26
2.3.4 Research by Liu et al. (2002).....	28
2.3.5 Research by Pampanin et al. (1992).....	30
2.3.6 Research on Joint Subassemblies with Shallow (Wide)	
Beam.....	33
2.3.6.1 Research by Popov et al. (1992).....	33
2.3.6.2 Research by Gentry and Wight (1994).....	35
2.3.6.3 Research by Abdouka (2003).....	37
2.4 RELEVANT RESEARCH PROJECTS ON SPACE FRAME	
BEAM-COLUMN JOINT.....	39
2.4.1 Research by Leon and Jirsa (1986).....	39
2.4.2 Research by Cheung et al. (1991).....	42
2.4.3 Research by Bolong and Yuzhou (1991).....	46
2.4.4 Research by Kurose et al. (1991).....	48
2.4.5 Research by Owada (2000).....	50
2.5 ANALYTICAL MODELING DEVELOPMENT.....	51
2.5.1 Multi-Spring Models.....	51
2.5.2 Finite Element Methods.....	54
2.5.3 Fiber Models.....	54
2.5.4 Simplified Models.....	54
2.6 ANALYTICAL MODEL.....	55
2.6.1 Basic Approach.....	55
2.6.2 Joint Deformation.....	56
2.6.3 Joint Moment-Rotation Relationship.....	56
2.6.4 Space Frame Interaction.....	58
2.6.5 Geometry of the Model.....	59
2.7 MEMBER STRENGTH AND DEFORMABILITY.....	60
2.7.1 Material Properties.....	60

2.7.2 Beam and Column Strength.....	61
2.7.3 Beam-Column Joint Shear Strength.....	61
2.8 SUMMARY.....	64
CHAPTER 3 TEST UNITS AND SETUP.....	65
3.1 INTRODUCTION.....	65
3.2 TEST UNIT DETAILS.....	68
3.2.1 Introduction.....	68
3.2.2 Plane Frame Units.....	69
3.2.2.1 General.....	69
3.2.2.2 Deep Beams Details.....	69
3.2.2.3 Shallow Beams Details.....	75
3.2.3 Space Frame Units.....	78
3.2.3.1 General.....	78
3.2.3.2 Unit DD-1.....	79
3.2.3.3 Unit DD-2.....	81
3.2.3.4 Unit DS.....	83
3.3 TEST SETUP.....	86
3.3.1 Design and Construction of the Test Rig.....	86
3.3.2 Instrumentation Setup.....	89
3.3.2.1 Hydraulic Actuator.....	90
3.3.2.2 Hydraulic Jack.....	90
3.3.2.3 Load Cells.....	90
3.3.2.4 Potentiometers.....	92
3.3.2.5 Strain Gauges.....	95
3.3.3 Loading Control.....	100
3.3.3.1 Displacement Control for Plane Frame Tests.....	101
3.3.3.2 Displacement Control for Space Frame Test.....	102
CHAPTER 4 PLANE FRAME TEST RESULTS.....	105
4.1 INTRODUCTION.....	105
4.2 DEEP BEAMS.....	106
4.2.1 Unit TDD-1.....	106
4.2.1.1 Crack Development and Damage.....	107

4.2.1.2 Hysteretic Response.....	109
4.2.1.3 Displacement Components.....	109
4.2.1.4 Force and Stress in the Joint.....	111
4.2.1.5 Summary.....	113
4.2.2 Unit TDP-1.....	113
4.2.2.1 Crack Development and Damage.....	113
4.2.2.2 Hysteretic Response.....	115
4.2.2.3 Displacement Components.....	116
4.2.2.4 Force and Stress in the Joint.....	117
4.2.2.5 Summary.....	119
4.2.3 Unit TDP-2.....	120
4.2.3.1 Crack Development and Damage.....	120
4.2.3.2 Hysteretic Response.....	123
4.2.3.3 Displacement Components.....	123
4.2.3.4 Force and Stress in the Joint.....	125
4.2.3.5 Joint Shear Deformation.....	125
4.2.3.6 Summary.....	128
4.2.4 Unit TDD-2.....	130
4.2.4.1 Crack Development and Damage.....	130
4.2.4.2 Hysteretic Response.....	133
4.2.4.3 Displacement Components.....	133
4.2.4.4 Force and Stress in the Joint.....	135
4.2.4.5 Summary.....	137
4.3 SHALLOW BEAMS.....	137
4.3.1 Unit TSP.....	138
4.3.1.1 Crack Development and Damage.....	138
4.3.1.2 Hysteretic Response.....	140
4.3.1.3 Displacement Components.....	141
4.3.1.4 Force and Stress in the Joint.....	142
4.3.1.5 Summary.....	144
4.3.2 Unit TSD.....	144
4.3.2.1 Crack Development and Damage.....	145
4.3.2.2 Hysteretic Response.....	148
4.3.2.3 Displacement Components.....	148

4.3.2.4 Force and Stress in the Joint.....	150
4.3.2.5 Summary.....	151
4.4 TESTS SUMMARY.....	152
4.4.1 Results Comparison.....	152
4.4.1.1 Hysteresis Response.....	152
4.4.1.1.1 Unit TDP-1 and TDD-1.....	154
4.4.1.1.2 Unit TSP and TSD.....	155
4.4.1.1.3 Unit TDP-1 and TSP.....	156
4.4.1.1.4 Unit TDD-1 and TSD.....	158
4.4.1.2 Joint Principal Tensile Stress.....	159
4.5 CONCLUSION.....	161
CHAPTER 5 SPACE FRAME TEST RESULTS.....	163
5.1 INTRODUCTION.....	163
5.2 DEEP-DEEP BEAMS.....	165
5.2.1 Unit DD-1.....	165
5.2.1.1 Crack Development and Damage.....	165
5.2.1.2 Hysteretic Response.....	168
5.2.1.3 Displacement Components.....	169
5.2.1.4 Force and Stress in the Joint.....	172
5.2.1.5 Joint Shear Deformation.....	175
5.2.1.6 Summary.....	176
5.2.2 Unit DD-2.....	177
5.2.2.1 Crack Development and Damage.....	177
5.2.2.2 Hysteretic Response.....	180
5.2.2.3 Displacement Components.....	181
5.2.2.4 Force and Stress in the Joint.....	184
5.2.2.5 Joint Shear Deformation.....	187
5.2.2.6 Summary.....	188
5.3 DEEP-SHALLOW BEAMS.....	190
5.3.1 Unit DS.....	192
5.3.1.1 Crack Development and Damage.....	190
5.3.1.2 Hysteretic Response.....	193
5.3.1.3 Displacement Components.....	194

5.3.1.4 Force and Stress in the Joint.....	197
5.3.1.5 Joint Shear Deformation.....	200
5.3.1.6 Summary.....	200
5.4 TESTS SUMMARY.....	202
5.4.1 Results Comparison.....	202
5.4.1.1 Hysteresis Response.....	202
5.4.1.2 Joint Principal Tensile Stress.....	204
5.5 BIAXIAL EFFECT.....	207
5.5.1 Hysteresis Response.....	207
5.5.2 Joint Principal Tensile Stress.....	207
5.6 CONCLUSION.....	209
CHAPTER 6 ANALYTICAL-EXPERIMENTAL COMPARISONS.....	210
6.1 INTRODUCTION.....	210
6.2 PLANE FRAME BEAM-COLUMN JOINTS.....	210
6.2.1 Unit TDD-1.....	210
6.2.2 Unit TDP-1.....	211
6.2.3 Unit TDP-2.....	212
6.2.4 Unit TDD-2.....	212
6.2.5 Unit TSP.....	213
6.2.6 Unit TSD.....	214
6.3 SPACE FRAME BEAM-COLUMN JOINTS.....	215
CHAPTER 7 CONCLUSION AND RECOMMENDATIONS FOR FUTURE RESEARCH.....	216
7.1 GENERAL.....	216
7.2 CONCLUSION FROM QUASI STATIC CYCLIC LOADING TESTS.....	217
7.2.1 Plane Frame Beam-Column Joint Subassemblies.....	217
7.2.2 Space Frame Beam-Column Joint Subassemblies.....	219
7.3 RECOMMENDATIONS AND SUGGESTIONS FOR FUTURE RESEARCH.....	221
REFERENCES.....	222

NOTATION

A_j	= area of joint section
b_c	= column width
b_w	= beam width
C_c	= concrete compression force
C_s	= compression for of reinforcement
D	= deformed bars
f'_c	= concrete compressive strength
f_u	= reinforcement ultimate strength
f_y	= reinforcement yield strength
F	= lateral force
F_x	= lateral force in x axis
h	= storey height or vertical distance between the column end pins
h_b	= beam depth
h_c	= column depth
j_d	= distance from extreme compression fiber of beam to centroid of beam tension reinforcement
N	= column axial load
OTM	= over turning moment
P_i	= tributary gravity axial load
P_t	= joint principal tensile stress
R	= plain round bars
T, T'	= tension force in the beam bar
v_{jh}	= joint horizontal shear stress
V	= lateral load
V_b	= beam shear force
V_c	= column shear force
V_{jh}, V_j	= joint horizontal shear force
V_{jv}	= joint vertical shear force
V_s	= inter storey shear force
α	= power factor for yield interaction
γ	= joint rotation

σ_a	= column axial stress
ε_y	= reinforcement yield strain
θ_j	= joint rotation
ρ	= ratio of area of the top beam longitudinal bars to b_{jd} of beam
ρ'	= ratio of area of the bottom beam longitudinal bars to b_{jd} of beam
ρ_t	= ratio of area of the total column longitudinal bars to column gross area
Φ	= bar diameter

LIST OF FIGURES

<i>Figure 1.1 Joint failure in 1999 Chi-Chi, Taiwan earthquake (NISEE, University of California, Berkeley).....</i>	<i>4</i>
<i>Figure 1.2 Joint failure with stairway in 1999 Izmit, Turkey earthquake (NISEE, University of California, Berkeley).....</i>	<i>4</i>
<i>Figure 1.3 Joint failure from below in 1999 Izmit, Turkey earthquake (NISEE, University of California, Berkeley).....</i>	<i>5</i>
<i>Figure 1.4 Multiple joint failures in 1999 Izmit, Turkey earthquake (NISEE, University of California, Berkeley).....</i>	<i>5</i>
<i>Figure 2.1 Severe damage on corner joints in 1999 Izmit, Turkey earthquake (NISEE, University of California, Berkeley).....</i>	<i>13</i>
<i>Figure 2.2 Capacity design concept, Park and Paulay (1975).....</i>	<i>14</i>
<i>Figure 2.3 Different type of mechanism.....</i>	<i>15</i>
<i>Figure 2.4 Typical pre-1970s reinforced concrete beam-column joint in New Zealand, Hakuto (1995).....</i>	<i>17</i>
<i>Figure 2.5 Detailing of pre-1970s reinforced concrete structures in the Mediterranean countries (Italy), Pampanin (2003).....</i>	<i>18</i>
<i>Figure 2.6 Reinforcement detailing from the 1950s code.....</i>	<i>19</i>
<i>Figure 2.7 Soft-storey mechanism observed in 1999 Chi-Chi Earthquake in Taiwan due to the effect of the use of infills, Uang (1999).....</i>	<i>20</i>
<i>Figure 2.8 Specimens details, Aycardi et al. (1994).....</i>	<i>23</i>
<i>Figure 2.9 Lateral force vs drift graph of the specimens, Aycardi et al. (1994).....</i>	<i>24</i>
<i>Figure 2.10 Specimens details, Hakuto et al. (1995).....</i>	<i>25</i>
<i>Figure 2.11 Damage observed, Hakuto et al. (1995).....</i>	<i>26</i>
<i>Figure 2.12 Specimens details, Beres et al. (1996).....</i>	<i>27</i>
<i>Figure 2.13 Lateral force versus drift of the specimens, Beres et al. (1996).....</i>	<i>28</i>
<i>Figure 2.14 Specimens details, Liu et al. (2002).....</i>	<i>29</i>
<i>Figure 2.15 Damage observed, Liu et al. (2002).....</i>	<i>30</i>
<i>Figure 2.16 Specimens details, Pampanin et al. (2002).....</i>	<i>31</i>
<i>Figure 2.17 Damage observed and test results, Pampanin et al. (2002).....</i>	<i>31</i>
<i>Figure 2.18 Specimens details, Popov et al. (1992).....</i>	<i>34</i>

<i>Figure 2.19 Specimens details, Gentry and Wight (1994)</i>	36
<i>Figure 2.20 Lateral force versus drift of the specimens, Gentry and Wight (1994)</i> ...	36
<i>Figure 2.21 Specimens details, Abdouka (2003)</i>	37
<i>Figure 2.22 Damage observed, Abdouka (2003)</i>	38
<i>Figure 2.23 Specimens details, Leon and Jirsa (1986)</i>	40
<i>Figure 2.24 Test result, Leon and Jirsa (1986)</i>	40
<i>Figure 2.25 Specimens details, Cheung et al. (1991)</i>	43
<i>Figure 2.26 Damage observed, Cheung et al. (1991)</i>	46
<i>Figure 2.27 Specimens details, Bolong and Yuzhou (1991)</i>	47
<i>Figure 2.28 Damage observed, Bolong and Yuzhou (1991)</i>	47
<i>Figure 2.29 Specimens details, Kurose et al. (1991)</i>	48
<i>Figure 2.30 Damage observed, Kurose et al. (1991)</i>	49
<i>Figure 2.31 Specimens details, Owada (2000)</i>	50
<i>Figure 2.32 Test result and damage observed, Owada (2000)</i>	50
<i>Figure 2.33 Proposed model by Elmorsi et al. (2000)</i>	52
<i>Figure 2.34 Proposed model by Youssef and Ghobarah (2001)</i>	53
<i>Figure 2.35 Proposed model by Lowes and Altoontash (2003)</i>	53
<i>Figure 2.36 Proposed model by Pampanin et al. (2003)</i>	55
<i>Figure 2.37 Giberson one component beam, Carr (2004)</i>	56
<i>Figure 2.38 Joint shear deformation</i>	56
<i>Figure 2.39 Advanced hysteresis rule with pinching (Pampanin) and available in Ruaumoko, Carr (2004)</i>	57
<i>Figure 2.40 Reinforced concrete column interaction surface in space frame, Carr (2004)</i>	59
<i>Figure 2.41 Proposed model</i>	60
<i>Figure 2.42 Forces on beam-column joints (Cheung et al. 1991)</i>	61
<i>Figure 2.43 Proposed Principal tensile stress limits, Pampanin (2003)</i>	63
<i>Figure 2.44 Hierarchy of strength analysis for Specimen TDP-1</i>	63
<i>Figure 3.1 Forces acting on the column under lateral load in different directions</i> ...	66
<i>Figure 3.2 Hierarchy of strength of a beam-column joint</i>	67
<i>Figure 3.3 Corner joint</i>	67
<i>Figure 3.4 Loading history used for previous bi-directional research</i>	68
<i>Figure 3.5 Single degree of freedom structure behaviour under earthquake</i>	68
<i>Figure 3.6 Plane frame beam-column joint subassembly specimens</i>	69

<i>Figure 3.7 Details of Unit TDP-1.....</i>	<i>71</i>
<i>Figure 3.8 Details of Unit TDD-1.....</i>	<i>72</i>
<i>Figure 3.9 Details of Unit TDP-2.....</i>	<i>73</i>
<i>Figure 3.10 Details of Unit TDD-2.....</i>	<i>74</i>
<i>Figure 3.11 Details of Unit TSP.....</i>	<i>76</i>
<i>Figure 3.12 Details of Unit TSD.....</i>	<i>77</i>
<i>Figure 3.13 Overall geometry of space frame units.....</i>	<i>78</i>
<i>Figure 3.14 Details of Unit DD-1.....</i>	<i>80</i>
<i>Figure 3.15 Details of Unit DD-2.....</i>	<i>82</i>
<i>Figure 3.16 Geometry details of unit DS.....</i>	<i>84</i>
<i>Figure 3.17 Details of Unit DS.....</i>	<i>85</i>
<i>Figure 3.18 Details of joint core area.....</i>	<i>86</i>
<i>Figure 3.19 Details of plane frame test rig.....</i>	<i>87</i>
<i>Figure 3.20 Details of space frame test rig.....</i>	<i>88</i>
<i>Figure 3.21 Axial load variation related with lateral force.....</i>	<i>90</i>
<i>Figure 3.22 Positions of load cells.....</i>	<i>91</i>
<i>Figure 3.23 Positions of potentiometers h_1 and h_2 in plane frame setup.....</i>	<i>93</i>
<i>Figure 3.24 Positions of potentiometers in joint area in plane frame setup.....</i>	<i>93</i>
<i>Figure 3.25 Positions of potentiometers R_1, R_2, h_2 and h_3 in space frame setup.....</i>	<i>94</i>
<i>Figure 3.26 Positions of potentiometers in joint area in space frame setup.....</i>	<i>94</i>
<i>Figure 3.27 Positions of strain gauges for Unit TDP-1.....</i>	<i>96</i>
<i>Figure 3.28 Positions of strain gauges for Unit TDD-1.....</i>	<i>96</i>
<i>Figure 3.29 Positions of strain gauges for Unit TDP-2.....</i>	<i>96</i>
<i>Figure 3.30 Positions of strain gauges for Unit TDD-2.....</i>	<i>97</i>
<i>Figure 3.31 Positions of strain gauges for Unit TSP.....</i>	<i>97</i>
<i>Figure 3.32 Positions of strain gauges for Unit TSD.....</i>	<i>98</i>
<i>Figure 3.33 Positions of strain gauges for Unit DD-1.....</i>	<i>99</i>
<i>Figure 3.34 Positions of strain gauges for Unit DD-2.....</i>	<i>99</i>
<i>Figure 3.35 Positions of strain gauges for Unit DS.....</i>	<i>100</i>
<i>Figure 3.36 Lateral displacement history.....</i>	<i>101</i>
<i>Figure 3.37 Bi-directional lateral displacement history.....</i>	<i>103</i>
 <i>Figure 4.1 Positive loading and displacement.....</i>	 <i>105</i>
<i>Figure 4.2 Cracks development of Unit TDD-1.....</i>	<i>107</i>

<i>Figure 4.3 Lateral force versus Top displacement of Unit TDD-1</i>	110
<i>Figure 4.4 Members displacement contribution of Unit TDD-1</i>	110
<i>Figure 4.5 Force and stress in the joint core of Unit TDD-1</i>	112
<i>Figure 4.6 Cracks development of Unit TDP-1</i>	114
<i>Figure 4.7 Lateral force versus Top displacement of Unit TDP-1</i>	115
<i>Figure 4.8 Members displacement contribution of Unit TDP-1</i>	116
<i>Figure 4.9 Force and stress in the joint core of Unit TDP-1</i>	118
<i>Figure 4.10 Cracks development of Unit TDP-2</i>	120
<i>Figure 4.11 Lateral force versus Top displacement of Unit TDP-2</i>	123
<i>Figure 4.12 Members displacement contribution of Unit TDP-2</i>	124
<i>Figure 4.13 Force and stress in the joint core of Unit TDP-2</i>	126
<i>Figure 4.14 Joint principal tensile stress versus Joint rotation of Unit TDP-2</i>	127
<i>Figure 4.15 Cracks development of Unit TDD-2</i>	131
<i>Figure 4.16 Lateral force versus Top displacement of Unit TDD-2</i>	133
<i>Figure 4.17 Members displacement contribution of Unit TDD-2</i>	134
<i>Figure 4.18 Force and stress in the joint core of Unit TDD-2</i>	136
<i>Figure 4.19 Cracks development of Unit TSP</i>	138
<i>Figure 4.20 Lateral force versus Top displacement of Unit TSP</i>	140
<i>Figure 4.21 Members displacement contribution of Unit TSP</i>	141
<i>Figure 4.22 Force and stress in the joint core of Unit TSP</i>	143
<i>Figure 4.23 Cracks development of Unit TSD</i>	145
<i>Figure 4.24 Lateral force versus Top displacement of Unit TSD</i>	148
<i>Figure 4.25 Members displacement contribution of Unit TSD</i>	149
<i>Figure 4.26 Force and stress in the joint core of Unit TSD</i>	150
<i>Figure 4.27 Hysteresis envelopes of Units TDP-1 (deep-plain) and TDD-1 (deep-deformed)</i>	155
<i>Figure 4.28 Hysteresis envelopes of Units TSP (shallow-plain) and TSD (shallow-deformed)</i>	156
<i>Figure 4.29 Strain distribution on beam reinforcement for Unit TSP (shallow-plain)</i>	157
<i>Figure 4.30 Hysteresis envelopes of Units TDP-1 (deep-plain) and TSP (shallow-plain)</i>	157
<i>Figure 4.31 Hysteresis envelopes of Units TDD-1 (deep-deformed) and TSD (shallow-deformed)</i>	158

Figure 4.32 Strength degradation curve for Units TDP-1 (deep-plain-4-2), TDP-2 (deep-plain-4-4) and TDD-2 (deep-deformed-6-4).....	159
Figure 4.33 Strength degradation curve for Units TDP-1, TDP-2 and TDD-2.....	160
Figure 4.34 Strength degradation curve for exterior joints.....	161
Figure 5.1 Positive loading and displacement.....	163
Figure 5.2 Cracks of Unit DD-1.....	166
Figure 5.3 Lateral force versus Top displacement of Unit DD-1.....	168
Figure 5.4 Members displacement contribution of Unit DD-1.....	170
Figure 5.5 Force and stress in the joint core of Unit DD-1.....	173
Figure 5.6 Joint principal tensile stress $(P_t)/\sqrt{f'_c}$ versus Joint rotation of Unit DD-1.....	175
Figure 5.7 Cracks of Unit DD-2.....	178
Figure 5.8 Lateral force versus Top displacement of Unit DD-2.....	181
Figure 5.9 Members displacement contribution of Unit DD-2.....	182
Figure 5.10 Force and stress in the joint core of Unit DD-2.....	185
Figure 5.11 Joint principal tensile stress $(P_t)/\sqrt{f'_c}$ versus Joint rotation of Unit DD-2.....	188
Figure 5.12 Cracks of Unit DS.....	191
Figure 5.13 Lateral force versus Top displacement of Unit DS.....	193
Figure 5.14 Members displacement contribution of Unit DS.....	195
Figure 5.15 Force and stress in the joint core of Unit DS.....	198
Figure 5.16 Joint principal tensile stress $(P_t)/\sqrt{f'_c}$ versus Joint rotation (N-S) of Unit DS.....	200
Figure 5.17 Hysteresis envelopes of Units DD-1 (deep-deep-one joint stirrup), DD-2 (deep-deep-no joint stirrup), DS (deep-shallow).....	204
Figure 5.18 Joint principal tensile stress envelopes of Units DD-1 (deep-deep-one joint stirrup), DD-2 (deep-deep-no joint stirrup), DS (deep-shallow).....	205
Figure 5.19 Proposed strength degradation for smooth bars without joint stirrup.....	206
Figure 5.20 Proposed strength degradation curves for smooth bars with joint stirrup.....	206
Figure 5.21 Hysteresis envelopes of Units DD-1 (deep-deep) and TDP-2 (deep-plain).....	208
Figure 5.22 Joint principal tensile stress of Units DD-1 (deep-deep) and TDP-2 (deep-plain).....	208

<i>Figure 6.1 Analytical-experimental comparison of Unit TDD-1.....</i>	<i>211</i>
<i>Figure 6.2 Analytical-experimental comparison of Unit TDP-1.....</i>	<i>211</i>
<i>Figure 6.3 Analytical-experimental comparison of Unit TDP-2.....</i>	<i>212</i>
<i>Figure 6.4 Analytical-experimental comparison of Unit TDD-2.....</i>	<i>213</i>
<i>Figure 6.5 Analytical-experimental comparison of Unit TSD.....</i>	<i>213</i>
<i>Figure 6.6 Analytical-experimental comparison of Unit TSD.....</i>	<i>214</i>
<i>Figure 7.1 Strength degradation curve for exterior joints.....</i>	<i>218</i>
<i>Figure 7.2 Proposed strength degradation curves for corner joints.....</i>	<i>219</i>

LIST OF TABLES

<i>Table 3.1 Concrete properties of test units (deep beams).....</i>	<i>74</i>
<i>Table 3.2 Reinforcing steel properties of test units (deep beams).....</i>	<i>75</i>
<i>Table 3.3 Concrete properties of test units (shallow beams).....</i>	<i>77</i>
<i>Table 3.4 Reinforcing steel properties of test units (shallow beams).....</i>	<i>78</i>
<i>Table 3.5 Concrete properties of unit DD-1.....</i>	<i>81</i>
<i>Table 3.6 Reinforcing steel properties of unit DD-1.....</i>	<i>81</i>
<i>Table 3.7 Concrete properties of unit DD-2.....</i>	<i>82</i>
<i>Table 3.8 Reinforcing steel properties of unit DD-2.....</i>	<i>83</i>
<i>Table 3.9 Concrete properties of unit DS.....</i>	<i>86</i>
<i>Table 3.10 Reinforcing steel properties of unit DS.....</i>	<i>86</i>
<i>Table 4.1 Reinforcing details of plane frame test units.....</i>	<i>106</i>
<i>Table 4.2 Material strength of plane frame test units.....</i>	<i>106</i>
<i>Table 4.3 Plane frame test result.....</i>	<i>153</i>
<i>Table 4.4 Limit state based on joint shear deformation.....</i>	<i>164</i>
<i>Table 5.1 Reinforcement details of space frame test units.....</i>	<i>164</i>
<i>Table 5.2 Material properties of space frame test units.....</i>	<i>164</i>
<i>Table 5.3 Summary of space frame units global behaviour.....</i>	<i>203</i>
<i>Table 5.4 Summary of force and stress in joint of space frame units.....</i>	<i>203</i>
<i>Table 6.1 Pampanin hysteresis parameter for Unit TDD-1.....</i>	<i>210</i>
<i>Table 6.2 Pampanin hysteresis parameter for Unit TDP-2.....</i>	<i>212</i>
<i>Table 6.3 Pampanin hysteresis parameter for Unit TDD-2.....</i>	<i>213</i>
<i>Table 6.4 Pampanin hysteresis parameter for Unit TSP.....</i>	<i>214</i>
<i>Table 6.5 Pampanin hysteresis parameter for Unit TSD.....</i>	<i>214</i>

CHAPTER 1

INTRODUCTION

1.1 SEISMIC VULNERABILITY ASSESSMENT OF EXISTING REINFORCED CONCRETE BUILDINGS

Around the world, and more specifically in seismic prone countries, there are still an impressive number of reinforced concrete structures which were not originally designed to resist the seismic hazard. Most of these structures have been typically designed before the 1970s when ‘capacity design’ philosophy was not yet widely introduced in seismic design codes. Current seismic design procedures around the world have advanced significantly when compared to the time when those reinforced concrete structures were built. The main advances are the understanding of the post-elastic seismic behaviour of the structures, the “capacity design” design philosophy and the improvement in the structural detailing to enhance the ductility capacity at section, member or whole structure level. Therefore, many existing reinforced concrete structures designed and constructed before the 1970s may lack basic seismic design principles now widely adopted in present code design provisions.

The importance of the seismic assessment of existing reinforced concrete structures with the lack of seismic details has in a relatively recent past received more and more attention following the high level of damage and direct or indirect socio-economical losses and consequences observed as a result of recent severe earthquake events. Several recent earthquakes, such as Hyogo-ken Nanbu Earthquake in Japan (1995), Chi-Chi Earthquake in Taiwan (1999), Izmit Earthquake in Turkey (1999), and more recently, 2003 Bingol Earthquake in Turkey, caused heavy damage and/or collapse to an excessively high number of existing reinforced concrete structures designed to outdated codes. The 1995 Hyogo-ken Nanbu Earthquake in Kobe resulted for example in heavy damage to about 3900 reinforced concrete structures, with about 330 structures of them collapsing. More than 10000 buildings suffered moderate level of damage to full collapse with 2469 victims died and more than 11000 injured in the 1999 Chi-Chi Earthquake in Taiwan (EERI 2001). In the same year about 115000 buildings collapse or were heavily damaged and 17439 people were killed and 43953 injured in the Izmit Earthquake in Turkey. The 2003 Bingol Earthquake in

Turkey resulted in heavy damage to about 2874 buildings, among which about 308 existing reinforced concrete structures collapsed and left 177 dead and 530 injured (EERI 2003). Economical and social sectors were severely hit as the result of the extent of damage. For example, in the Chi-Chi Earthquake, the estimated loss was in the order of 20-30 billion US\$. On the other hand, most of the reinforced concrete structures built recently and designed according to modern seismic code provisions, did not suffer significant damage, proving the current knowledge on seismic design to be relatively advanced and the correspondent design guidelines adequate in limiting the disastrous consequences observed in the past.

Seismic assessment is the first step within the retrofit strategy aiming to reduce the seismic risk (combination of hazard and vulnerability). A good understanding of the weak point of a structure under seismic loading could allow to complement and design the most appropriate retrofit solution to reduce the seismic vulnerability, thus the expected damage for the target (expected) intensity of the seismic event.

As a result, the activities in the assessment of the seismic vulnerability of existing reinforced concrete structures have been increasing rapidly in many countries in order to establish appropriate retrofit strategies. The seismic risk of a structure, which is determined by its seismic vulnerability to its area seismic hazard, has to be identified accurately to provide a good seismic assessment.

During recent years, many countries have developed several seismic assessment procedures, which are established using different principles. The current code, FEMA 356 (NEHRP 2000), requires the assessment to be based on the performance of the building under seismic loading. Performance based seismic assessment procedures have been developed during the past decade with particular focus on displacement based design approaches, in recognition to the role of displacement as major damage indicator (Calvi and Priestley 1991, Priestley 1997, Calvi 1999, Glaister and Pinho 2003).

The general seismic assessment procedure for an existing structure as described by FEMA 356 (NEHRP 2000) can be conceptually summarized as:

1. Obtain the as-built information of the structure.
2. Choose the rehabilitation method that will be applied to the structure.

3. Analyze the structure seismically according to the seismic hazard to find the performance of the components and the global structure.
4. Decide the rehabilitation strategy suitable for the structure.

Limit states based on the deformation of the structure globally (i.e. interstorey drift ratio, ductility) as well as for each component (beams, columns, joints, infills) have to be used to determine the necessity of rehabilitation for the structure.

The proper understanding of the ‘hierarchy of strength’ concept is also essential to avoid major mistakes in assessing the structure and choosing the suitable retrofit strategy.

Some of the seismic assessment procedures are already advanced using capacity design philosophy and taking into account the global structural behaviour in the post-elastic range. Experimental research to investigate the possible seismic behaviour of pre-1970s reinforced concrete structures have been carried out in the past. However, there is still a need of further investigation on to understand more the behaviour of reinforced concrete structure under seismic loading.

The objectives of these experiments are to further study the cyclic loading behaviour of reinforced concrete of the structures designed with older code provisions.

The research work presented in this thesis aims at investigating the seismic behaviour of substandard beam-column joints using different types of detailing.

1.2 BACKGROUND OF THIS RESEARCH PROJECT

A significant amount of research investigations have been carried out in the past to improve the seismic behaviour of beam-column joints. Most of these works were however focused on the need to come out with proper guidelines for the new design of seismic-resisting structure. On the contrary, a substantial lack of information and experimental investigation on the seismic behaviour of substandard beam-column joints has to be recognized. Furthermore, due to the need and intention to limit the complexity of the set-up and extent of the investigation, there has been little number of tests on the three-dimensional seismic behaviour of beam-column joint. In particular the aforementioned recent earthquake events have highlighted a peculiar vulnerability of exterior (corner) beam-column joints when subjected to a combined

bi-directional cyclic response. Fig. 1.1 to Fig. 1.4 show some example of damage on the beam-column joint of a structure observed during recent earthquake events



**Figure 1.1 Joint failure in 1999 Chi-Chi, Taiwan earthquake
(NISEE, University of California, Berkeley)**

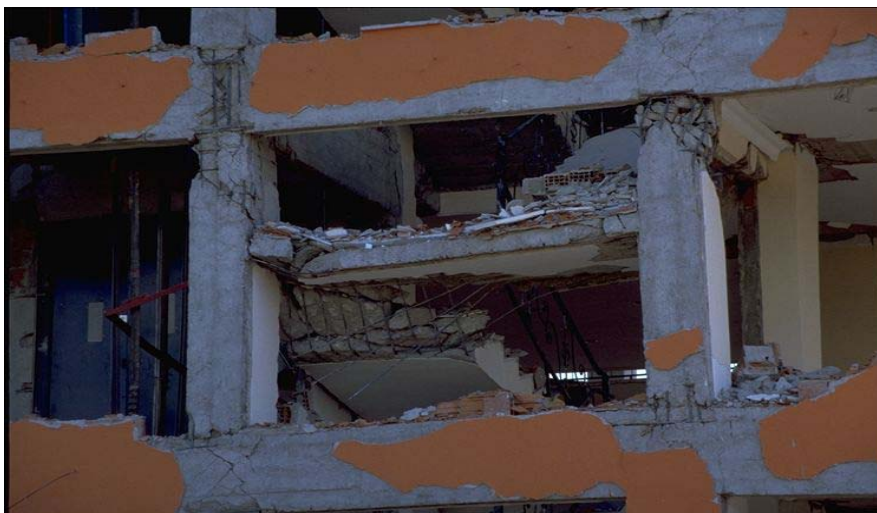


**Figure 1.2 Joint failure with stairway in 1999 Izmit, Turkey earthquake
(NISEE, University of California, Berkeley)**



**Figure 1.3 Joint failure from below in 1999 Izmit, Turkey earthquake
(NISEE, University of California, Berkeley)**



**Figure 1.4 Multiple joint failures in 1999 Izmit, Turkey earthquake
(NISEE, University of California, Berkeley)**

To understand more about the seismic behaviour of reinforced concrete structures, numerous amount of research have been and are being done around the world. United States of America, Japan and New Zealand are some of the leading countries in the research on the seismic behaviour of reinforced concrete structure. In New Zealand particularly, the FRST-NZ (Foundation of Research on Science and Technology New Zealand) has been one of the main institution that helps to provide the fund for various number of research on reinforced concrete structure.

The University of Canterbury has been developing a research program on Seismic Assessment and Retrofit of Existing Reinforced Concrete Structures for several years sponsored by the Earthquake Commission of New Zealand. Investigations of existing reinforced concrete structures built in 1950s in New Zealand had been done (Hakuto et al. 2000, Liu et al. 2001) in past years. Cyclic loading tests of reinforced concrete columns and beam-column joint prototypes with reinforcing details typical of the 1950s have been completed. Unfortunately, most of the tests used deformed bars for longitudinal reinforcement. This does not express the real peculiarities of typical 1950s reinforced concrete structures, where plain round bar reinforcement was still commonly used. The deformed bar reinforcement has higher bond strength compared to plain bar reinforcement. Bond strength between the longitudinal reinforcement and the concrete around it has the main role in the behaviour of reinforced concrete components. The old codes were still using conventional theory for flexure and shear with the assumption of no bond problems between the longitudinal reinforcement and the surrounding concrete. Therefore, the seismic behaviour of reinforced concrete members using plain round bars as longitudinal reinforcement can be very different from the theoretical calculation. The information from the tests using deformed longitudinal reinforcement may give misleading results in assessing the seismic behaviour of reinforced concrete structures with plain round bar longitudinal reinforcement.

There is still an absence of experimental tests on the 3-D response of existing beam-column joints under bi-directional cyclic loading, such as corner joints. Moreover, the different structure detailing can lead to different mechanisms, therefore it is important to conduct more tests varying the structural details used before 1970.

Furthermore, in most of the previous beam-column joint tests available in the literature, the axial column load was maintained as constant, without considering the

real effects during the building sway mechanisms. The axial load on the column can become smaller or bigger depending on the movement of the structure. Therefore, it is important to investigate the influence of axial load in the column on the seismic behaviour of beam-column joint regions, since the variation in axial load on the column will always exist. It will affect the bond performance of the beam bars passing through the joint core and the joint shear capacity, especially when plain round bars are used for longitudinal reinforcement. The compression from the axial column load can help to confine the joint core but also increase the force distribution by bond within the joint core, which will accelerate the joint shear failure.

1.3 OBJECTIVES OF THIS RESEARCH PROJECT

The objectives of this research project are:

1. To gather the information on the cyclic loading behaviour of existing reinforced concrete members with plain round bars as the longitudinal reinforcement, which is needed for the seismic assessment of pre-1970s reinforced concrete structures.
2. To investigate the behaviour of beam-column joints with different detailing:
 - plain round bars with hook-end and deformed bars bent into the joint
 - single joint transverse reinforcement and no joint transverse reinforcement
 - use of deep beam and shallow beam.
3. To investigate the effect of bi-axial loading in space frame on the behaviour of the exterior beam-column joints.
4. To develop a further refined existing analytical procedure and numerical models to predict the seismic behaviour of pre-1970s reinforced concrete structures. Information from tests available in literature as well as from those performed within this project, will be used to further validate and calibrate recently proposed hysteresis loop with pinching behaviour, appropriate for the seismic behaviour of poorly detailed structural member.

1.4 ORGANIZATION OF THE THESIS

This thesis consists of seven Chapters and can be conceptually divided into five parts.

Part 1, which consists of Chapter 2, reviews the seismic deficiencies of pre-1970s concrete frame structures and the previous research projects relevant to this project available in literature both experimentally and analytically. Review of the seismic deficiency of pre-1970s concrete frame structures clarify the importance of understanding the actual local behaviour of concrete structure components for conducting the seismic assessment of the structures which were under-designed for seismic excitation. The review of previous researches carried out worldwide on the topic is to identify what has been done in this research topic and what still needs to be done for a more comprehensive understanding of the seismic performance of existing frame buildings, as a fundamental platform to define an appropriate retrofit strategy. The analytical modelling and basic theory used for the assessment (prediction) of the hierarchy of strength, sequence of events as well as the cyclic behaviour of the test units are also described.

In part 2, which includes Chapters 3, the test set up and loading procedure adopted for the quasi-static tests (either uni-directional or bi-directional) in this project, is described first. The description of the test specimens, including mechanical and geometrical properties are also described along with the instrumentation.

In Part 3, which include Chapters 4 and 5, test results are presented. Chapter 4 introduces the results from the tests on six 2D as-built exterior beam-column joint units, while Chapter 5 discusses the results from the tests done on three 3D as-built exterior beam-column joint units. Emphasis is placed on studying the effects of the different structural details used, varying axial column load and the biaxial effect on the seismic behaviour of existing reinforced concrete structures.

In Part 4, which includes Chapter 6, a critical comparison between test result and analytical prediction, in terms of hierarchy of strength and sequence of events, is carried out. In addition, further validation of the efficiency of the lumped plasticity approach numerical model herein adopted with the used of a recently proposed hysteresis with pinching behaviour is performed.

In Part 5, which consist of chapter 7, summarise the conclusions reached in this project, and gives the suggestions for further developments and future research investigations.

CHAPTER 2

REVIEW ON STRUCTURAL DEFICIENCIES IN PRE-1970'S REINFORCED CONCRETE STRUCTURE AND PREVIOUS INVESTIGATIONS ON BEAM-COLUMN JOINT

2.1 INTRODUCTION

The construction and design practice of reinforced concrete structures have significantly advanced around the world since about the 1970s, mainly in the understanding of the seismic hazard. Current seismic design provisions require a structure to have adequate reinforcement detailing to provide an adequate ductile behaviour necessary to survive a targeted level (i.e. for a given return period) earthquake. Up to the 1970s, most of the structures were not designed using 'capacity design' concepts and the seismic details were poor when compared to those currently implemented in more recent design codes.

The lack of seismic detailing and, in general, of capacity design principle, in the pre-1970s reinforced concrete structures leads to an expectable lack of ductility, at both local or global level, which can result in heavy damage or total collapse under seismic excitation. Therefore it is extremely important to assess the deficiencies in the pre-1970s reinforced concrete structures to find the possible retrofit method for the structure to survive the expected earthquake ground motions.

A large number of research investigations on the seismic behaviour on frame system beam-column joint subassemblies have been carried out in the past with the intent to develop and further refine appropriate seismic design guidelines for framed buildings.

Due to main focus given to the design of new structures (Leon and Jirsa, 1986, Cheung et al., 1991, Bolong and Yuzhou, 1991, Popov et al., 1992, Gentry and Wight, 1994, Owada, 2001, Abdouka, 2003) and the relatively more recent growing interest on seismic assessment and rehabilitation of the existing heritage (Hakuto et al., 1995, Beres et al., 1996, Liu et al., 2002, Pampanin et al.), there is still a significant need for further investigation on the behaviour of under-detailed existing building particularly

when considering the behaviour under bi-directional excitation as in the case of exterior corner beam-column joints.

However, most of the tests focused on the current design code, and not assessing the existing reinforced concrete structure designed with outdated codes. There is still a need in investigating the behaviour of existing reinforced concrete structures, which were not designed seismically. Apart from that, some more limitations can be taken from the previous research.

Typical limits observed in past experimental investigation on b-c joints are for example given by the following points:

1. The variation of axial load in the column due to the sway mechanism, typically taken into account within testing regime. An increase or reduction of the axial load in the column can in fact alter the failure mechanism in a beam-column joint unit.
2. Typical biaxial lateral loading histories used for space frame reinforced concrete beam-column joint experiments were either performed following a fixed diagonal direction (i.e. fixed angle of attack) or imposing orthogonal loading one after the other once the target cyclic peak in one direction has been achieved.

A more complex and realistic bi-directional lateral loading history with interaction between the two orthogonal is needed to capture the behaviour of a beam-column joint under a real earthquake.

3. Previous experimental tests on reinforced concrete beam-column joints were mostly done on interior beam-column joints. Information of the behaviour of poorly detailed exterior beam-column joint unit is still widely needed.

The evolution of computer modeling to help more in-depth analysis is reviewed. A few of the modeling approaches have been proposed in the literature, from empirical methods to finite element methods. Multi-spring macro-models usually require a lot of input-parameters as well as appropriate constitutive-laws for the material. This complexity discourages people from using them as analytical tool.

This chapter reviews the typical detailing and the deficiencies of pre-1970s reinforced concrete structures when compared to those designed according to current codes and the previous researches relevant to this thesis. The vulnerability of pre-1970s

reinforced concrete structures under seismic loading is discussed and photos of damaged structures in recent earthquakes are presented to show the scale of destruction that can occur. Researches both for plane and space frame that had been done in the past years are also mentioned and summarized. A simple analytical model for joint behaviour is proposed as a feasible tool for analytical purposes on the seismic response of existing frames. A rotational spring, dominating the beams and columns relative rotation, is used to represent the joint behaviour in the linear and non-linear range according to the lumped plasticity approach. A newly proposed hysteresis rule with pinching behaviour to take into account the slipping of the bars and the joint shear cracking is used to perform the analysis. In the second phase, the force transfer mechanism in a beam-column joint is discussed. Test units were assessed theoretically to predict the possible behaviour under the seismic loading. The strength of the members and deformability are evaluated to make a hierarchy of strength diagrams that is used to predict the sequence of failure. Strength degradation curves (Priestley, 1997, Pampanin, 2003) were used to predict the joint strength.

2.2 TYPICAL DESIGN APPROACH AND STRUCTURAL DETAILING IN PRE-1970S REINFORCED CONCRETE BUILDINGS

2.2.1 Introduction

Code requirements and details for reinforced concrete structures were dramatically revolutionized in the 1970s mainly thanks to the introduction of ‘capacity design’ principles, a wider acceptance of ductile behavior and the development of appropriate structural detailing to achieve desired inelastic mechanisms at both local and global level.

The beam-column joint of frame buildings designed before the 1970s (i.e. primarily designed for gravity loads only) typically lacks of appropriate transverse reinforcement as well as anchorage and bond details for seismic consideration, thus becoming the likely weakest link of the “chain”. Joint damage or failure can lead to brittle collapse mechanism of the overall building with consequent loss of human life. To prevent this from happening, it is important to investigate the behaviour of the beam-column joint under seismic loading.

The objective of this research is to contribute to the investigation on the seismic behaviour of beam-column joints with typical detailing used before 1970 reinforced concrete buildings both in plane frames and space frames (2D and 3D response), in order to improve and refine the basic knowledge on the topic as a support of the implementation of appropriate retrofit solutions. Lessons learned from past earthquake events, experimental observations, have suggested and confirmed, respectively, that an exterior beam-column joint is inherently more vulnerable than an interior beam-column joint due to the inefficiency of the shear transfer mechanism through the development of a reliable compression strut after first cracking.



**Figure 2.1 Severe damage on corner joints in 1999 Izmit, Turkey earthquake
(NISEE, University of California, Berkeley)**

Furthermore, in a space frame building, the corner exterior joint was in most cases demonstrated the most critical joint, and should thus be expected, to be particularly

prone to suffer high level of damage if not a total collapse (Fig. 2.1). The biaxial effect on the joint contributes to weaken the joint strength and deformation capacity, but limited information are available in literature on this complex bi-axial behavior of under-designed joints, as briefly mentioned and further emphasized in the literature review of Chapter 3.

To identify the possible structural deficiencies expected in existing reinforced concrete buildings constructed before 1970s under seismic excitation, a review of pre-1970s design codes and design code developments are given below.

2.2.2 Development of Design Codes

Early design codes were not yet implementing ‘capacity design’ concepts (Park and Paulay 1975, Paulay and Priestley 1992) as part of the seismic design process, which were only in the 1970s widely adopted in seismic code provisions worldwide.

Behind the concept of capacity design is the clear intent to “tell the structure what to do” (Paulay). The designer selects the most appropriate and desire inelastic mechanism of the structure under seismic loading by choosing the critical regions of the members who should sustain the inelastic demand. These locations, typically referred to as *plastic hinge* regions, are detailed sufficiently to enable inelastic flexural action and act as an artificial fuse (according to the concept of weakest link of the chain, Fig. 2.2).

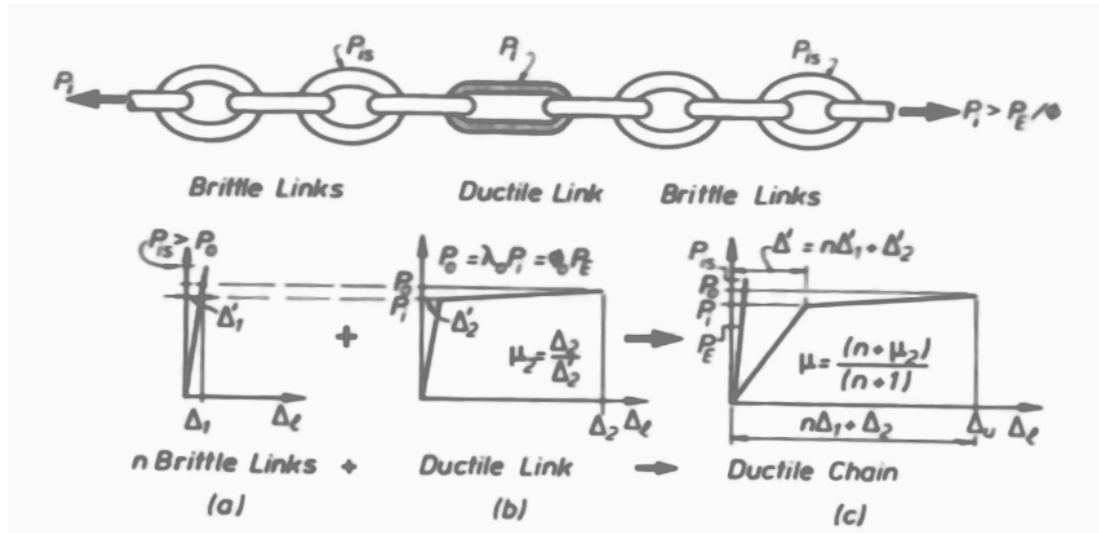


Figure 2.2 Capacity design concept, Park and Paulay (1975)

The other (adjacent) structural elements (i.e. column versus beams) are designed for a greater strength than that corresponding to the fuse mechanism developed in the selected chosen plastic regions.

A beam sway mechanism, as opposite to column sway, is for example the most desirable inelastic mechanism for a reinforced concrete frame subjected under seismic loading. To achieve that, the beams are designed to yield in plastic hinge regions, providing sufficient ductility to the structure while columns remain elastic (apart from the base-column sections). Fig. 2.3 shows the different types of mechanism.

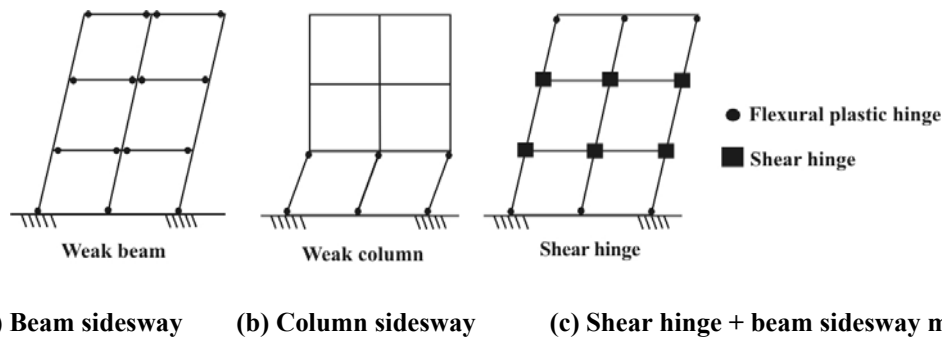


Figure 2.3 Different types of mechanism

As mentioned most of the pre-1970s reinforced concrete structures were not designed with capacity design philosophy, which means an undesirable seismic mechanism such as a soft-storey mechanism might occur. It is found that back then; columns were designed to provide strength only to restrain the lateral load applied on the structure, not on the possible load coming from the beams. This will lead to weak column-strong beam mechanism which will have disastrous outcomes.

There was also lack of seismic details to provide sufficient ductility for the structure under seismic excitation. Due to the scale of damage caused by earthquakes around the world, there is an extreme necessity in understanding the behaviour of the structure under seismic excitation to avoid heavy damage or even collapse of the structure. The capacity design philosophy was used for the base of current seismic codes, taking into account the seismic performance of structures during cycles of lateral loading in the post-elastic range imposed by seismic excitation. Aspects of proportioning and detailing to achieve a structure's overall strength and ductility needed to survive severe earthquakes were developed.

2.2.3 Typical Detailing of Pre-1970s Reinforced Concrete Structures

Due to the absence of ‘capacity design’ philosophy before the 1970s, the lack of ductility has been acknowledged as one of the main reason of the unsatisfactory seismic performance of the reinforced concrete structures designed during that period and which is accentuated by poor reinforcement detailing. Typical structural deficiencies found in these buildings are:

1. lack of appropriate confinement through transverse reinforcement in the plastic hinge regions;
2. lack or even absence of transverse reinforcement in the joint core;
3. moment capacity of the column is lower than that of the beam;
4. use of plain round bars versus deformed bars and inadequate reinforcement anchorage;
5. lapped splices located in potential member (column) plastic hinge region;
6. low strength and poor quality material when compared to present practice;
7. presence of masonry infill walls with complex interaction with the bare frame;

Most of the reinforced concrete structures designed in the pre-1970s exhibit a lack of shear reinforcement in the joint. Sometimes, one stirrup only or no shear reinforcement at all was provided in the joint core. Due to the gradient of bending moment demand between the top and bottom column section within a beam column joint, the shear force in the joint panel zone can be as large as 9 times the shear in the adjacent column (simple calculation) and concrete alone will likely not to be able to resist all the shear force without a contribution from shear reinforcement. Without adequate shear reinforcement in the joint, the concrete has to resist all the forces from the beam and the column passing through the joint, which may lead to a joint shear failure mechanism. High diagonal compressive and tensile stresses occur in the joint as the result of the shear forces. The cracking in the concrete develops according to the tensile stresses and it will lead to a large shear distortion of the joint. The term ‘shear hinge’ (Pampanin et al., 2003) has been used to describe this mechanism, alternative and dual to a typical flexural plastic hinge. As noted in Pampanin et al. (2003), a shear hinge mechanism can delay the occurrence of undesirable column sway mechanism because the concentration of shear deformation in the joint area can

reduce the deformation demand on adjacent structural members and also spreading the interstorey drift demand along two storeys. However, the main shortcoming of a shear hinge mechanism is the intrinsic lack of ductility due to the rapid strength degradation in the joint after first cracking. As suggested by Pampanin and Christopoulos (2003) as part of a multi-level performance based retrofit strategy, a shear hinge mechanism should not be allowed to occur in the exterior joint, since the exterior joints are more vulnerable and unable to maintain the strength once the shear hinge occurs. Figs. 2.4 and 2.5 show the example of typical detailing of pre-1970s reinforced concrete structures.

In most of pre-1970s reinforced concrete structures, the columns were mainly designed for gravity load only or to resist the bending moment from the low level of lateral forces specified by the code (typically a small portion of the building weight) without consideration on the relative hierarchy of strength with the beam moment capacity. This may cause the columns to be weaker than the beams, and possibly resulting in the column side sway mechanism (i.e. soft story mechanism), rather than the preferred beam sway mechanism.

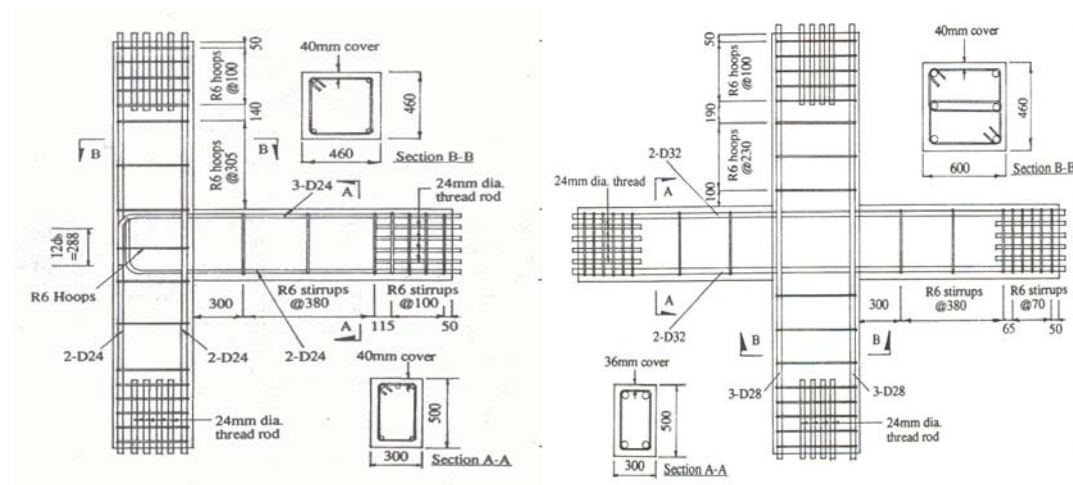


Figure 2.4 Typical pre-1970s reinforced concrete beam-column joint in New Zealand, Hakuto (1995)

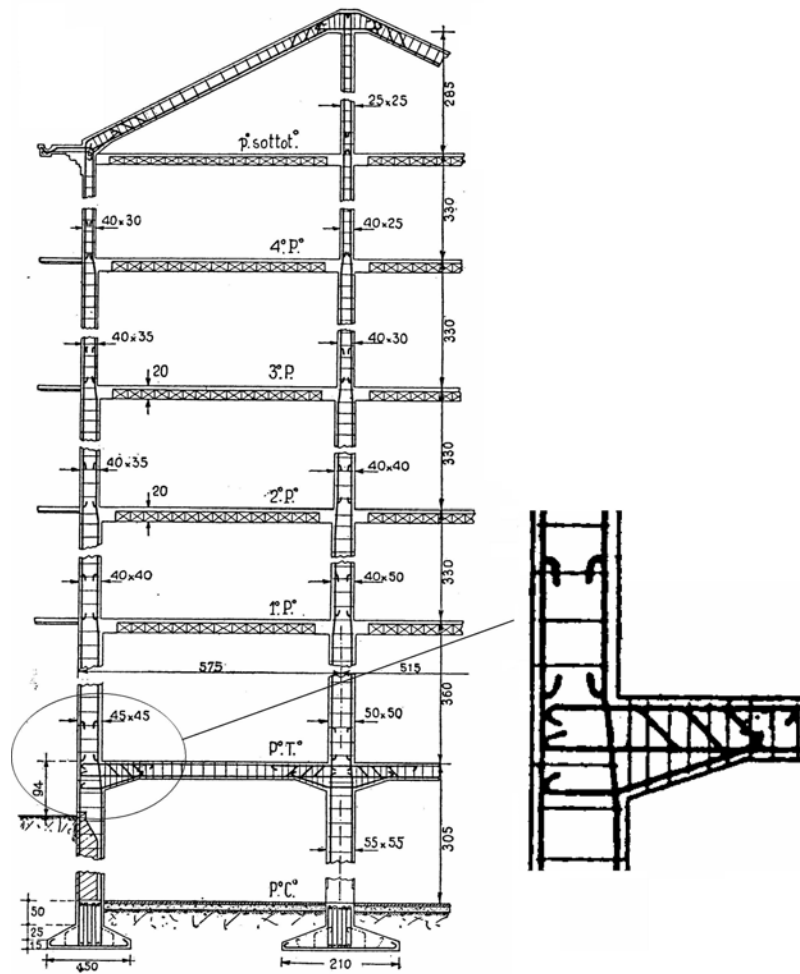
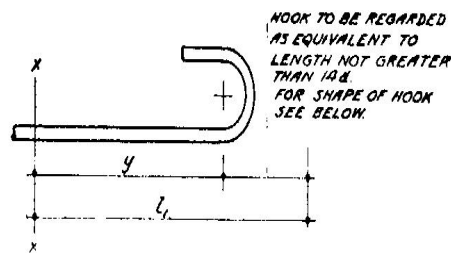


Figure 2.5 Detailing of pre-1970s reinforced concrete structures in the Mediterranean countries (Italy), Pampanin (2003)

In addition, as mentioned, plain round bars with hook-end were widely used for longitudinal reinforcement in the reinforced concrete structures before the 1970s (with consistent use around the world when going back to the 1950s). The performance of a structure using plain round bars with end hooks as the longitudinal reinforcement can result to a very poor behavior under reversed cyclic inelastic loading due to the lack of bond strength between the steel and the concrete which leads to bar slipping and high global deformation of the system. Anchorage provided by hook-end bars was likely to be not sufficient to prevent the bars from slipping, and the concentration of strut and compression force at the hook, due to bars slipping, can lead to a peculiar damage and failure mechanism due to the expulsion of a ‘concrete wedge’ (Pampanin 2003). Plain round bars with hook-end were commonly used for longitudinal reinforcement in the reinforced concrete structures before the 1970s (Fig. 2.6). The

performance of a structure using plain round bars as the longitudinal reinforcement will be very poor under cyclic inelastic loading due to the lack of bond strength between the steel and the concrete so the bars slip easily. Anchorage provided by hook-end bars was not sufficient enough to prevent the bars from slipping, and the concentration of strut and compression force at the hook, due to bars slipping, lead to the expulsion of a ‘concrete wedge’ (Pampanin 2003).

Hooked anchorage:



... all tensile and shear reinforcement should have hooked ends, ...

(a) NZ Code

CHAPTER 8 — DETAILS OF REINFORCEMENT*

801—Hooks and bends¹

(a) *Hooks*—The term “standard hook” as used herein shall mean either

1. A semicircular turn plus an extension of at least four bar diameters but not less than 2½ in. at the free end of the bar, or
2. A 90-deg turn plus an extension of at least 12 bar diameters at the free end of the bar, or
3. For stirrup and tie anchorage only, either a 90-deg or a 135-deg turn plus an extension of at least six bar diameters but not less than 2½ in. at the free end of the bar.

(b) *Minimum radii*—The radii of bend measured on the inside of the bar for standard hooks shall not be less than the values of Table 801(b), except that for sizes #6 to #11, inclusive, in structural and intermediate grades of bars only, the minimum radius shall be 2½ bar diameters.

(b) ACI Code

Figure 2.6 Reinforcement detailing from the 1950s code

The location of lapped splices of the longitudinal reinforcement is another seismic inadequacy typically found in pre-1970s reinforced concrete structures. Lapped splices are usually located in the plastic hinge regions of the beams and/or just above the beam-column joint area where the maximum moments develop. This will lead to inadequate local ductility for the beams and columns (Hakuto et al, 1999, Calvi et al., 2003).

The presence of infills could also provide controversial effects to the structural capacity as well as increase the seismic demand (Crisafulli, 1997, Magenes and Pampanin, 2004). Infill walls provide additional stiffness to the structure reducing the deformation demand. On the other hand, the increment of structure’s lateral stiffness will reduce its fundamental period; therefore there will be an increase in seismic actions. If the use of infills is not distributed evenly in the frame, it can alter the structural mechanism. For example, in 1999 Chi-Chi Earthquake in Taiwan, a lot of buildings have soft-storey mechanisms due to the uneven distribution of infill walls as

shown in Fig. 2.7. The infill walls were used in the higher storeys while the first storey did not have any infill walls.



Figure 2.7 Soft-storey mechanism observed in 1999 Chi-Chi Earthquake in Taiwan due to the effect of the use of infills, Uang (1999)

Moreover, the low strength material, both concrete and steel, used in the construction worsen the seismic behaviour of the pre-1970s reinforced concrete structure.

Flat slabs, often waffle slabs, were widely used in the pre-1970s reinforced concrete structures. Researches done on investigating the seismic behaviour of reinforced concrete waffle slab frame structures (Rodriguez and Diaz, 1989, Rodriguez et al., 1995 and Saunders, 2004) show that the waffle slab structures have moderate energy-dissipation capacity, low displacement ductility factors and high lateral flexibility. It is advised to have other structural elements that can help to increase the lateral strength and stiffness of the structure. On the other hand, the higher flexibility due also to the use of plain round bars have been found in some cases to be a safe mechanism to an under-designed structure, by limiting the amount of internal forces in the members as well by increasing the overall period (thus input loads) during the major event.

Amongst all the aforementioned sources of seismic vulnerability of the pre-1970s reinforced concrete structure, recent studies (Hakuto et al., 1995, Liu et al., 2002 and Pampanin et al., 2003) have emphasized the significant vulnerability of the joint panel zone. Therefore, this research aims to investigate the joint panel zone behaviour from the effect of the use of different structural details, reinforcement types, and bi-axial loading (corner joint).

2.2.4 Shallow or Wide Beams

The use of shallow beams, also typically referred to as wide beams, where the depth of the beam is far less than its width, which itself is much wider than the column which it is anchored to, was also quite typical of pre-1970s reinforced concrete structures around the world. In pre-1970s the codes did not specify the minimum depth of the beam so that there is no prohibition in the use of a shallow beam in construction in the pre-1970s building design code. Even now, some countries still allow the use of the shallow beam in their codes. The main purpose of using the shallow beam is dictated by architectural reason, to maintain the depth of the beam within the depth of the slab, as well as, in a more general sense, to increase the inter-storey living space.

A shallow beam has excellent performance in carrying the gravity load due to the width of the beam but clearly is not very efficient against lateral loading, due to the limited flexural stiffness. In addition the reduced depth of the beam may lead to punching shear failure from the column (Gentry and Wight, 1994) and the construction eccentricity between the beam and column axis could create critical flexural-torsion effects due to the slab weight.

2.3 RELEVANT PLANE FRAME BEAM-COLUMN JOINT RESEARCH PROJECTS

Although, as mentioned plain round bars were typically used instead of deformed bars in construction practice between the 1950s and 1970s in most of major seismic-prone countries, the number of experimental investigation on b-c joints where plain round has been adopted is very limited, mainly due (but not limited) to a common difficulty to find steel reinforcing bars with same properties of those adopted decades ago. Also critically limited information are available on the seismic performance of existing frame systems with shallow (wide) beam, which were not only widely adopted in older construction practice, but are still allowed to be used in few current seismic code provisions (i.e. U.S. and Italy).

2.3.1 Research by Aycardi et al. (1994)

Aycardi et al. (1994) performed two tests on gravity-load-design reinforced concrete slab-beam-column units using deformed longitudinal bars. The specimens were one-

third scale and taken from a prototype reinforced concrete frame designed non-seismically designed according to the ACI 318-89. The units consisted of one exterior specimen and one interior specimen and tested under simulated seismic loading using a shake table. This is a part of a series of research investigation on the seismic behaviour of gravity load design reinforced concrete buildings (Aycardi et al., 1994, Kunnath et al., 1995, Bracci et al., 1995). More specific and broad details of the research investigation can be found in literature. This section focuses on the part of the test series on the beam-column joint.

The objective of this research was to examine the effects of detailing deficiencies on the seismic performance of gravity-design-load structure, such as location of lap splices in potential plastic hinge areas, little transverse reinforcement in beam-column joints and discontinuous bottom beam longitudinal reinforcement in the joint area.

Not typically of similar experimental tests carried out in literature, the axial load on the column was varied during the test depending on the lateral force. The relationship equation is $P = P_i + 2V$ where P_i is the tributary gravity axial load and V is the lateral load. The coefficient 2 was taken based on the result form analysis of entire frames under combined gravity and lateral earthquake loading. Figs. 2.8 and 2.9 show the specimens details and lateral force versus drift of the specimens.

The exterior slab-beam-column unit showed progressive damage in the beam due to the bottom beam longitudinal reinforcement pullout and later continuing in the column. In the interior slab-beam-column unit progressive damage was instead observed only in the column with minor damage in the beam.

Conclusions drawn from this research were:

1. Structural components with detailing deficiencies such as lap splices located in potential plastic hinge area, lack of transverse reinforcement in the joint core and discontinuous of bottom beam longitudinal reinforcement in joint core could still reach their flexural strength and sustain the gravity load during large cyclic deformations.
2. The exterior unit maintained 50 percent of its maximum load capacity for few cycles at 4 percent of drift while the interior unit was able to maintain about 85 percent of its maximum load capacity for two cycles at 4 percent drift. This

shows that total drift limit of 1 percent suggested by some codes is really conservative, even for non-seismic detailing used in this research.

3. The results showed that the complete structural frame is likely to have a hybrid type of failure mechanism. The exterior unit showed a strong column-weak beam mechanism while the interior unit showed a strong beam-weak column mechanism.

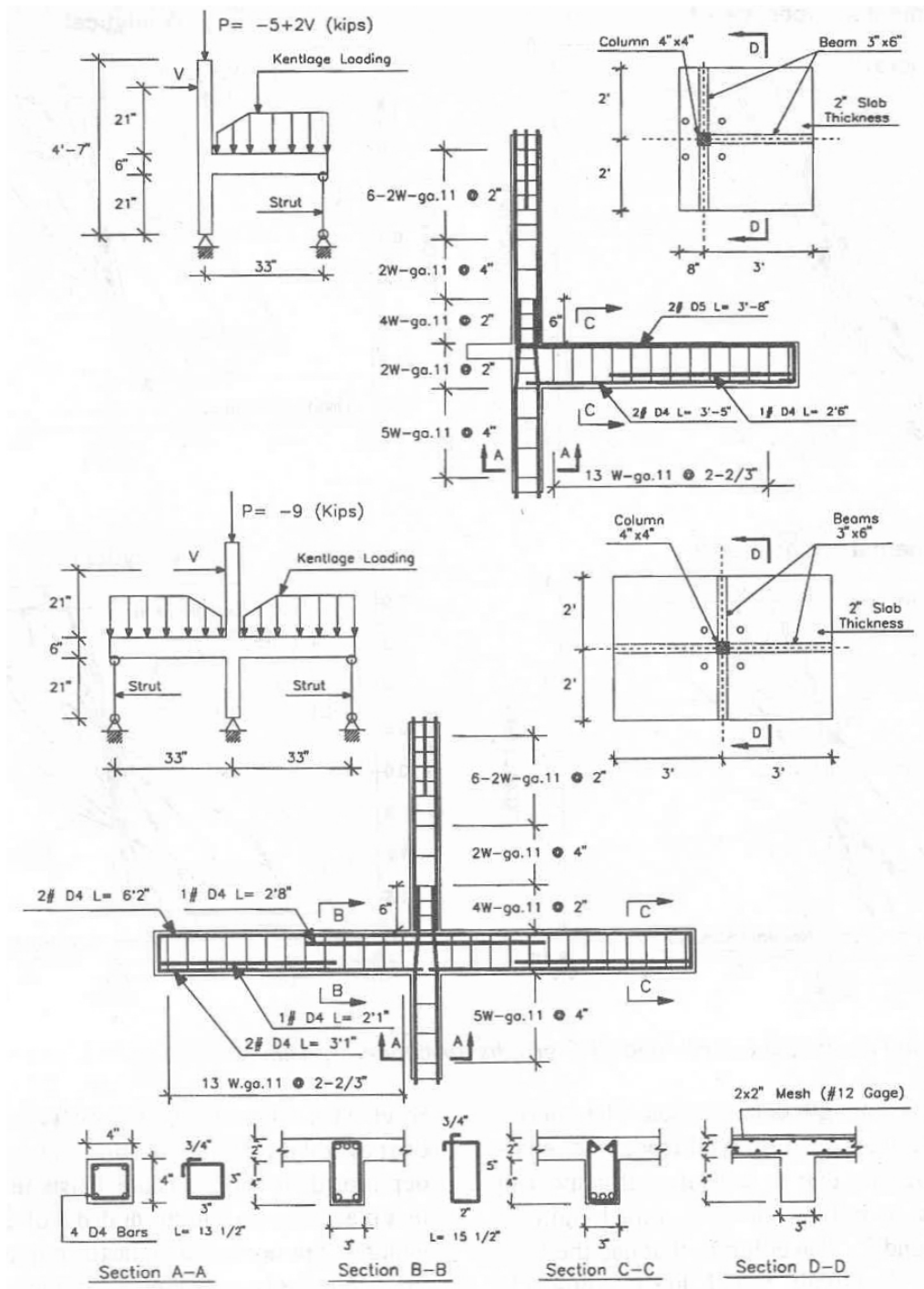


Figure 2.8 Specimens details, Aycardi et al. (1994)

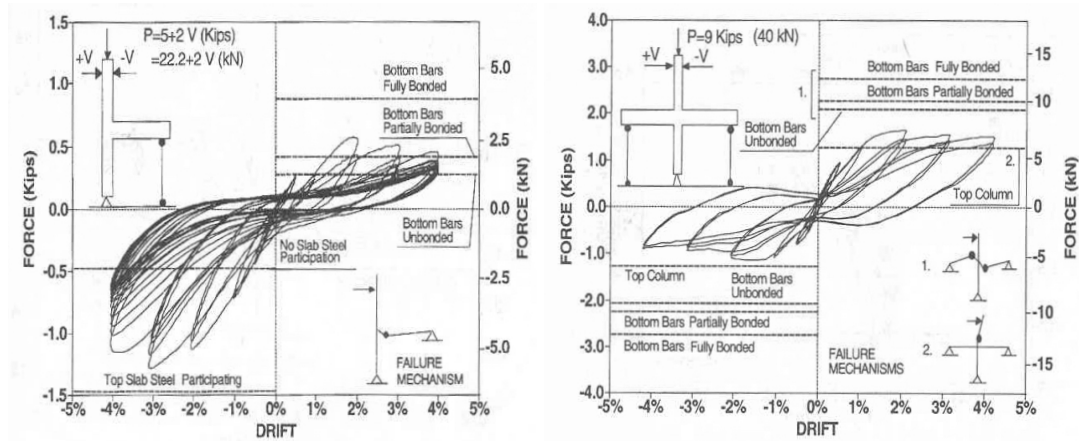


Figure 2.9 Lateral force vs. drift graph of the specimens, Aycardi et al. (1994)

Given the prevalence of flexural behaviour in the beams and columns, no specific information could be derived on the behaviour of the full subassembly and frame system when shear damage mechanism occur into the joint core, as frequently observed after moderate-severe earthquake events in the recent past.

2.3.2 Research by Hakuto et al. (1995)

Hakuto et al. (1995) carried out a series of tests on as-built reinforced concrete beam-column joint units with deformed longitudinal bars. The specimens were full scale and taken from a typical reinforced concrete moment resisting frame designed in the late 1950s in New Zealand. Five beam-column joint specimens were constructed including three interior joint and two exterior joint subassemblies and tested under simulated seismic loading. The objective of this research was to gather more information on the seismic behaviour of structures designed according to older codes in NZ. All the specimens were lacking joint transverse reinforcement as typical of 1950s reinforced concrete frames. The details of the specimens and damage observed in this research are shown in Figs. 2.10 and 2.11.

Most of the specimens suffered extensive joint damage on the form of diagonal shear cracks due to the lack of joint transverse reinforcement able to provide a reliable source of a shear transverse mechanism. The lateral strength of the specimens is expected to reduce along with increasing level of the joint deformation. In the exterior joint with beam longitudinal bar bent into the joint, the diagonal compression strut mechanism can instead be developed adequately to maintain the subassembly lateral strength and provide satisfactory performance under seismic loading.

Figure 2.10 Specimens details, Hakuto et al. (1995)

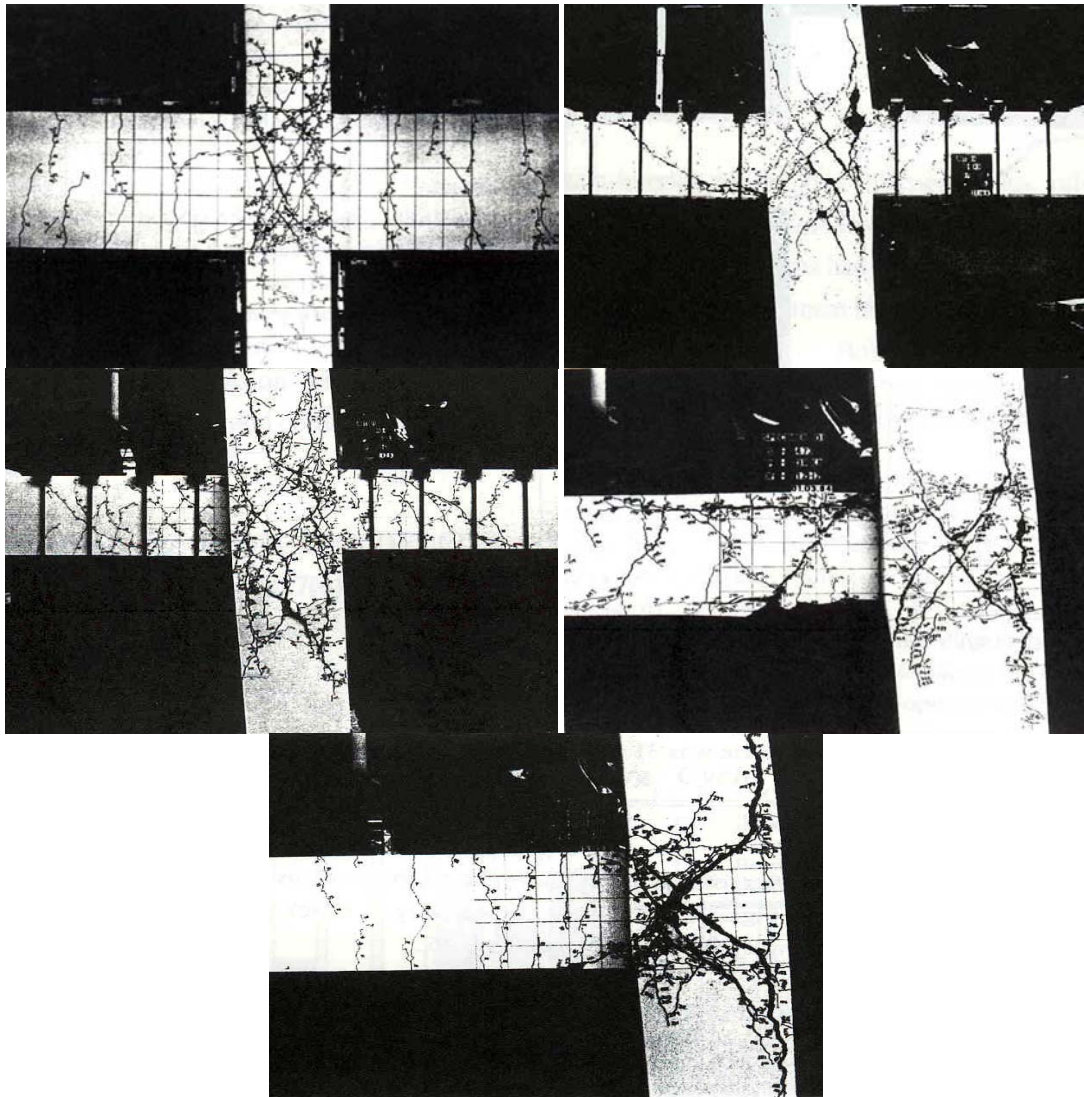


Figure 2.11 Damage observed, Hakuto et al. (1995)

2.2.4 Research by Beres et al. (1996)

Beres et al. (1996) carried out a series of tests on as-built reinforced concrete beam-column joint units with deformed longitudinal bars. The specimens were designed for gravity load only according to U.S. construction practice in the 1950-1970 with typical structural deficiencies mentioned previously, i.e. low column longitudinal reinforcement (though the minimum level of 2% is higher than that used in Mediterranean country, as low as 0.8%), lapped splices of column longitudinal reinforcement just above the joint, insufficient amount of column ties, absence or lack of transverse reinforcement in the beam-column joint core and discontinuity of the beam reinforcement in the column. Thirty-four beam-column joint subassemblies were constructed in full scale and tested under simulated seismic loading at Cornell

University. The objective of this research is to investigate the damage mechanisms and the effect of critical details on strength and deformations.

The specimens were divided into three groups:

1. Six interior beam-column joints with continuous top beam longitudinal reinforcement through the joint panel
2. Fourteen interior beam-column joints with discontinuous top beam longitudinal reinforcement into the column
3. Fourteen exterior beam-column joints with different column axial force, column reinforcement and joint transverse reinforcement.

Figs. 2.12 and 2.13 provide an example of a typical joint specimen detail along with some global force-displacement experimental behaviour.

The test results confirmed that interior joint specimens can reach higher lateral strength capacity than the exterior joint, thanks to the inherent capacity to develop a strut mechanism to transfer shear force in absence of appropriate transverse reinforcement in the joint region. Damage in the specimens occurred mostly in the form of diagonal cracking in the joint-panel area and the surrounding regions, leading to a progressive and critical loss of strength capacity. The causes of these damages were related to the pullout of beam reinforcement, the buckling of the column bars, and loss of anchorage of the beam reinforcement within the joint (opening of the bent bars). Effect of axial load was also confirmed to have not-negligible effects with higher levels of axial load providing additional confinement to the longitudinal reinforcement in the joint, delaying the pullout occurrence.

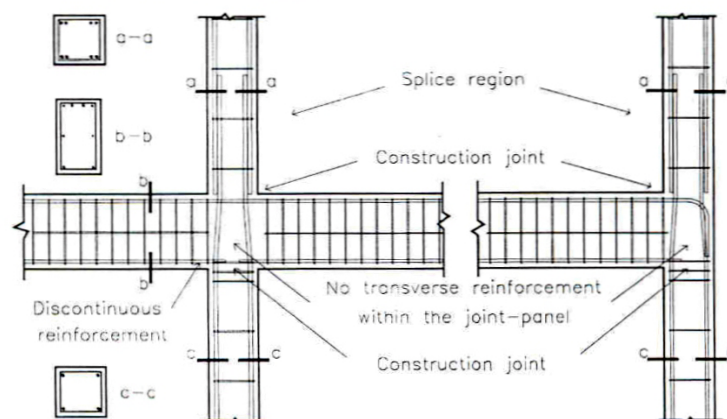


Figure 2.12 Specimens details, Beres et al. (1996)

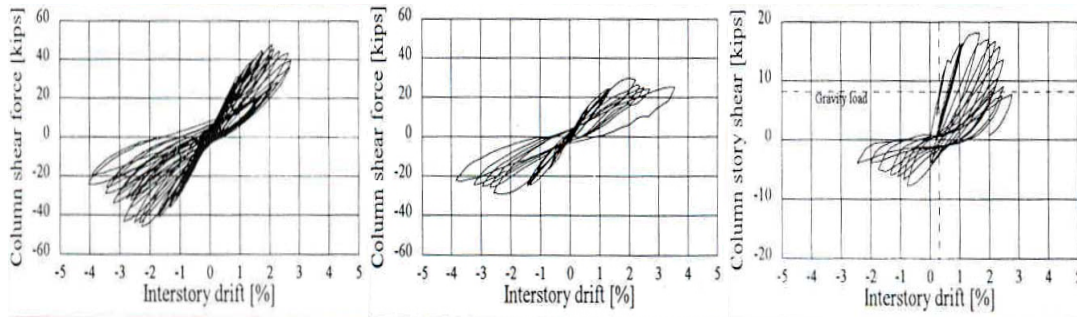


Figure 2.13 Lateral force versus drift of the specimens, Beres et al. (1996)

2.3.4 Research by Liu et al. (2002)

Liu et al. (2002) performed a series of tests on as-built reinforced concrete beam-column joint subassemblies typical of NZ construction practice in the 1950s, following and extending the aforementioned previous contribution by Hakuto et al. (1995) by adopting plain round longitudinal bars. Two interior and four exterior full-scale reinforced concrete beam-column joint units were tested under simulated seismic loading to investigate the post-elastic behaviour of as-built reinforced concrete components. The tests were again carried out at the University of Canterbury, Christchurch, New Zealand. A constant compression axial load was applied on the column top for some of the specimens. Details of the specimens and test program used in this research are shown in Figs. 2.14 and 2.15.

Tests on the interior beam-column joint units result in a poor seismic behaviour in terms of stiffness and strength. Severe bond degradation and column bar buckling from the use of plain round bars led to the final failure of the units.

From the tests on the exterior beam-column joint units, severe bond degradation was also observed while there was no column bar buckling because the columns were still in the elastic range. The bond deterioration helps to avoid shear failure and instead results in flexural failure due to the degradation in flexural strength from the bar slip.

The conclusions drawn from the research are:

1. The compressive column axial load would not improve the joint shear performance in the interior beam-column joint units. For the exterior beam-column joint units, the compressive column axial load has a big beneficial effect in the seismic performance increasing the initial stiffness and storey strength.

2. The use of plain round longitudinal bars was found to enhance premature concrete tension cracking failure along the beam bar hooks. However due to the bond degradation and the slipping of the plain round longitudinal bars, shear failure in the beam and joint core can be avoided and altered to flexural failure of the beam. The bond and slipping problems also make the stiffness observed in the experiment to be lower than the theoretical value.
3. When plain round longitudinal bars are used for the reinforcement, the transverse reinforcement will have bigger effect in confining and preventing the bars from buckling rather than enhancing the shear capacity.

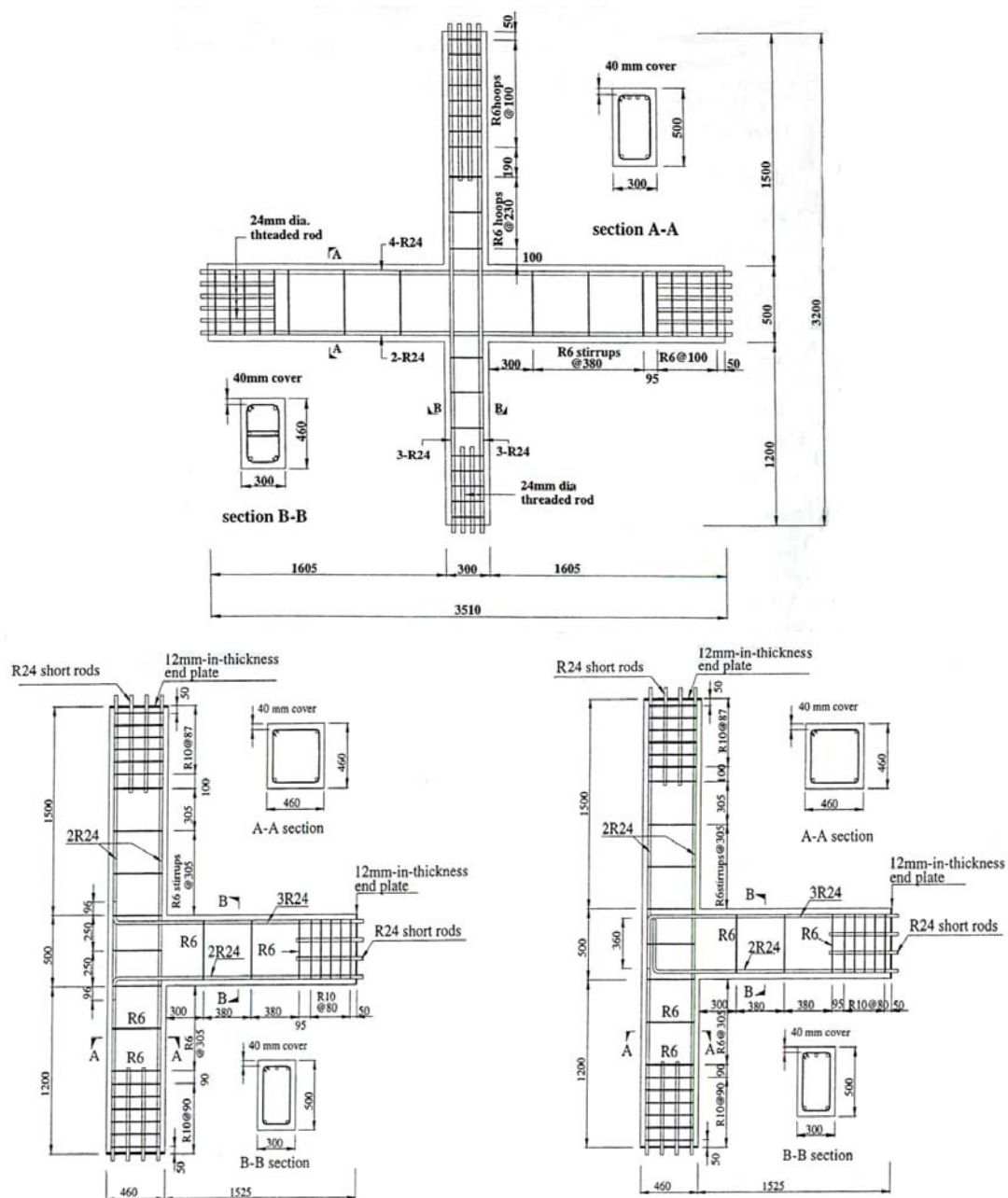


Figure 2.14 Specimens details, Liu et al. (2002)

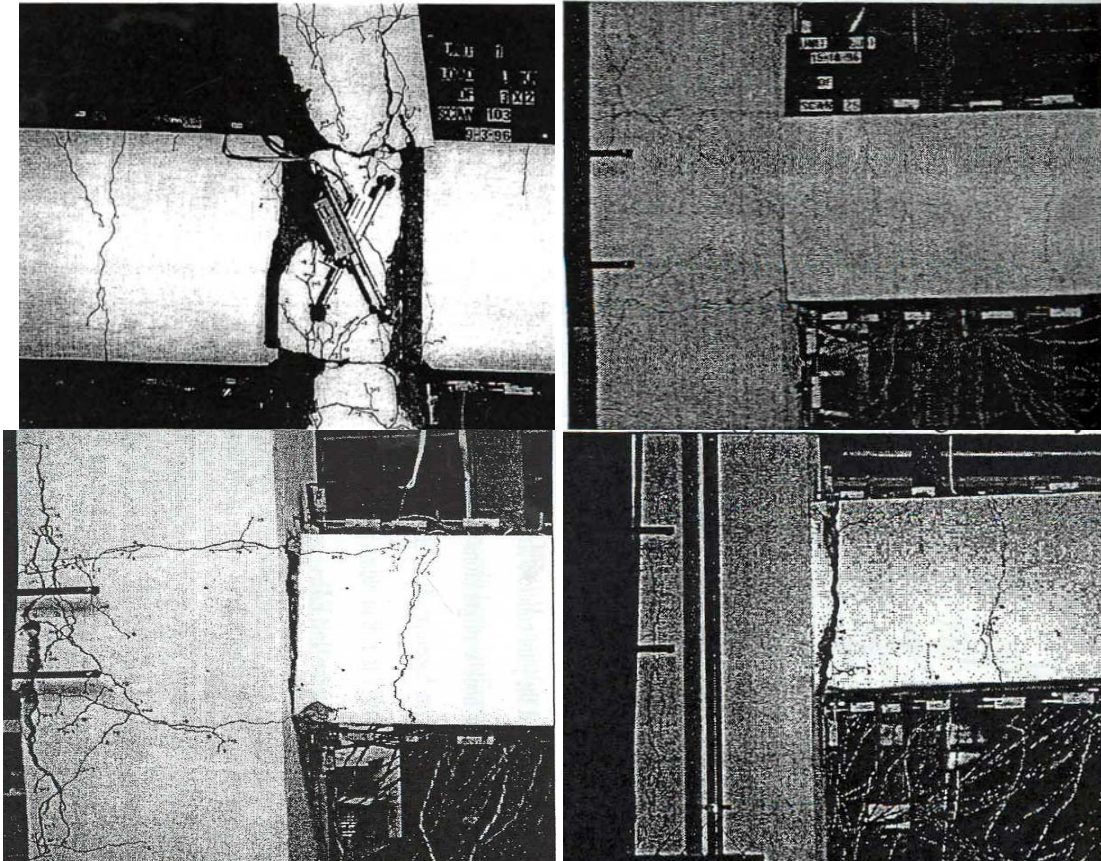


Figure 2.15 Damage observed, Liu et al. (2002)

2.3.5 Research by Pampanin et al. (2002)

Pampanin et al. (2002) carried a series of tests on existing reinforced concrete beam-column joint subassemblies and frame system with plain round bars as typical of (mainly) gravity load designed frame systems detailed according to the Italian construction practice of the 1950-1970s period. Two interior cruciform joints, two exterior knee-joints and two exterior tee-joints on 2/3 scale were tested under simulated seismic loading to get more information on the seismic behaviour of gravity load designed beam-column subassemblies. The tests were carried out at the University of Pavia, Italy. An example of specimen details and test results from this research is shown in Figs. 2.16 and 2.17. The level of the axial load was varied during the test as a function of the lateral load: $P = P_i + 1.44V$ where P_i is the tributary gravity axial load and V is the lateral load.

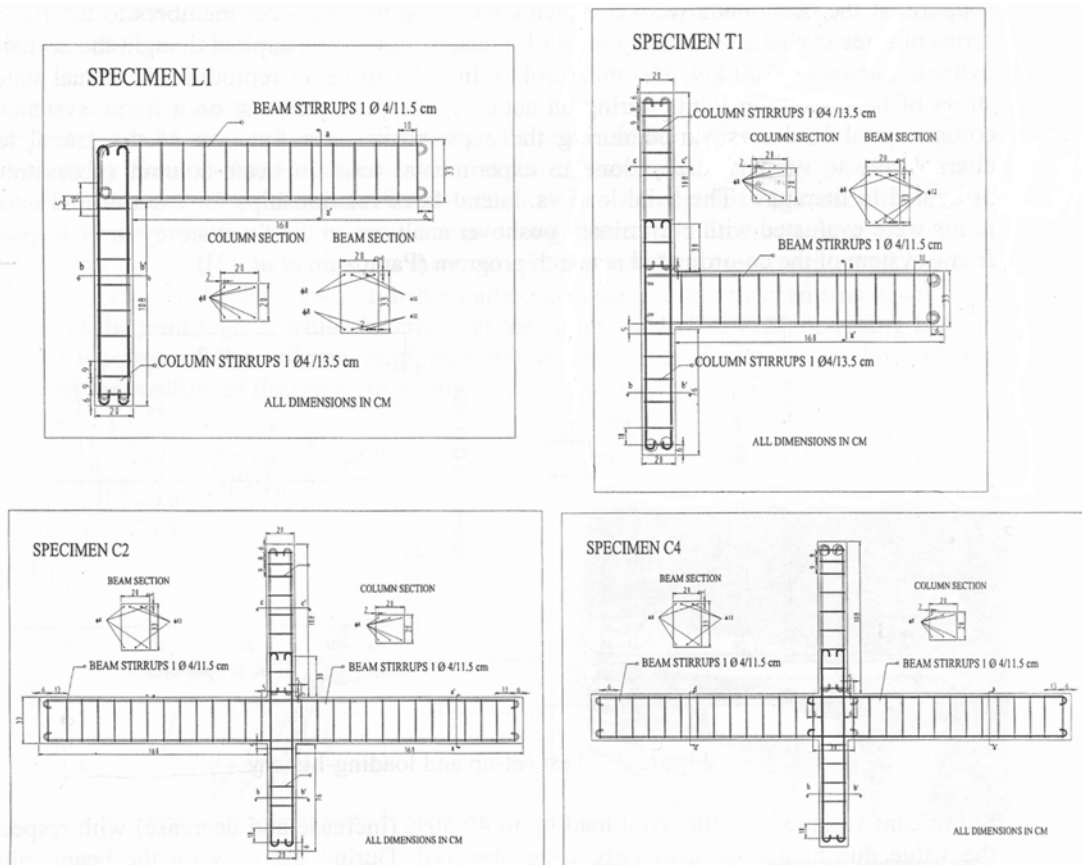
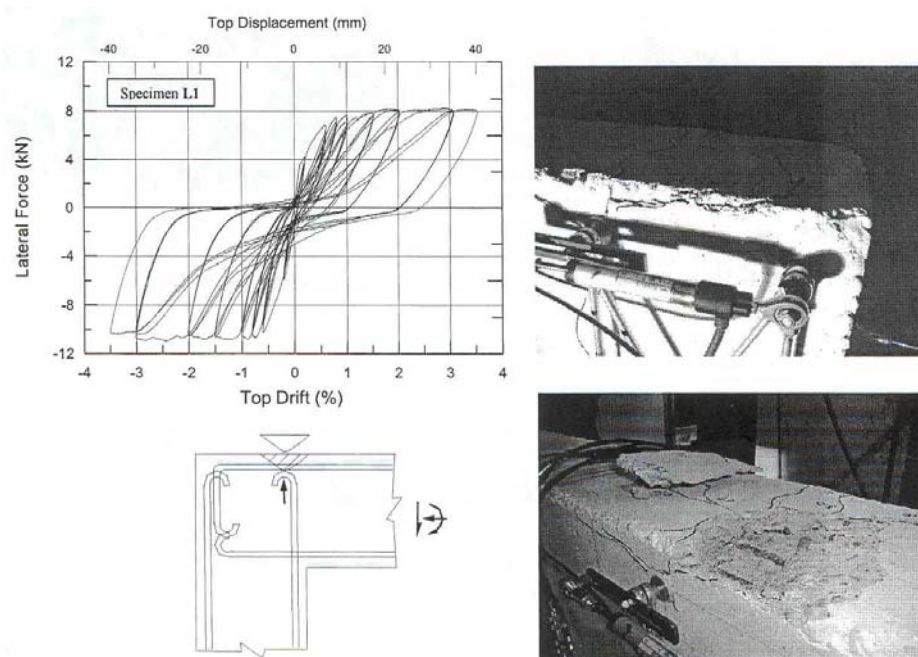
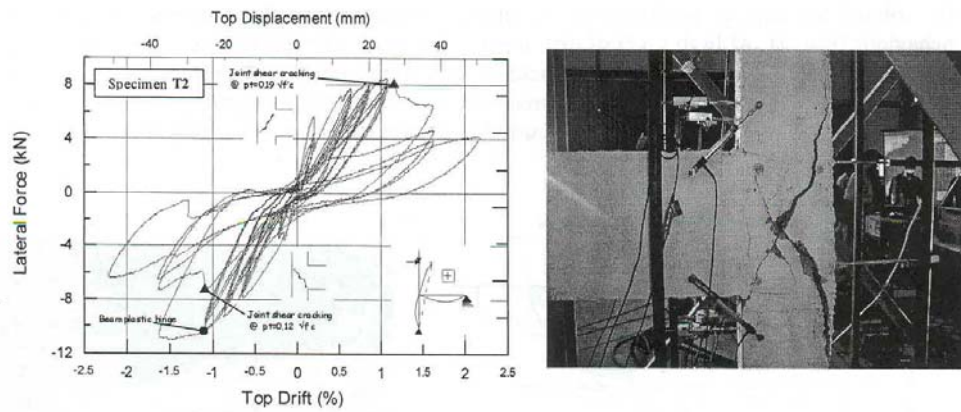


Figure 2.16 Specimens details, Pampanin et al. (2002)

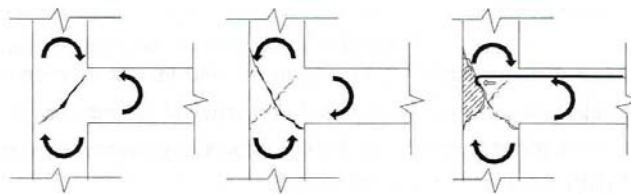


a) Corner joint

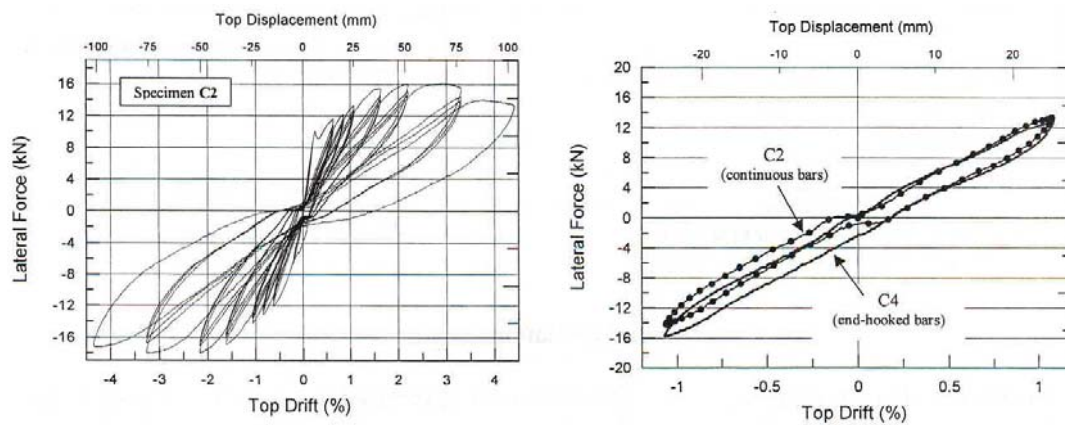
Figure 2.17 Damage observed and test results, Pampanin et al. (2002)



b) Tee joint



c) 'Concrete wedge' development



d) Interior joint

Figure 2.17 Damage observed and test results, Pampanin et al. (2002) (continued)

Exterior beam-column joint tests resulted in extensive joint shear damage in the joint panel zone, which would lead to a severe and critical reduction of gravity load capacity of the overall frame system. A critical discussion on the implication of joint damage and collapse on the overall behaviour of a frame system can be found in Calvi et al., (2002). The combination of hook-end anchorage with plain round bars can lead to a peculiar brittle mechanism consisting of the expulsion of a concrete wedge at the

outer side of the column due to the combined shear damage in the joint region and concentrated compression force at the end of the beam longitudinal bars.

Due to more favorable hierarchy of strength, the interior beam-column joint showed a quite displacement capacity, due to the formation of a flexural damage in the column which would act as a fuse for the joint, preserving it from excessive level of internal shear stresses and deformation.

The conclusions drawn from the research were:

1. In exterior beam-column joints, the use of plain round bars with end-hook anchorage can lead to brittle damage mechanisms after the first diagonal cracking occurred in the joint.
2. Relatively adequate deformation capacity can be provided from a combination of bar slip and low column reinforcement ratio as observed from the tests on knee-joints and interior joints. However, within a proper seismic assessment of the global frame system behaviour, the formation of plastic hinges on top and bottom of interior b-c joints could increase the chances to develop a soft-storey mechanism.
3. Minor differences in the anchorage solutions for the beam longitudinal reinforcement crossing the joint region in an interior beam-column unit showed an increase in the ability to deform without flexural strength reduction.

2.3.6 Research on Joint Subassemblies with Shallow (Wide) Beam

2.3.6.1 Research by Popov et al. (1992)

Popov et al. (1992) tested two interior beam-column joints with slab using deformed longitudinal bars. The specimens were at half-scale taken from a prototype 20-storey reinforced concrete building designed using ACI 318-89. The units consist of one interior narrow beam-column joint and one interior wide beam-column joint were tested under simulated seismic loading to investigate the behaviour of beams with some longitudinal reinforcement anchored outside the column core. Specimen detail used in this research is shown in Fig. 2.18. Constant axial load was applied on the top of the column to represent the gravity load.

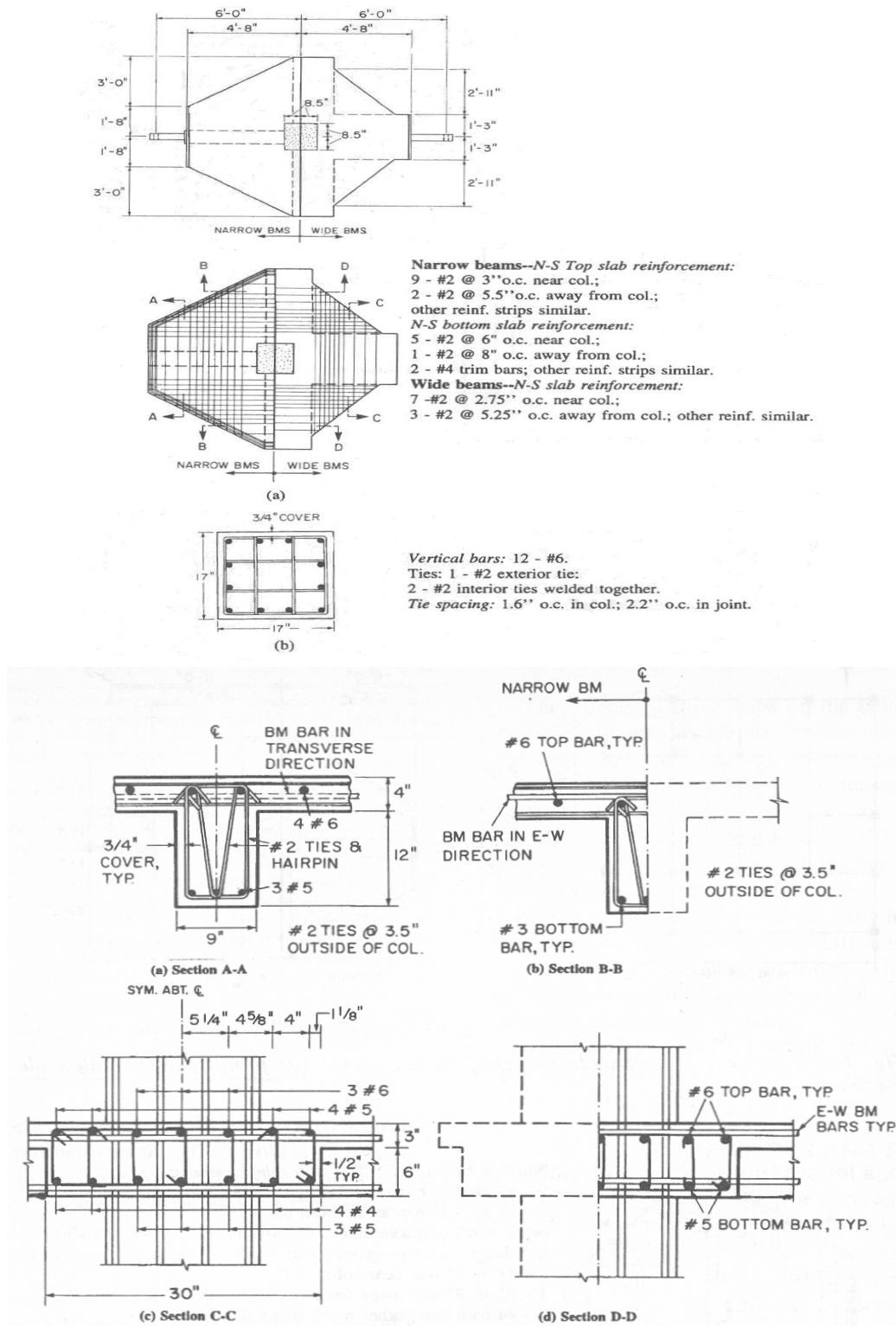


Figure 2.18 Specimens details, Popov et al. (1992)

The test results showed that the beam longitudinal reinforcing bars anchored outside the joint core can give a good contribution to the lateral resistance and provide sufficient energy dissipation. However, the good behaviour of the beam bars placed

outside of the columns might be due to the contribution of the large well-reinforced transverse beams.

2.3.6.2 Research by Gentry and Wight (1994)

Gentry and Wight (1994) performed a series of tests on four exterior beam-column joints using wide beams and deformed longitudinal bars, designed according to ACI 318-89. The specimens were $\frac{3}{4}$ -scale and tested under simulated seismic loading at the University of Michigan, USA. The objective of the tests was to provide rational provisions and limitations for the use of wide beam-column joints in seismic regions. Details of the specimens and test results from the research are shown in Figs. 2.19 and 2.20. Constant compressive axial load was applied to the column to rule out any tension in the column during testing.

The tests show that the stiffness and strength of the transverse beams can govern the behaviour of the exterior wide beam-column joints. Cracking in the transverse beam due to torsional moment reduces the moment strength of the connection because the anchorage of the longitudinal beam bars became ineffective.

The conclusions drawn from the tests were:

1. The limit on the width of wide beams was proposed to be: $b_w \leq b_c + 2h_c$, compared to the limit in ACI 318-89: $b_w \leq b_c + 1.5h_b$, where b_w is the width of the wide beam, b_c is the width of the column, h_c is the depth of the column and h_b is the depth of the wide beam.
2. The low flexural stiffness of the wide beams must be adequately increased in the design to ensure the structure can meet the lateral drift requirements from the code.
3. Slip of the exterior column bar may occur in wide beam-column connections, therefore it has to be controlled properly.

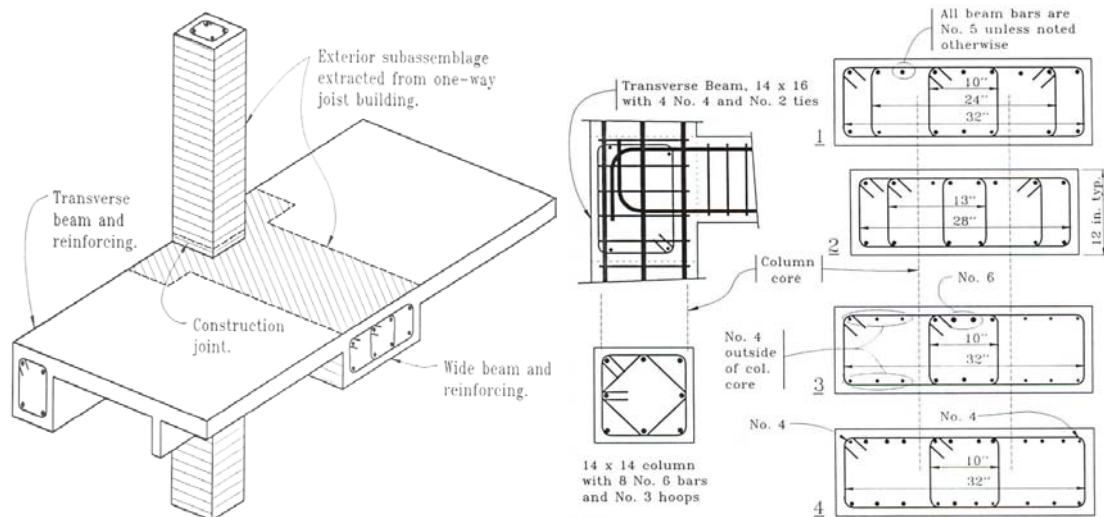


Figure 2.19 Specimens details, Gentry and Wight (1994)

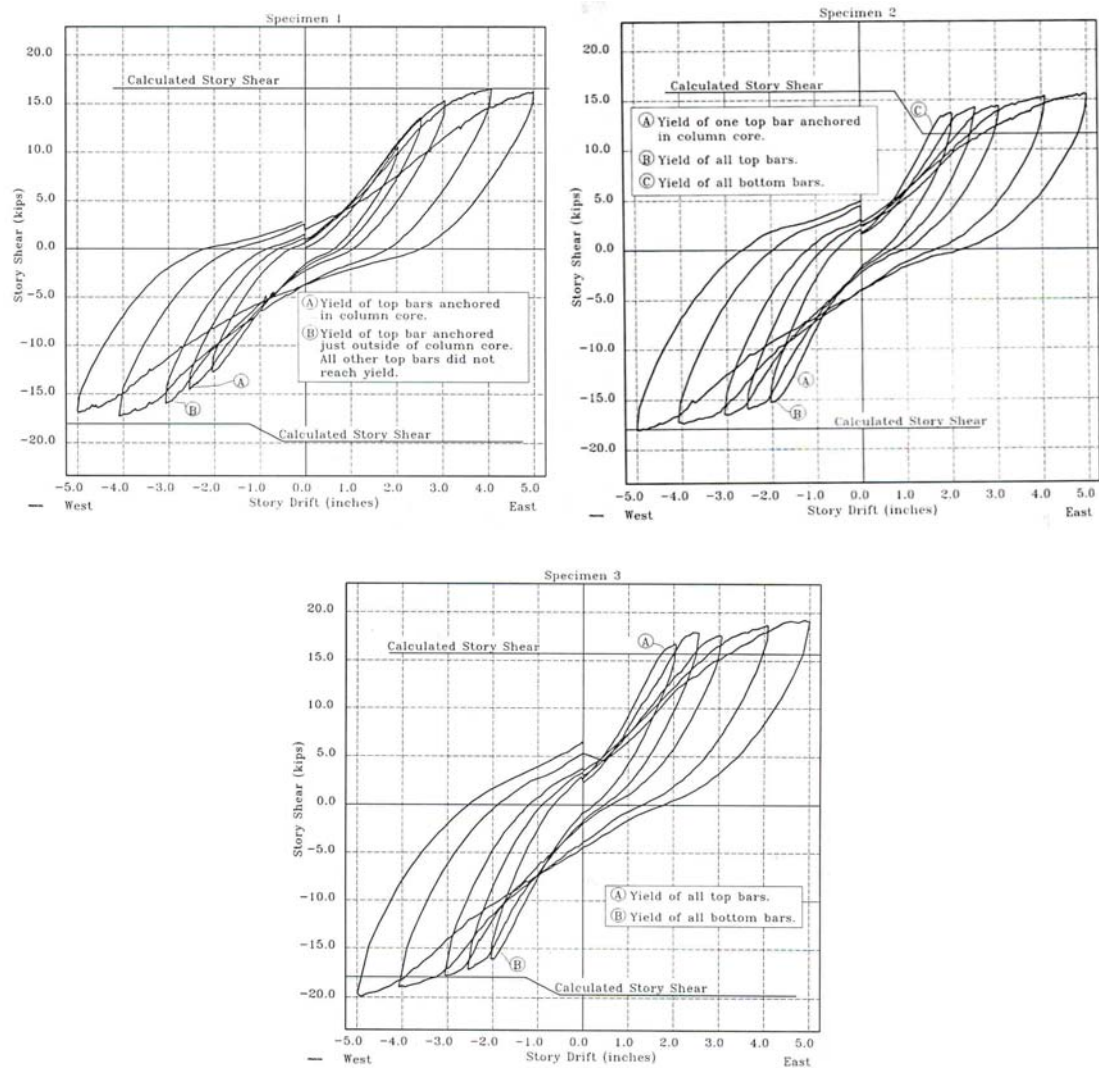


Figure 2.20 Lateral force versus drift of the specimens, Gentry and Wight (1994)

2.3.6.3 Research by Abdouka (2003)

Abdouka (2003) tested two exterior wide beam-column joint units with transverse beams using deformed longitudinal bars of reinforced concrete structure designed according to the current Australian Standard for Concrete Structures AS 3600-1994. The units were half scale models and tested under simulated seismic loading. The tests were carried out at the University of Melbourne, Australia. Figs. 2.21 and 2.22 show the details of the specimens along with the observed damage. Constant compression axial load of 300 kN was applied on the top column top during the test.

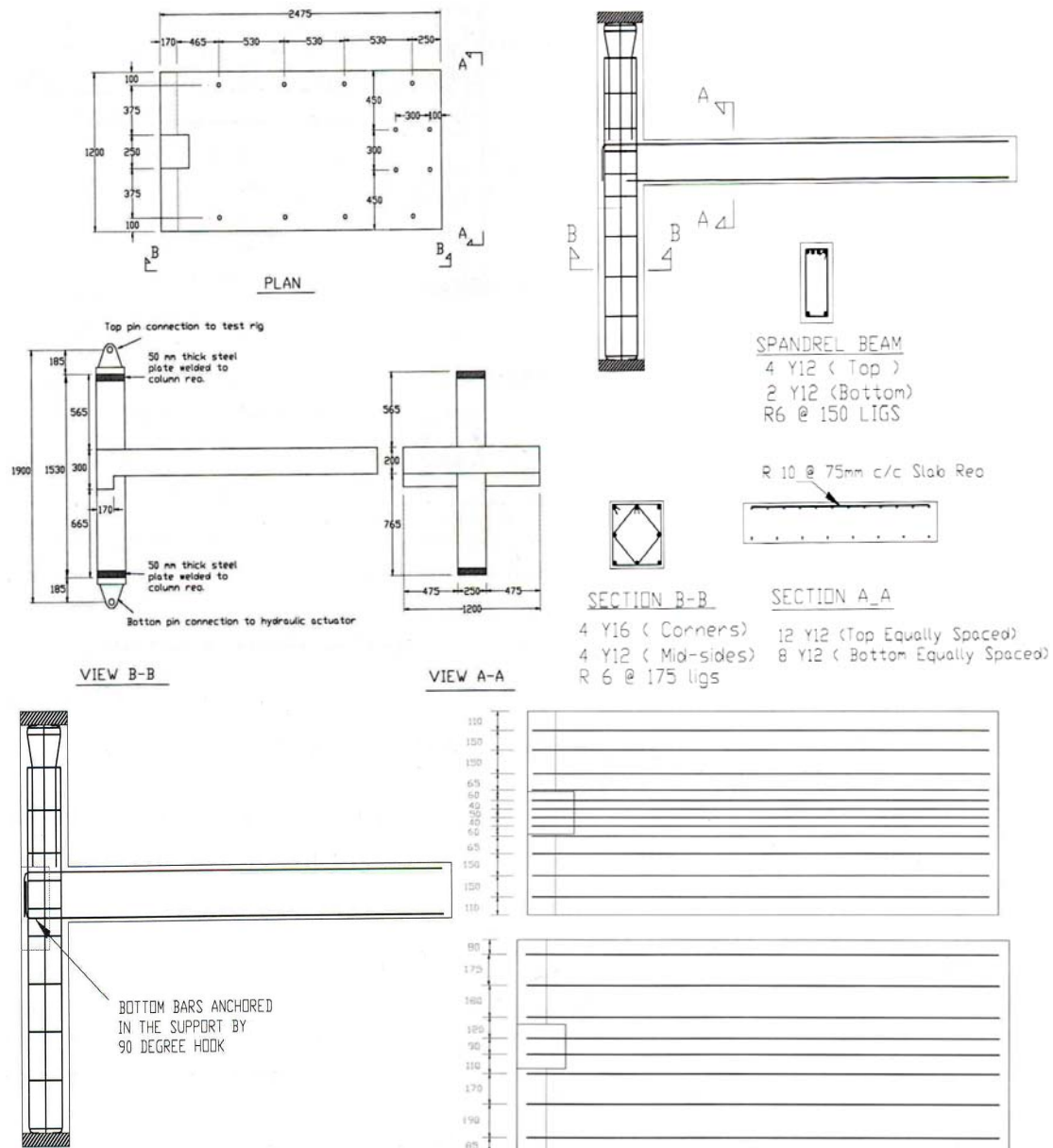


Figure 2.21 Specimens details, Abdouka (2003)

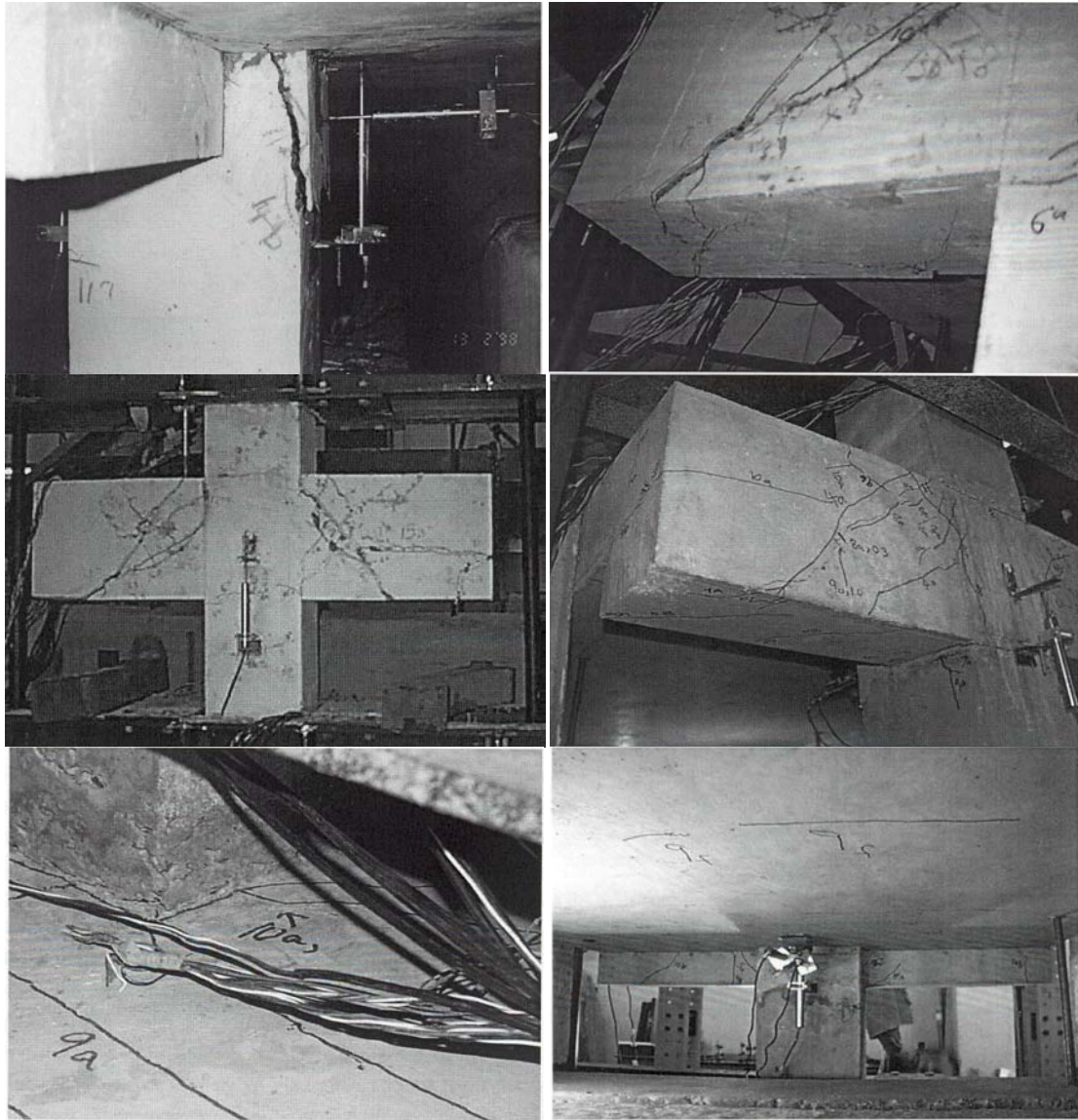


Figure 2.22 Damage observed, Abdouka (2003)

The behaviour of both units was considered very satisfactory in terms of displacement ductility. Unit EXT-2 performed better than Unit EXT-1 with a more evenly distributed cracking pattern and smaller crack width. Concrete spalling was only observed in the Unit EXT-1 and not in Unit EXT-2.

The conclusions drawn from the research were:

1. Wide beam-column joint subassemblies designed according to the Australian Standard for Concrete Structures AS 3600-1994 have acceptable performance under seismic loading with sufficient displacement ductility.
2. Reinforcement detailing used in Unit EXT-2 is highly recommended for exterior connection to improve the behaviour of the connection under seismic loading.

2.4 RELEVANT RESEARCH PROJECTS ON SPACE FRAME BEAM-COLUMN JOINT

The direction of attack of an earthquake ground motion is clearly likely to not be along the strong axis of the structure, thus leading to a 3-D behaviour of the full structure. In some older construction realities (i.e. Mediterranean countries) a typical geometrical and plan configuration would consist of frames running in one direction only and lightly reinforced slab in the orthogonal direction. In this case, plane frame tests (2-D) can provide a realistic representation of the seismic response of the whole building. However, when space frame systems are used as structural skeleton (maybe in combination with cast-in-situ floor system) a more adequate bi-directional testing protocol could provide more accurate information on the actual seismic behaviour.

However, in spite of the high number of space frames and particularly on the high seismic vulnerability of exterior corner beam-column joint observed during recent earthquake events, a relatively small number of experimental research investigation on as-built under-designed space frame beam-column joints (particularly exterior) have been carried out in the past years. A summary of some major contribution is herein reported and reviewed.

2.4.1 Research by Leon and Jirsa (1986)

Leon and Jirsa (1986) performed a series of tests on plane and space frame behaviour beam-column subassemblies. A total of twelve interior beam-column joint units (eleven without slab and one with slab) and two exterior beam-column joint units (with and without slab) were tested under simulated seismic loading. The units were full-scaled and represented a properly seismically designed beam-column joint (weak beam, strong column mechanism) and thus adopting deformed longitudinal bars. The objective of the tests was to investigate the effect of biaxial loading, beam reinforcement size, beam geometry and floor slabs on the seismic behaviour of b-c joint. Tests were carried out at the University of Texas, Austin, USA. Details of the specimens and test results from this research are shown in Figs. 2.23 and 2.24. Constant compressive axial load was applied in most of the specimens during the test.

Test	Reinforcement			Mom. Ratio (4)	Load	Variable
	Column (1)	Beam Neg. (2)	Beam Pos. (3)			
BCJ1	12 # 9	3 #10	3 # 8	1.00	UC	UC loading
BCJ2	12 # 9	3 #10	3 # 8	1.00	BA	BA loading
BCJ3	12 # 9	3 #10	3 # 8	0.77	BS	BS loading
BCJ4	12 # 9	2 #10	2 # 8	1.19	BS	Bar number
BCJ5	12 # 9	3 # 8	3 # 6	1.27	BS	Bar size
BCJ6	12 # 9	3 # 8	3 # 6	1.28	MS	MS loading
BCJ7	12 # 9	3 # 8	3 # 6	1.28	BS	Joint rein.
BCJ8	12 # 9	3 # 8	3 # 6	1.26	BS	No axial load
BCJ9	12 # 9	3 # 8	3 # 6	1.16	BS	Slab
BCJ9A	12 # 9	3 # 8	3 # 6	1.26	BS	Slab
BCJ10	12 # 9	3 # 8	3 # 6	1.13	BS	Wide beams
BCJ11	8 #11	2 #10	2 # 8	1.26	BS	Nar. beams
BCJ12	12 # 9	3 # 8	3 # 6	1.13	BS	Wide beams
BCJ13	12 # 9	3 # 8	3 # 6	1.38	BS	Exterior
BCJ14	12 # 9	3 # 8	3 # 6	1.38	BS	Ext. w/slab

(1) All columns 15" by 15".
 (2) All beams 18" by 13", except BCJ11 (8.75" x 18") and BCJ12 (18" x 18").
 (3) All specimens had 2 #4 joint ties, except BCJ7 which had 10 joint ties.
 (4) Column moment vs. beam capacities utilizing actual material properties at yield.

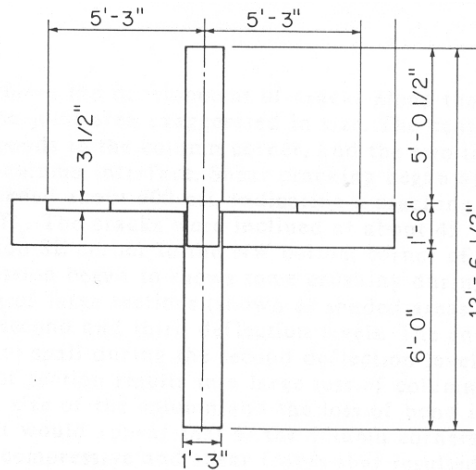


Figure 2.23 Specimens details, Leon and Jirsa (1986)

Test	Maximum shear (biaxial, kips)			Concrete Strength (psi)	Max. Shear $\frac{1}{f'_c b d}$
	1st Level	2nd Level	3rd Level		
BCJ1	324	363	327	4.90	28.0
BCJ2	372	397	330	4.25	33.0
BCJ3	316	342	286	4.50	27.6
BCJ4	351	346	283	4.25	29.1
BCJ5	318	303	254	4.20	27.7
BCJ6	307	316	312	4.40	25.8
BCJ7	322	328	287	4.85	25.5
BCJ8	302	305	264	4.25	25.1
BCJ9	372	379	315	4.40	30.5
BCJ11	257	264	180	4.30	21.3
BCJ12	335	339	286	4.50	27.3
BCJ13	206	166	172	4.40	16.4
BCJ14	290	276	227	4.80	21.7

Figure 2.24 Test result, Leon and Jirsa (1986)

From the test results, the conclusions drawn are:

1. The biaxial loading has a big influence on the column performance but no significant effect on joint shear capacity, herein properly designed and detailed with transverse reinforcement.
2. The beam reinforcement size is not a critical aspect in determining the bond strength.
3. Transverse reinforcement used in the joint provides additional confinement in the joint panel area and will influence the overall mechanism of the unit, but does not improve the global moment capacity, primarily governed by flexural mechanism in the beam.
4. Axial load on the column gives additional confinement to the column preventing the cracks from happening. However, the effect of axial load on the joint strength seems not be significant. Actually such an effect could not be appropriately appreciated since the damage and inelastic behaviour is concentrated in the adjacent beam and column.
5. The presence of the floor slab reduces, by flange effects in the beam, the column-to-beam-moment capacity ratio increasing the possibility of formation of a column plastic hinge and forming a soft storey mechanism. On the other hand, the floor slab provides additional confinement to the joint region, reducing the extent of damage.
6. The dimension of the transverse beam influence the strength degradation curve by providing joint confinement and preventing early cracking or spalling that can lead to extensive loss in strength.
7. Exterior joints are confirmed to be inherently more vulnerable than interior joints under seismic loading. In addition to a less efficient compression strut mechanism, in fact, the anchorage of beam bars in the joint can cause, by bond deterioration, damage of the concrete cover, with subsequent spalling and partial loss of anti-buckling protection to the column longitudinal bars.

2.4.2 Research by Cheung et al. (1991)

Cheung et al. (1991) performed a series of tests on full scale plane and space frame behaviour beam-column joint units with slab, designed according to the New Zealand design code (NZS 3101:1982). Deformed longitudinal bars were thus used.

One plane frame interior beam-column-slab joint, one space frame interior beam-column-slab joint and one space frame exterior beam-column-slab joint unit were tested under simulated seismic loading. The objectives of the tests were to investigate the behaviour of the subassemblies under seismic loading and the effects of biaxial loading, transverse beam presence and floor slab. Tests were carried out at the University of Canterbury, Christchurch, New Zealand. Figs. 2.25 and 2.26 show the specimen details and damage observed in this research.

The behaviour of all units was satisfactory and complied with the performance criteria in the New Zealand loading code. Plastic hinges occurred in the beams and columns during the inelastic range loading. Few diagonal cracks occurred in the joint core regions without however causing strength loss.

From the test results, the conclusions drawn are:

1. The floor slab or the presence of the transverse beam seemed not to provide confinement to the joint cores during biaxial seismic loading whereby the performance would have been improved.
2. The joint regions were sufficiently reinforced with stirrups to prevent extensive level of damage and inelastic shear deformation to occur. However, the contribution of joint deformation was up to 26% of the total interstorey drift.
3. The strength and stiffness of the units reduced if loaded biaxially mainly due to the change of slab reinforcement contribution to the beam flexural strength.

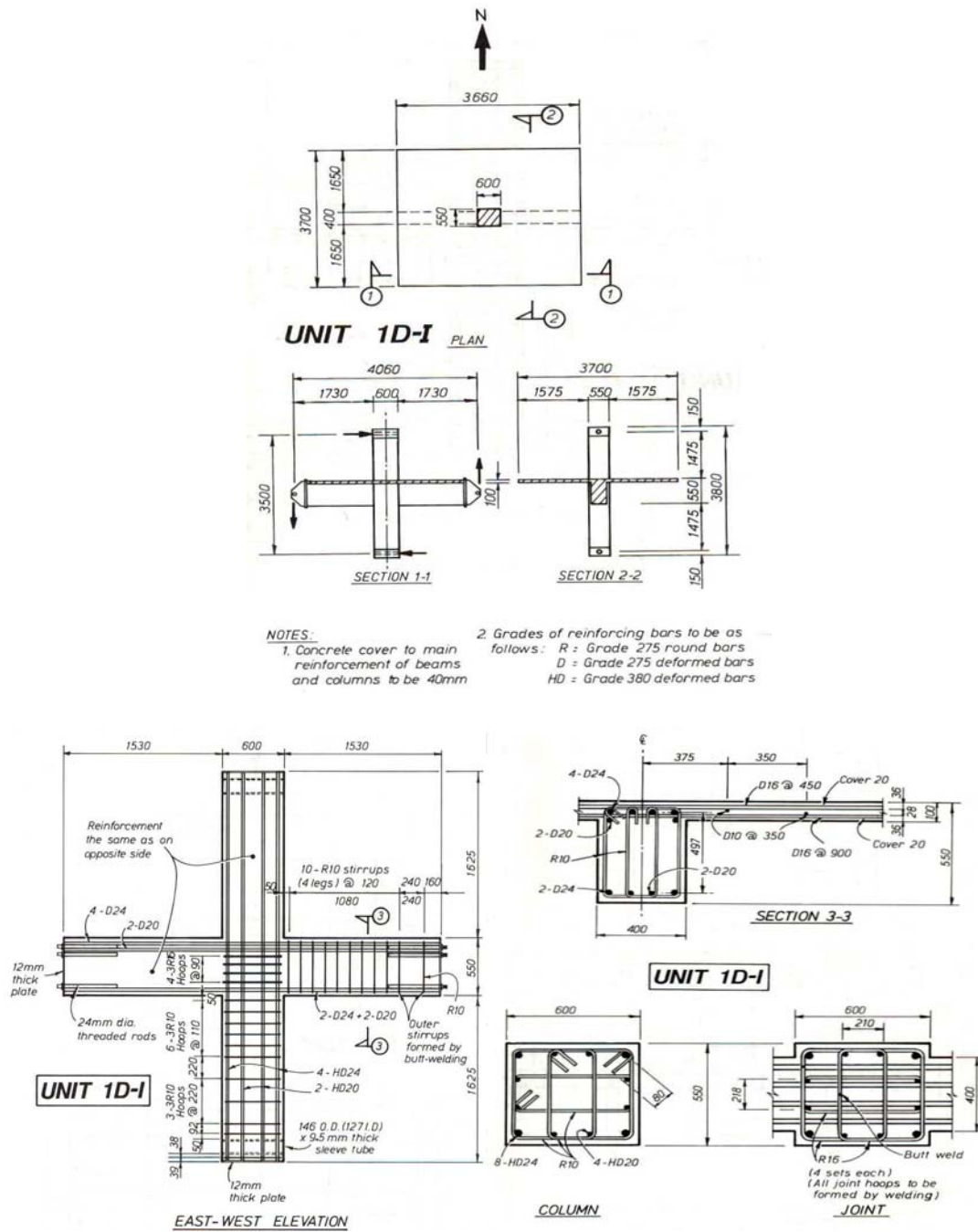
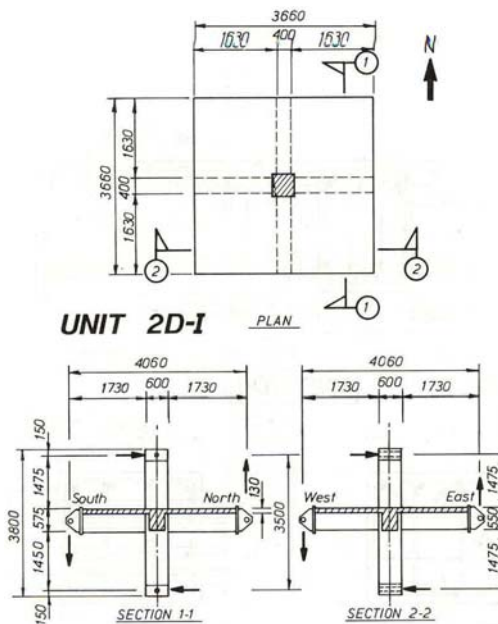


Figure 2.25 Specimens details, Cheung et al. (1991)



NOTES :

1. Unless otherwise noted
concrete cover to main
reinforcement to be as follows:
40mm for beams & columns
20mm for slabs
2. Grades of reinforcing to
be as follows:
R : Grade 275 round bars
D : Grade 275 deformed bars
HD : Grade 380 deformed bars

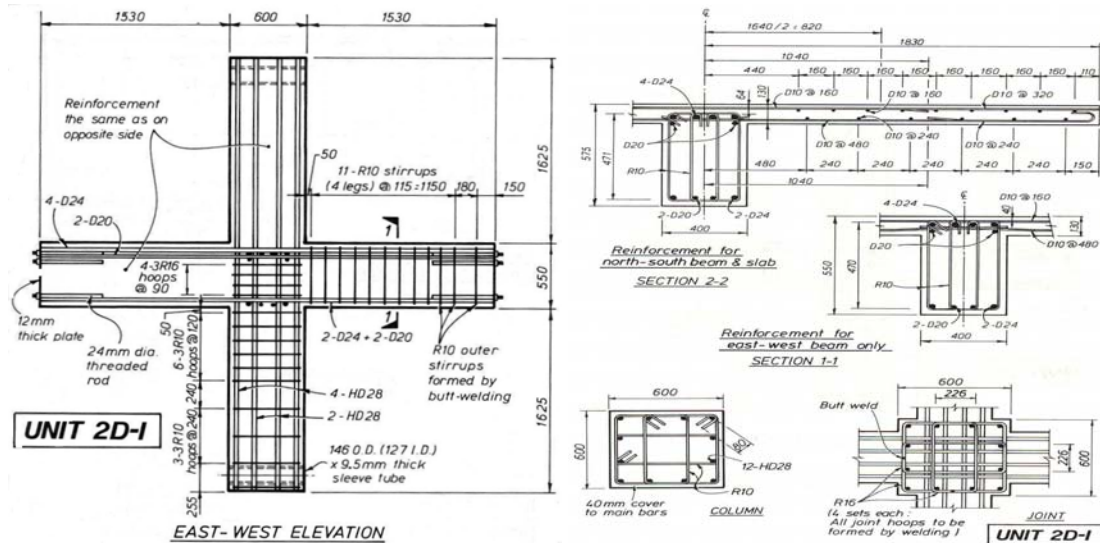
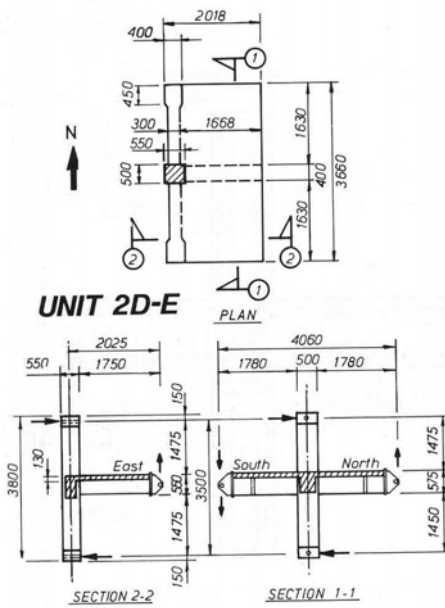


Figure 2.25 Specimens details, Cheung et al. (1991) (continued)



NOTES:

1. Unless otherwise noted concrete cover to main reinforcement to be as follows :

- 40mm for beams & columns
- 20mm for slabs

2 Grade of reinforcing bars
to be as follows :
R - Grade 275 round bars
D = Grade 275 deformed bars
HD = Grade 380 deformed bars

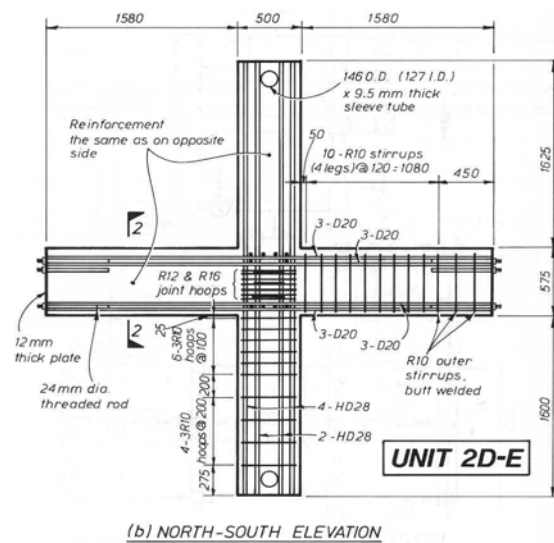


Figure 2.25 Specimens details, Cheung et al. (1991) (continued)

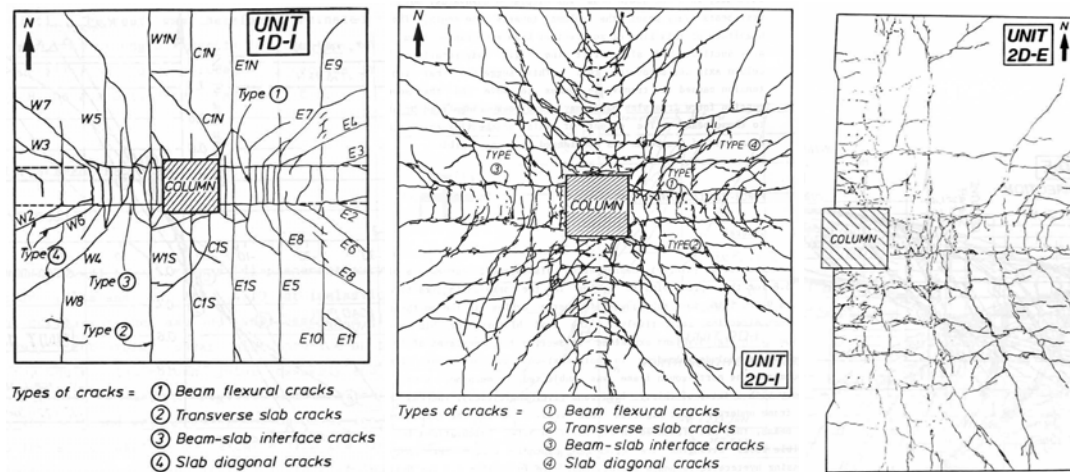


Figure 2.26 Damage observed, Cheung et al. (1991)

2.4.3 Research by Bolong and Yuzhou (1991)

Bolong and Yuzhou (1991) performed a series of tests on plane and space frame r. c. beam-column joint units. One plane frame exterior beam-column joint, one space frame exterior beam-column joint and one space frame exterior beam-column-slab joint units were tested under simulated seismic loading. The units were full-scaled units taken from the design of Beijing Hospital of Traditional Chinese Medicine and deformed longitudinal bars were used. The objective of the tests was to investigate the behaviour of beam-column joints designed according to the China building code. Tests were done at the Tongji University, Shanghai, China. Figs. 2.27 and 2.28 show the specimens details and damage observed from this research. Constant compressive axial load was applied on the column top during the test.

The performance of all units was satisfactory when compared with the design requirements. Cracks occurred mostly in the beam region, followed by joint and the slab (only for Unit J6 with slab). The failure mechanisms of all specimens were quite similar.

From the test results, the conclusions drawn are:

1. For the exterior joint, the transverse beams are also subjected to the torque action, not only subjected to the bi-directional bending moment and shear. Therefore the longitudinal reinforcement area in the joint and transverse beam should be increased.

2. The presence of the slab has a significant influence of the stiffness and strength of the beam. It can revert the hierarchy of strength between beam and column; therefore, when similar cast-in-situ floor configurations are adopted, the effect of the slab should be appropriately taken into account in the capacity design process.

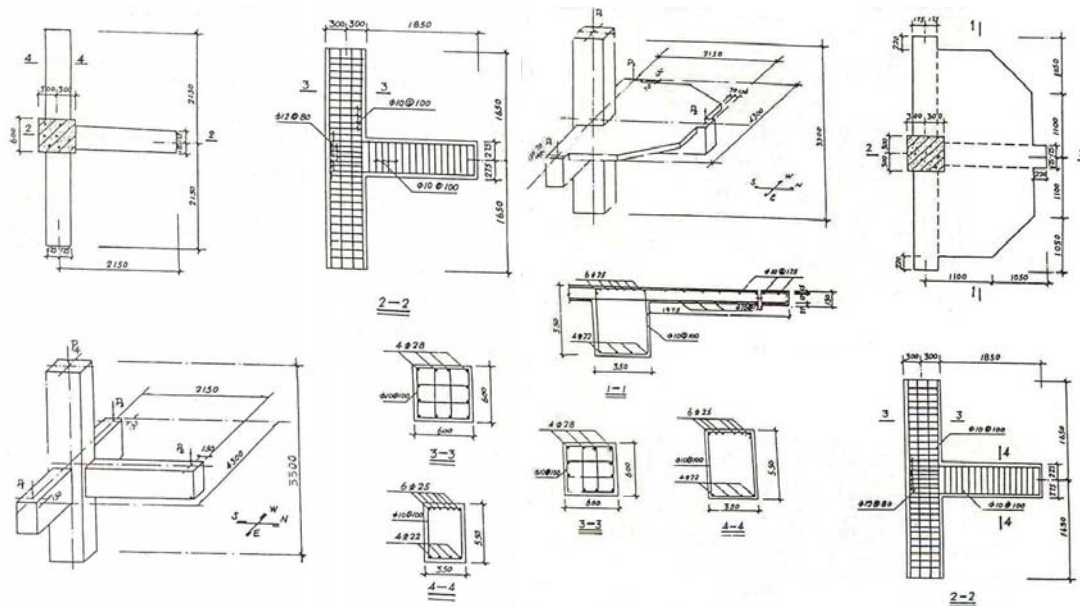


Figure 2.27 Specimens details, Bolong and Yuzhou (1991)

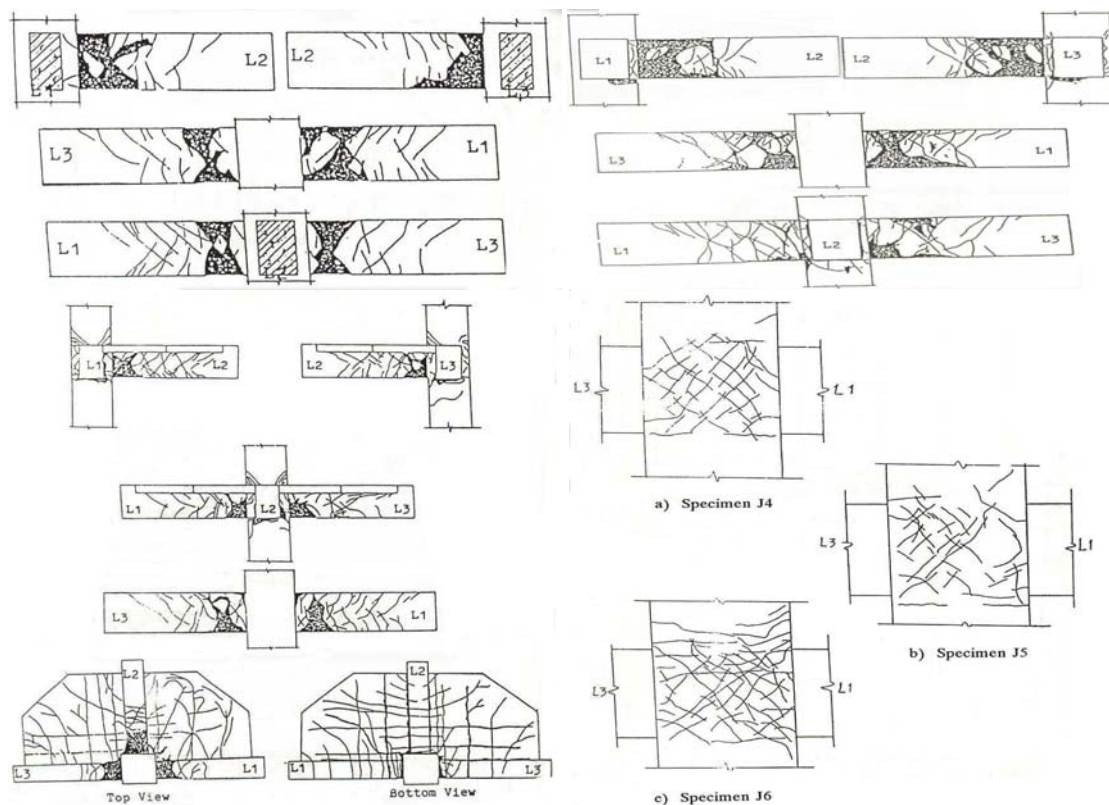


Figure 2.28 Damage observed, Bolong and Yuzhou (1991)

2.4.4 Research by Kurose et al. (1991)

Kurose et al. (1991) performed a series of test on plane and space frame reinforced concrete slab-beam-column connections. One plane frame interior beam column joint with slab, one space frame slab-beam-column and one space frame exterior slab-beam-column units using deformed longitudinal bars were tested under simulated seismic loading. The units were full-scaled units and designed according to ACI 352 R-85. The objective of the tests was to evaluate the behaviour of the slab-beam-column connections designed according to the ACI 352 R-85. Tests were carried out at the University of Texas, Austin, USA. Figs. 2.29 and 2.30 show the specimens details and the damage observed from this research. No axial load was applied on the column during the test.

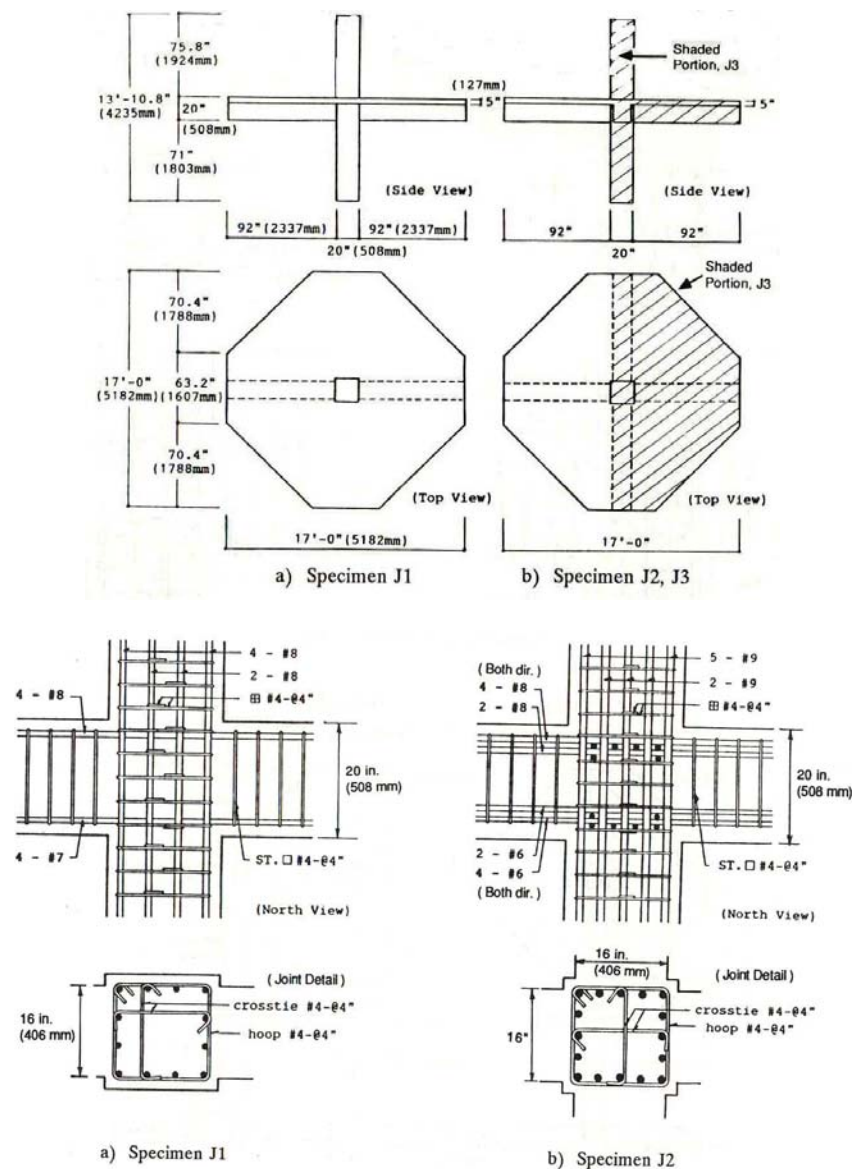


Figure 2.29 Specimens details, Kurose et al. (1991)

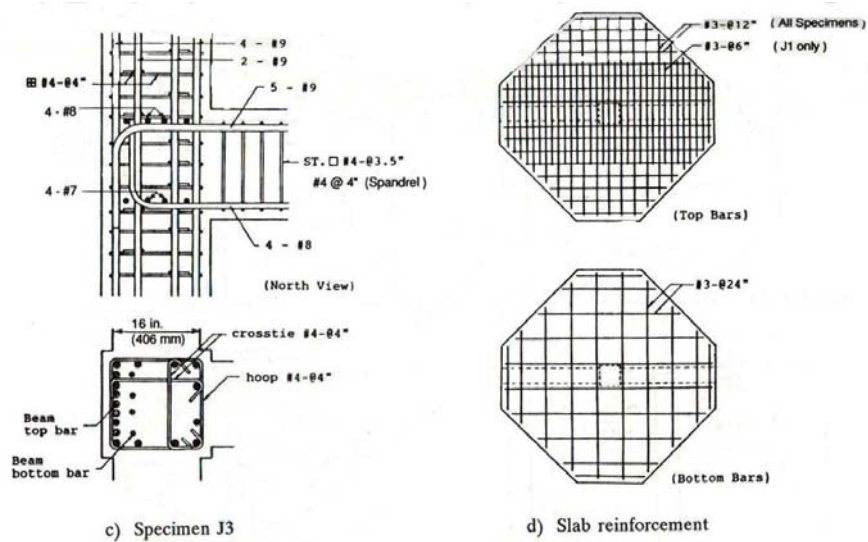


Figure 2.29 Specimens details, Kurose et al. (1991) (continued)

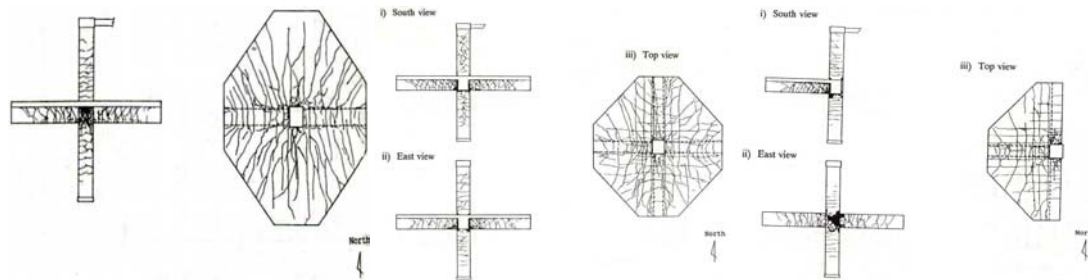


Figure 2.30 Damage observed, Kurose et al. (1991)

Flexural cracks occurred in the slab, beams and column in all the specimens. Diagonal cracking in the joint were observed in Specimen J1 and Specimen J3.

Conclusions drawn from the results are:

1. All specimens suffered a joint shear failure at 4% drift, after the formation of plastic hinges in the beam and consequent development of ductility demand. Specimen J3 also had anchorage distress in top beam bars at the same stage.
2. All specimens reached higher strength than predicted based on a pure beam-hinge mechanism.
3. Loading in one direction during bidirectional load cycles resulted in reduced story shear in the orthogonal direction.
4. The unidirectional story shear levels measured for all specimens were higher than those calculated to correspond to a joint shear failure.

5. Bidirectional strengths for Specimens J2 and J3 exceeded the unidirectional strengths.

2.4.5 Research by Owada (2000)

Owada (2000) tested one plane frame interior beam-column joint and one space frame interior beam-column joint. The units were one-quarter scaled using deformed longitudinal bars and tested under simulated seismic loading. The objective of the test was to investigate the three-dimensional behaviour of the interior beam-column joint. Details of the specimens and test program used in this research are shown in Figs. 2.31 and 2.32. Constant compressive axial load of 10 kN was applied on the column during the test.

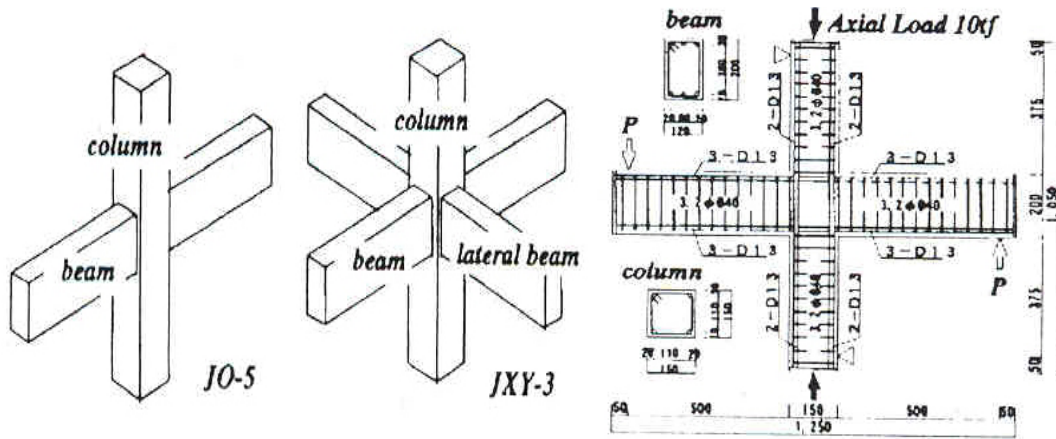


Figure 2.31 Specimens details, Owada (2000)

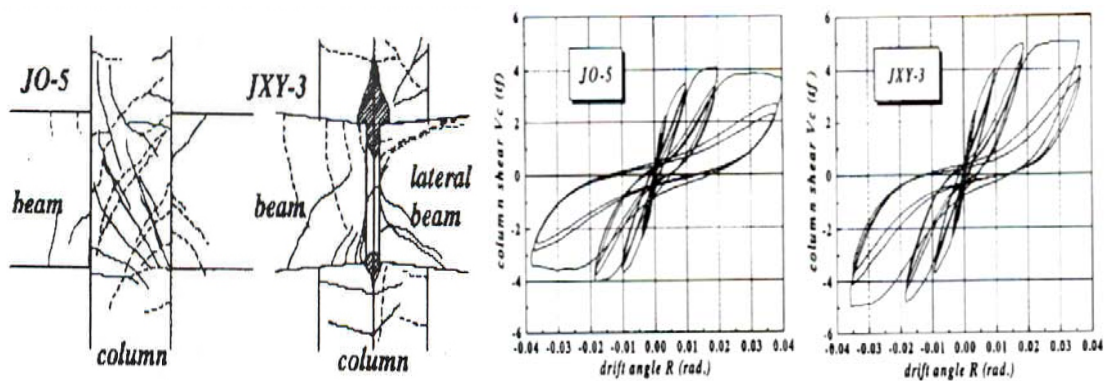


Figure 2.32 Test result and damage observed, Owada (2000)

Unit JO5 had diagonal shear cracks in the joint panel area at the first loading cycle and the width was extending during testing leading to concrete crushing and spalling

at the end of test. Joint failure occurred for Unit JO5 without any column or beam yielding. Unit JXY-3 had shear cracks on the sides of all four beams, however the width is smaller when compared to Unit JO5. For Unit JXY-3 the joint failure occurred after the column yielding.

From the test results, the conclusion drawn was that the lateral beams in the space frame beam-column joint subassembly increases the confinement of the joint preventing it from early failure.

2.5 ANALYTICAL MODELING DEVELOPMENT

There are a large number of methods for analyzing the seismic behaviour of existing reinforced beam-column joints ranging from simplified empirical approaches to complex finite element models. A good approach should take into account all parameters to model the behaviour as realistically as possible. However, the closer a model is to the real behaviour, the more complex it is. An ideal model will be a compromise between accuracy and simplicity. The development of the beam-column joint modeling is discussed here.

2.5.1 Multi-Spring Models

Some models using multi-spring/multi-node to simulate the behaviour of beam-column joint element have been proposed recently (Elmorsi, 2000, Youssef and Ghobarah, 2001, Lowes and Altoontash, 2003). The spring/node elements were used to model the joint deformation taking into account some factors such as bond slip and concrete crushing.

Elmorsi et al. (2000) proposed a model to simulate the behaviour of a beam-column joint element under cyclic loading. The joint panel is represented by a 12-node inelastic plane stress element. Inelastic truss elements are used to model the beam flexural reinforcement in the joint panel. Bond slip relationship between concrete and reinforcing steel is represented by using bond-slip contact element. A finite element method was used first to model the bond-slip behaviour. Fig. 2.33 shows the proposed model with detail on the bond slip relationship model.

The model works well in analyzing the beam-column joint behaviour with bond-slip of the beam flexural reinforcement. However, further calibration has to be done to find the ideal parameters used for this model.

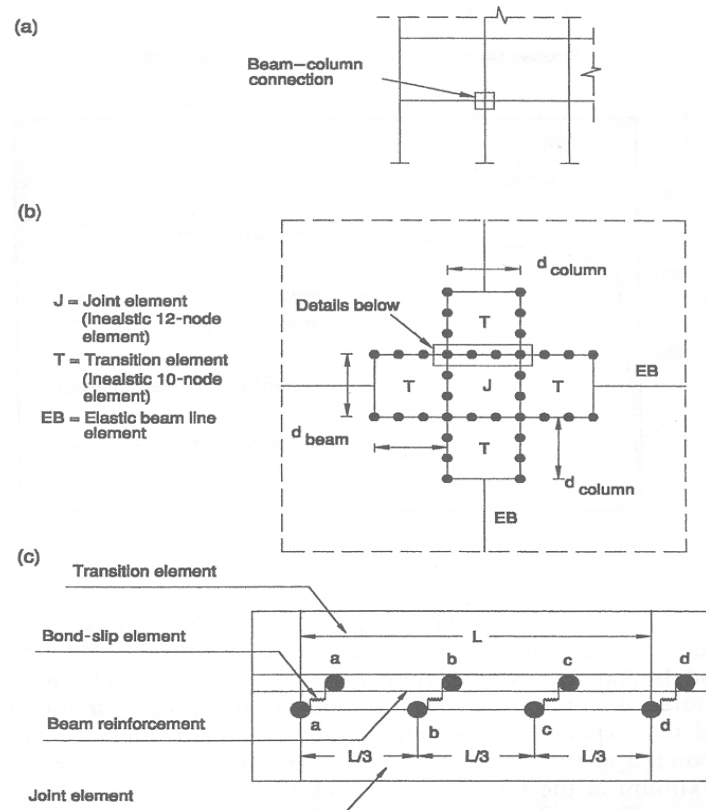


Figure 2.33 Proposed model by Elmorsi et al. (2000)

Youssef and Ghobarah (2001) proposed a model of beam-column joint that can take into account the contribution of shear and bond slip to the joint deformation. Twenty six springs were used to model the joint deformation, as shown in Fig. 2.34. Four rigid members used to model the joint region and the members attached to the joint are modeled using elastic elements. The connection between the joint and the members idealize the bond slip and concrete crushing by using three concrete springs and three steel springs. The springs represent the stiffness of the steel and concrete.

The steel spring models the behaviour of the steel bars which idealizes the relationship between the force in the steel bars and the bond slip. Relationships between the axial force-displacement of an identified concrete strut are modeled by the concrete spring. And finally, the shear spring models the shear force-displacement behaviour of the joint.

The proposed model gives a satisfactory representation of the behaviour of the beam-column joint, unfortunately the number of parameters that have to be calculated for the input discourages people from using the model.

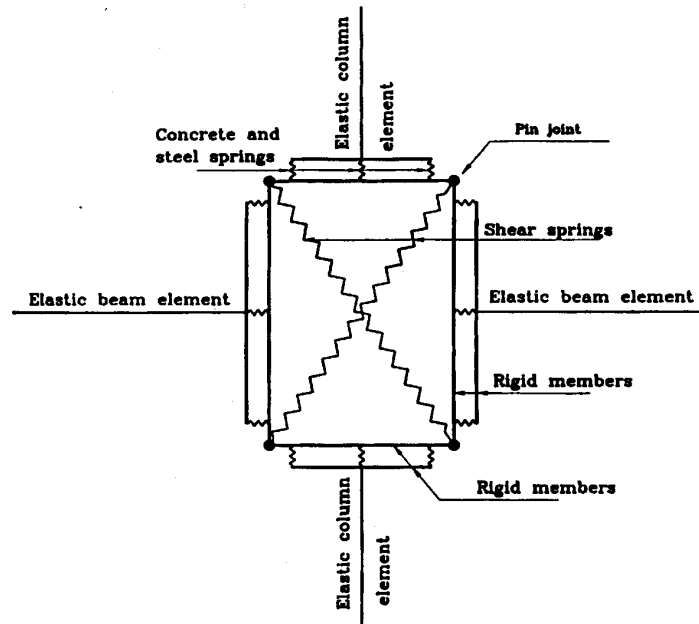


Figure 2.34 Proposed model by Youssef and Ghobarah (2001)

Lowes and Altoontash (2003) proposed a model to simulate a reinforced concrete beam-column joint behaviour as shown in Fig. 2.35. Two translation springs and one rotational spring are used to define the element displacement field at the every perimeter of the joint. The bar slip is modeled by the translation springs while the shear deformation of the joint is modeled by the rotational springs. This model works well to represent the basic characteristic of joint response under shear demands.

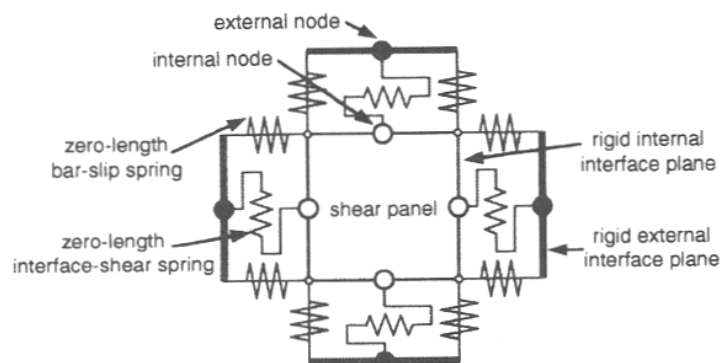


Figure 2.35 Proposed model by Lowes and Altoontash (2003)

2.5.2 Finite Element Models

Finite Element Method (FEM) has been well-known as one of the powerful and reliable tool for evaluating the as-built structures and designing new structures. One of the advantages of FEM is that it can be used to model structure members accurately. Many FEM models have been proposed, ranging from analyzing the behaviour of the total structure (i.e. Kwak and Filippou, 1990), the members (i.e. Ngo and Scordelis, 1967, Hoehler and Ozbolt, 2001) to the bond relationship (i.e. Monti et al., 1993, Lettow et al., 2004). However, due to the large amount and complexity of the analysis that have to be done to obtain the good modeling, this method is not commonly used.

2.2.6 Fiber Models

In this method, the element is divided into longitudinal fibers which relation with each other is derived by the integration of the response of the fibers. This model is commonly used to simulate the behaviour of members like beams or columns. Some researches have been done in using fiber model. (Taucer et al., 1991, Zeris and Mahin, 1991, Kaba and Mahin, 1994). The model usually requires a large number of integration and matrix operations which discourages people from using it.

2.2.7 Simplified Model

Pampanin et al. proposed a model to simulate the behaviour of a reinforced concrete beam-column joint, which takes into account the joint strength. A rotational spring is used to represent the joint behaviour both in the linear and the non-linear range. The linkage between the joint panel and the beam and column element are modeled by rigid element. The moment-rotation relationship of the spring is derived from the principal tensile stress versus shear deformation relationship. Figure 2.36 shows the reinforced concrete beam-column joint model proposed by Pampanin et al. (2003). Unfortunately, this model does not allow the effect of varying axial load to the joint strength.

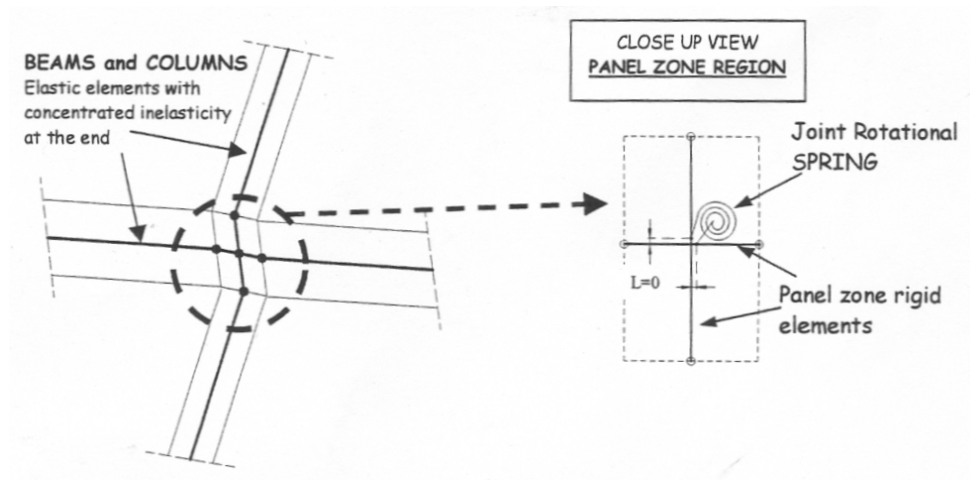


Figure 2.36 Proposed model by Pampanin et al. (2003)

2.6 ANALYTICAL MODEL

A simple yet reasonably accurate model is proposed to model the behaviour of reinforced concrete beam-column joint. The basic principal and assumption are similar to the model proposed by Pampanin et al. (2003). The model can take into account the contribution of the axial load to the joint strength. Details of the model, including the basic assumptions and principal are explained.

2.6.1 Basic Approach

One of the ideal method which lies in the middle ground between accuracy and simplicity is the lumped plasticity approach. Preliminary analysis is used to determine the parts of members which are likely to experience plastic deformation and only those areas will be modeled as plastic regions later.

The beam column joint modeled in this research has three areas of lumped plasticity: column plastic hinge region, beam plastic hinge region and shear hinge in the joint. The other parts of the members are modeled as linear elastic elements, called the Giberson one component beam model as shown in Fig. 2.37. Standard bending theory is used to model the elastic region, while for the plastic region a more empirical relationship has to be used.

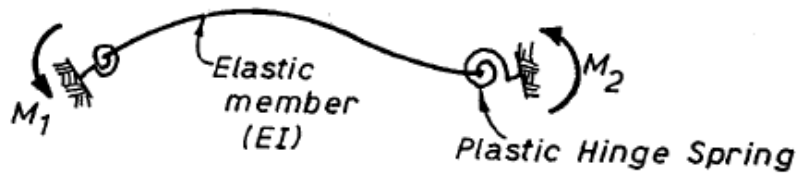


Figure 2.37 Giberson one component beam, Carr (2004)

2.6.2 Joint Deformation

It is assumed in the model that the joints suffer pure shear distortion therefore only the joint shear deformation is concerned. Based on the assumption, the opposite faces of the joint will always remain parallel, so the columns and the beams remain parallel to each other as well as shown in Fig. 2.38.

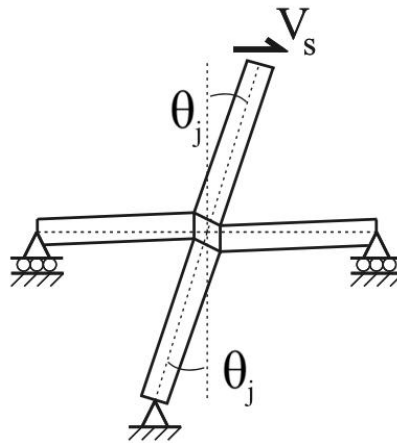


Figure 2.38 Joint shear deformation

2.6.3 Joint Moment-Rotation Relationship

To simplify the complex behaviour of the joint, two parameters are taken to illustrate the joint behaviour, which are joint principal tensile stress and rotation. The principal tensile stress is chosen instead of the horizontal shear stress because it can take into account the effect of axial load on the joint. However, to find the relationship between the two parameters, experimental results are needed since it is phenomenological not an empirical approach. Since the ultimate goal of the model is to simulate the seismic behaviour of the joint then the moment-rotation relationship of the joint must show the cracking, yielding, hysteretic behaviour, pinching and strength degradation. An advanced hysteresis loop with pinching behaviour, proposed by

Pampanin to model the behaviour of a gravity load-design joint, shown in Fig. 2.39, has been implemented in Ruaumoko (Carr, 2004), based on the experimental tests carried out at the University of Pavia (Pampanin, 2002) and herein adopted to predict the experimental behaviour, while allowing for further validation and calibrations of the parameters.

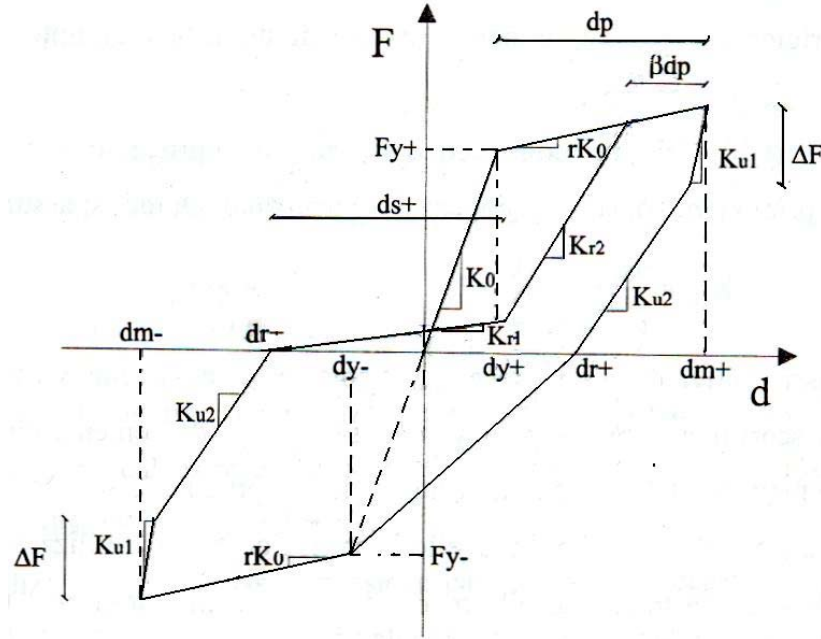


Figure 2.39 Advanced hysteresis rule with pinching (Pampanin) and available in Ruaumoko, Carr (2004)

The yield moment is calculated using the upper limit of the joint principal tensile stress. The yield condition can be calculated by this equation:

$$P_t = -\frac{\sigma_a}{2} + \sqrt{\left(\frac{\sigma_a}{2}\right)^2 + (\nu_{jh})^2} \quad (1)$$

where:

σ_a = column axial stress

ν_{jh} = joint horizontal shear stress

Substitute the formula in terms of the joint horizontal shear stress:

$$\nu_{jh} = \sqrt{(P_t)^2 - P_t \sigma_a} \quad (2)$$

From the horizontal shear stress we can find the inter-storey shear from this relationship:

$$V_{jh} = v_{jh} A_j = \frac{V_s h}{jd} - V_s \quad (3)$$

then find the relationship between principal tensile stress and inter-storey shear with:

$$V_s = A_j \sqrt{P_t^2 + P_t \sigma_a \left(\frac{jd}{h - jd} \right)} \quad (4)$$

Using Equation 4, the yield moment can be calculated using the maximum limit of the principal tensile stress in the joint.

2.6.4 Space Frame Interaction

The relationship between the moment and rotation of joint in plane frame has been under development to simulate the joint behaviour. However, in space frames, the joint shear acts in more than one direction, and there will be an effect of the joint shears one to another. The joint capacity in one direction is suspected to be reduced due to the shear stress from the other direction.

Much research has been done to investigate the behaviour of reinforced concrete in space frames. Furlong analyzed square columns loaded in two principal axes. The columns were loaded by axial load and moments on their both principal axes. He computed the ordinates of points on the failure surface using the concrete compression stress block assumption to make a failure surface image. As shown in Fig. 2.40, Furlong found that the moment capacity in square columns is lower about the non-principal axis.

This simplified equation for the interaction of principal axis moment capacity on a plane of constant axial load is proposed by Bresler:

$$\left(\frac{M_{xy}}{M_{xyo}} \right)^\alpha + \left(\frac{M_{zy}}{M_{zyo}} \right)^\alpha = 1.0 \quad (5)$$

This interaction model can be the basic to find the interaction of many different members by calibrating the parameter α .

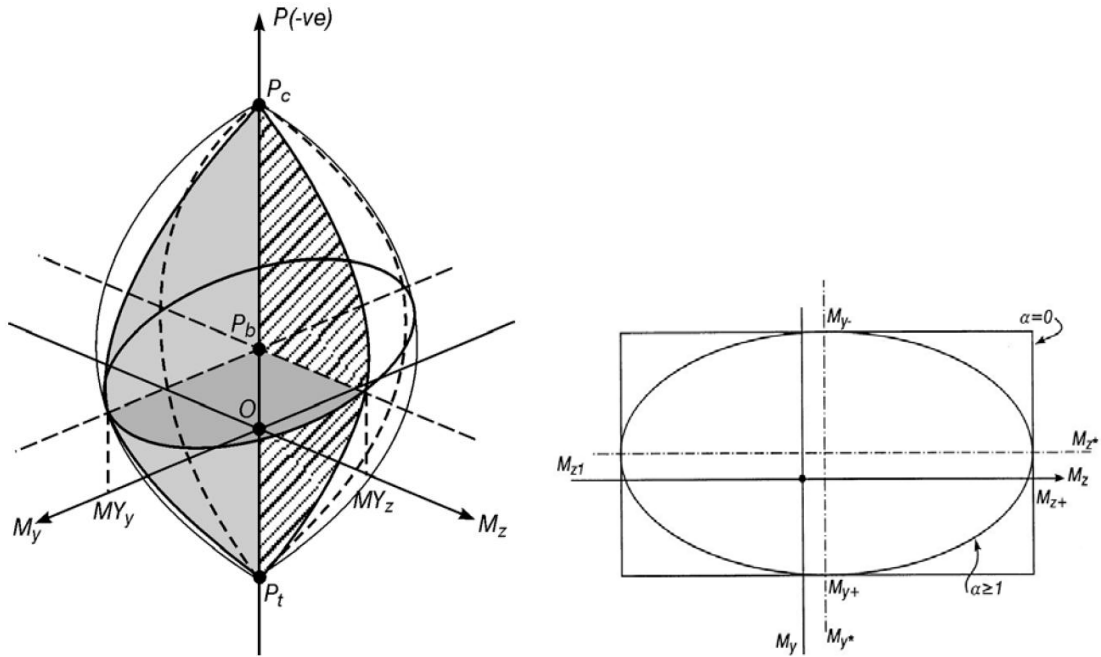


Figure 2.40 Reinforced concrete column interaction surface in space frame, Carr (2004)

Still, the interaction relationship obtained by Furlong is for flexural strength only and can only be used to make a coarse prediction on what the shear strength interaction relationship might be.

Preliminary work to derive appropriate values of the parameter α for the shear interaction surface in a 3-D behaviour of beam-column joint failing in shear can be found in Trowland, 2004 (Modeling the Shear Hinge in Beam-Column Joints). Based on the experiments done by Leon and Jirsa (1986) on a series of reinforced beam-column joints, he proposed $\alpha = 1.3-1.4$ to be used.

2.6.5 Geometry of the Model

Figure 2.41 shows the geometry and details of the proposed model for reinforced concrete beam-column joint. A rotational spring is used to model the joint and connect the beam to the column. The end of the upper column is slaved to the end of the lower column both in translation and rotation. In this way, the joint will be the member which transfers the force from column to beam and/or from beam to column. Therefore, the axial load applied on the top of the column can be passed through the joint and effect the joint behaviour. The rotation spring used to model the joint has to be split into two springs to connect the column and beam and to receive the axial load. Properties of the two springs are the same, half of the joint strength and stiffness.

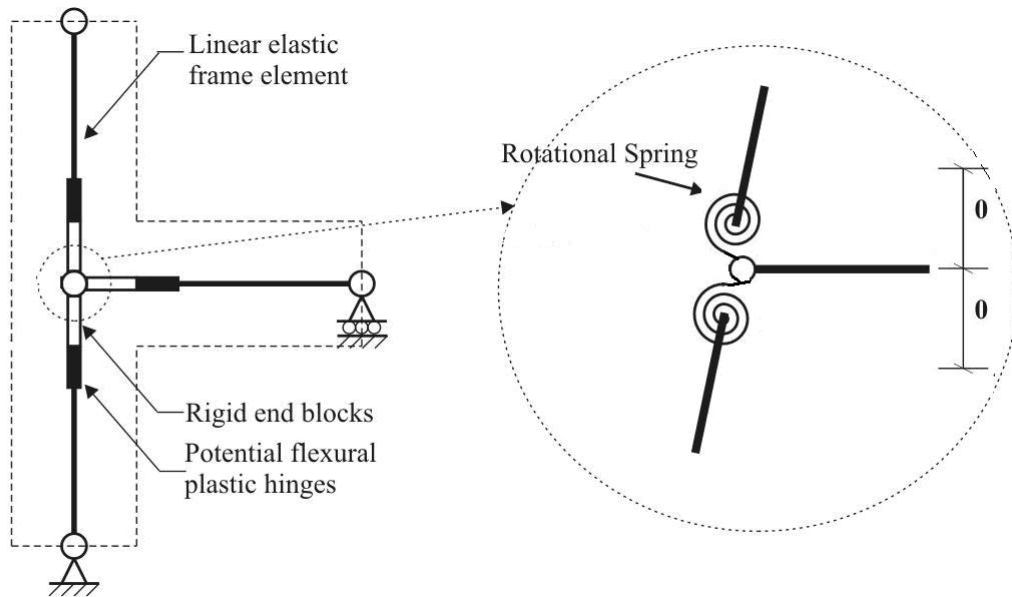


Figure 2.41 Proposed model

2.7 MEMBER STRENGTH AND DEFORMABILITY

The failure mechanism of a structure can be determined using the knowledge of member's strength and deformation capacity. A proper assessment method to assess the member strength and deformation properties has to be used for existing reinforced concrete members.

2.7.1 Material Properties

The specified or nominal material strengths can not be used to calculate the member strength. For the reinforcement, it is important to have yield tests on samples of the steel used to get a better estimation of the yield strength. If it is not possible to have the yield test, then an increment of 10% of nominal yield strength ($1.1 f_y$) should be used.

For the concrete, it is also important to have a compressive test on samples of the concrete used for the construction. The real compressive strength of the concrete can be up to 30% lower or higher than the nominal strength. For existing reinforced concrete structures, the compressive strength of the concrete is likely to exceed the nominal value as a result of aging. A value of 1.5 times the nominal compressive strength is considered to be appropriate for assessment purposes if further data is not available.

2.7.2 Beam and Column Strength

There are two major factors for beam and column strengths, the flexural and the shear strengths. To calculate the flexural and shear strength of the beam and column, standard reinforced concrete beam/column theory with the assumption of a strength reduction factor can be used.

2.7.3 Beam-Column Joint Shear Strength

The strength of the beam-column joint is governed by the shear strength. Forces introduced in joint core come from beam and column reacting to the loads applied on the structure. Figure 2.42 shows the forces acting on beam-column joints. Therefore, for interior joint, considering free body diagram in the mid depth of the joint, the horizontal joint shear force V_{jh} is:

$$V_{jh} = T_1 + C_{c2} + C_{s2} - V'_c \quad (6) \text{ (Cheung et al. 1991)}$$

and considering the free body diagram in mid width of the joint, the vertical joint shear force V_{jv} is:

$$V_{jv} = T' + C_c'' + C_s'' - V_{b1} \quad (7) \text{ (Cheung et al. 1991)}$$

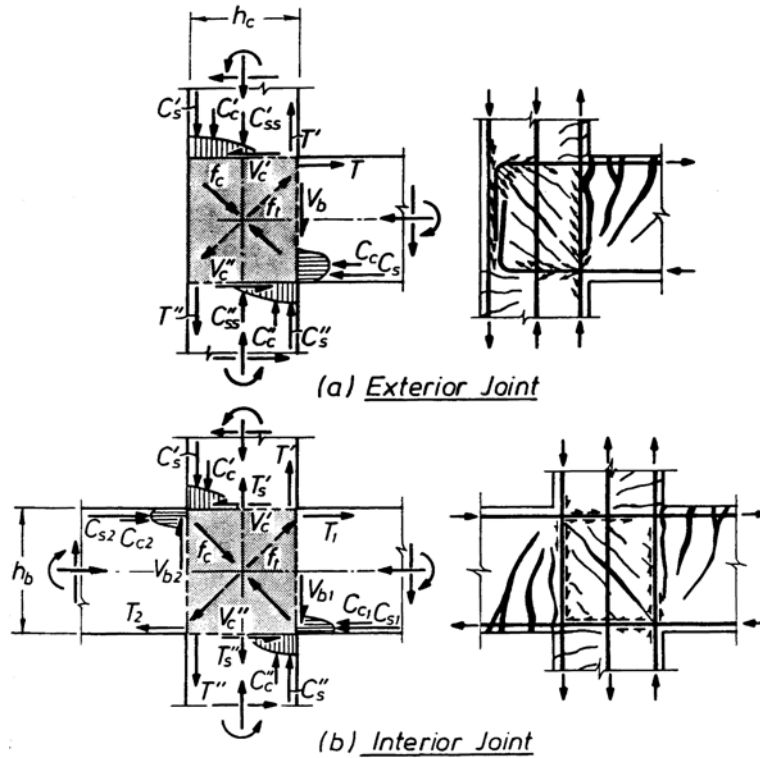


Figure 2.42 Forces on beam-column joints (Cheung et al. 1991)

While for exterior joint, the horizontal and vertical joint shear force are:

$$V_{jh} = T_1 - V'_c \quad (8)$$

$$V_{jv} = T'_1 + C''_c + C''_s - V_b \quad (9)$$

It is assumed that the shear capacity of the beam-column joint is when the initial diagonal tension cracking occurs in the joint core. Instead of using horizontal and vertical joint shear forces and stresses, the principal tensile stress is used as an index in determining the joint shear capacity. The principal tensile stress is contributed to by the column axial force and horizontal shear stress in the joint, with the following equation

$$P_t = -\frac{\sigma_a}{2} + \sqrt{\left(\frac{\sigma_a}{2}\right)^2 + (v_{jh})^2} \quad (10)$$

where:

$$c_a = \text{column axial stress} \left(\frac{N}{A_c} \right)$$

$$v_{jh} = \text{joint horizontal shear stress} \left(\frac{V_{jh}}{A_j} \right)$$

Some limits for the principal tensile stress and the post-cracking behaviour of reinforced concrete beam-column joints have been proposed by Priestley (1997) and extended by Pampanin (2003) for different types of joint, reinforcement and detailing. After the initial diagonal cracking occurs in the joint, the strength will reduce. The amount of the reduction depends on the joint type, reinforcement used and detailing, as shown in Fig. 2.43.

A simple analysis to predict the sequence of event within a beam-column joint system is discussed here. The expected sequence of event is carried out by comparing the capacity and demand curves in M-N (Moment-Axial load) diagram. Fig. 2.44 shows the evaluation of Specimen TDP-1 as an example.

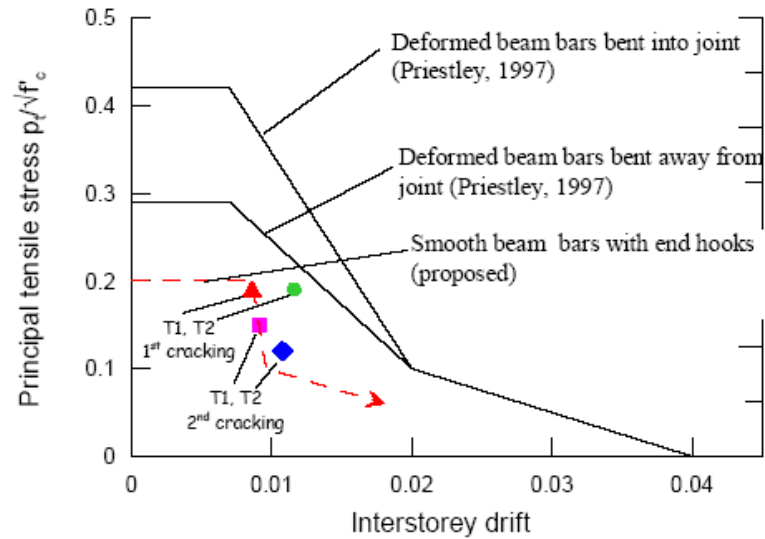
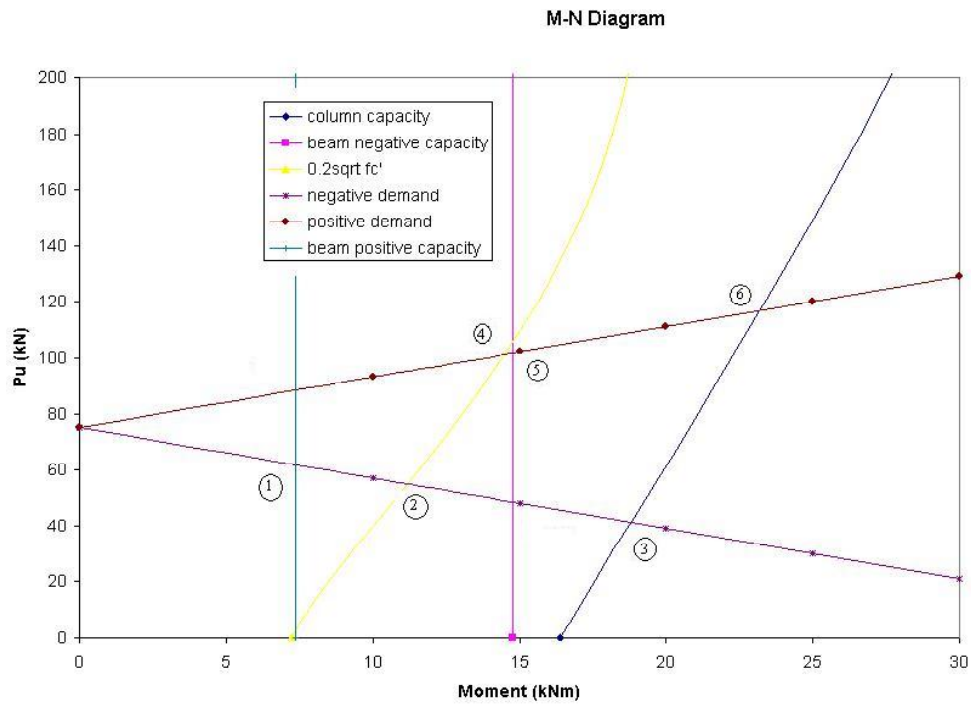


Figure 2.43 Proposed Principal tensile stress limits, Pampanin (2003)



Lateral Force Type	No	Event	Lateral Force (kN)
Open joint ($F < 0$)	1	Beam yielding	7.4
	2	Joint crack ($P_t = 0.19\sqrt{f_c}$)	12.2
	3	Column yielding	18.7
Close joint ($F > 0$)	4	Joint crack ($P_t = 0.19\sqrt{f_c}$)	14.6
	5	Beam yielding	14.8
	6	Column yielding	22.4

Figure 2.44 Hierarchy of strength analysis for Specimen TDP-1

The capacities of the beam, column and joint are referred to a given limit state (for joints: cracking, ‘yielding’, or severe damage and collapse) and evaluated in terms of equivalent moment in the column at that stage, based on equilibrium considerations in the beam-column joint specimen.

2.8 SUMMARY

Buildings designed and constructed in pre-1970s period were typically adopting (in particular in the 1950s) plain round bars as the longitudinal reinforcement. It is thus important to gather more information on the behaviour with plain round bars in addition to the situation deformed bars in order to assess their strength. Based on the available literature, it is clear that there is a need for more experimental tests on reinforced concrete beam-column joints using plain round bars as the longitudinal reinforcement and with reinforcement detailing as typical in the pre-1970 period.

The contribution of axial load on the behaviour of the beam-column joint response has not been typically accounted for during experimental tests. A variation of axial load on the column can alter the hierarchy of strength in a beam-column joint unit, thus yielding to alternative undesired damage and failure mechanisms. This matter will be further discussed in Chapter 4. Therefore it is important to take into account the variation of axial load on the column, which is related to the base shear force.

The biaxial lateral loading protocol used for the space frame reinforced concrete beam-column joint experiments mentioned before were in most cases independent between one direction and the orthogonal one. Under a real earthquake, a column is subjected to a complicated motion in random directions. This will also be discussed further in Chapter 4. A bi-directional lateral loading regime with step-by step interaction between the two orthogonal axes directions is needed to simulate as close as possible the behaviour of a beam-column joint under a real earthquake.

The previous experimental tests on reinforced concrete beam-column joint were also mostly concentrating on interior beam-column joints. Interior joints are expected to perform better than the exterior joints due to the presence of an additional beam on the side of the column which can provide adequate anchorage. Comprehensive information of the behaviour of poorly detailed exterior beam-column joint unit, based on both experimental and numerical investigation, is still of wide interest.

CHAPTER 3

TEST UNITS AND SETUP

3.1 INTRODUCTION

Review of previous researches in the beam-column joint subassemblies, both in two-dimensional and three-dimensional, described in Chapter 2, shows that effect of varying axial load on the column to represent what happened to the column in the real structure under earthquake excitation was not taken into account. The column will receive compression or tension load depending on the lateral loading direction, as described in Fig. 3.1. The axial load is really important because it can change the sequence of the failure of the member, predicted from the hierarchy of strength, using the Moment-Axial Force interaction diagram. To explain this, an example of a hierarchy of strength is shown in Fig. 3.2. The sequence of failure of the beam-column joint if the column is in tension is, joint failure, followed by beam failure and the last will be column failure. We can see if the axial load is in compression, the sequence of failure will change to beam failure, followed by joint failure and ended by column failure.

The other thing is the use of deep beams ($h_b \geq 2b_w$), instead of the shallow beams or wide beams, which were commonly used in the practice since it was allowed by the codes at that time. The advantage of using a shallow beam is to have a large storey height without having to worry about the total height of the structure.

In addition, the previous tests of the three-dimensional beam-column joints were focused on interior and exterior beam-column joint subassemblies; while the weakest part will be the corner beam-column joint subassemblies especially if the anchorage detailing is poor (see Fig. 3.3). The bi-directional loading was applied on the unit strong axes on sequence, without any interaction between one axis to the other as shown in Fig. 3.4. In the reality, the earthquake will strike the structure from any direction it wants, so it is impossible to predict the direction. The response of a column in the real structure under earthquake excitation is plotted in Fig. 3.5. A bi-directional loading history with interaction between the directions of the strong axes will represent the behaviour more precisely.

This research project studied the seismic behaviour of existing beam-column joint subassemblies with plain round longitudinal bars with typical detailing of the pre-1970s design. The effects of different reinforcement detailing, variation of axial load and beam geometry are investigated. The behaviour of the beam-column joint in three-dimensional under interacted-bi-directional loading is also tested. The main objective is to get more information about the joint behaviour with different detailing and the concept of shear hinge in the joint.

This chapter introduces the units tested in this research project.

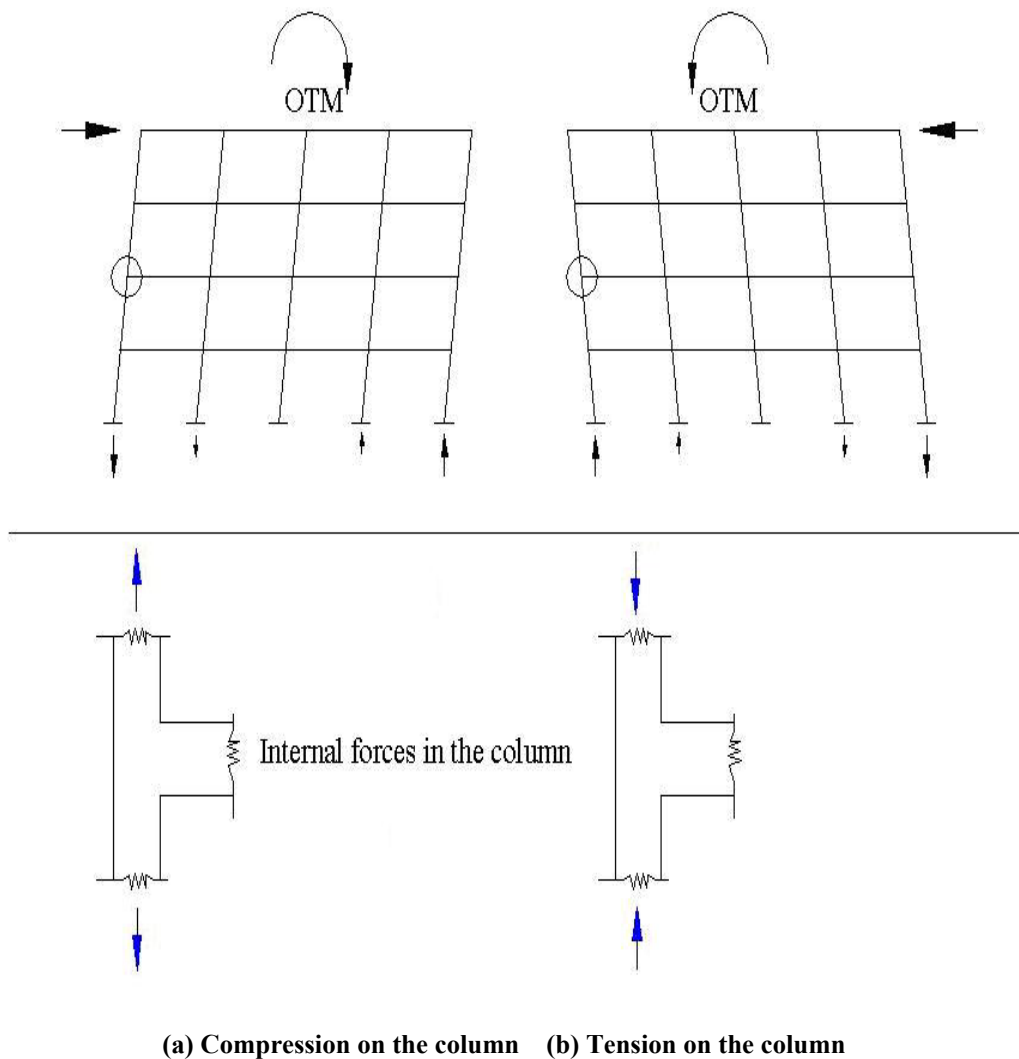


Figure 3.1 Forces acting on the column under lateral load in different directions

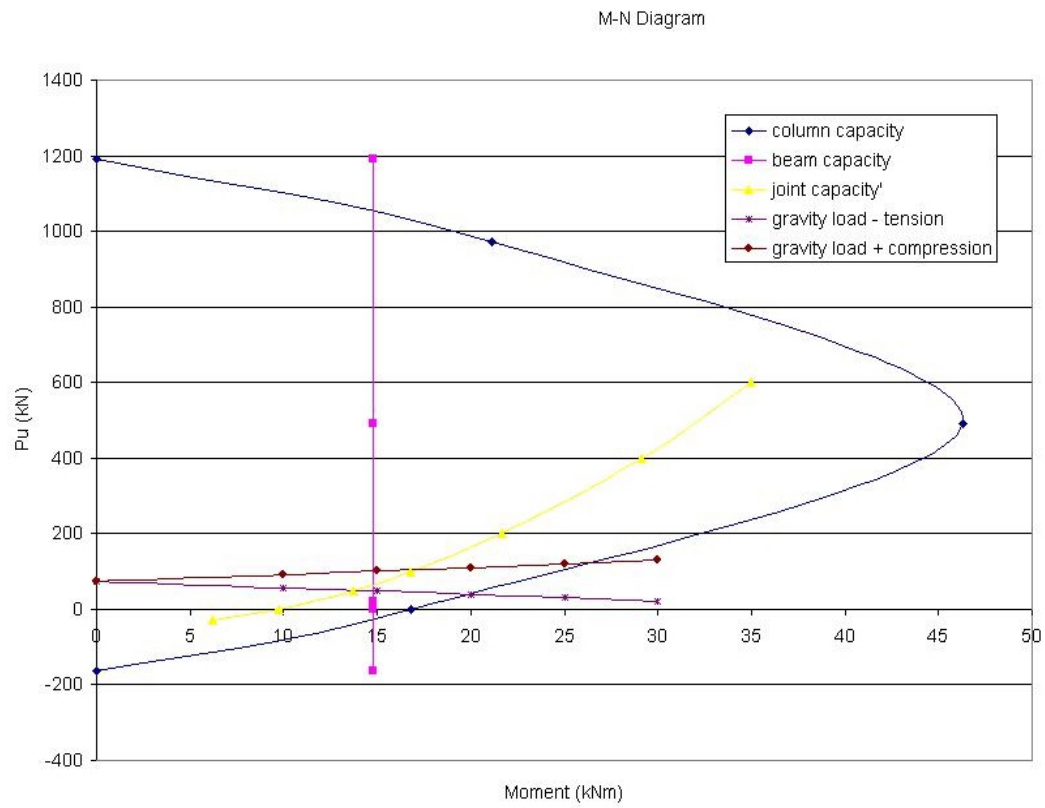


Figure 3.2 Hierarchy of strength of a beam-column joint

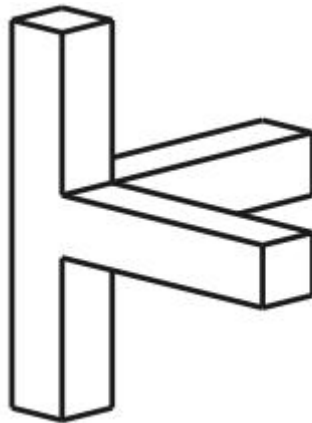


Figure 3.3 Corner joint

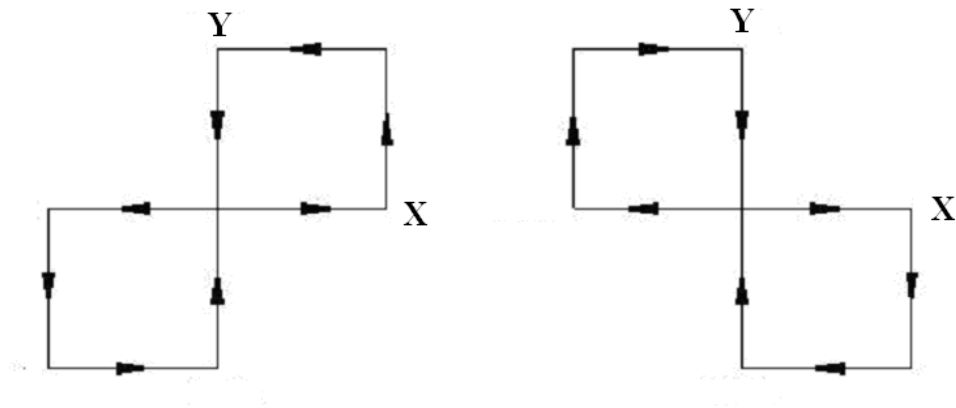


Figure 3.4 Loading history used for previous bi-directional research

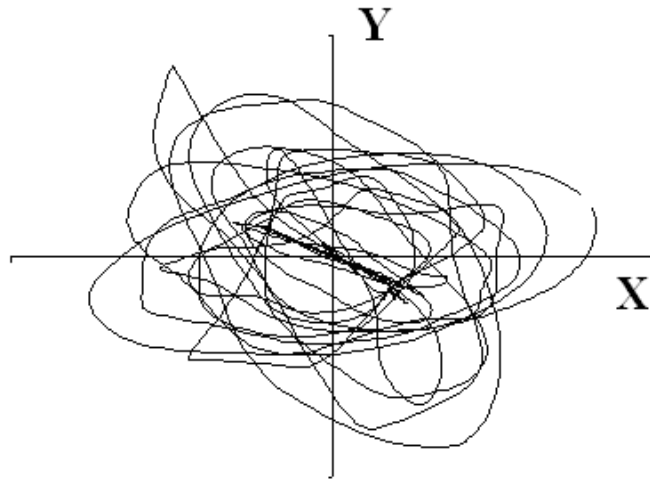


Figure 3.5 Single degree of freedom structure behaviour under earthquake

3.2 TEST UNIT DETAILS

3.2.1 Introduction

The existing beam-column joint subassemblies, reinforced by plain round longitudinal bars with hooked ends are representative of the reinforced concrete frame structure constructed before 1970. The test aimed at investigating the influence of different kinds of detailing in the joint area and beam geometry to the member local behaviour. This project involved six existing two-third-scale plane frame exterior beam-column joint units and three existing two-third-scale space frame corner-exterior beam-column joint units. The six existing plane frame units include two units with deep

beam and plain round longitudinal bars, two units with deep beam and deformed longitudinal bars, one unit with shallow beam and plain round longitudinal bars, and one unit with shallow beam and deformed longitudinal bars. The three existing space frame units, all using plain round longitudinal bars, consist of two units with deep beam-deep beam combination and one unit with deep beam–shallow beam combination.

3.2.2 Plane Frame Units

3.2.2.1 General

Six one-way exterior beam-column joint units were constructed, each two-third-scale in size. The units were divided into two main categories according to the beam geometry, deep beams and shallow beams. All of the units have identical parts between the mid-span of the beams and the mid-height of the columns of a common four-storey existing reinforced concrete frame structure constructed before 1970. The overall geometry of the beam-column joint subassemblies is shown in Fig. 3.6.

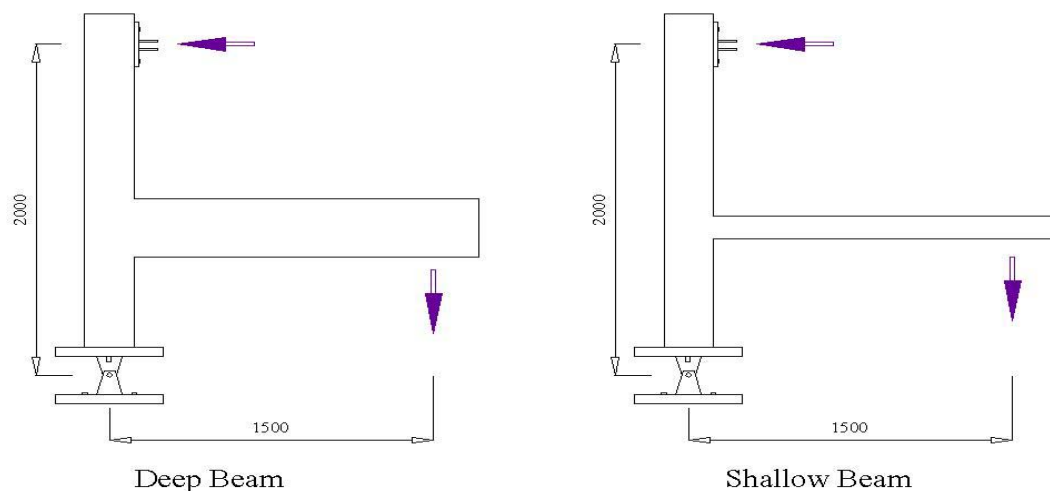


Figure 3.6 Plane frame beam-column joint subassembly specimens

3.2.2.2 Deep Beams Details

Four geometrically identical exterior beam-column joint units with deep beams, each different in reinforcement details, were constructed. The units are referred to as Units TDP-1, TDD-1, TDP-2 and TDD-2. Units TDP-1 and TDP-2 used plain round

longitudinal reinforcement, while units TDD-1 and TDD-2 used deformed longitudinal reinforcement.

The beams of each unit were 330 mm in depth and 200 mm in width and the columns were 230 mm square. The size of these units is scaled down from the perimeter planar frame of the subject structure. The overall dimensions and reinforcing details of all the units are shown in Fig. 3.7 to 3.10.

The columns for all units were symmetrically reinforced on the strong axis, containing three 10 mm diameter Grade 300 plain round bars on both sides ($\rho_t = 0.0045$). The column transverse reinforcement was from 6 mm diameter Grade 300 plain round bars placed at 100 mm centers, and the first tie was 50 mm from the beam face. The beam-column joint core contained a single transverse reinforcement placed in the middle of the beam depth for every unit. The beam transverse reinforcement for all units used 6 mm diameter Grade 300 plain round bars placed at 135mm centers, and the first stirrup was 50 mm from the column face.

The beam for Unit TDP-1 was asymmetrically reinforced, contained four 10 mm diameter Grade 300 plain round bars in the top ($\rho = 0.0048$) and two 10 mm diameter Grade 300 plain round bars in the bottom ($\rho' = 0.0024$), with hooked anchorage. The beam for Unit TDD-1 was asymmetrically reinforced, contained four 10 mm diameter Grade 300 deformed bars in the top ($\rho = 0.0048$) and two 10 mm diameter Grade 300 deformed bars in the bottom ($\rho' = 0.0024$), with bars end bent into the joint core. The beam for Unit TDP-2 was symmetrically reinforced, contained four 10 mm diameter Grade 300 plain round bars in the top ($\rho = 0.0048$) and four 10 mm diameter Grade 300 plain round bars in the bottom ($\rho' = 0.0048$), with hooked anchorage. The beam for Unit TDD-2 was asymmetrically reinforced, contained six 10 mm diameter Grade 300 deformed bars in the top ($\rho = 0.0072$) and four 10 mm diameter Grade 300 deformed bars in the bottom ($\rho' = 0.0048$), with bars end bent into the joint core.

The four units were cast in the horizontal plane. Units TDP-1 and TDD-1 were cast on the same time, while units TDP-2 and TDD-2 were cast later. Table 3.1 lists details of concrete compressive cylinder strengths of all units at 28 days old and the time of testing. Table 3.2 lists details of the reinforcement for Units TDP-1, TDD-1, TDP-2 and TDD-2.

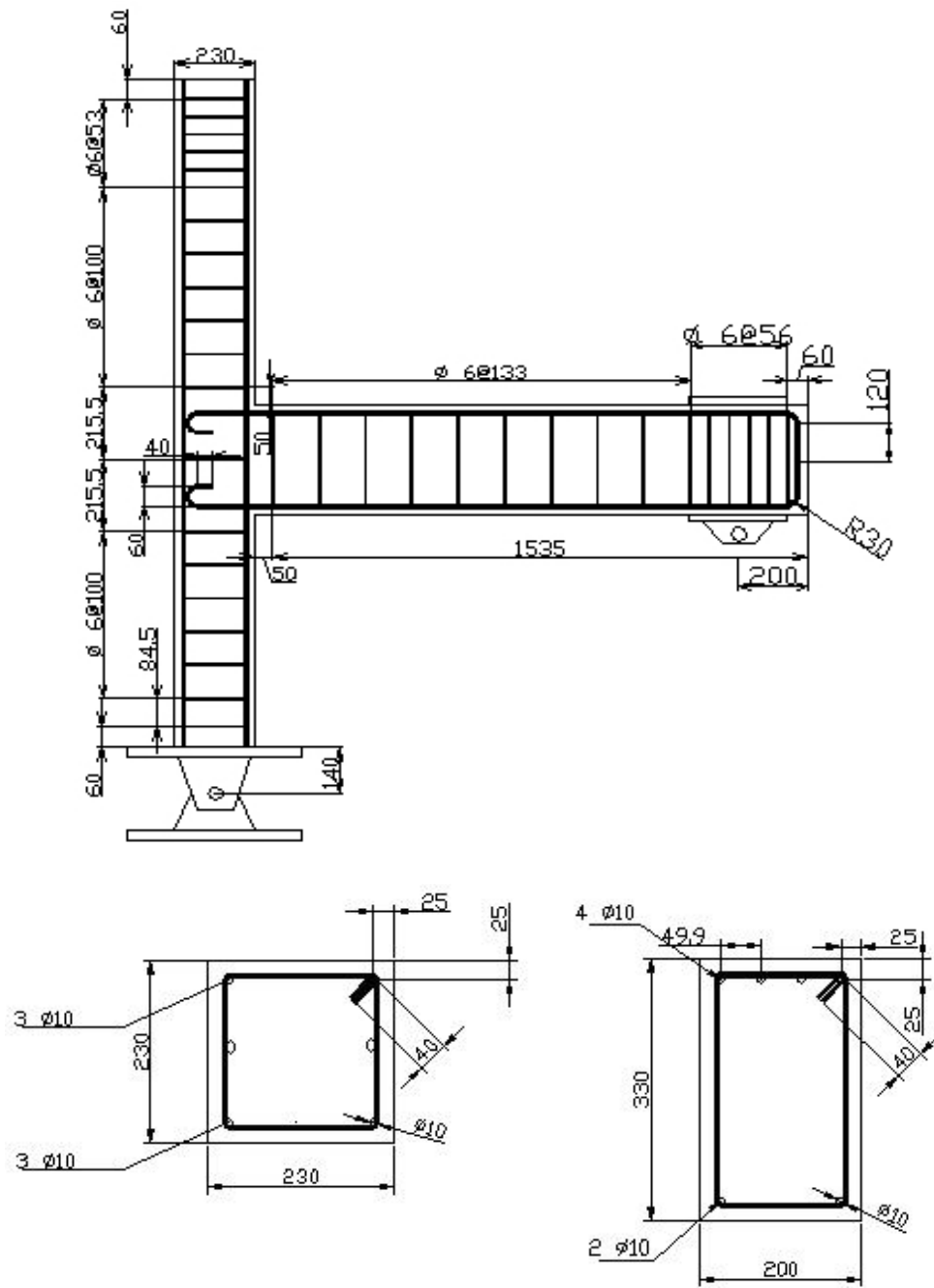


Figure 3.7 Details of Unit TDP-1

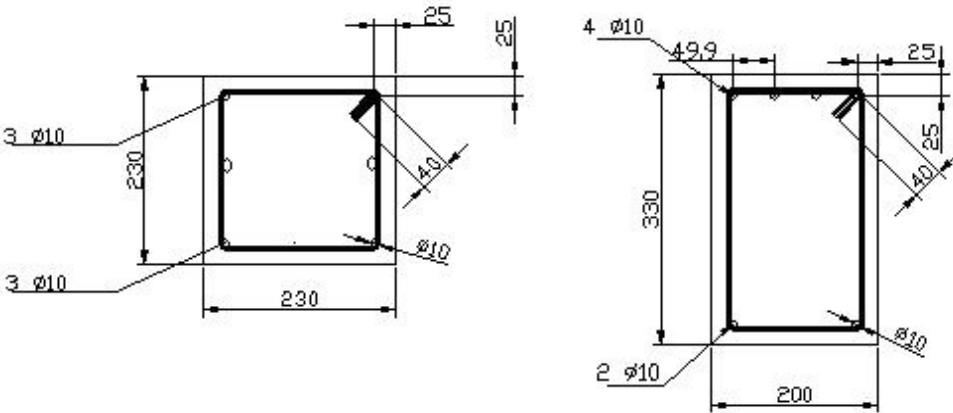


Figure 3.8 Details of Unit TDD-1

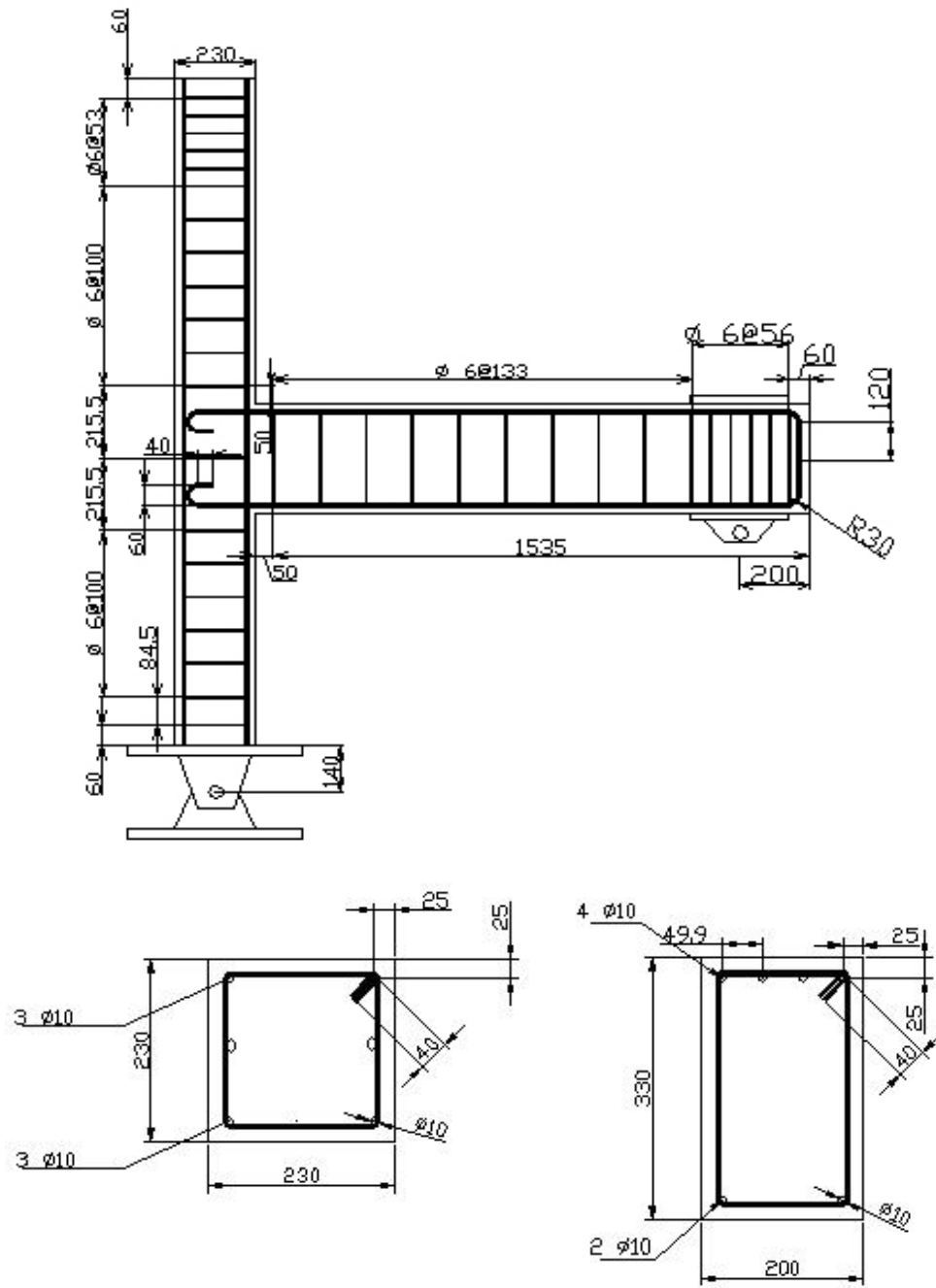


Figure 3.9 Details of Unit TDP-2

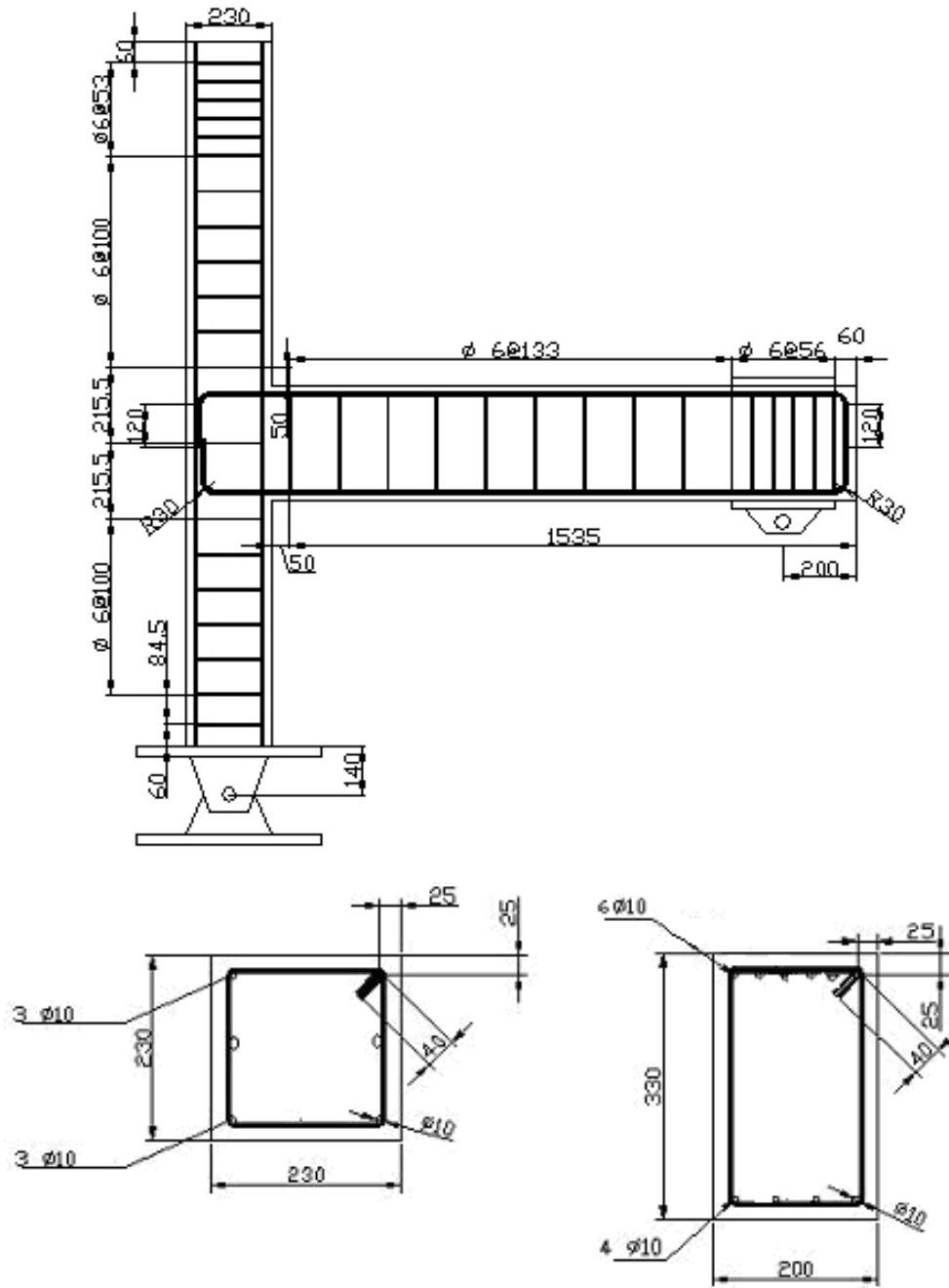


Figure 3.10 Details of Unit TDD-2

Test Unit	TDP-1	TDD-1	TDP-2	TDD-2
f'_c at 28 days (MPa)	21.4	21.4	23.3	23.3
age at test	45 days	50 days	48 days	56 days
f'_c at test day (MPa)	22.9	23.1	25	24.7

Table 3.1 Concrete properties of test units (deep beams)

Test Unit	TDP-1		TDD-1		TDP-2		TDD-2	
Grade of Steel (MPa)	300	300	300	300	300	300	300	300
Bar Size	R6	R10	R6	D10	R6	R10	R6	D10
Yield strength, f_y (MPa)	424	348	424	326	408	333	408	354
Yield strain, ϵ_y	0.0021	0.0018	0.0021	0.0017	0.0021	0.0015	0.0021	0.0015
Ultimate strength, f_u (MPa)	495	464	495	458	482	467	482	481

Table 3.2 Reinforcing steel properties of test units (deep beams)

3.2.2.3 Shallow Beams Details

Two geometrically identical exterior beam-column joint units with shallow beams, each different in reinforcement details, were constructed. The units are referred to as Units TSP and TSD. Units TSP used plain round longitudinal reinforcement, while units TSD used deformed longitudinal reinforcement.

The beams of each unit were 130 mm in depth and 535 mm in width and the columns were 230 mm square. The size of these units is scaled down from the perimeter planar frame of the subject structure. The overall dimensions and reinforcing details of the two units are shown in Fig. 3.11 to 3.12.

The columns for all units were symmetrically reinforced on the strong axis, containing three 10 mm diameter Grade 300 plain round bars on both sides ($\rho_t = 0.0045$). The column transverse reinforcement was from 6 mm diameter Grade 300 plain round bars placed at 100 mm centers, and the first tie was 50 mm from the beam face. The beam transverse reinforcement used was 6 mm diameter Grade 300 plain round bars placed at 135mm centers, and the first stirrup was 50 mm from the column face. The beam-column joint core contained a single transverse reinforcement placed in the middle of the beam depth and a single beam stirrup in the middle of the column depth.

The shallow beams were designed to have the same flexural capacity as Unit TDP and Unit TDD. The beam for Unit TSP was asymmetrically reinforced, contained twelve 10 mm diameter Grade 300 plain round bars in the top ($\rho = 0.013$) and six 10 mm diameter Grade 300 plain round bars in the bottom ($\rho' = 0.0066$), with hooked anchorage. The beam for Unit TSD was asymmetrically reinforced, contained twelve

10 mm diameter Grade 300 deformed bars in the top ($\rho = 0.013$) and six 10 mm diameter Grade 300 deformed bars in the bottom ($\rho' = 0.0066$), with bars end bent into the joint core.

The two units were cast in one stage in the horizontal plane. Table 3.3 lists details of concrete compressive cylinder strengths of all units at 28 days old and the time of testing. Table 3.4 lists details of the reinforcement for Units TSP and TSD.

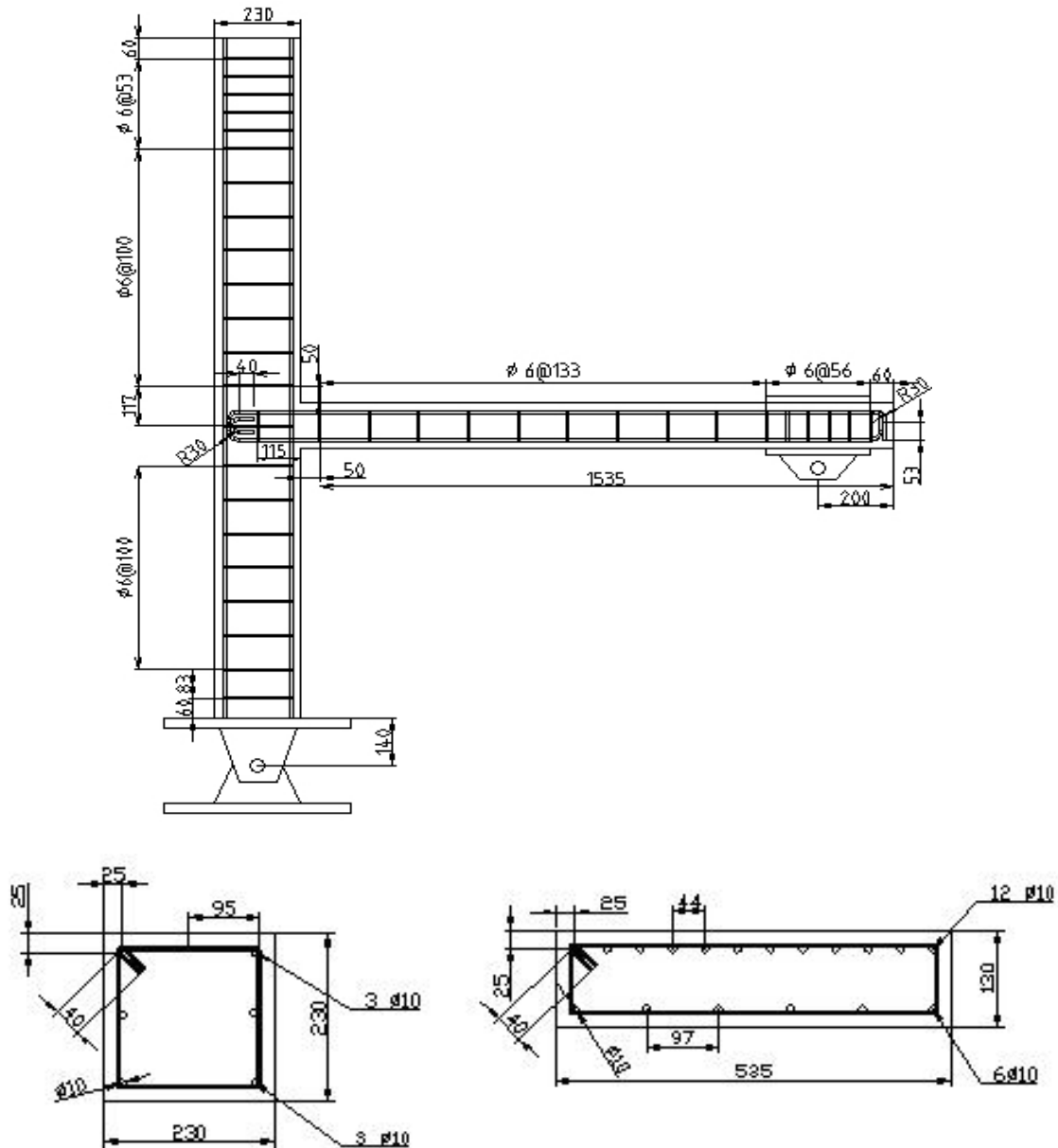


Figure 3.11 Details of Unit TSP

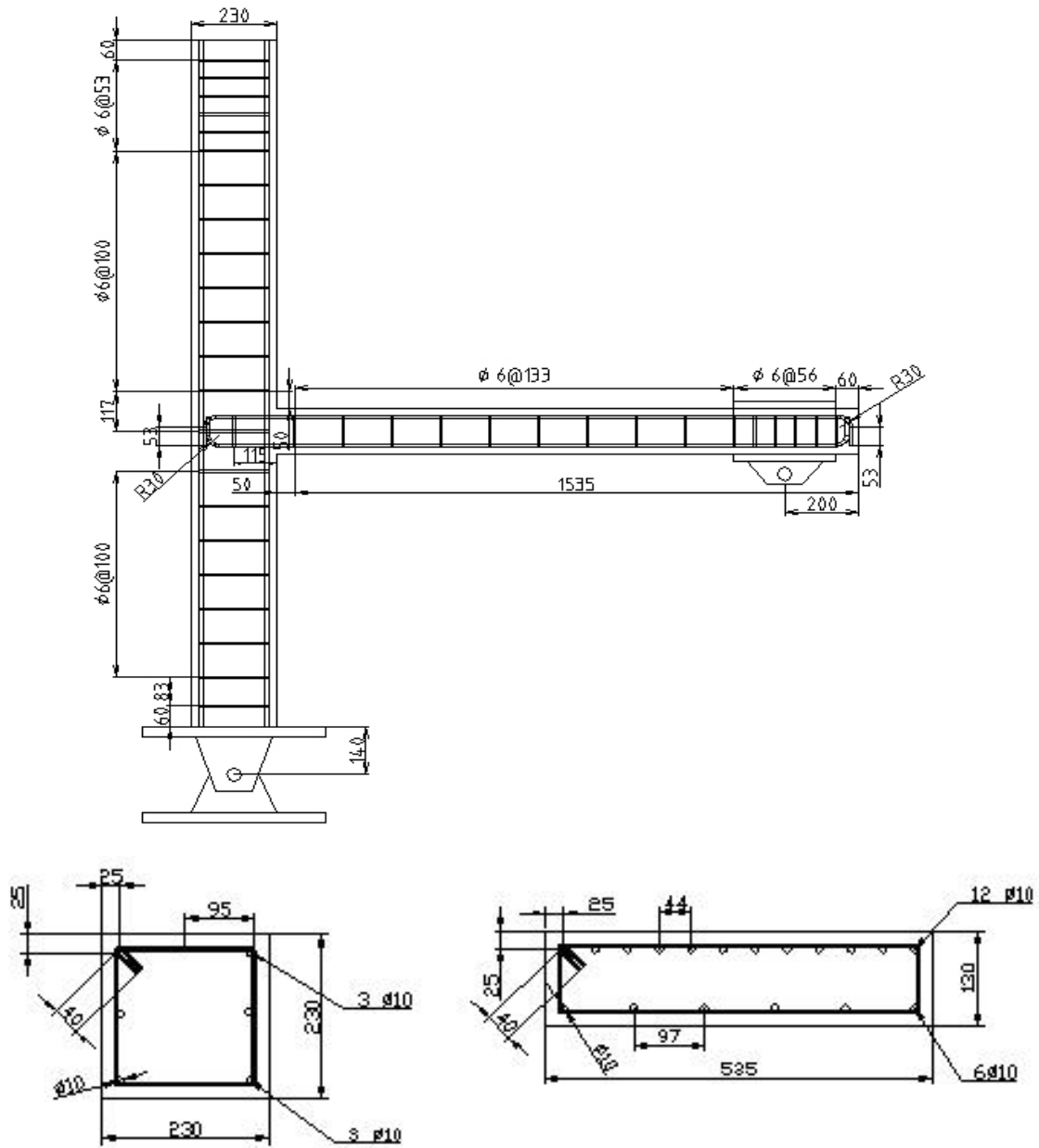


Figure 3.12 Details of Unit TSD

Test Unit	TSP	TSD
f'_c at 28 days (MPa)	21.4	21.4
Age at test	55 days	59 days
f'_c at test day (MPa)	23.4	23.6

Table 3.3 Concrete properties of test units (shallow beams)

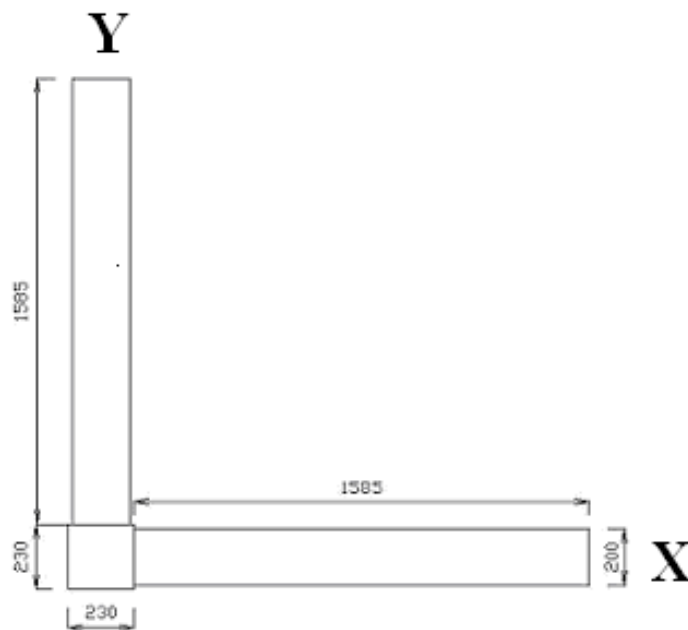
Test Unit	TSP		TSD	
Grade of Steel (MPa)	300	300	300	300
Bar Size	R6	R10	R6	D10
Yield strength, f_y (MPa)	424	348	424	326.3
Yield strain, ϵ_y	0.0021	0.0018	0.0021	0.0017
Ultimate strength, f_u (MPa)	495	464	495	458

Table 3.4 Reinforcing steel properties of test units (shallow beams)

3.2.3 Space Frame Units

3.2.3.1 General

Three two-way corner beam-column joint units constructed each two-third-scale in size. All of the units have identical parts between the mid-span of the beams and the mid-height of the columns of a common four-storey existing reinforced concrete frame structure constructed before 1970. These three units are referred to as Units DD1, DD2 and DS. Plain round longitudinal reinforcing bars with hooked anchorages were used for all the units. The global geometry used for the two-way units is the same with the one-way units. The overall geometry of the beam-column joint subassemblies is shown in Fig. 3.13.



Plan view

Figure 3.13 Overall geometry of space frame units

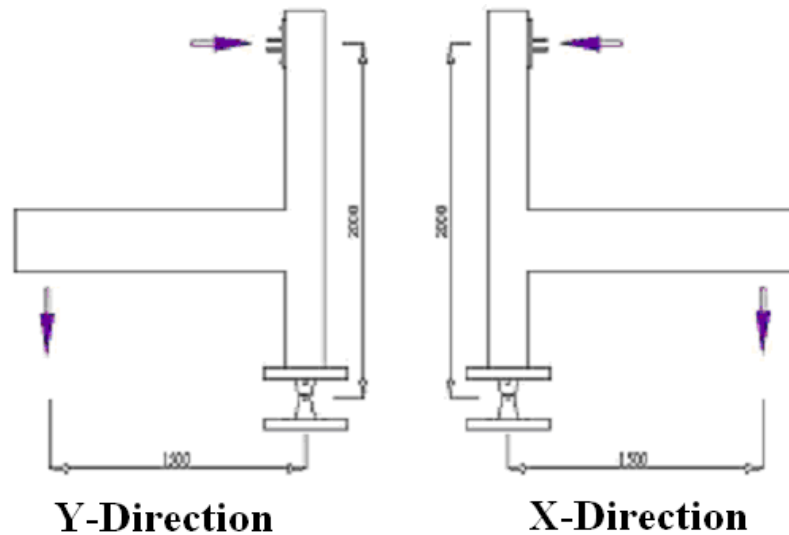


Figure 3.13 Overall geometry of space frame units (continued)

The two-way corner beam-column joint units are no more than the combination of the one-way exterior beam-column joint units described before. The objective is to find the member behaviour differences in two-dimensional and three-dimensional.

3.2.3.2 Unit DD-1

Unit DD-1 had identical beams in both Y and X directions. The beams were 330 mm in depth and 200 mm in width and the column was 230 mm square. The size of these units is scaled down from the corner space frame of the subject structure. The overall dimensions and reinforcing details of the unit are shown in Fig. 3.14.

The column was symmetrically reinforced on the Y direction, containing three 10 mm diameter Grade 300 plain round bars on both sides ($\rho_t = 0.0045$). The column transverse reinforcement was from 6 mm diameter Grade 300 plain round bars placed at 100 mm centers, and the first tie was 50 mm from the beam face. The beams were symmetrically reinforced, contained four 10 mm diameter Grade 300 plain round bars in the top ($\rho = 0.0048$) and four 10 mm diameter Grade 300 plain round bars in the bottom ($\rho' = 0.0048$). The beam transverse reinforcement used was 6 mm diameter Grade 300 plain round bars placed at 135mm centers, and the first stirrup was 50 mm from the column face. The beam-column joint core contained a single transverse reinforcement placed in the middle of the beam depth.

The unit was cast in one stage in the vertical plane. Table 3.5 lists details of concrete compressive cylinder strengths of the unit at 28 days old and the time of testing. Table 3.6 lists details of the reinforcement for Unit DD-1.

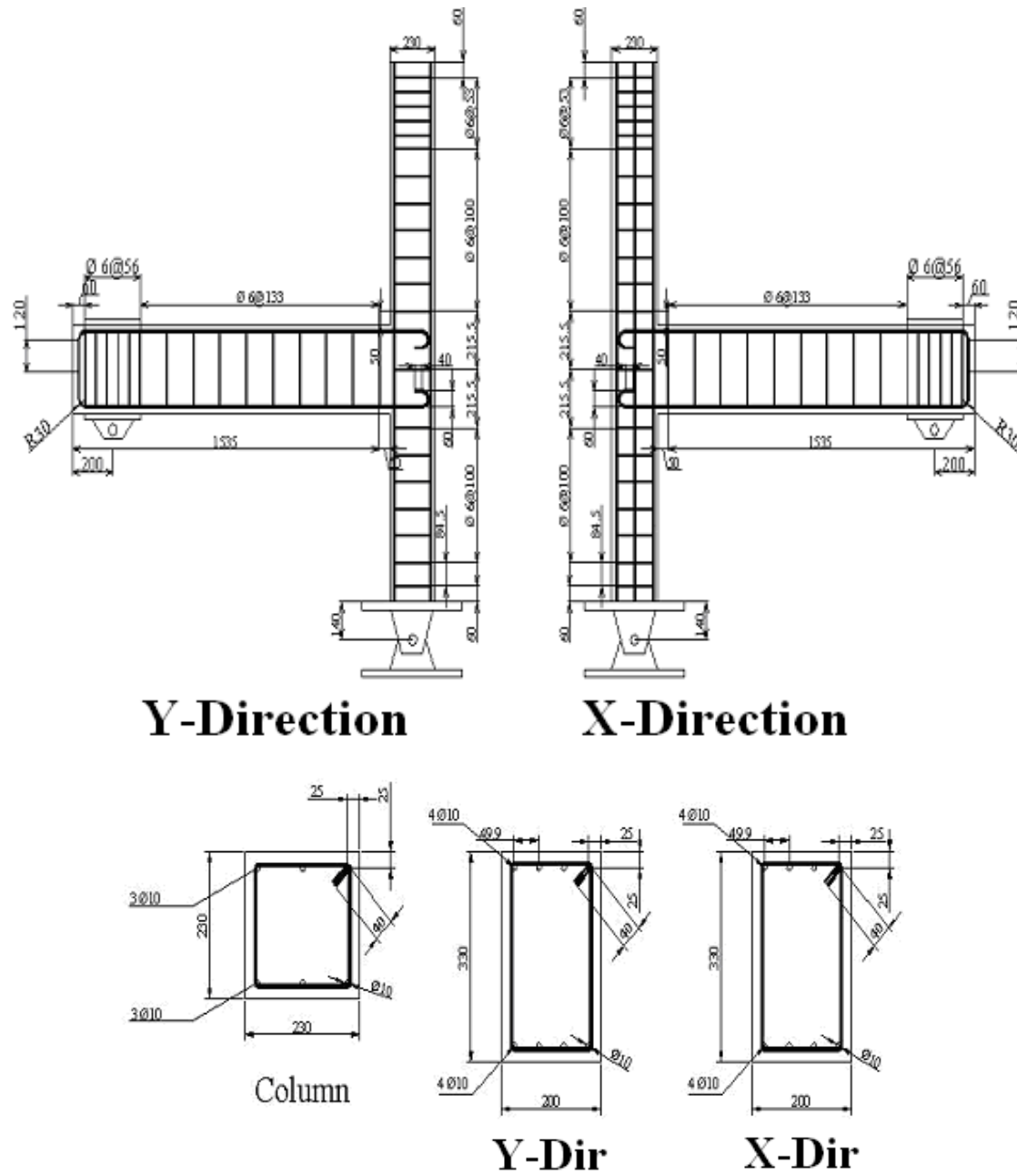


Figure 3.14 Details of Unit DD-1

Test Unit	DD-1
f'_c at 28 days (MPa)	24.82
Age at test	153 days
f'_c at test day (MPa)	24.2

Table 3.5 Concrete properties of unit DD-1

Test Unit	DD-1	
Grade of Steel (MPa)	300	300
Bar Size	R6	R10
Yield strength, f_y (MPa)	388	344
Yield strain, ϵ_y	0.0022	0.0015
Ultimate strength, f_u (MPa)	487	478

Table 3.6 Reinforcing steel properties of unit DD-1

3.2.3.3 Unit DD-2

Unit DD-2 had identical beams in both Y and X directions. The beams were 330 mm in depth and 200 mm in width and the column was 230 mm square. The size of these units is scaled down from the corner space frame of the subject structure. The overall dimensions and reinforcing details of the unit are shown in Fig. 3.15.

The column was symmetrically reinforced on the Y direction, containing three 10 mm diameter Grade 300 plain round bars on both sides ($\rho_t = 0.0045$). The column transverse reinforcement was from 6 mm diameter Grade 300 plain round bars placed at 100 mm centers, and the first tie was 50 mm from the beam face. The beams were symmetrically reinforced, contained four 10 mm diameter Grade 300 plain round bars in the top ($\rho = 0.0048$) and four 10 mm diameter Grade 300 plain round bars in the bottom ($\rho' = 0.0048$). The beam transverse reinforcement used was 6 mm diameter Grade 300 plain round bars placed at 135mm centers, and the first stirrup was 50 mm from the column face. The beam-column joint core contained no transverse reinforcement.

The unit was cast in one stage in the vertical plane. Table 3.7 lists details of concrete compressive cylinder strengths of the unit at 28 days old and the time of testing. Table 3.8 lists details of the reinforcement for Unit DD-2.

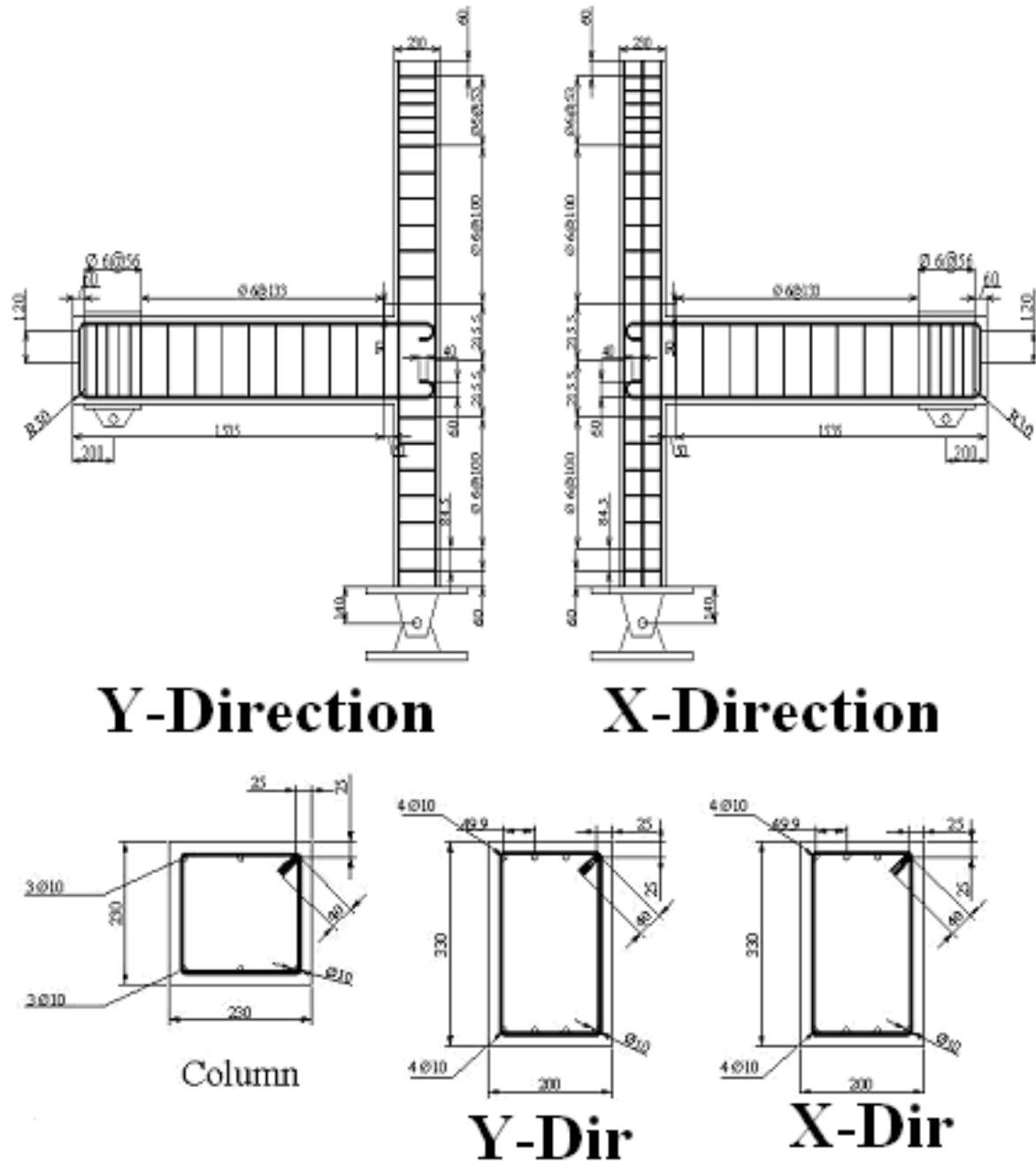


Figure 3.15 Details of Unit DD-2

Test Unit	DD-2
f'_c at 28 days (MPa)	28.9
Age at test	40 days
f'_c at test day (MPa)	27.4

Table 3.7 Concrete properties of unit DD-2

Test Unit	DD-2	
Grade of Steel (MPa)	300	300
Bar Size	R6	R10
Yield strength, f_y (MPa)	388	341
Yield strain, ϵ_y	0.0022	0.0018
Ultimate strength, f_u (MPa)	487	487

Table 3.8 Reinforcing steel properties of unit DD-2

3.2.3.4 Unit DS

Unit DS had deep beam in X direction and shallow beam in Y direction. The shallow beam's surface is at the same level with the deep beam, which means that the centerline of the shallow beam is above the centerline of the deep beam. The centerline of the shallow beam is not in the same plane as the column's either because the corner must be flat. The plan and section views of the unit are shown in Fig. 3.16.

The deep beam was 330 mm in depth and 200 mm in width, the shallow beam was 130 mm in depth and 535 mm in width and the column was 230 mm square. The size of these units is scaled down from the corner space frame of the subject structure. The overall dimensions and reinforcing details of the unit are shown in Fig. 3.17.

The column was symmetrically reinforced on the Y direction, containing three 10 mm diameter Grade 300 plain round bars on both sides ($\rho_t = 0.0045$). The column transverse reinforcement was from 6 mm diameter Grade 300 plain round bars placed at 100 mm centers, and the first tie was 50 mm from the beam face. The deep beam was symmetrically reinforced, contained four 10 mm diameter Grade 300 plain round bars in the top ($\rho = 0.0048$) and four 10 mm diameter Grade 300 plain round bars in the bottom ($\rho' = 0.0048$). The shallow beam was symmetrically reinforced, contained twelve 10 mm diameter Grade 300 plain round bars in the top ($\rho = 0.013$) and twelve 10 mm diameter Grade 300 plain round bars in the bottom ($\rho' = 0.013$). The beams transverse reinforcement used was 6 mm diameter Grade 300 plain round bars placed at 135mm centers, and the first stirrup was 50 mm from the column face.

The beam-column joint core contained a single transverse reinforcement placed in the middle of the deep beam depth and a single beam stirrup from the shallow beam in the

middle of the column depth. The joint core area reinforcing details is shown in Fig. 3.18.

The unit was cast in one stage in the vertical plane. Table 3.9 lists details of concrete compressive cylinder strengths of the unit at 28 days old and the time of testing. Table 3.10 lists details of the reinforcement for Unit DS.

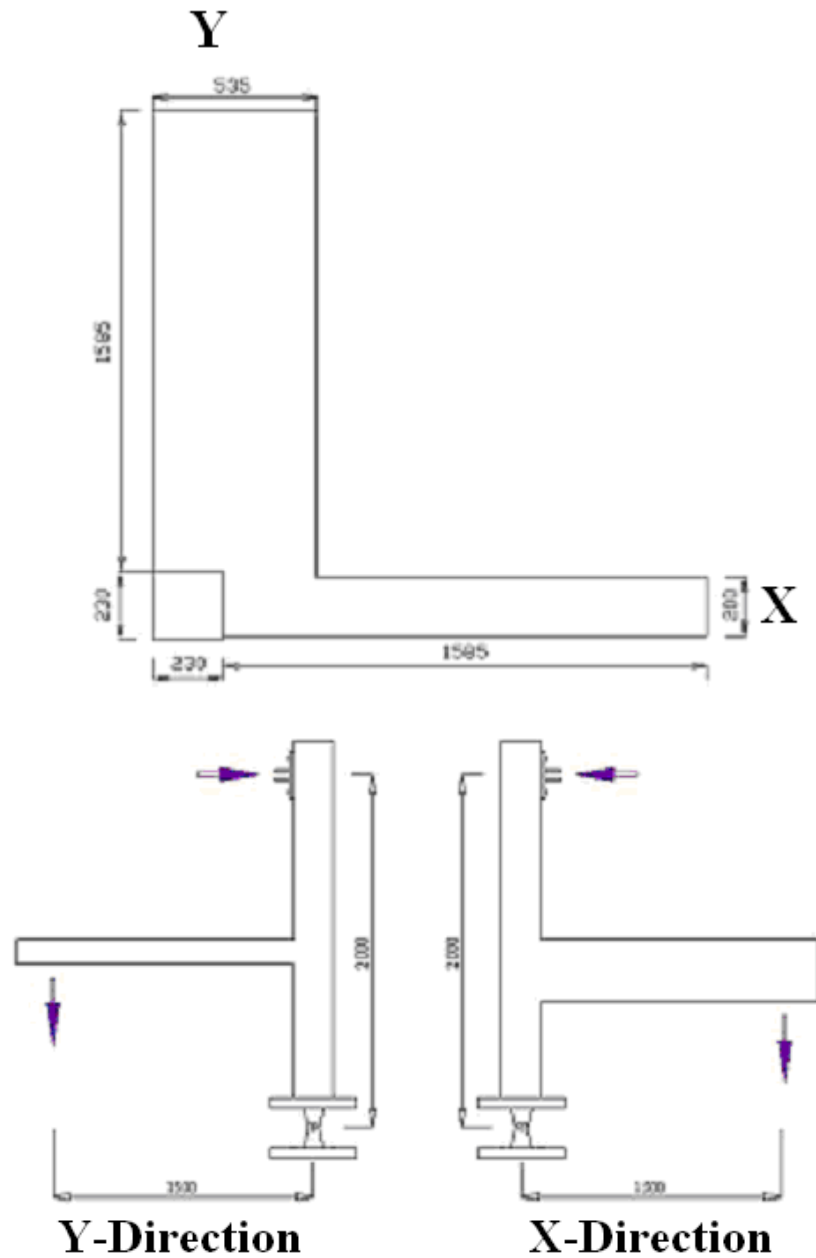


Figure 3.16 Geometry details of unit DS

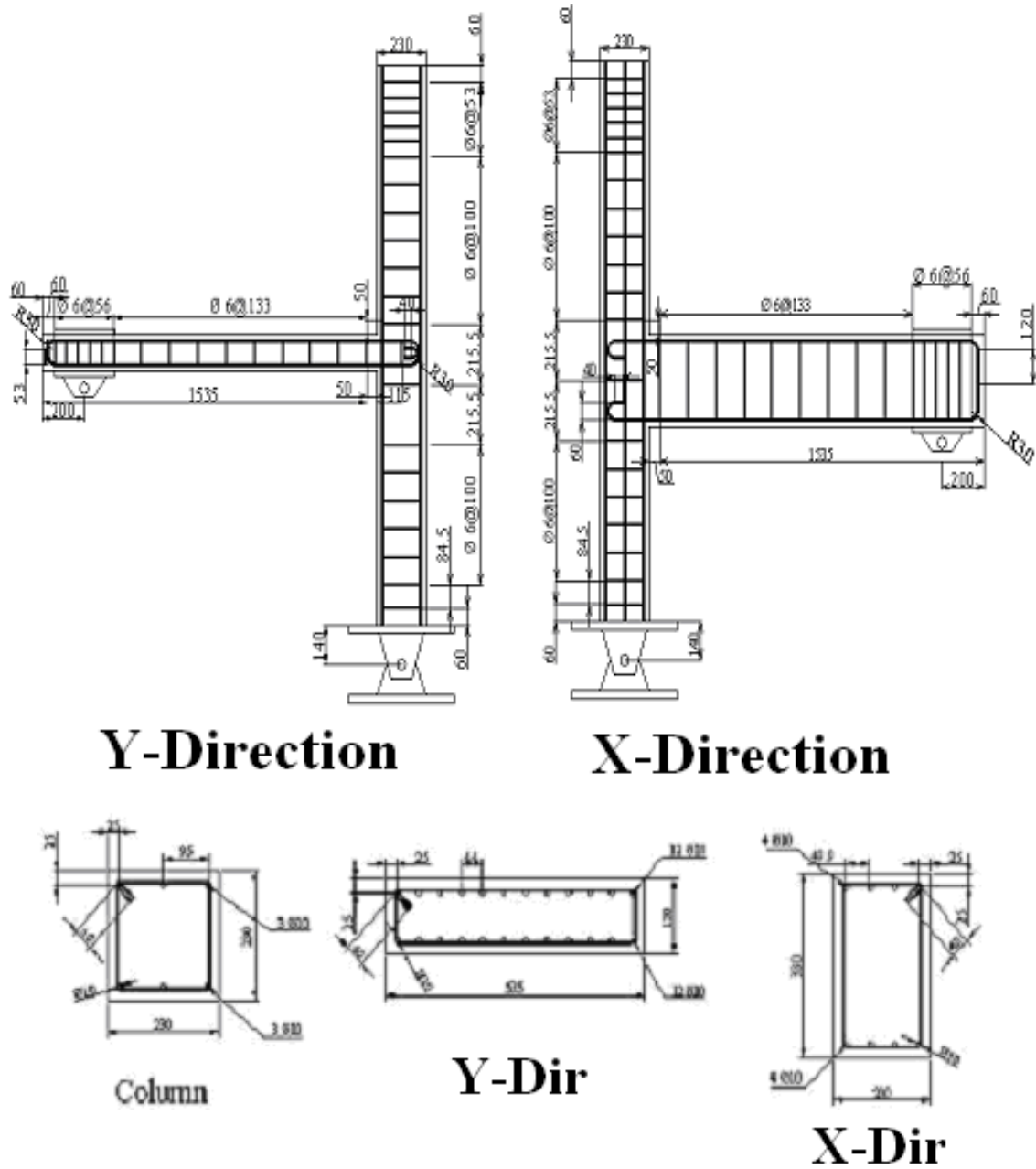


Figure 3.17 Details of Unit DS

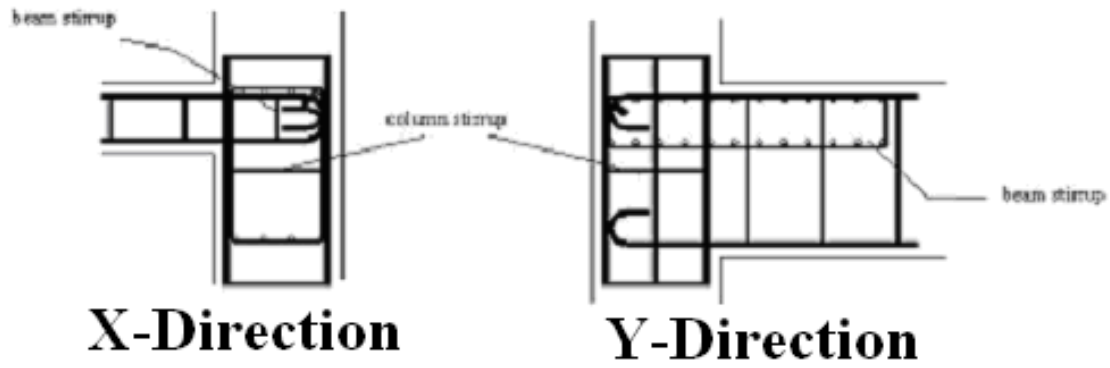


Figure 3.18 Details of joint core area

Test Unit	DS
f_c at 28 days (MPa)	21.1
Age at test	136 days
f_c at test day (MPa)	23.8

Table 3.9 Concrete properties of unit DS

Test Unit	DS	
Grade of Steel (MPa)	300	300
Bar Size	R6	R10
Yield strength, f_y (MPa)	388	344
Yield strain, ϵ_y	0.0022	0.0015
Ultimate strength, f_u (MPa)	487	478

Table 3.10 Reinforcing steel properties of unit DS

3.3 TEST SETUP

3.3.1 Design and Construction of the Test Rig

The design of the test rig had to take into account the positions of the inserts in the strong-floor and the capacity of the hydraulic actuator in the University of Canterbury's Structural Laboratory. The reaction frame was made of an I-section bolted to the strong floor. A hollow box section was used to brace the reaction frame

to the floor to minimize the deflection of the reaction frame from the lateral load. The reaction was transferred from the test specimen to the test rig by a hinge connection at the bottom of the column and a pin connection at the free end of the beam. The dimensions and details of the test rig are shown in Fig. 3.19.

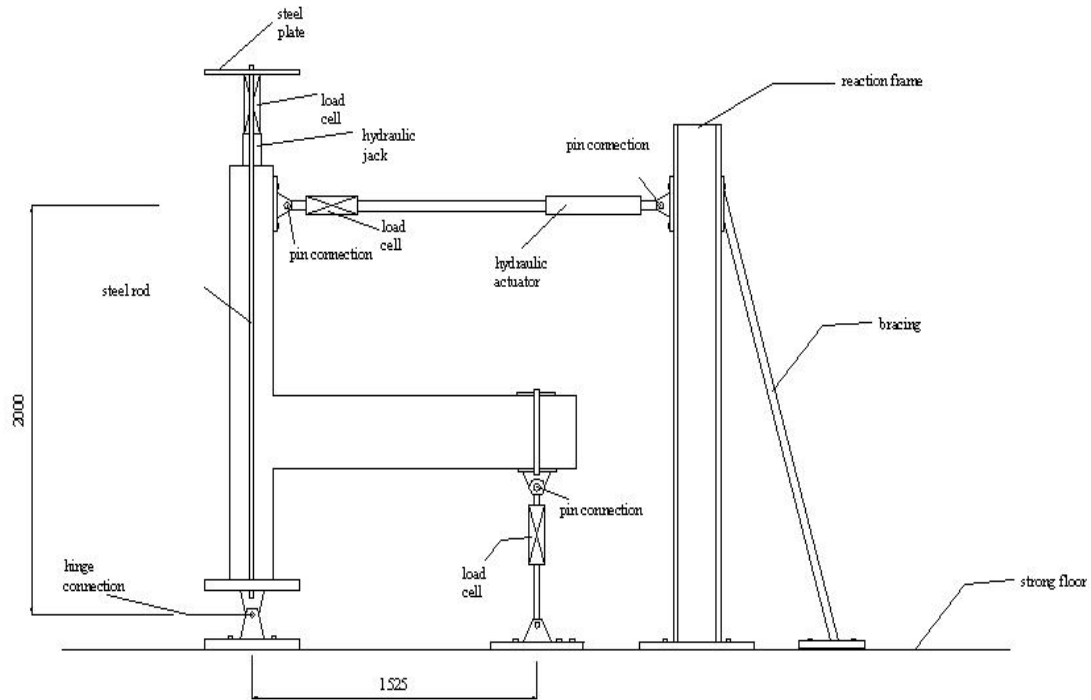


Figure 3.19 Details of plane frame test rig

For the two-way beam-column joint subassembly tests, the rig had to be modified. Another reaction frame was added in the transverse direction using an I-section bolted to the strong-floor. Universal beam was used to strengthen the reaction frame at the level of the lateral load. The beam was then braced to the floor using two hollow box sections to minimize the deflection of the reaction frame. Finally the two reaction frames were braced on the top using universal beam to prevent it from deflecting in angle. The details of the test rig used for bi-directional loading can be seen in Fig. 3.20.

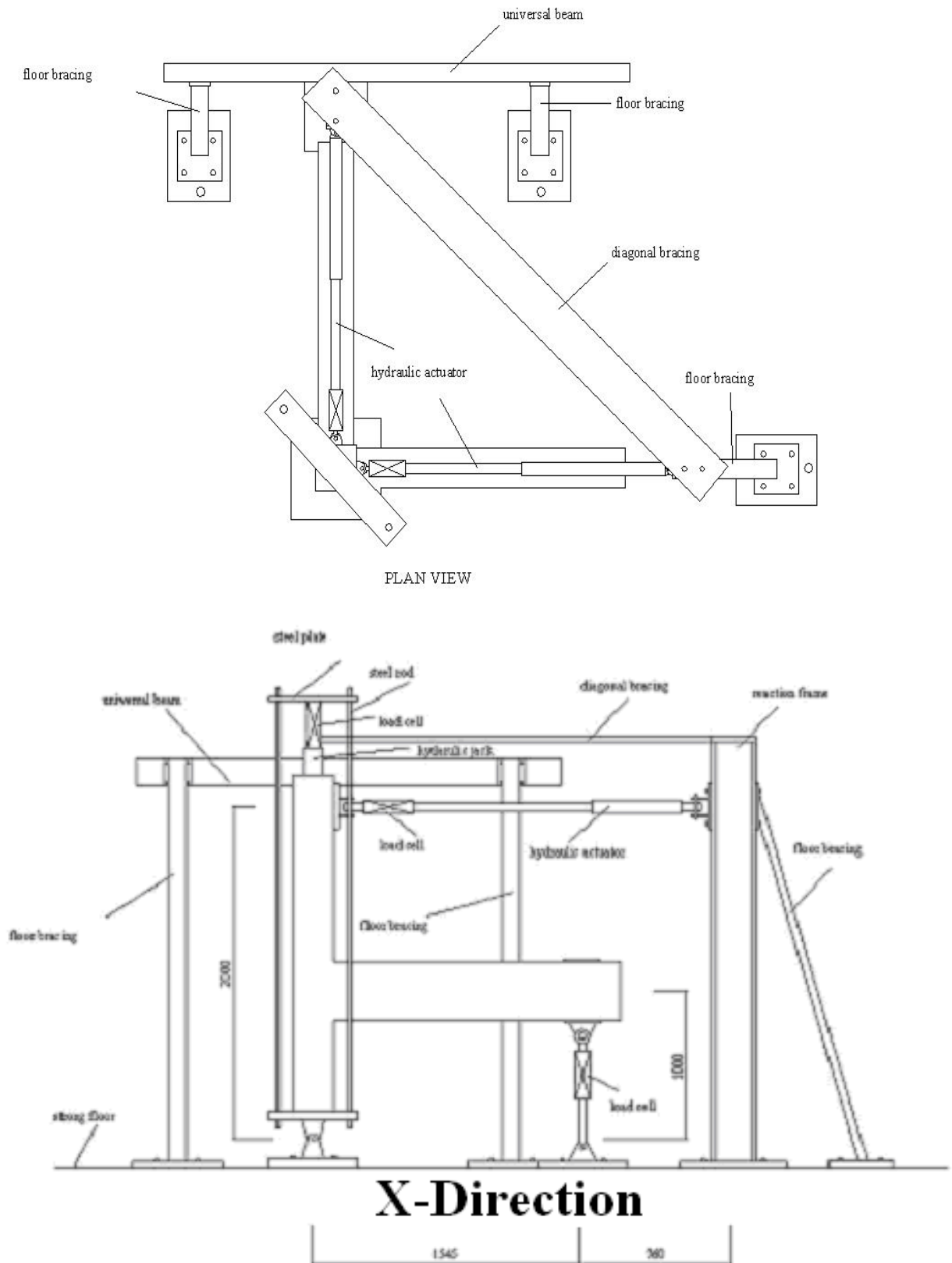


Figure 3.20 Details of space frame test rig

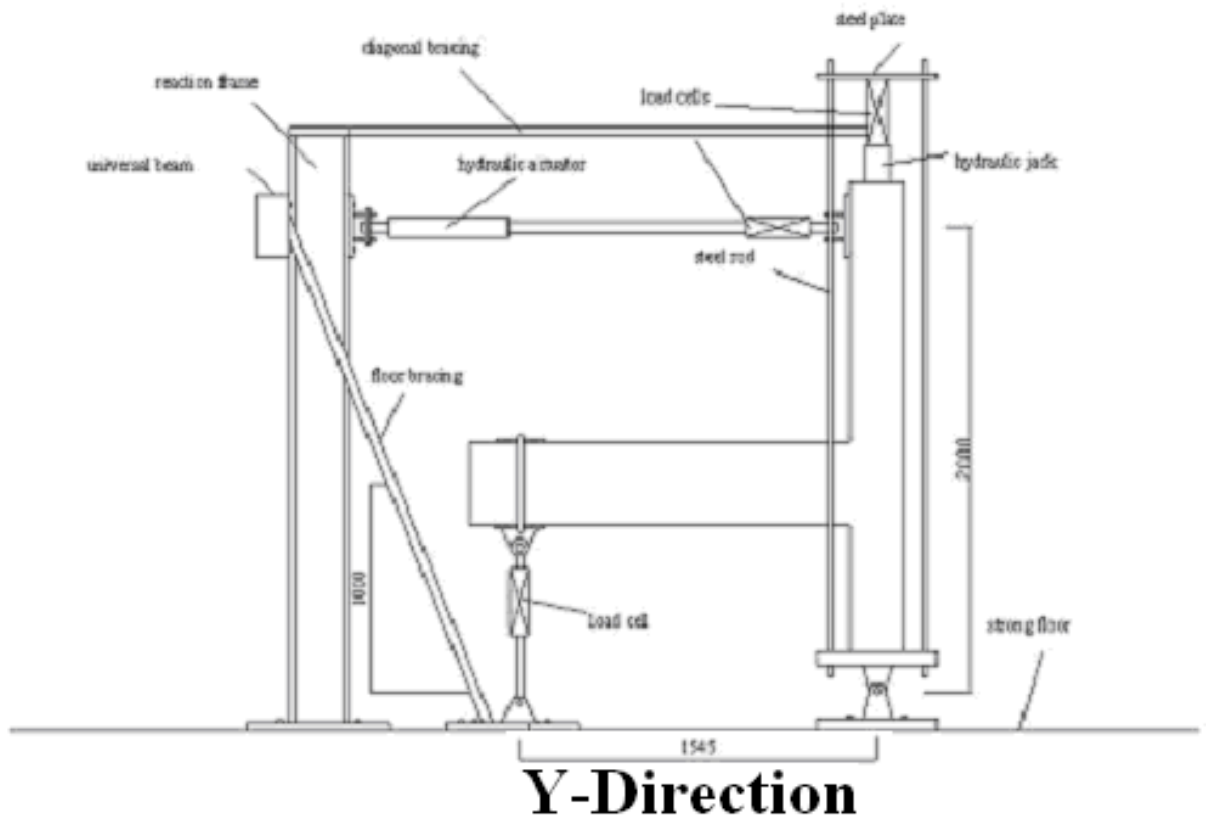


Figure 3.20 Details of space frame test rig (continued)

3.3.2 Instrumentation Setup

The lateral cycles of displacement and varying axial load were applied on the top of the column. Initial axial load, 75 kN, scaled from the dead and live load typically applied to the corner column of the structure, represents the gravity load on the column and was varied in proportion of lateral force with the equation:

$$N(kN) = 75 \pm 1.8 * F_x \quad (1)$$

where F_x is the lateral force. The constant number of 1.8 was determined from the relationship between the lateral load and the shear acting in the column. The relationship is shown in Fig. 3.21.

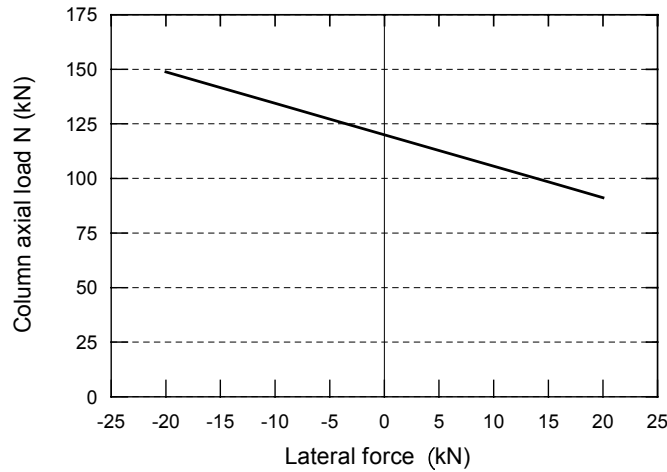


Figure 3.21 Axial loading variation related with lateral force

3.3.2.1 Hydraulic Actuator

The 450 mm stroke with 100 kN loading capacity hydraulic actuator was used to apply the lateral load to the column. The actuator was attached to the reaction frame using high strength bolts and connected to the column using pin connection.

In the space frame test, an additional 300 mm stroke with 100 kN loading capacity hydraulic actuator was used for the Y direction. Valve controllers, attached on the hydraulic actuators were used to control the lateral loading automatically. The lateral loading direction was the interaction between the two hydraulic actuators.

3.3.2.2 Hydraulic Jack

To apply the varying axial load on the column, a hydraulic jack was attached on the top of the column. The jack was clamped to the column top using a steel plate with a ball joint and two steel rods attached to the hinge to allow it to rotate with the column.

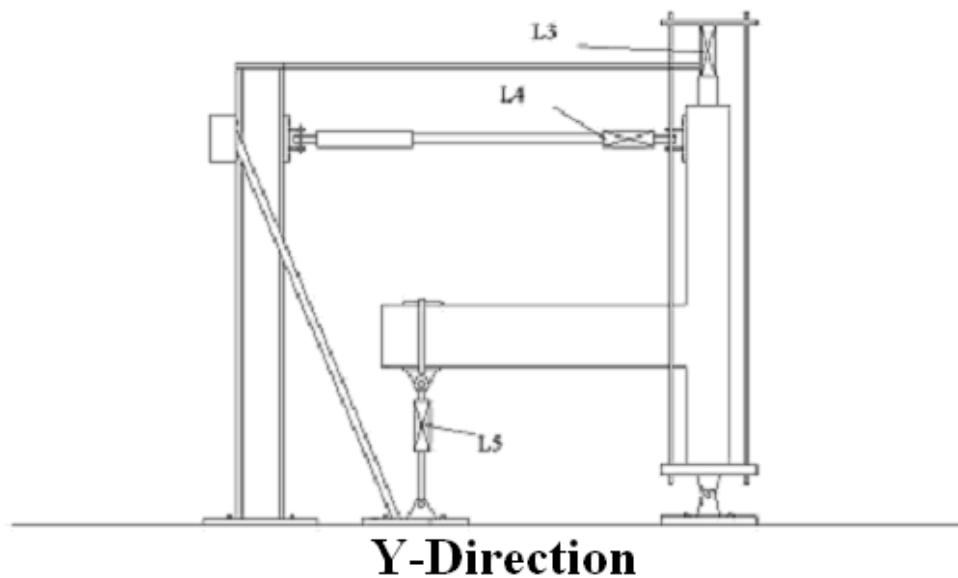
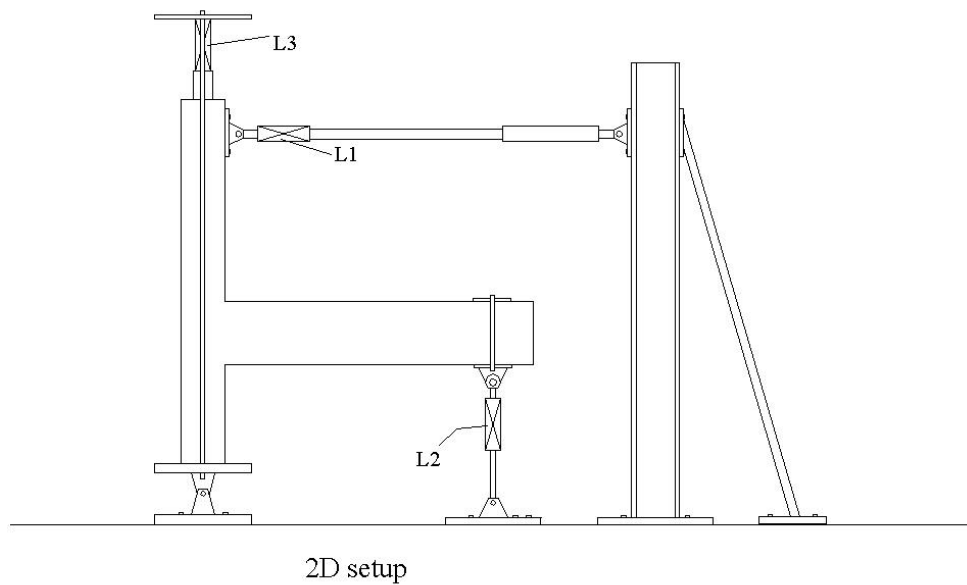
A controller for the hydraulic jack was also used in the space frame test to control the axial load automatically. The axial load changed according to the lateral load force, so the controller automatically read from the hydraulic actuators and send the command to the hydraulic jack controller.

3.3.2.3 Load Cells

For each exterior one-way beam-column joint unit, three load cells were used to measure loads. Load cells L1 and L3 were used to measure the lateral and axial loads applied to the column. L1 was attached on the end of the hydraulic actuator, while L3

was attached to the hydraulic jack. Load cell L2 was attached on the pin connection at the free end of the beam to measure the beam end shear force.

For each corner two-way beam-column joint unit, two load cells had to be added in the transverse direction. Load cell L4 was attached on the end of the hydraulic actuator to measure the lateral load applied to the column, while load cell L5 was attached on the pin connection at the free end of the beam to measure the beam end shear force. The load cells position for both setups is shown in Fig. 3.22.



NOTE:

The plane frame setup is the same with the X direction of the space frame setup

Figure 3.22 Positions of load cells

3.3.2.4 Potentiometers

Fourteen potentiometers were used for all one-way beam-column joint tests. One linear potentiometer of 200 mm travel, h_1 was used to measure the horizontal movement of the column. To measure the horizontal displacement at the free end of the beam, a linear potentiometer with 100 mm travel, h_2 was used. Twelve small linear potentiometers with ball joint connections at the ends and 30 mm of travel were used to measure the deformation in the member. Two potentiometers were attached on the joint panel area at one end and the beam plastic hinge region in the other end to measure the beam deformation relative to the joint. Two other potentiometers were attached on the column above and below the joint panel area at one end and the joint panel area at the other end to measure the column deformation relative to the joint. The rest of the potentiometers were attached in the joint panel area to vertically, horizontally and diagonally to measure the joint deformation. Details and dimensions of the potentiometers position are shown in Fig. 3.23 and Fig. 3.24.

Rotary potentiometers, R_1 and R_2 were used for all two-way beam-column joint tests, replacing the linear potentiometer to measure the top column displacement, due to the use of the controller. They were attached to a rigid frame in some distance from the column and connected to the column using a thin string. One linear potentiometer with 120 mm travel, h_3 and another 12 small linear potentiometers with 30 mm travel were added to measure the displacement at the free end of the beam and the deformation of the members in the joint region. Fig. 3.25 and Fig. 3.26 show the dimensions and details of the potentiometer positions for the space frame test setup.

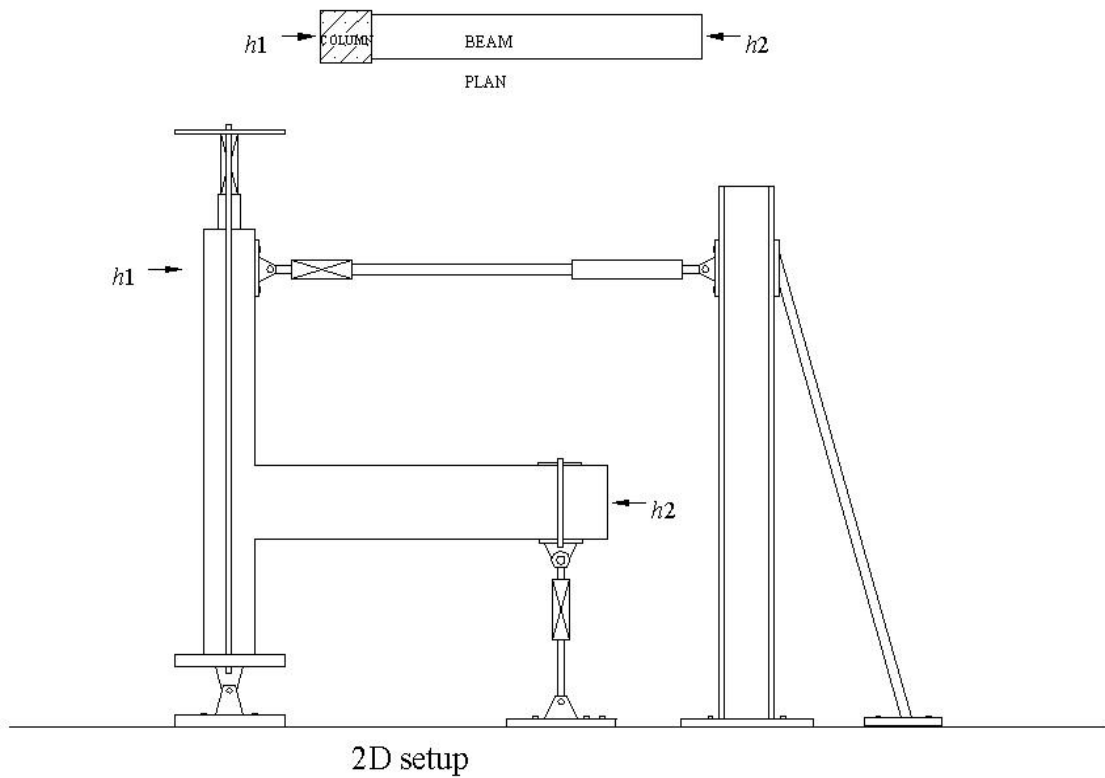


Figure 3.23 Positions of potentiometers h_1 and h_2 in plane frame setup

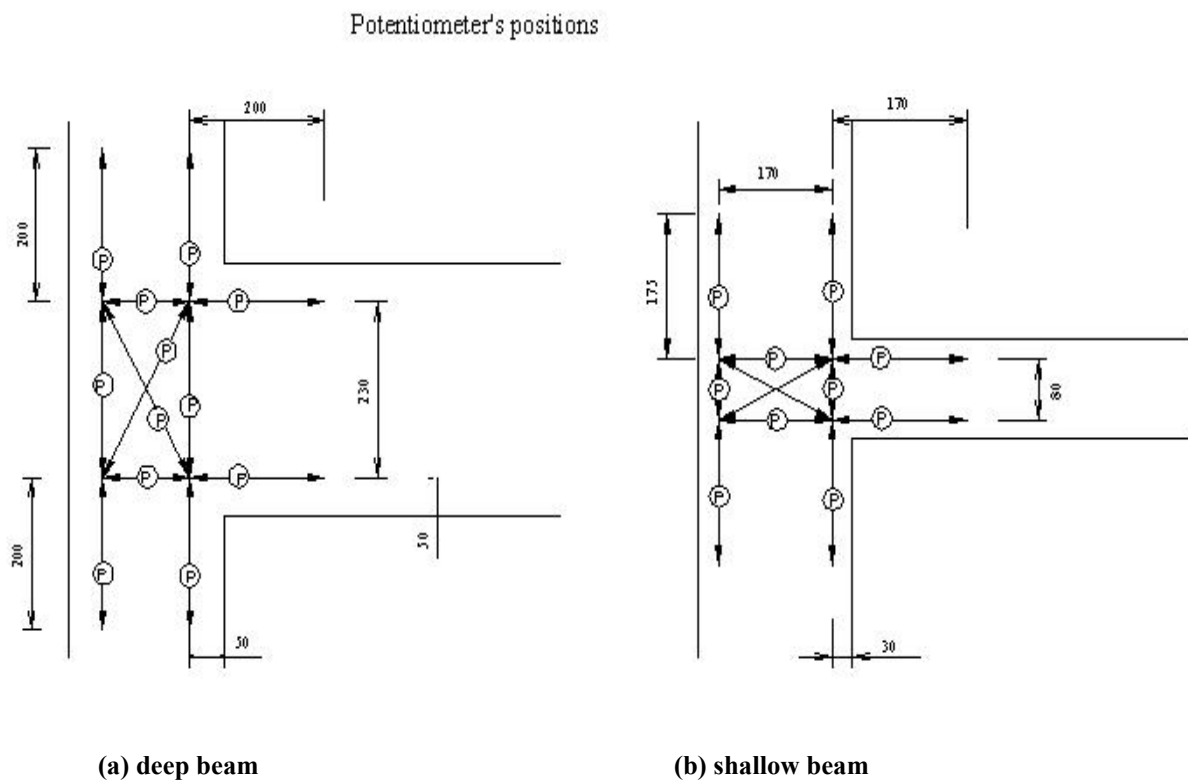


Figure 3.24 Positions of potentiometers in joint area in plane frame setup

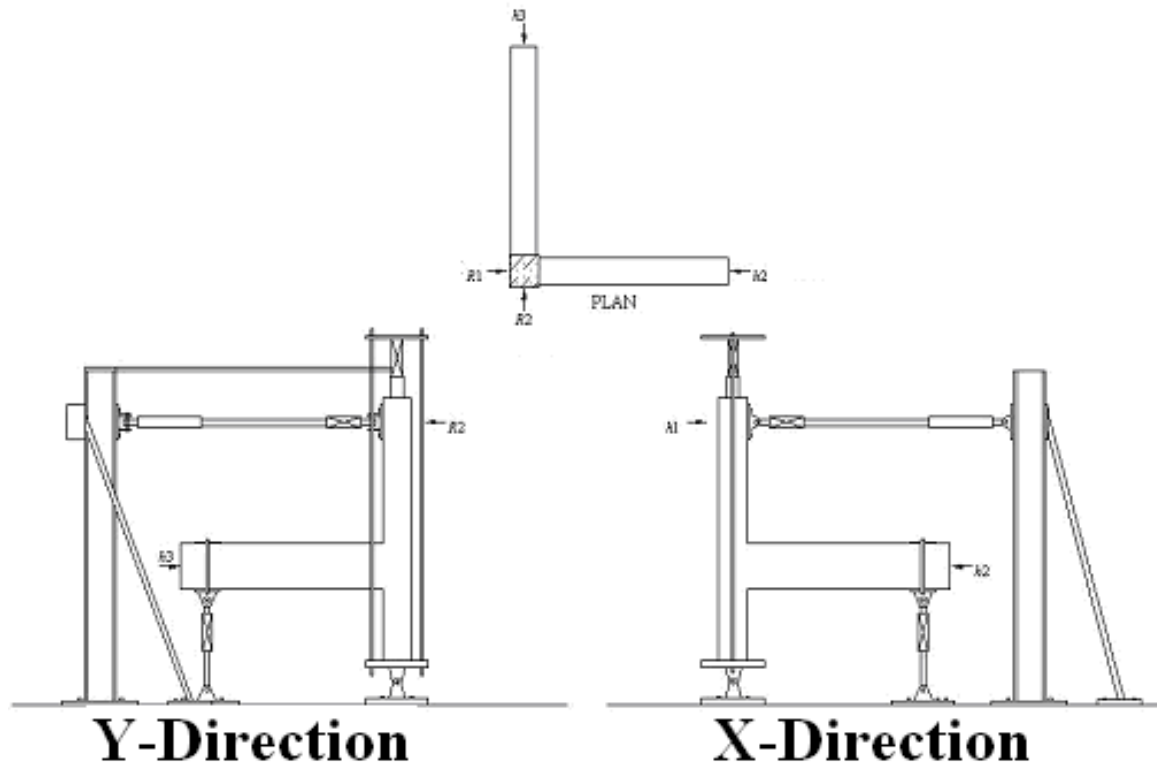
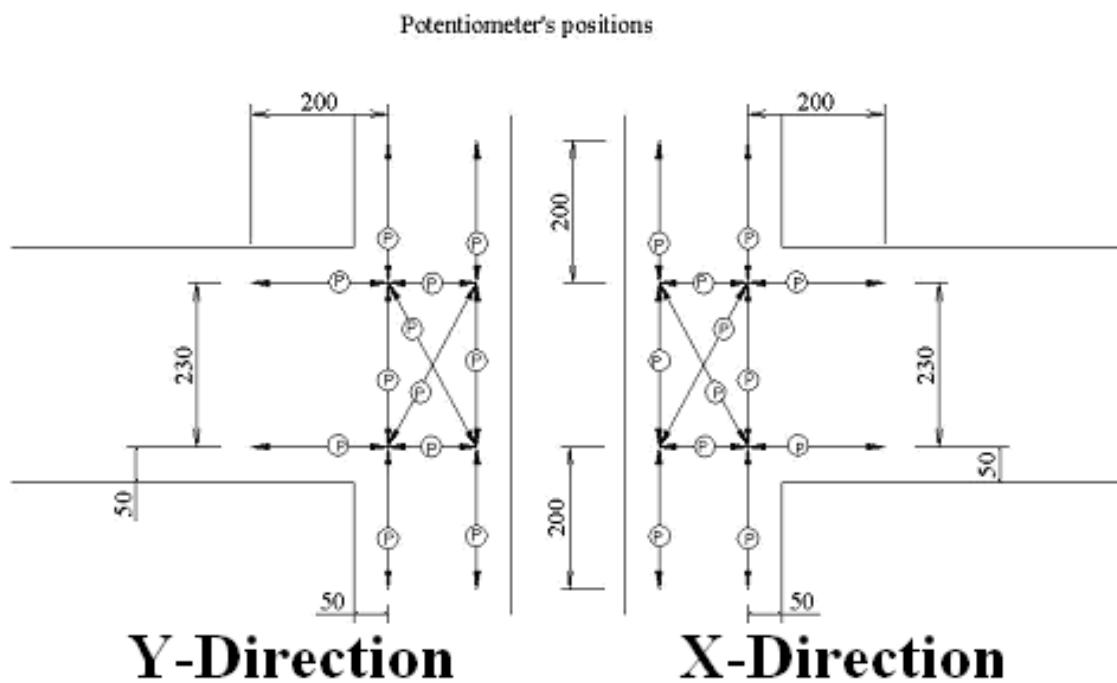
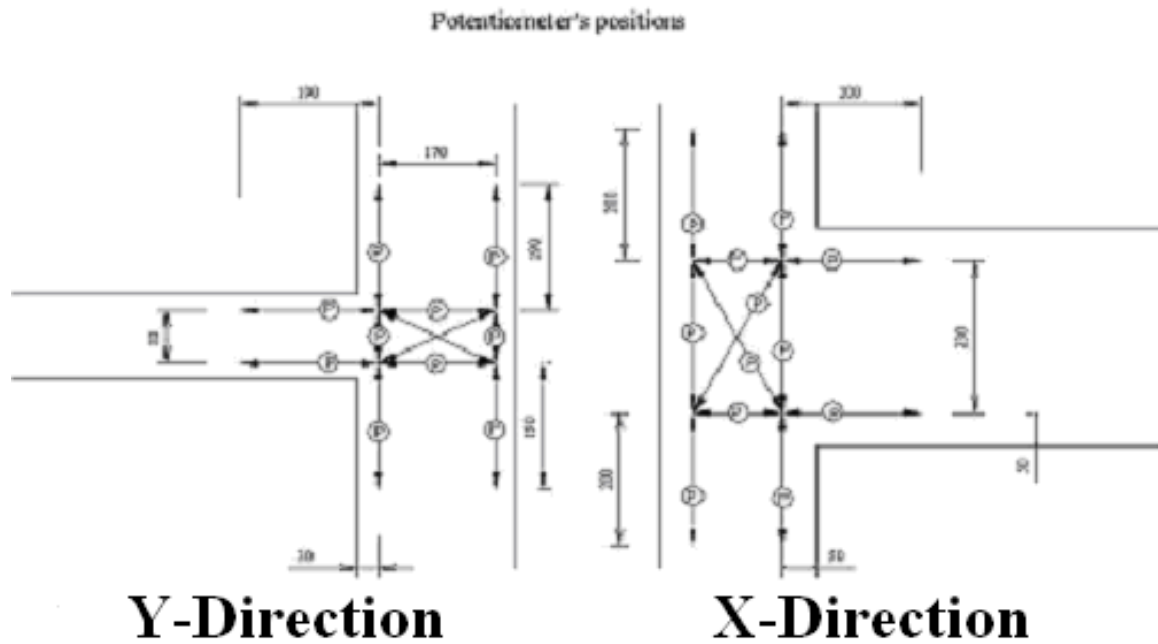


Figure 3.25 Positions of potentiometers R_1 , R_2 , h_2 and h_3 in space frame setup



(a) Units DD-1 and DD-2

Figure 3.26 Positions of potentiometers in joint area in space frame setup



(b) Unit DS

Figure 3.26 Positions of potentiometers in joint area in space frame setup (continued)

3.3.2.5 Strain Gauges

TML 120-ohm electrical resistance strain gauges (Type FLA-3-11-3L) were used to measure the reinforcement strains. The electrical strain gauges were attached to the sides of the bars, assumed to be their 'neutral axis'. Arrangement of electrical strain gauges for the four one-way exterior beam-column joint units with deep beam (TDP-1, TDP-2, TDD-1 and TDD-2) is shown in Fig. 3.27 to 3.30. The arrangement of the strain gauges for the two one-way exterior beam-column joint units with shallow beam (TSP-1 and TSD-1) is slightly different due to the number of longitudinal reinforcement in the beam, and is shown in Fig. 3.31 and 3.32. Twenty strain gauges were used to monitor the steel strain variation along the longitudinal and transverse reinforcement in the beams and joints of each one-way exterior beam-column joint unit.

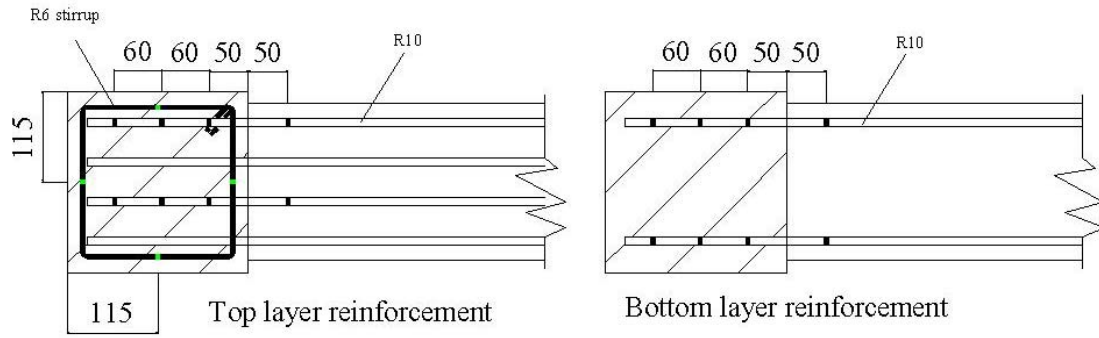


Figure 3.27 Positions of strain gauges for Unit TDP-1

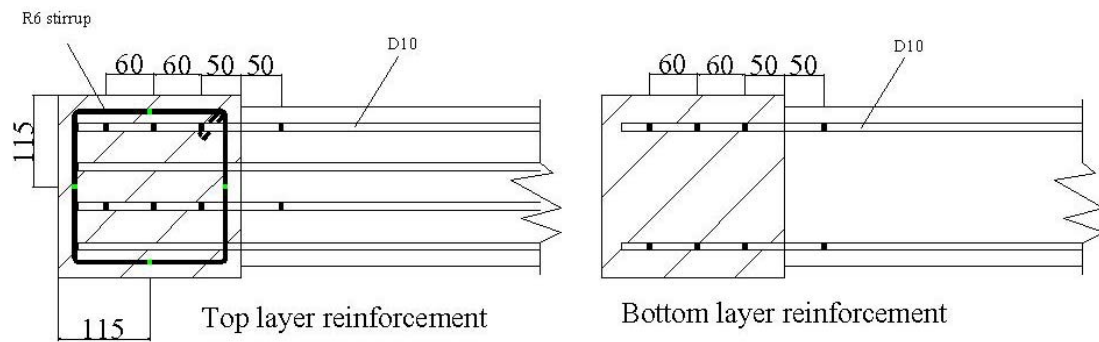


Figure 3.28 Positions of strain gauges for Unit TDD-1

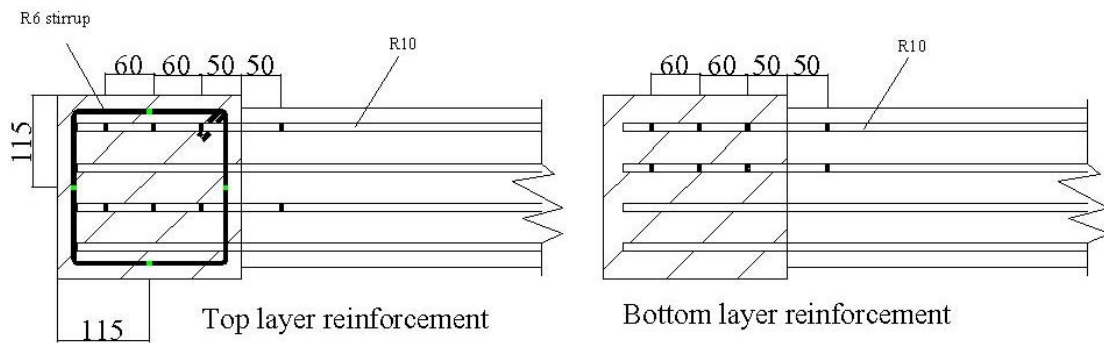


Figure 3.29 Positions of strain gauges for Unit TDP-2

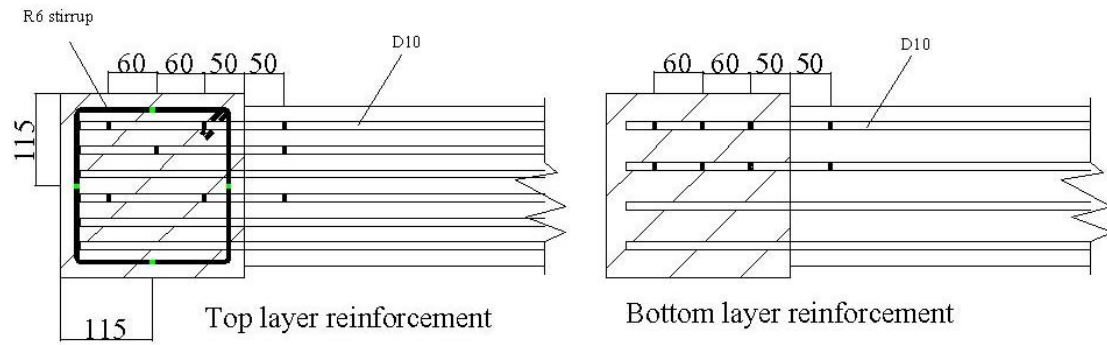


Figure 3.30 Positions of strain gauges for Unit TDD-2

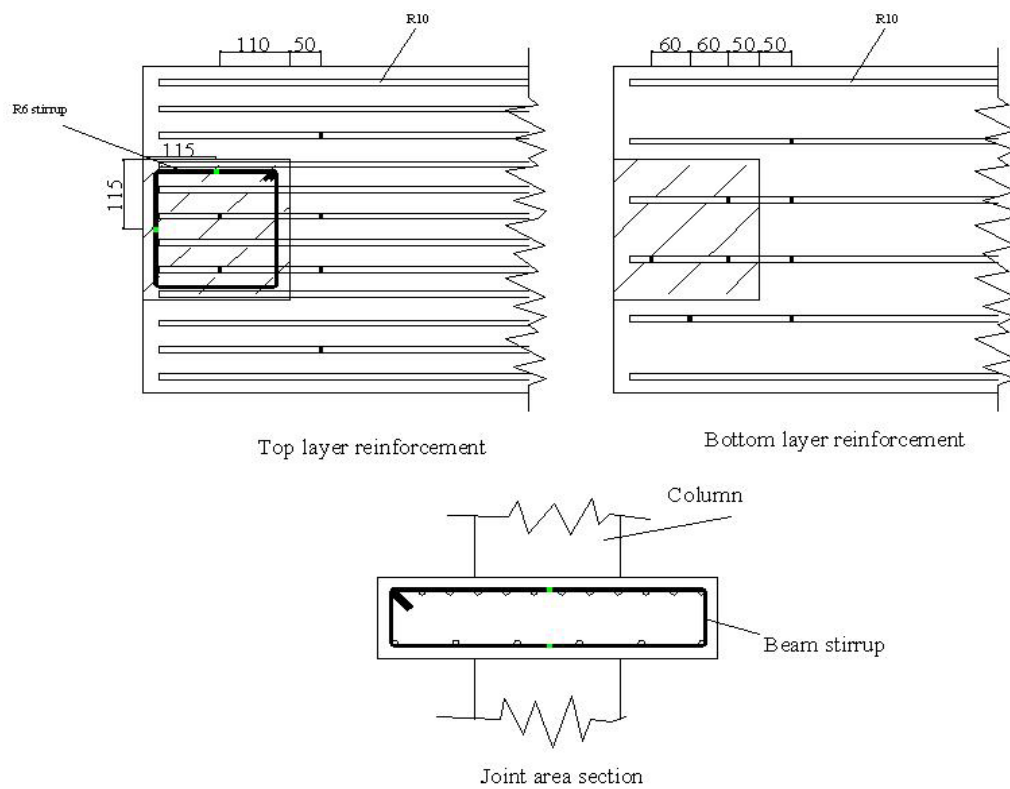


Figure 3.31 Positions of strain gauges for Unit TSP

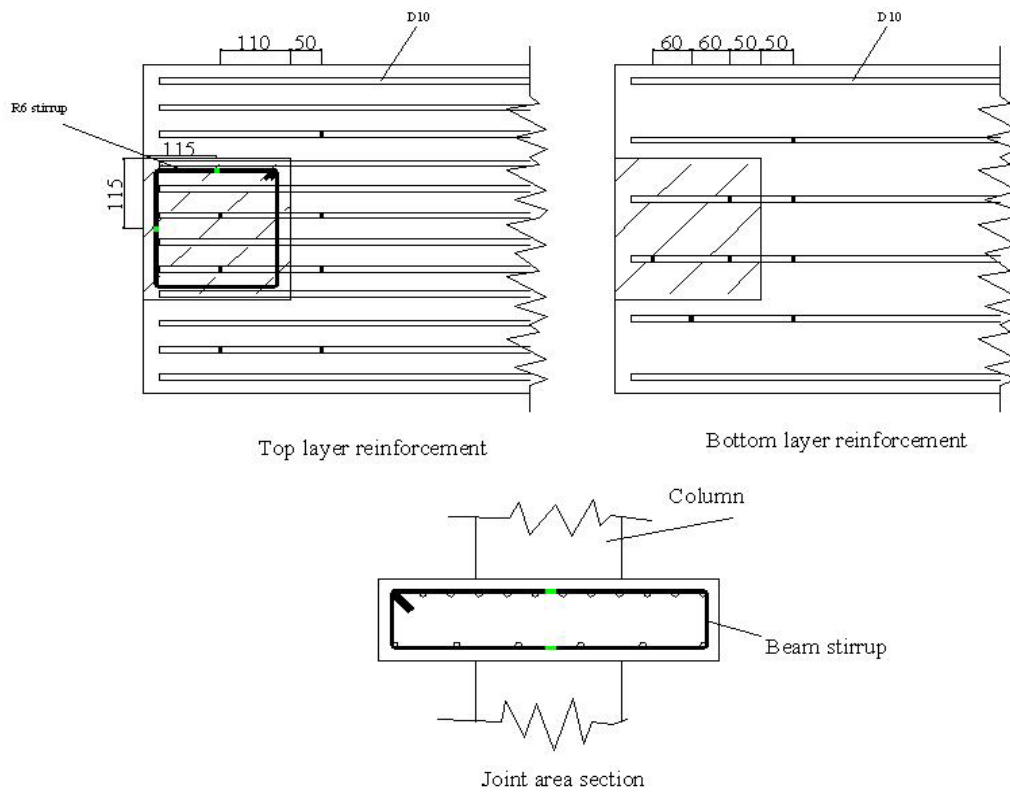


Figure 3.32 Positions of strain gauges for Unit TSD

For the two-way corner beam-column joint units, the arrangement of the strain gauges is similar as the one-way units according to the beam geometry, with the number of the strain gauges doubled. Thirty-six electrical resistance strain gauges for Unit DD-1, thirty-two electrical resistance strain gauges for Unit DD-2, and thirty-nine electrical resistance strain gauges for Unit DS were used to monitor the steel strain variation along the longitudinal and transverse reinforcement in the beams and joints. The position of the strain gauges used in Units DD-1, DD-2 and DS is shown in Fig. 3.33 to Fig. 3.35.

The electrical resistance strain gauges were attached to the sides of the bars, assumed to be their 'neutral axis' and concentrated within the joint region to carefully investigate the steel strains in the joint core.

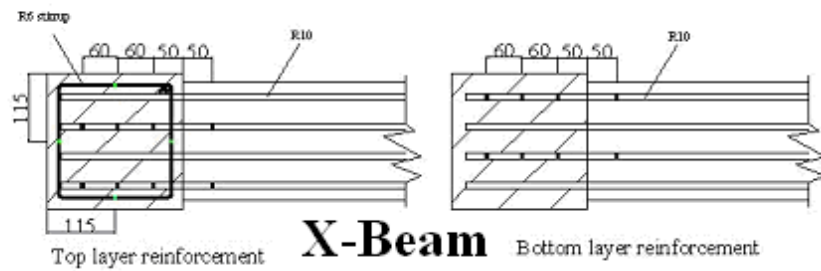
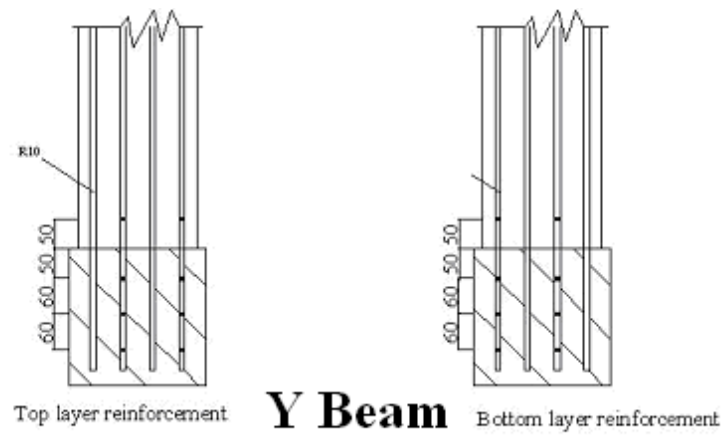


Figure 3.33 Positions of strain gauges for Unit DD-1

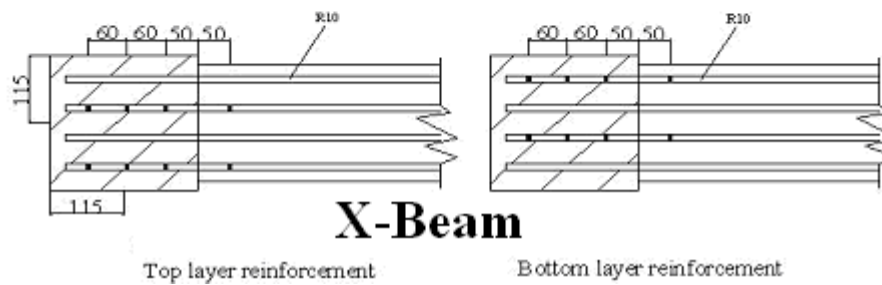
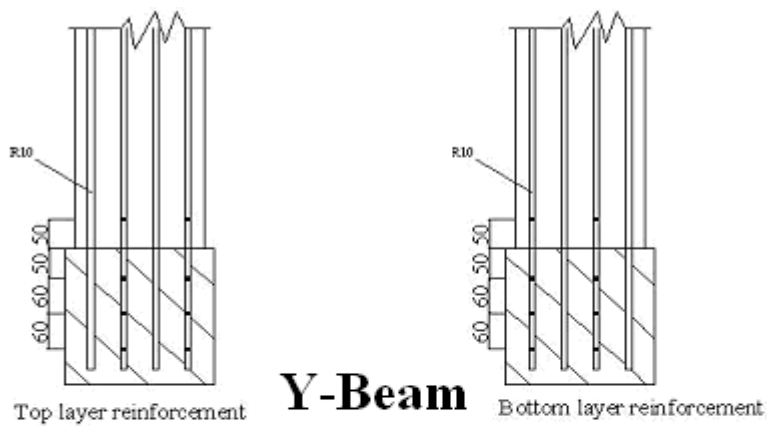
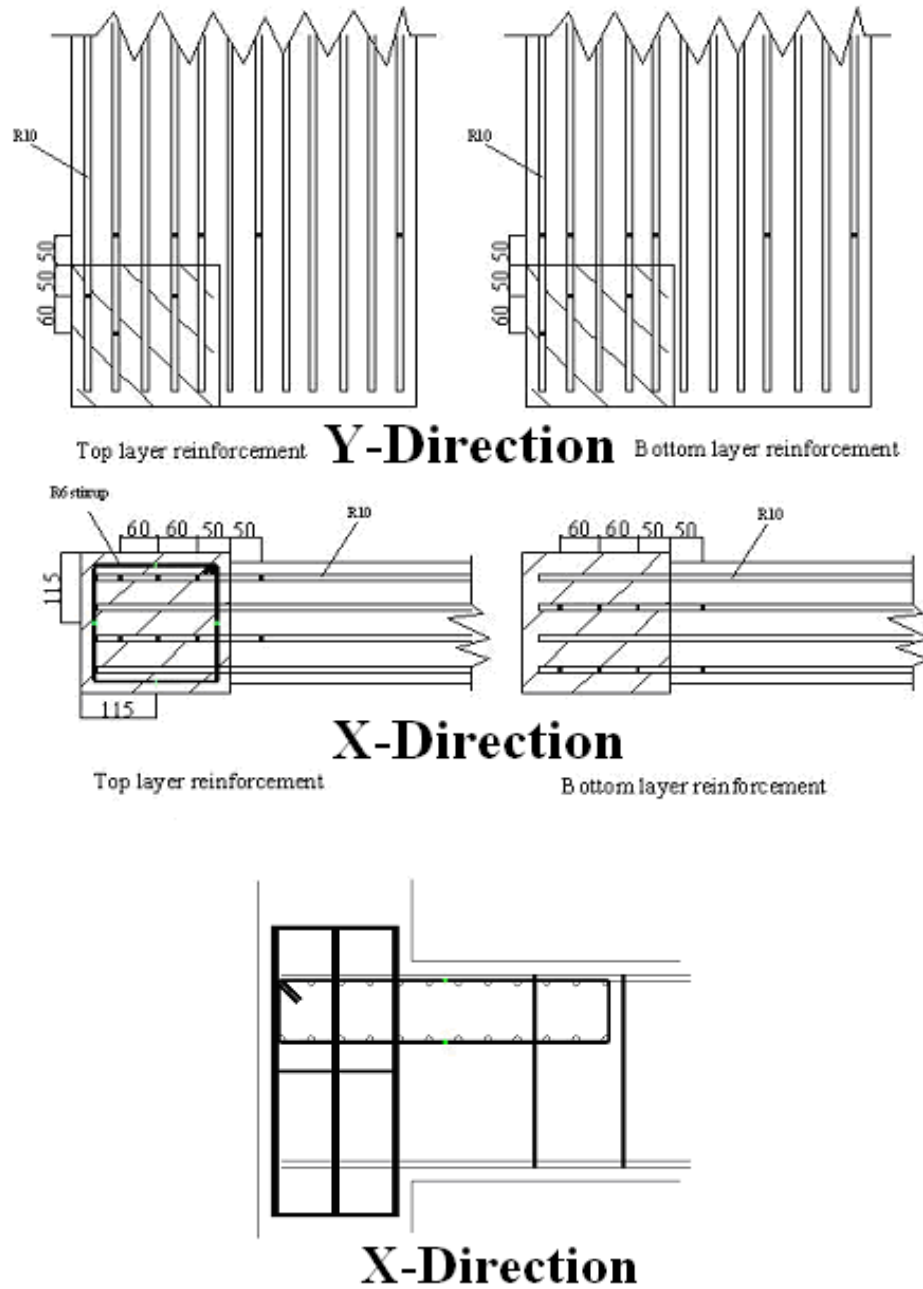


Figure 3.34 Positions of strain gauges for Unit DD-2



NOTE:

1. Two strain gauges were attached on the side of the Y beam stirrup in the joint area. The positions were in the middle top and middle bottom of the stirrup.
2. The first X beam stirrup to the column was not plot in the sake of clarity.

Figure 3.35 Positions of strain gauges for Unit DS

3.3.3 Loading Control

All the tests on the beam-column joint units used a cyclic lateral displacement control, which was applied on the column top. Axial load was also applied on the top of the

column, with 75 kN initial loads representing the gravity load. The axial load was then varied during the test in the proportion of the lateral load (Eq. 3.1)

3.3.3.1 Displacement Control for Plane Frame Tests

The lateral displacement cycle used for the tests started in small increments of 0.1% up to 0.2% drift ratio with a repeat of 2 cycles at each drift ratio, then to increase the lateral displacement in increment of 0.3% up to 0.5% drift, and finally to increase the lateral displacement in increments of 0.5% drift up to 3%, then to 4% ratios with a repeat of 2 cycles and 1 small cycle of 0.2% drift at the end for each drift ratio. The small cycles are required by the current code for the plastic region of the behaviour. Drift ratio is the ratio of the relative displacement between the ends of the column divided by the distance between these ends. The lateral displacement history is shown in Fig. 3.36.

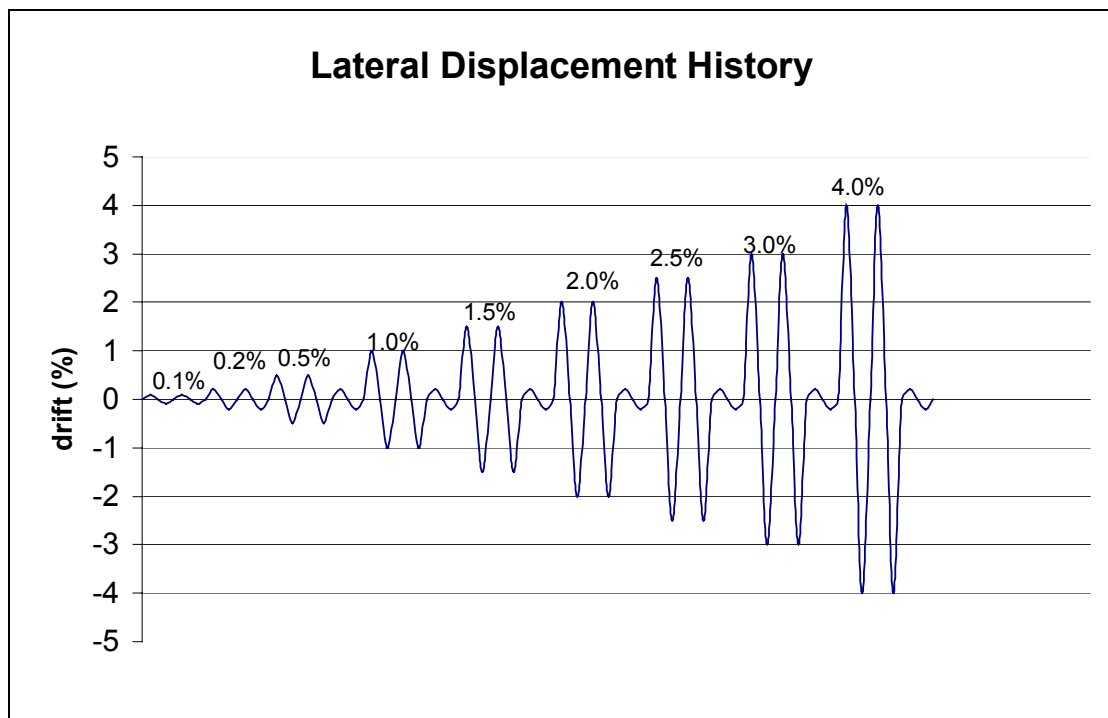


Figure 3.36 Lateral displacement history

Initial axial load with the value of 75 kN was applied on the top of the column before the lateral displacement started, to represent the gravity load. Since, the axial load was varied in proportion of the lateral load; the axial load history has the same cycle with the lateral displacement history.

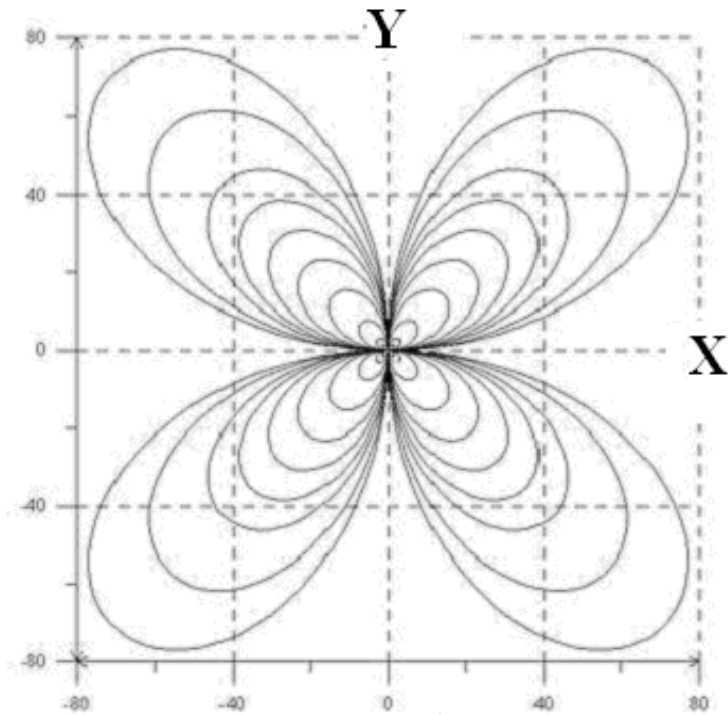
Hydraulic actuator and hydraulic jack were used to apply each lateral displacement and axial load. The loadings were controlled manually by reading the measurement from the potentiometer on the top of the column. The hydraulic actuator was run using a hydraulic motor, while the hydraulic jack was pumped by hand.

3.3.3.2 Displacement Control for Space Frame Tests

The lateral displacement used for the space frame tests was chosen to model as realistic as possible to the behaviour of a column in the structure during earthquake (Fig. 3.5). The direction of the displacement was the combination of X and Y directions, not focused on one direction only. Target drift used for the test was the ratio of resultant of the two directions to the height of the column. The cloverleaf shape displacement history was chosen and is shown in Fig. 3.37.

An automatic controller program was used to improve the accuracy of the test. The rotary potentiometers on the top of the column provide the information about the column displacement, which then later processed to give command to the valve on the hydraulic actuator for the movement and direction.

Axial load was also controlled automatically by using another controller on the hydraulic jack. Information from the load cells at the end of the hydraulic actuator was transferred to the program to later provide the command to the valve on the hydraulic jack.



NOTE:

1. The units are mm of displacement for both X and Y direction
2. The drift sequence was 0.1%, 0.2%, 0.5%, 1%, 1.5%, 2%, 2.5%, 3% and 4%

Y direction

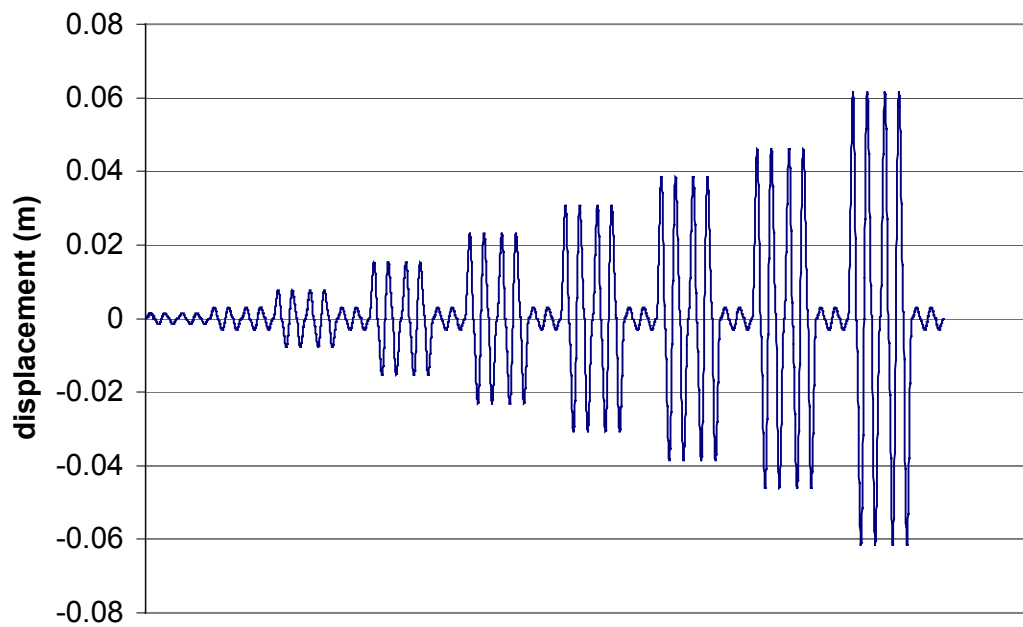
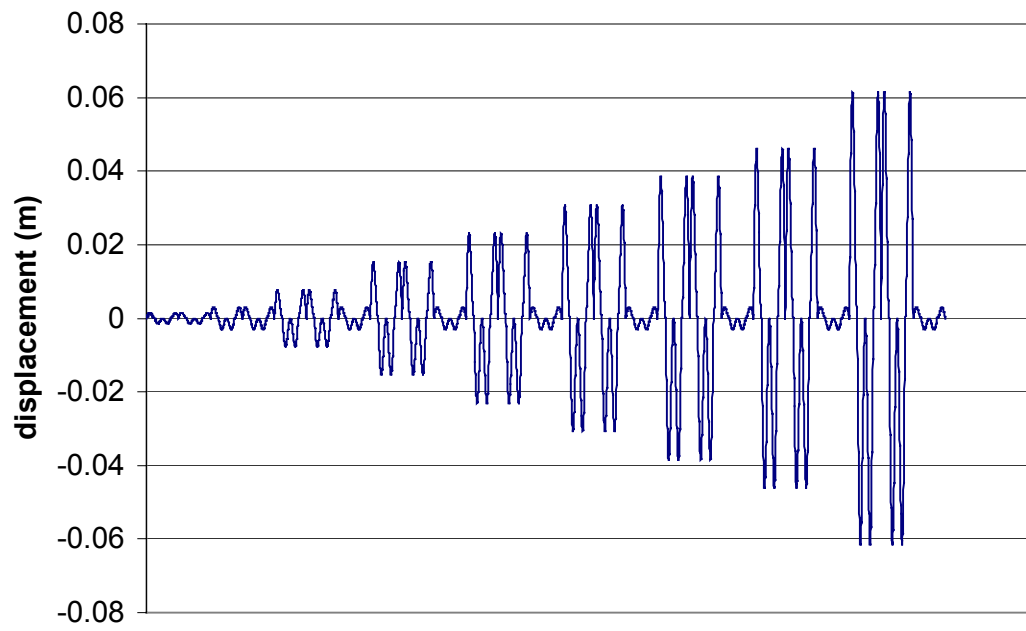


Figure 3.37 Bi-directional lateral displacement history

X direction**Figure 3.37 Bi-directional lateral displacement history (continued)**

CHAPTER 4

PLANE FRAME TEST RESULTS

4.1 INTRODUCTION

The plane frame test consists of six two-third scaled as-built reinforced concrete beam-column joint units, tested under simulated seismic loading with varying axial load on the column, using 75 kN as the initial axial load. The units were divided into two main categories according to the beam geometry, deep beams and shallow beams. The joint cores of all units contained single shear reinforcement, typical in pre-1970s construction. Tables 4.1 and 4.2 show the reinforcing details and material strength of the plane frame test specimens.

This chapter reports the results of the series of tests conducted on the plane frame units.

To clarify the signs and directions of the loading and the displacement, Fig. 4.1 shows the sign convention.

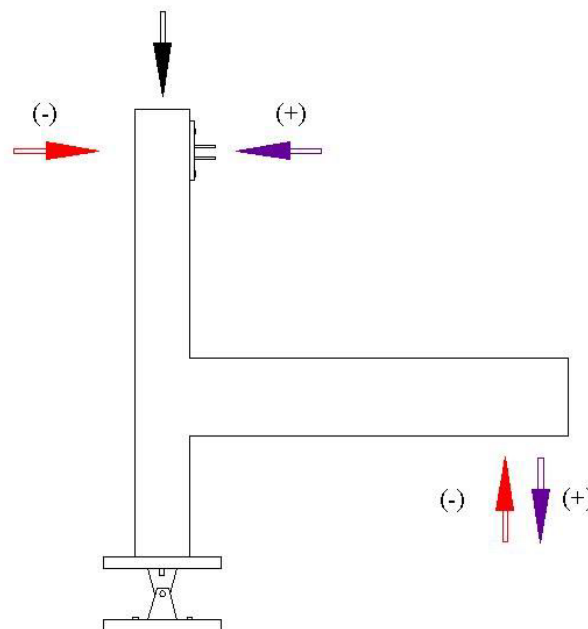


Figure 4.1 Positive loading and displacement

Test Unit	Bars type	Column			Beam		
		Dimension (mm ²)	Reinforcement		Dimension (mm ²)	Reinforcement	
			bars number (mm)	Stirrups		bars number (mm)	Stirrups
Unit TDP-1	Plain	230x230	6Φ10	Φ6-100	200x330	4Φ10 top - 2Φ10 bottom	Φ6-133
Unit TDD-1	Deformed	230x230	6Φ10	Φ6-100	200x330	4Φ10 top - 2Φ10 bottom	Φ6-133
Unit TSP	Plain	230x230	6Φ10	Φ6-100	130x535	12Φ10 top - 6Φ10 bottom	Φ6-133
Unit TSD	Deformed	230x230	6Φ10	Φ6-100	130x535	12Φ10 top - 6Φ10 bottom	Φ6-133
Unit TDP-2	Plain	230x230	6Φ10	Φ6-100	200x330	4Φ10 top - 4Φ10 bottom	Φ6-133
Unit TDD-2	Deformed	230x230	6Φ10	Φ6-100	200x330	6Φ10 top - 4Φ10 bottom	Φ6-133

Table 4.1 Reinforcing details of plane frame test units

Test Unit	Concrete strength (fc')		age at test	Reinforcing bars strength (fy)		
	(MPa)			MPa		
	28 days	at test day		(days)	Plain Φ10	Deformed Φ10
Unit TDP-1	21.3	22.9	45	348.1	-	424.3
Unit TDD-1	21.3	23.1	50	-	326.3	424.3
Unit TSP	21.3	23.4	55	348.1	-	424.3
Unit TSD	21.3	23.6	59	-	326.3	424.3
Unit TDP-2	23.3	25	48	333.1	-	407.9
Unit TDD-2	23.3	24.7	56	-	353.7	407.9

Table 4.2 Material strength of plane frame test units

4.2 DEEP BEAMS

Four geometrically identical exterior beam-column joint units with deep beams, each different in reinforcement details, were constructed. The units are referred to as Units TDP-1, TDD-1, TDP-2 and TDD-2. Units TDP-1 and TDP-2 used plain round longitudinal reinforcement, while units TDD-1 and TDD-2 used deformed longitudinal reinforcement. Grade 300 plain round steel was used for the longitudinal and transverse reinforcement. The joint cores contained one transverse reinforcement, typical in pre-1970's building construction.

4.2.1 Unit TDD-1

Unit TDD-1 used deformed bars as the longitudinal reinforcement in the column and beam. The beam bars were bent 90 degrees into the joint core area. The aim of this test is to show the desirable seismic mechanism, with a plastic hinge forming in the

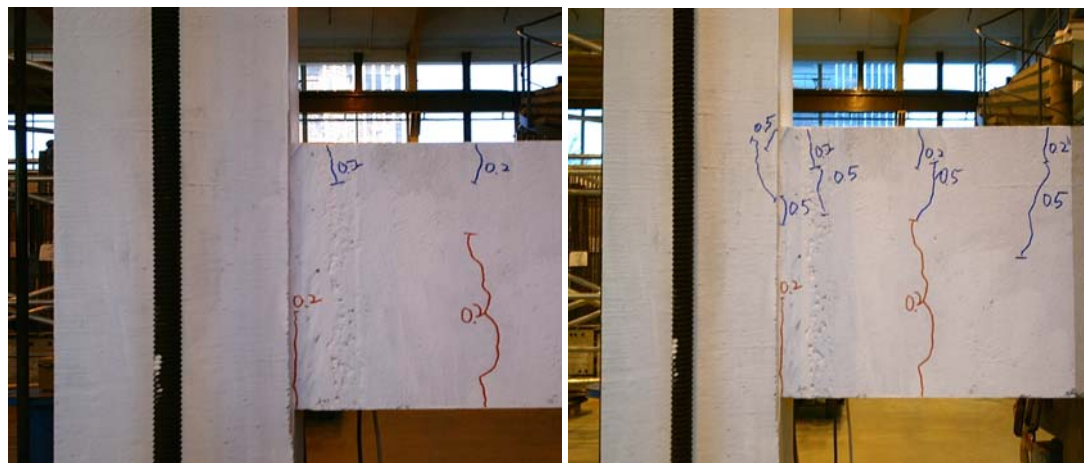
beam as calculated theoretically. Initial axial load of 75 kN was applied on the top of the column to represent the gravity load.

4.2.1.1 Crack Development and Damage

Flexural cracks at the beam bottom, the positive flexural reinforcement sides started to open at 0.2% of drift. For the negative side, the flexural cracks started to occur at 0.5% of drift. Horizontal cracks initiated at the outer layer of column longitudinal reinforcements just above the joint core at about 1.5% of drift due to the tension force from the beam longitudinal reinforcement in the joint core. These cracks later prompted angled cracks at the outer layer of the column due to lack of transverse reinforcement in the joint core to deal with the tension force from the beam longitudinal reinforcement. The existing cracks then extending and widening with the increase of the drift.

The concrete in the outer layer of the column was spalling at the end of test since the opening was really wide and the bond was totally destroyed. The unit reached its ultimate strength at about 2.5% of drift when the crack in the beam plastic hinge region became wider and caused the unit strength to degrade. The test was stopped at 3% of drift after one cycle, rather than 4% as planned because the strength degradation of the unit was so severe and the unit was considered near collapse.

Figure 4.2 shows the crack development and the final appearance of Unit TDD-1.

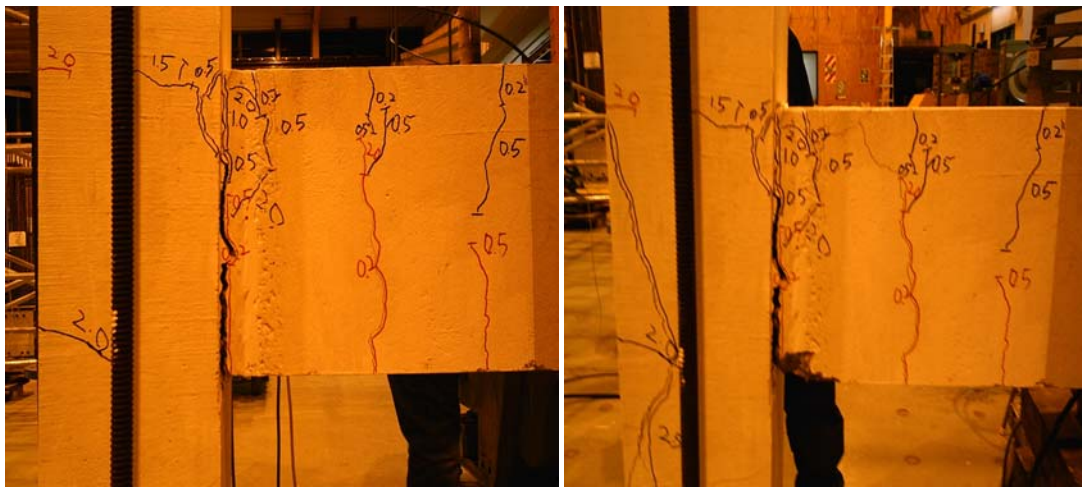


(a) At 0.2% of drift

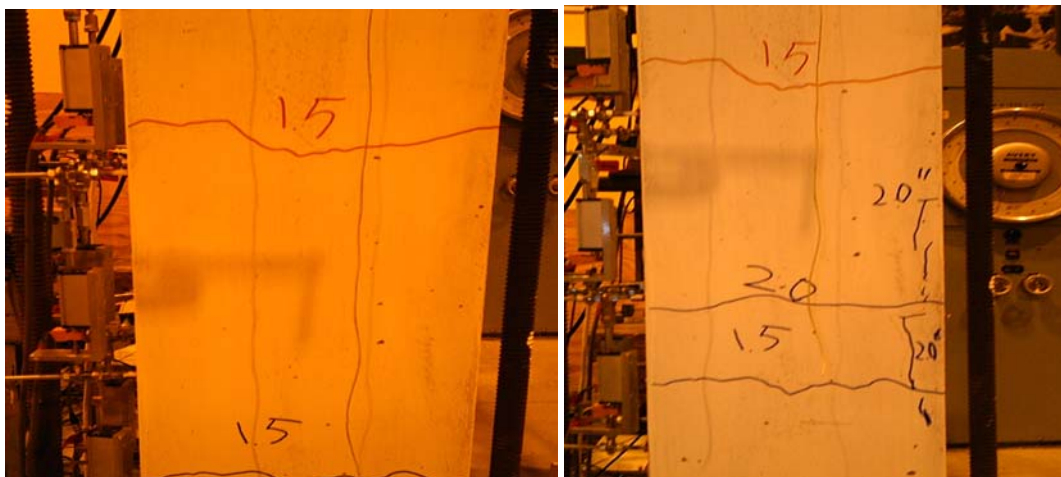
(b) At 0.5% of drift

Figure 4.2 Cracks development of Unit TDD-1

(d) At 1.5% of drift

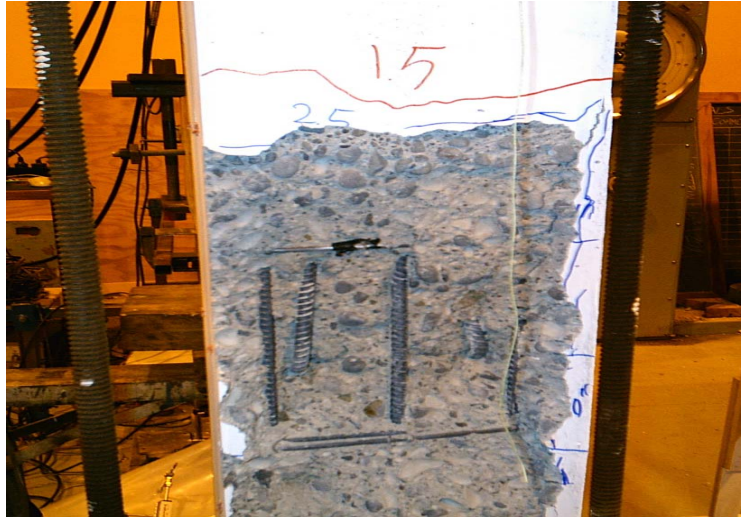


(f) At the end of test



(h) Column cracks at 2% of drift

Figure 4.2 Cracks development of Unit TDD-1 (continued)



(i) Column appearance at the end of test

Figure 4.2 Cracks development of Unit TDD-1 (continued)

4.2.1.2 Hysteretic Response

The lateral force versus the top column displacement of Unit TDD-1 is shown in Fig. 4.3. The beam started to form a plastic hinge at 0.6% and 0.4% of drift for positive and negative loading directions respectively. This is quite low compared to modern codes, which usually require the building to be designed for 2% of drift. The maximum lateral force that can be resisted by Unit TDD-1 was 16.8 kN and 10.2 kN for positive and negative loading directions respectively.

4.2.1.3 Displacement Components

The column at the start of the test governed the displacement of Unit TDD-1, until the plastic hinge formed in the beam and the beam started to govern. The joint's displacement contribution was really small (about 2%), since there was no critical deformation in the joint core. The maximum column displacement contribution was about 55% and the maximum beam displacement contribution was up to 80%. Figure 4.4 shows the members contribution of Unit TDD-1 total displacement.

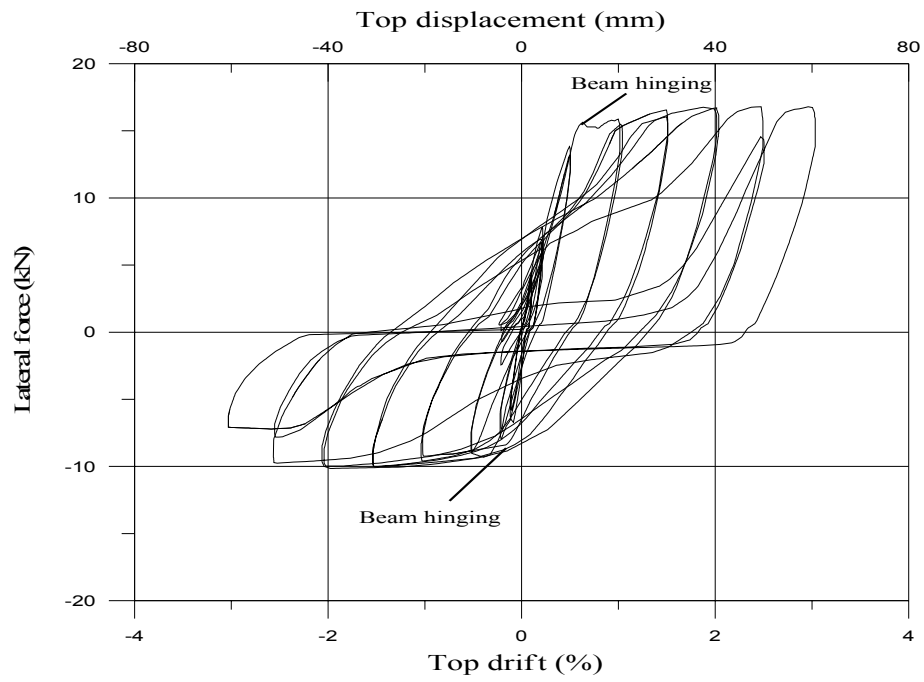
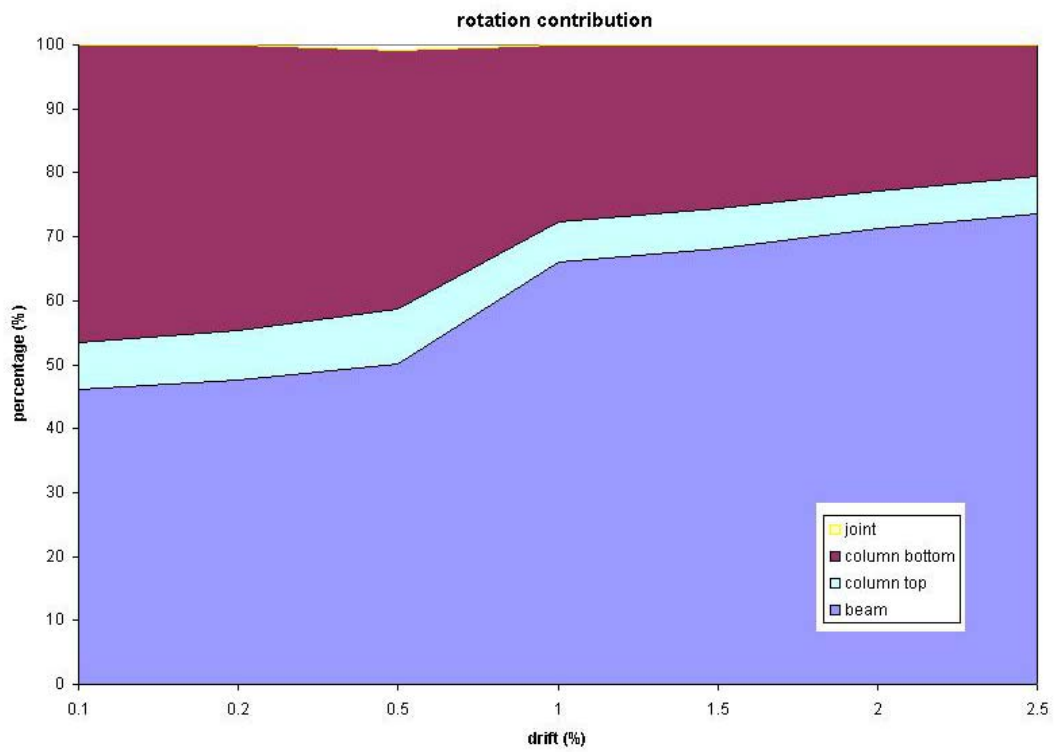
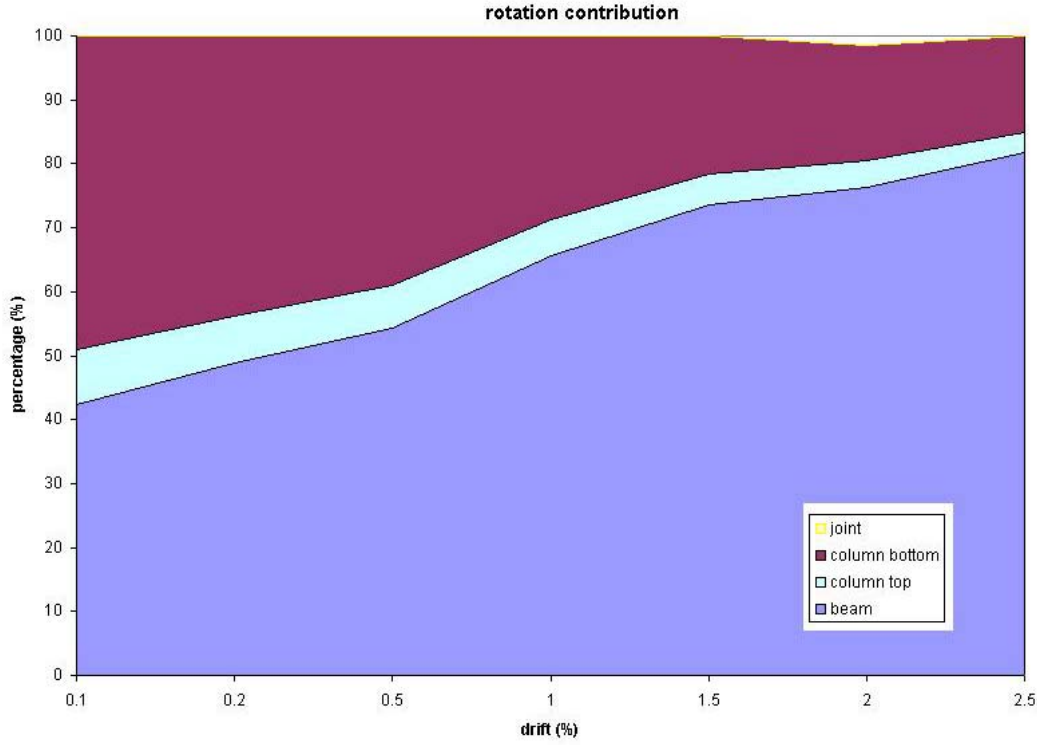


Figure 4.3 Lateral force versus Top displacement of Unit TDD-1



(a) positive loading direction

Figure 4.4 Members displacement contribution of Unit TDD-1



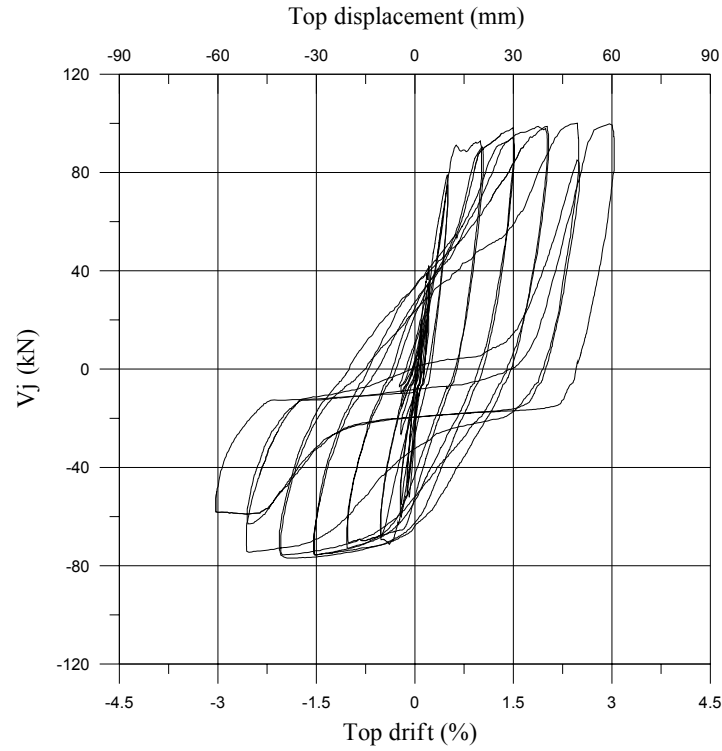
(b) negative loading direction

Figure 4.4 Members displacement contribution of Unit TDD-1 (continued)

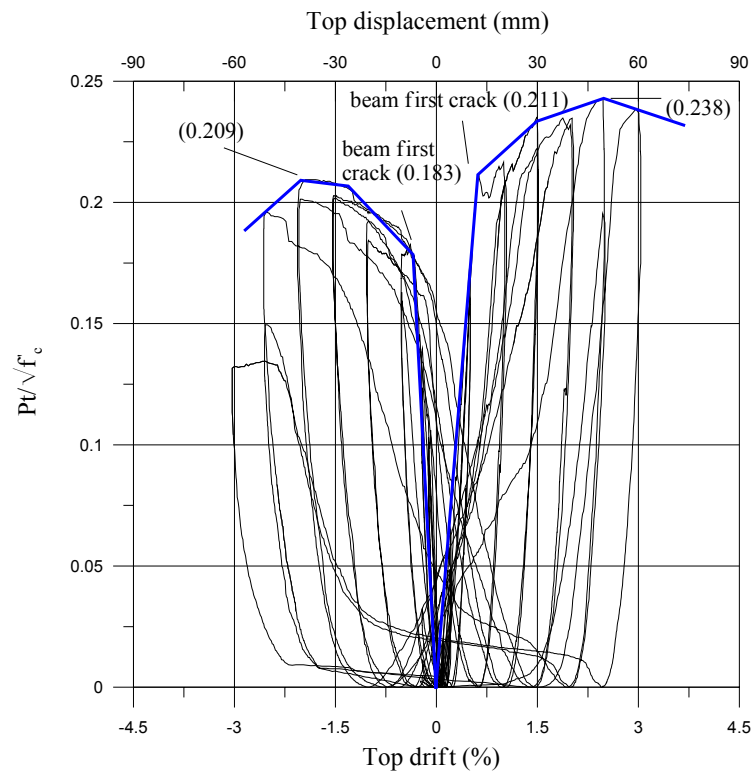
4.2.1.4 Force and Stress in the Joint

The beam was the critical member for Unit TDD-1, therefore there is no damage in the joint core. The forces in the joint were increasing up to the level when Unit TDD-1 suffered heavy damage and lost its strength. From that point, the forces in the joint started to degrade as the beam steel tension was reducing as well.

The horizontal shear in the joint area reached 100 kN and -77 kN in the positive and negative loading direction respectively. The principal tensile stress reached $0.238\sqrt{f'_c}$ and $0.209\sqrt{f'_c}$ in the positive and negative loading direction respectively. The axial load applied to the top of column was varied from $0.22\sqrt{f'_c}$ to $0.41\sqrt{f'_c}$. Figure 4.5 shows the joint horizontal shear force versus top drift (a) and the joint horizontal principal tensile stress versus top drift (b).



(a) Horizontal shear (V_j) versus Top drift of Unit TDD-1



(b) Principal tensile stress ($P_t/\sqrt{f'_c}$) versus Top drift of Unit TDD-1

Figure 4.5 Force and stress in the joint core of Unit TDD-1

4.2.1.5 Summary

Unit TDD-1, an as-built two third scale beam-column joint unit was tested under a simulated seismic loading with varying axial load. Initial axial load of 75 kN was applied representing the gravity load on the column. The deficiency of Unit TDD-1 is the lack of transverse reinforcement in the joint core.

From this test we can conclude:

1. Desirable mechanism under seismic loading

The unit developed the desirable mechanism under seismic loading which is to form a plastic hinge in the beam so that other members are safe from major damage. But on the other hand, the plastic hinge occurred too early compared to what is expected in modern codes, which is at 2% of drift.

2. Lack of transverse reinforcement in the joint

The concrete cover of column outer layer was spalling when the high level of drift was applied on the unit. The reason is because of not enough transverse reinforcement to confine the concrete under the beam steel tension force acting in the joint core.

4.2.2 Unit TDP-1

Unit TDP-1 used plain round bars as the longitudinal reinforcement in the column and beam. The beam bars were hooked in the joint core area. The aim of this test is to investigate the behaviour of the unit with different reinforcement detailing and anchorage. Initial axial load of 75 kN was applied on the top of the column to represent the gravity load.

4.2.2.1 Crack Development and Damage

An accident happened while preparing the test set up and caused a crack in the beam plastic hinge region at the bottom side. Therefore the mechanism of the unit was altered from joint shear hinge to beam plastic hinge.

Disregarding the initial crack from the accident, flexural cracks at the beam bottom, the positive flexural reinforcement side, at 1% of drift. For the negative side, the flexural cracks started to occur at 0.5% of drift. A diagonal crack in the joint core occurred at 1.5% of drift in the positive loading direction. Minor diagonal cracks

were spread in the joint core area due to the lack of transverse reinforcement in the joint. The existing cracks were extending and widening with the increase of drift.

The unit was loaded until 4% of drift when the unit strength reduced significantly due to the damage in the beam and joint area.

Figure 4.6 shows the crack development and the final appearance of Unit TDP-1.

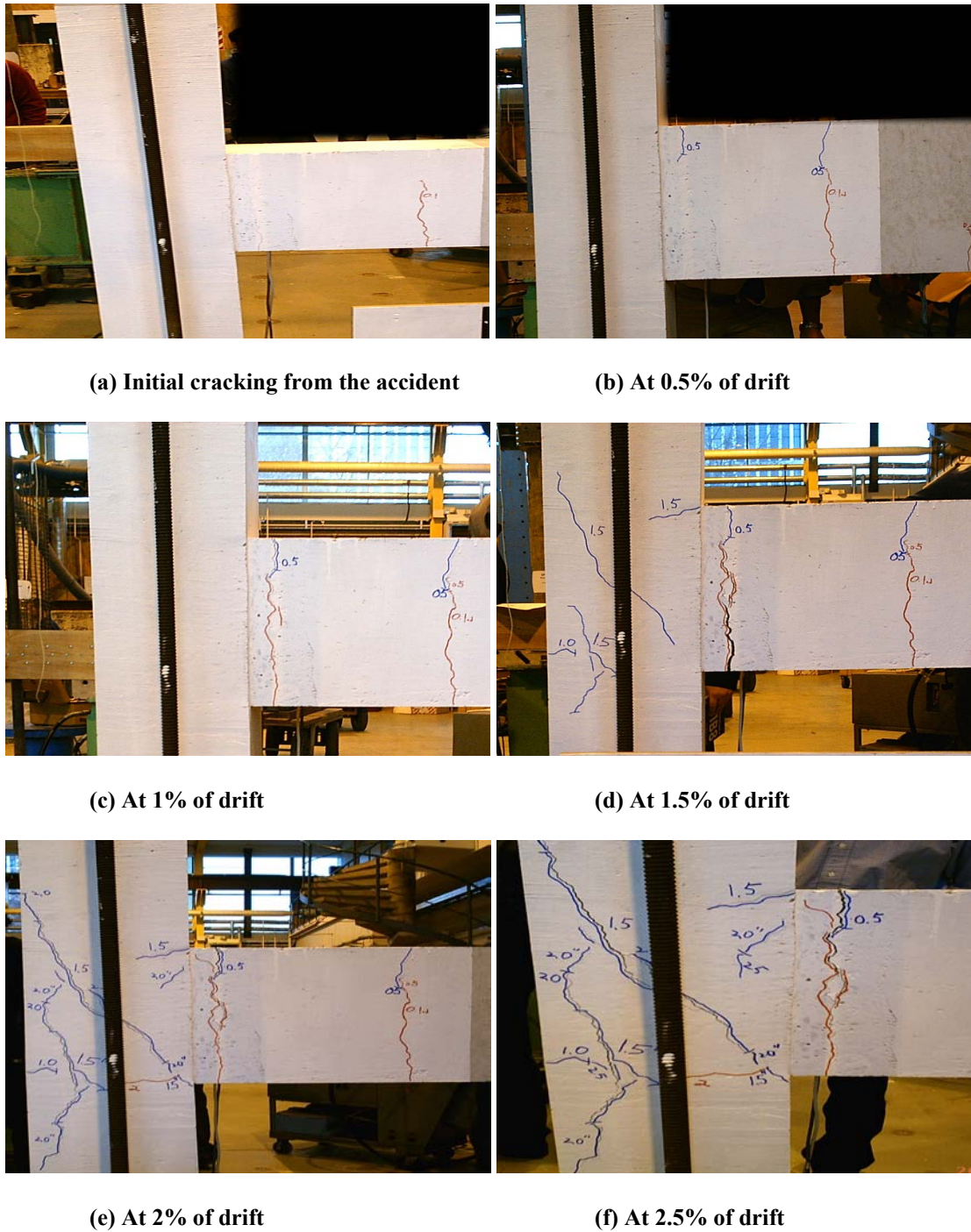
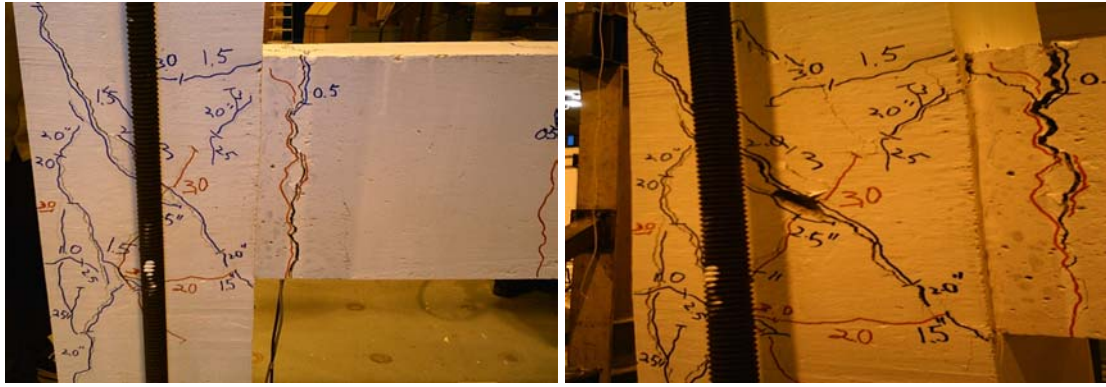


Figure 4.6 Cracks development of Unit TDP-1



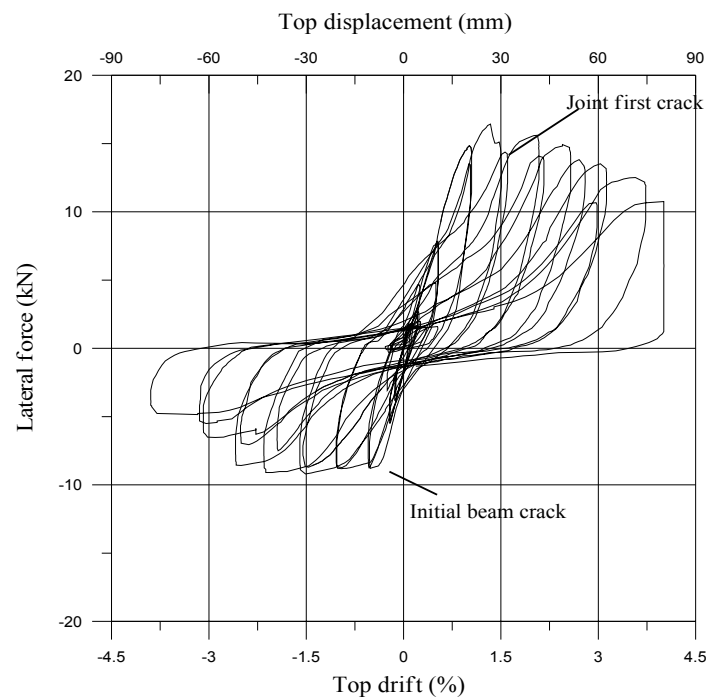
(g) At 3% of drift

(h) At the end of the test

Figure 4.6 Cracks development of Unit TDP-1 (continued)

4.2.2.2 Hysteretic Response

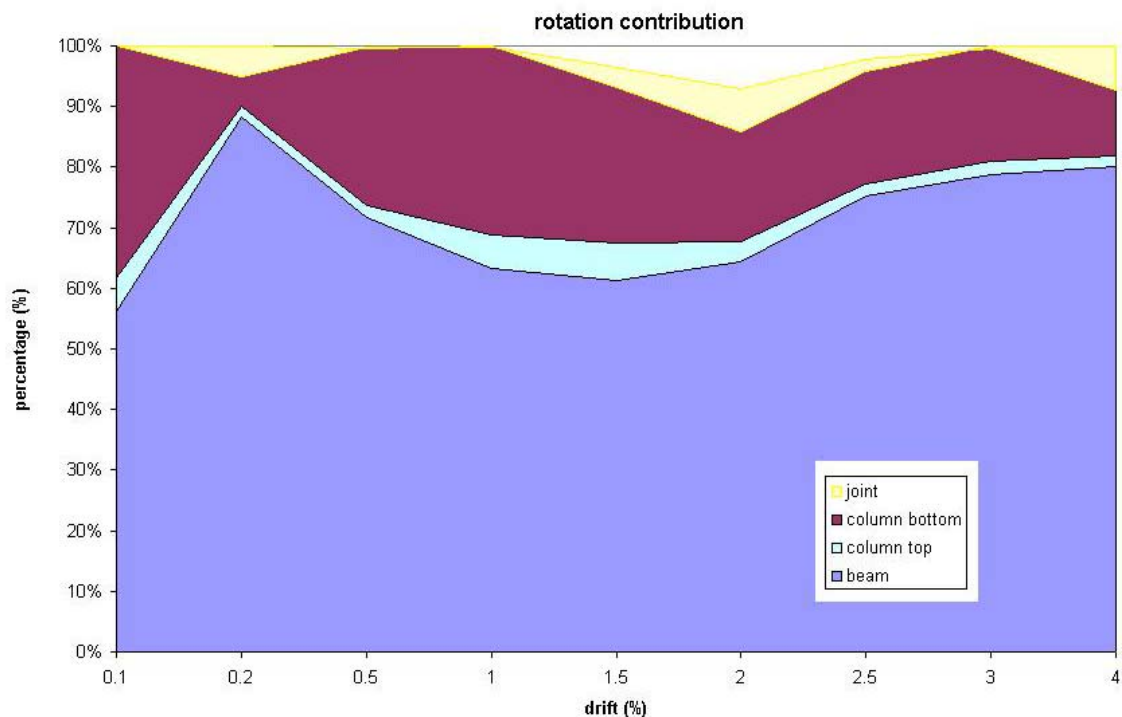
The lateral force versus the top column displacement of Unit TDP-1 is shown in Fig. 4.7. The initial beam cracking at the bottom caused the premature loss of strength of the beam in the negative loading direction. The beam positive longitudinal reinforcement yielded at about 0.4% of drift and the first joint cracking in the positive loading direction started to occur at 1.3% of drift. The maximum lateral force that can be resisted by Unit TDP-1 was 16.4 kN and 9.2 kN for positive and negative loading directions respectively.

**Figure 4.7 Lateral force versus Top displacement of Unit TDP-1**

4.2.2.3 Displacement Components

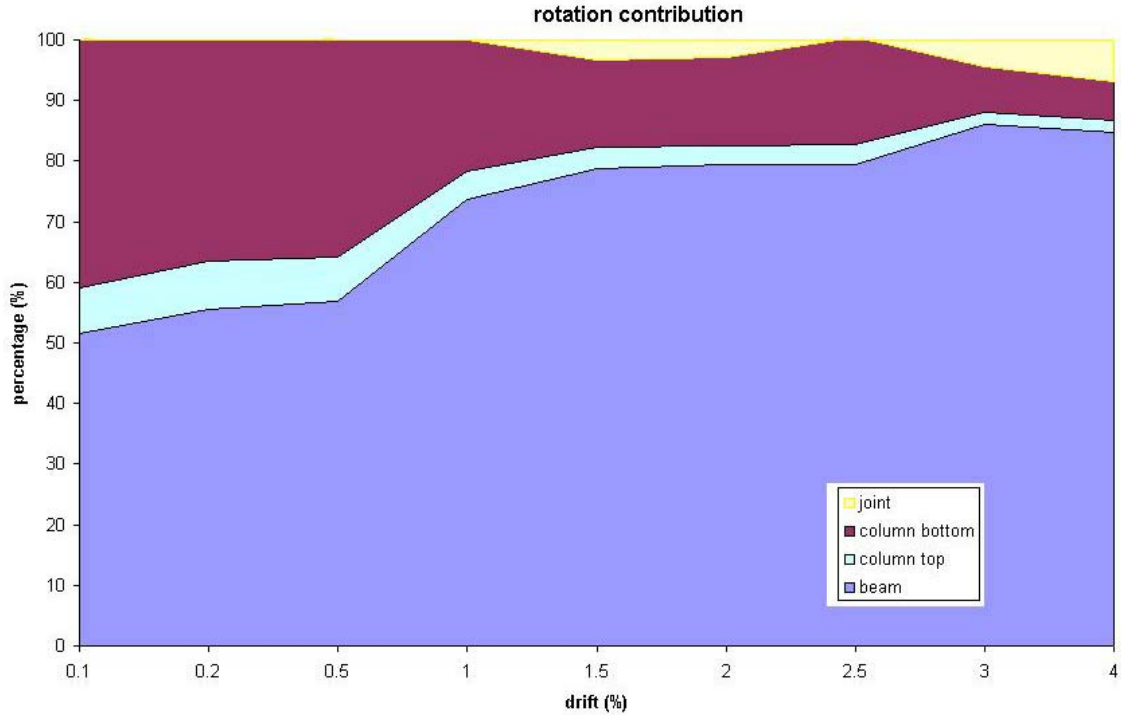
There were some difficulties in measuring the actual displacement of the unit. The cracks opened at the hole drilled to anchor the potentiometer. Therefore, once the crack started to open, the potentiometer was no longer fixed to one point of the concrete surface and it became quite flexible. The data recorded from the potentiometers had to be observed in test of Unit TDP-1 to approximate the actual displacement as close as possible.

At the start of the test, the column governed the displacement of Unit TDP-1, until the plastic hinge formed in the beam and the beam started to govern. The joint's displacement contribution was really small until the first joint cracking occurred in the positive loading direction at about 1.3% of drift. The maximum column displacement contribution was about 50%, the maximum beam displacement contribution was up to 80% and the maximum joint displacement contribution was up to 10%. Figure 4.8 shows the members contribution of Unit TDP-1 total displacement.



(a) positive loading direction

Figure 4.8 Members displacement contribution of Unit TDP-1



(b) negative loading direction

Figure 4.8 Members displacement contribution of Unit TDP-1 (continued)

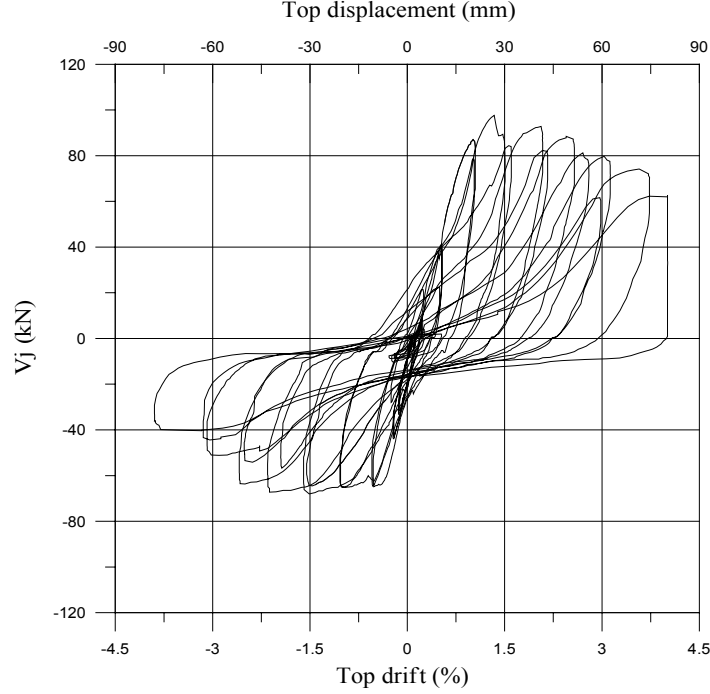
4.2.2.4 Force and Stress in the Joint

The assessment in Chapter 2 shows that the joint was supposed to be the critical member for Unit TDP-1. But due to the accident before the test that caused a major crack at the bottom of the beam in the plastic hinge area, the beam became the weakest member for the unit.

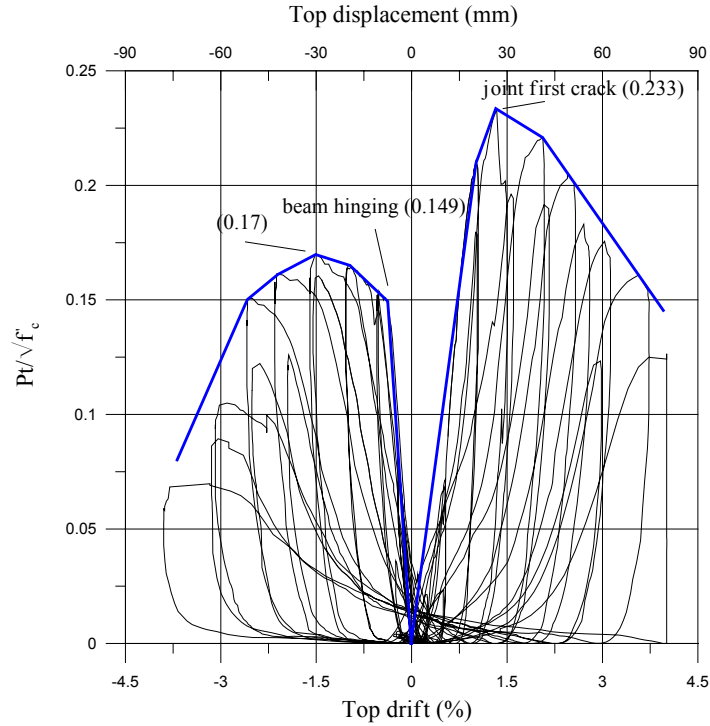
In the positive loading direction, the principal tensile stress in the joint was increasing up to $0.233\sqrt{f'_c}$ when the first joint diagonal cracking occurred. From that point, the forces in the joint started to degrade as the unit lost its strength quite significantly. In the negative loading direction, the forces in the joint were increasing up to the level when the beam suffered heavy damage and lost its strength.

The horizontal shear in the joint area reached 97 kN and -67 kN in the positive and negative loading directions respectively. The principal tensile stress reached $0.233\sqrt{f'_c}$ and $0.17\sqrt{f'_c}$ in the positive and negative loading directions

respectively. The axial load applied to the top of column was varied from $0.21\sqrt{f'_c}$ to $0.42\sqrt{f'_c}$. Figure 4.9 shows the joint horizontal shear force versus top drift (a) and the joint horizontal principal tensile stress versus top drift (b).



(a) Horizontal shear (V_j) versus Top drift of Unit TDP-1



(b) Principal tensile stress ($P_t/\sqrt{f'_c}$) versus Top drift of Unit TDP-1

Figure 4.9 Force and stress in the joint core of Unit TDP-1

4.2.2.5 Summary

Unit TDP-1, an as-built two third scale beam-column joint unit was tested under a simulated seismic loading with varying axial load. Initial axial load of 75 kN was applied representing the gravity load on the column. The deficiencies of Unit TDP-1 are the lack of transverse reinforcement in the joint core, the use of plain round longitudinal reinforcement and the hook anchorage of the beam longitudinal reinforcement in the joint core.

From this test we can conclude:

1. Poor seismic behaviour

The overall performance of the unit was poor. After the joint cracked at 1.3% of drift, the strength started to reduce significantly. The use of plain round longitudinal reinforcement caused a loss in bond strength and the bar slipping which can be seen in the pinching of the hysteresis loop of the unit. Hook anchorages worsen the behaviour of the unit because the tension forces from the beam longitudinal reinforcement were not transferred properly to the joint core but concentrated in the hooks and initiated the concrete wedge phenomena

2. Lack of transverse reinforcement in the joint

Diagonal cracks occurred in the joint area due to the shear forces working in the joint could not be resist by the single transverse reinforcement in the joint. The concrete cover of column outer layer was spalling when the high level of drift was applied on the unit. However, the joint first cracking occurred when the principal tensile stress in the joint reached $0.233\sqrt{f'_c}$, which is higher than $0.2\sqrt{f'_c}$ proposed by Pampanin. The joint transverse reinforcement helps the concrete confinement so it makes the joint slightly stronger than the unit tested by Pampanin, which did not use any transverse reinforcement in the joint core.

3. Contribution of varying axial load

The variation of axial load can both strengthens and weakens the joint core. In the positive loading direction, the joint strength is slightly higher than the negative one due to the different axial load applied on the column. The axial load applied in the positive loading direction can be up to double the axial load applied in the negative

loading direction, although the difference in terms of joint principal tensile stress is not that high.

4.2.3 Unit TDP-2

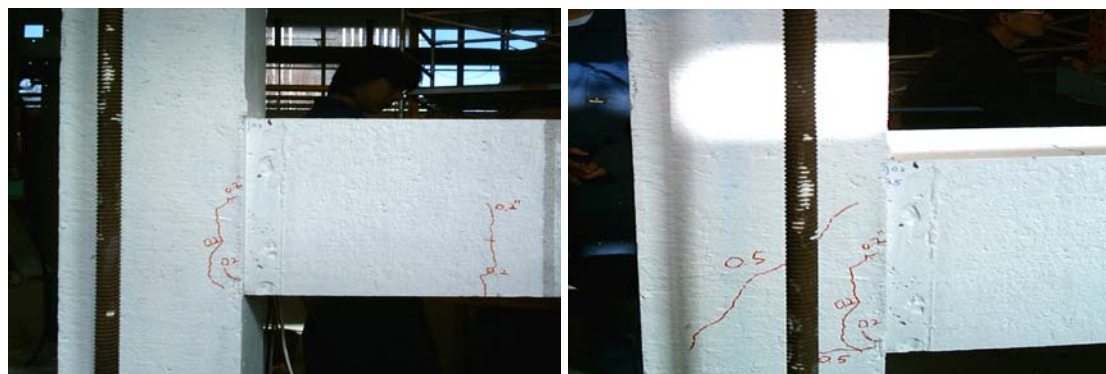
Unit TDP-2 used plain round bars as the longitudinal reinforcement in the column and beam. The beam bars were hooked in the joint core area. The aim of this test is to investigate the behaviour of the unit with different reinforcement detailing and anchorage and to complete the information gathered from Unit TDP-1. Initial axial load of 75 kN was applied on the top of the column to represent the gravity load.

4.2.3.1 Crack Development and Damage

Minor cracks started to occur at the location of the beam stirrups at 0.2% of drift. At the outer layer of the column, a horizontal crack occurred at 0.5% of drift. The diagonal joint crack occurred at 1% and 0.5% of drift for positive and negative loading directions. Minor diagonal cracks were spread into the joint core area due to the lack of transverse reinforcement in the joint. The existing cracks were extending and widening with the increase of the drift.

The concrete in the outer layer of the column was spalling at the end of test since the opening was really wide and the bond was totally destroyed. The unit was deformed until 4% of drift when the unit strength reduced significantly due to the damage in the beam and joint area.

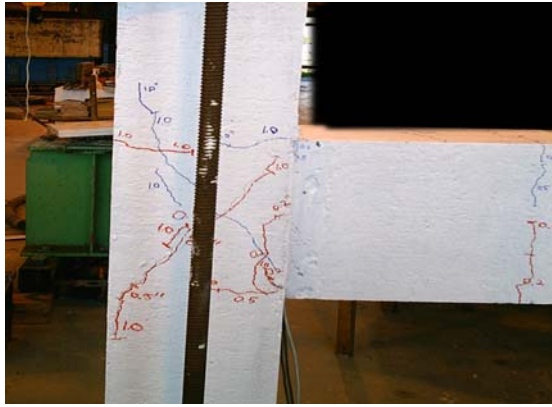
Figure 4.10 shows the crack development and the final appearance of Unit TDP-2.



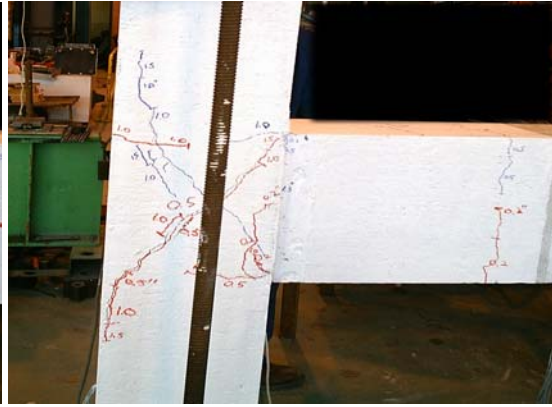
(a) At 0.2% of drift

(b) At 0.5% of drift

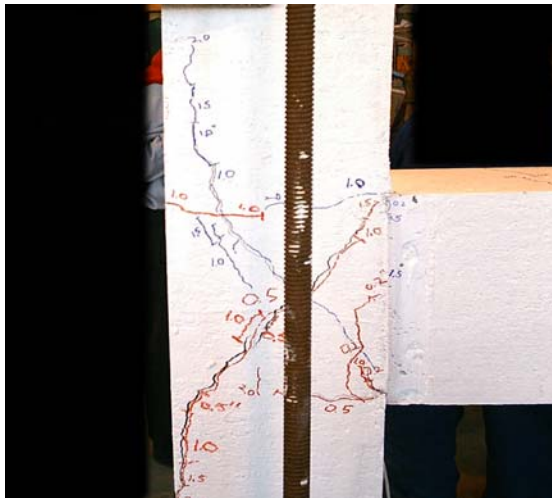
Figure 4.10 Cracks development of Unit TDP-2



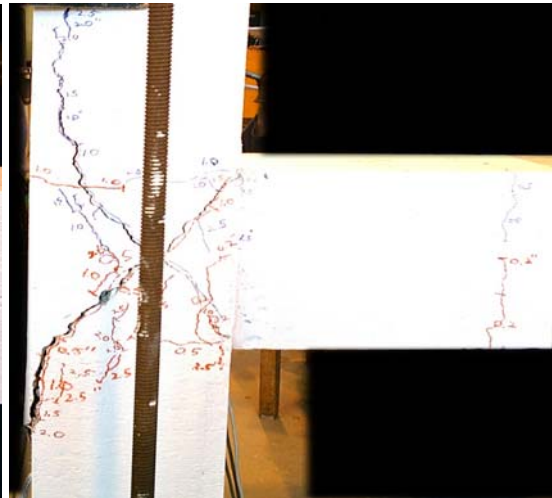
(c) At 1% of drift



(d) At 1.5% of drift



(e) At 2% of drift



(f) At 2.5% of drift



(g) At 3% of drift



(h) At the end of the test

Figure 4.10 Cracks development of Unit TDP-2 (continued)



(i) Column crack at 0.5% of drift



(j) Column crack at 1% of drift



(k) Column crack at 2% of drift



(l) Column crack at 2.5% of drift



(m) Column crack at the end of the test

Figure 4.10 Cracks development of Unit TDP-2 (continued)

4.2.3.2 Hysteretic Response

The lateral force versus the top column displacement of Unit TDP-2 is shown in Fig. 4.11. The first cracking in the joint occurred at 0.7% and 0.5% of drift in the positive and negative loading directions respectively. The stirrup in the joint core helped to confine the concrete so that the strength can be maintained up to certain level before degrading. The maximum lateral force that can be resisted by Unit TDP-2 was 16 kN and 14.6 kN for the positive and negative loading directions respectively.

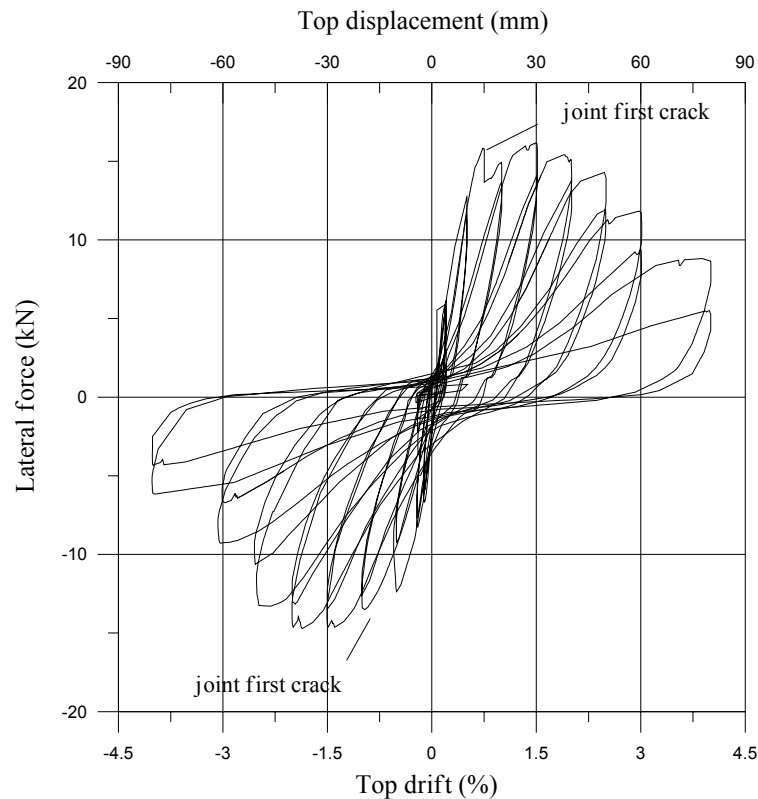


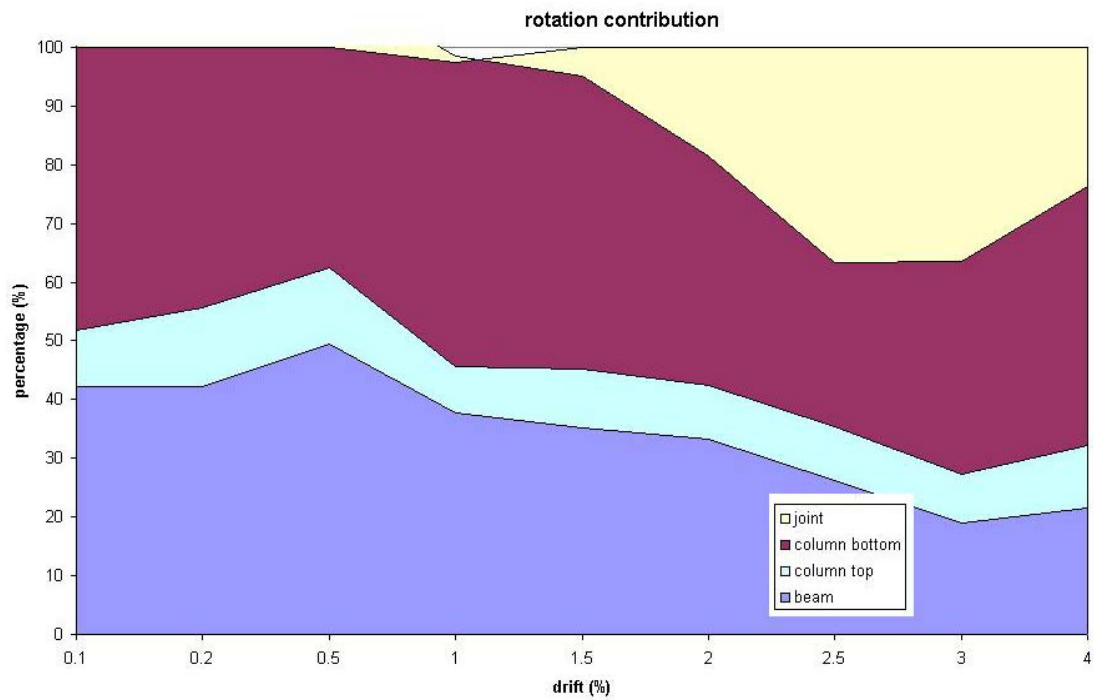
Figure 4.11 Lateral force versus Top displacement of Unit TDP-2

4.2.3.3 Displacement Components

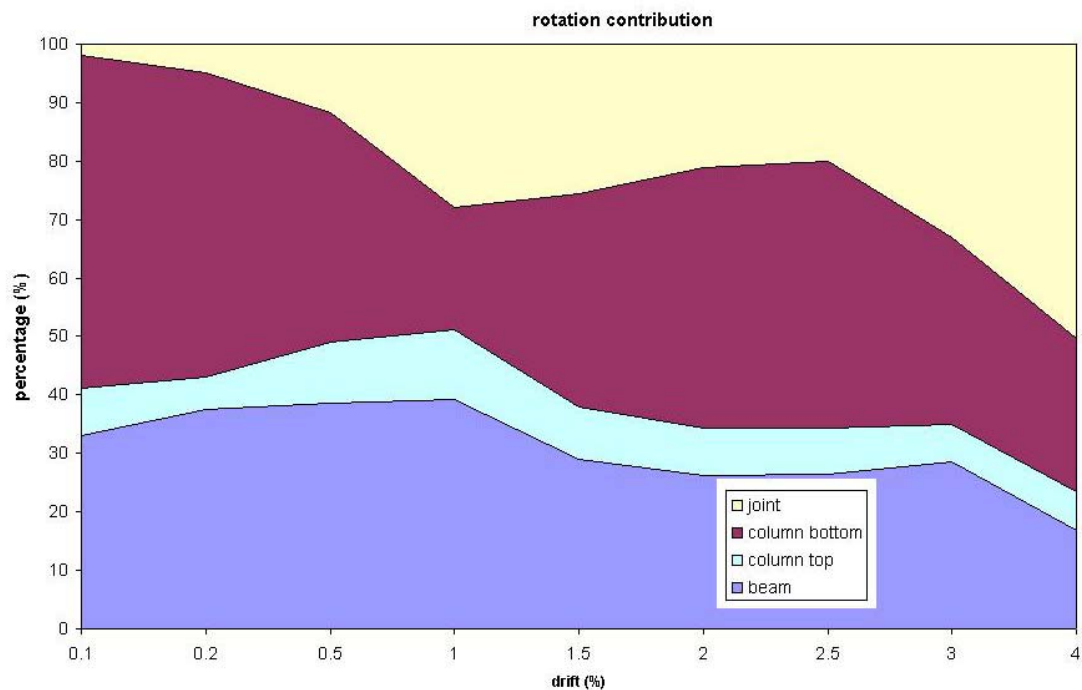
The same difficulties in measuring the actual displacement also happened for this unit. The data recorded from the potentiometers had to be observed in test of Unit TDP-2 to approximate the actual displacement as close as possible.

At the start of the test, the column governed the displacement of Unit TDP-2, until the joint first crack and the joint started to increase its contribution. The maximum column displacement contribution was about 60%, the maximum beam displacement contribution was up to 45% and the maximum joint displacement contribution was up

to 50%. Figure 4.12 shows the members contribution of Unit TDP-2 total displacement.



(a) positive loading direction



(b) negative loading direction

Figure 4.12 Members displacement contribution of Unit TDP-2

4.2.3.4 Force and Stress in the Joint

The assessment in Chapter 2 shows that the joint was the critical member for Unit TDP-2. The joint will crack both in positive and negative directions and preventing the plastic hinge occurring in the beam.

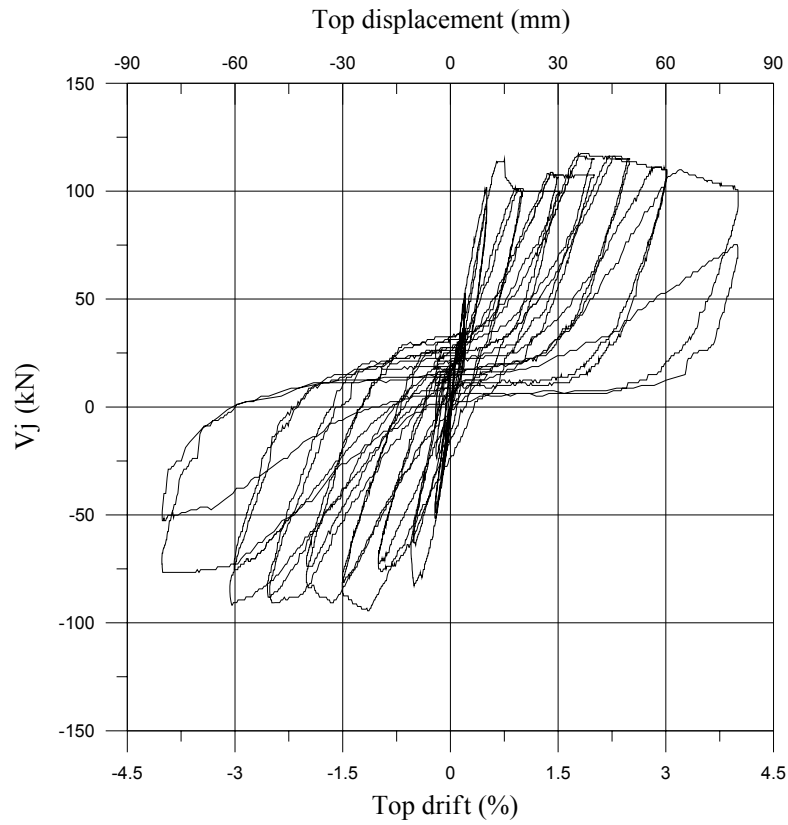
In the positive loading direction, the principal tensile stress in the joint was increasing up to $0.28\sqrt{f'_c}$ when the first joint diagonal cracking occurred. From that point, the principal tensile stress in the joint increased a little bit due to the contribution of the stirrup in the joint core up to $0.3\sqrt{f'_c}$ before it started to degrade as the unit lost its strength quite significantly. In the negative loading direction, the principal tensile stress in the joint was increasing up to $0.228\sqrt{f'_c}$ when the first joint diagonal cracking occurred. From that point, the principal tensile stress in the joint increased a little bit due to the contribution of the stirrup in the joint core up to $0.272\sqrt{f'_c}$ before it started to degrade as the unit lost its strength quite significantly.

The horizontal shear in the joint area reached 117 kN and -94 kN in the positive and negative loading directions respectively. The principal tensile stress reached $0.3\sqrt{f'_c}$ and $0.272\sqrt{f'_c}$ in the positive and negative loading directions respectively.

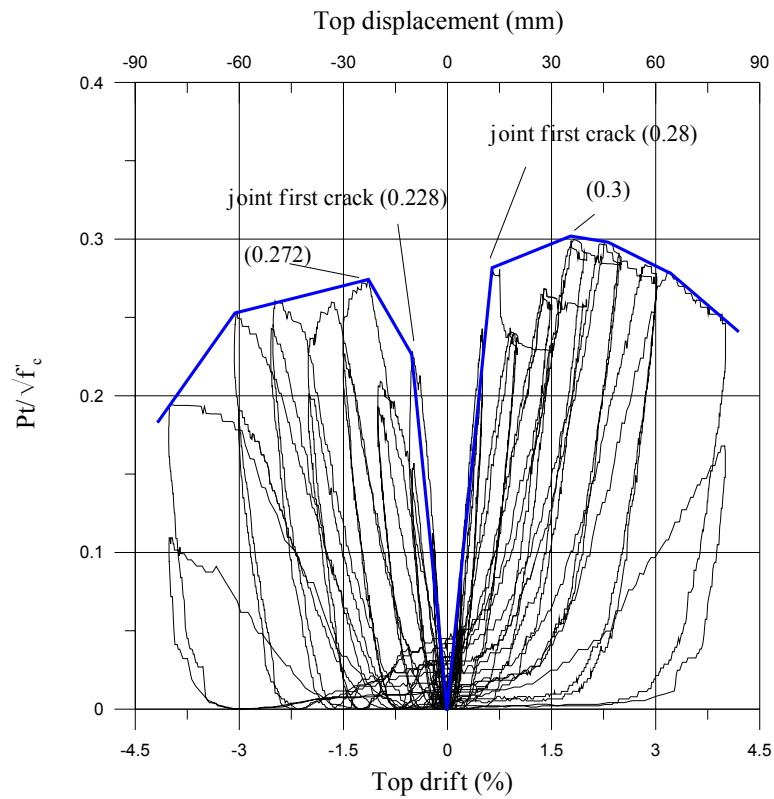
The axial load applied to the top of column was varied from $0.17\sqrt{f'_c}$ to $0.4\sqrt{f'_c}$. Figure 4.13 shows the joint horizontal shear force versus top drift (a) and the joint horizontal principal tensile stress versus top drift (b).

4.2.3.5 Joint Shear Deformation

The data recorded from the potentiometers located in the joint area for this unit was better than the other specimen although the potentiometers became flexible as well once the cracks started to open. After processing the data from the potentiometers, the joint behaviour in term of principal tensile stress versus the joint rotation can be plotted, as shown in Fig. 4.14.



(a) Horizontal shear (V_j) versus Top drift of Unit TDP-2



(b) Principal tensile stress ($P_t/\sqrt{f'_c}$) versus Top drift of Unit TDP-2

Figure 4.13 Force and stress in the joint core of Unit TDP-2

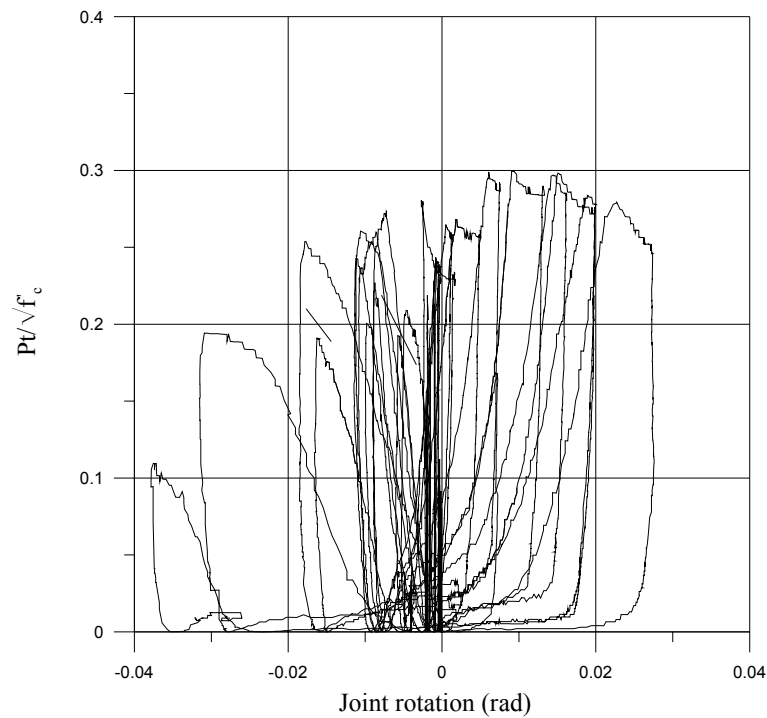


Figure 4.14 Joint principal tensile stress versus Joint rotation of Unit TDP-2

Pampanin et al (2003) proposed a limit state for exterior joints with substandard details:

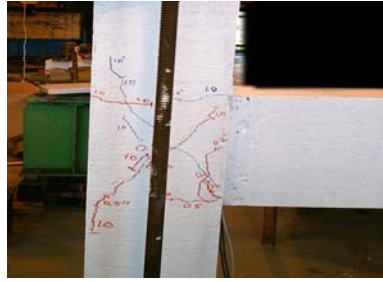
- Undamaged (uncracked): $\gamma < 0.0002$
- Limited damage: $0.0002 \leq \gamma < 0.005$
- Extensive damage: $0.005 \leq \gamma < 0.01$
- Critical damage: $0.01 \leq \gamma < 0.015$
- Collapse: $\gamma \geq 0.015$

From the damage in the unit observed during the test, the limit state in term of joint rotation (γ) is proposed as follows:

- Undamaged: $\gamma < 0.0007$



- Limited damage: $0.0007 \leq \gamma < 0.006$



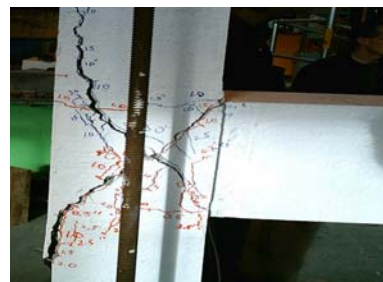
- Extensive damage: $0.006 \leq \gamma < 0.01$



- Critical damage: $0.01 \leq \gamma < 0.016$



- Collapse: $\gamma \geq 0.016$



4.2.3.6 Summary

Unit TDP-2, an as-built two third scale beam-column joint unit was tested under a simulated seismic loading with varying axial load. Initial axial load of 75 kN was applied representing the gravity load on the column. The deficiencies of Unit TDP-2

are the lack of transverse reinforcement in the joint core, the used of plain round longitudinal reinforcement and the hook anchorage of the beam longitudinal reinforcement in the joint core.

From this test we can conclude:

1. Poor seismic behaviour

The overall performance of the unit was poor. After the joint cracked at 1% of drift, the strength started to reduce significantly. The use of plain round longitudinal reinforcement caused loss in bond strength and the bar slipping which can be seen in the pinching of the hysteresis loop of the unit. Hook anchorage worsen the behaviour of the unit because the tension forces from the beam longitudinal reinforcement were not transferred properly to the joint core but concentrated in the hooks and initiated the concrete wedge phenomena

2. Lack of transverse reinforcement in the joint

Diagonal cracks occurred in the joint area due to the shear forces working in the joint could not be resist by the single transverse reinforcement in the joint. The concrete cover of column outer layer was spalling when the high level of drift was applied to the unit. However, the joint first cracking occurred when the principal tensile stress in the joint reached $0.28\sqrt{f'_c}$ to $0.3\sqrt{f'_c}$, which is higher than $0.2\sqrt{f'_c}$ proposed by Pampanin. The joint transverse reinforcement helps the concrete confinement so it makes the joint slightly stronger than the unit tested by Pampanin, which did not use any transverse reinforcement in the joint core.

3. Contribution of shear reinforcement in the joint

The single shear reinforcement placed in the joint core helped to confine the concrete so though the crack has already occurred in the joint, the strength can still increase before degrading.

4. Contribution of varying axial load

Refer to Section 4.2.2.6.

5. Limit state in term of joint rotation (γ)

Proposed limit state:

- Undamaged: $\gamma < 0.0007$

- Limited damage: $0.0007 \leq \gamma < 0.006$
- Extensive damage: $0.006 \leq \gamma < 0.01$
- Critical damage: $0.01 \leq \gamma < 0.016$
- Collapse: $\gamma \geq 0.016$

4.2.4 Unit TDD-2

Unit TDD-2 used deformed bars as the longitudinal reinforcement in the column and beam. The beam bars were bent 90 degrees into the joint core area. The aim of this test is to investigate the behaviour of the unit with different reinforcement detailing and anchorage to compare with the information gathered from Unit TDP-1 and Unit TDP-2. Initial axial load of 75 kN was applied on the top of the column to represent the gravity load.

4.2.4.1 Crack Development and Damage

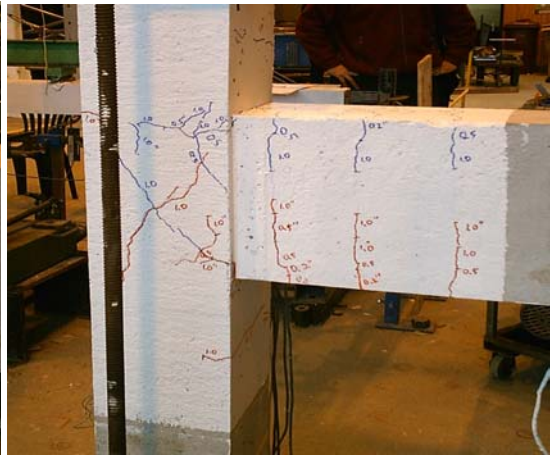
Minor cracks started to occur at the location of the beam stirrups at 0.2% of drift. At the outer layer of the column, a horizontal crack occurred at 0.5% of drift. The diagonal joint crack occurred at 1% of drift for both positive and negative loading directions. Minor diagonal cracks were spread in the joint core area due to the lack of transverse reinforcement in the joint. The existing cracks were extending and widening along the increase of the drift.

The concrete in the outer layer of the column was not spalling at the end of test due to the better bond for the deformed longitudinal reinforcement. The unit was loaded until 4% of drift when the unit strength reduced significantly due to the damage in the beam and joint area.

Figure 4.15 shows the crack development and the final appearance of Unit TDD-2.



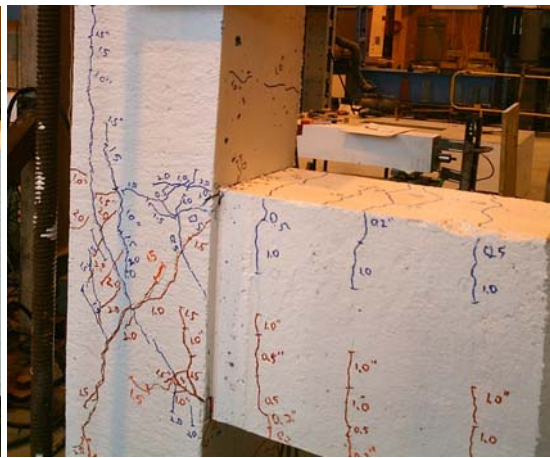
(a) At 0.5% of drift



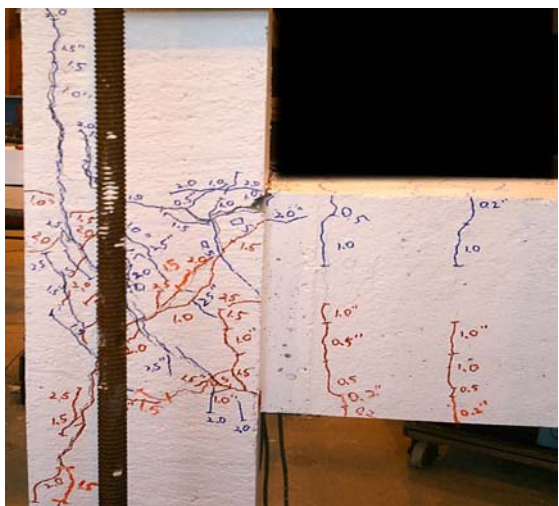
(b) At 1% of drift



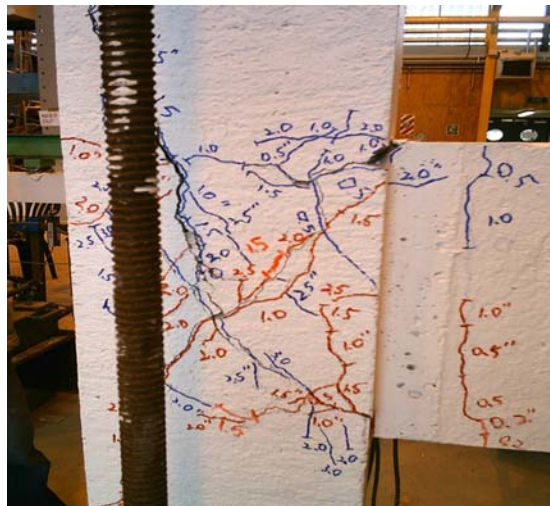
(c) At 1.5% of drift



(d) At 2% of drift



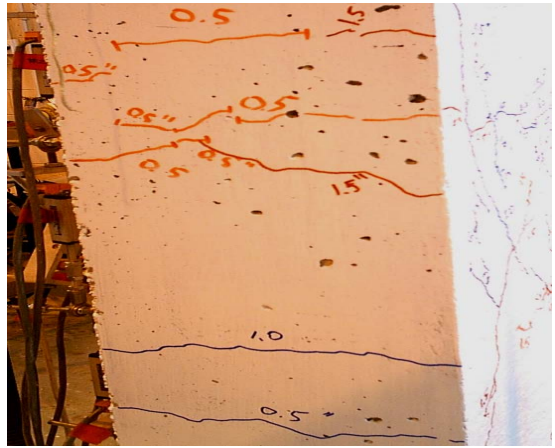
(e) At 2.5% of drift



(f) At 3% of drift

Figure 4.15 Cracks development of Unit TDD-2

(h) Column crack at 0.5% of drift



(j) Column crack at 1.5% of drift



(I) Column crack at the end of the test

Figure 4.15 Cracks development of Unit TDD-2 (continued)

4.2.4.2 Hysteretic Response

The lateral force versus the top column displacement of Unit TDD-2 is shown in Fig. 4.16. The first cracking in the joint occurred at 0.7% of drift both in positive and negative loading direction. The maximum lateral force that can be resisted by Unit TDD-2 was 23 kN and 16 kN for positive and negative loading direction respectively.

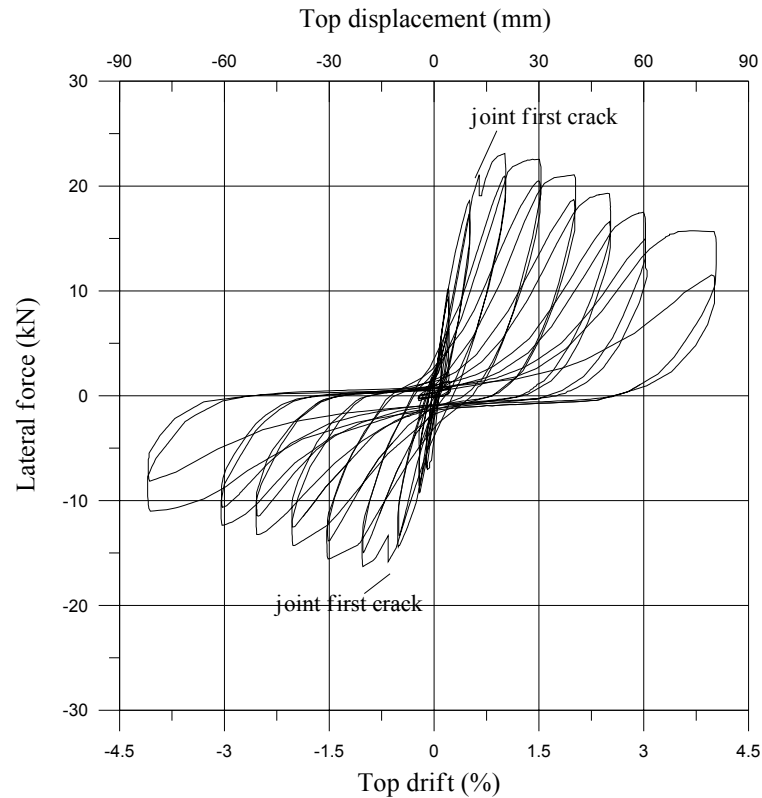


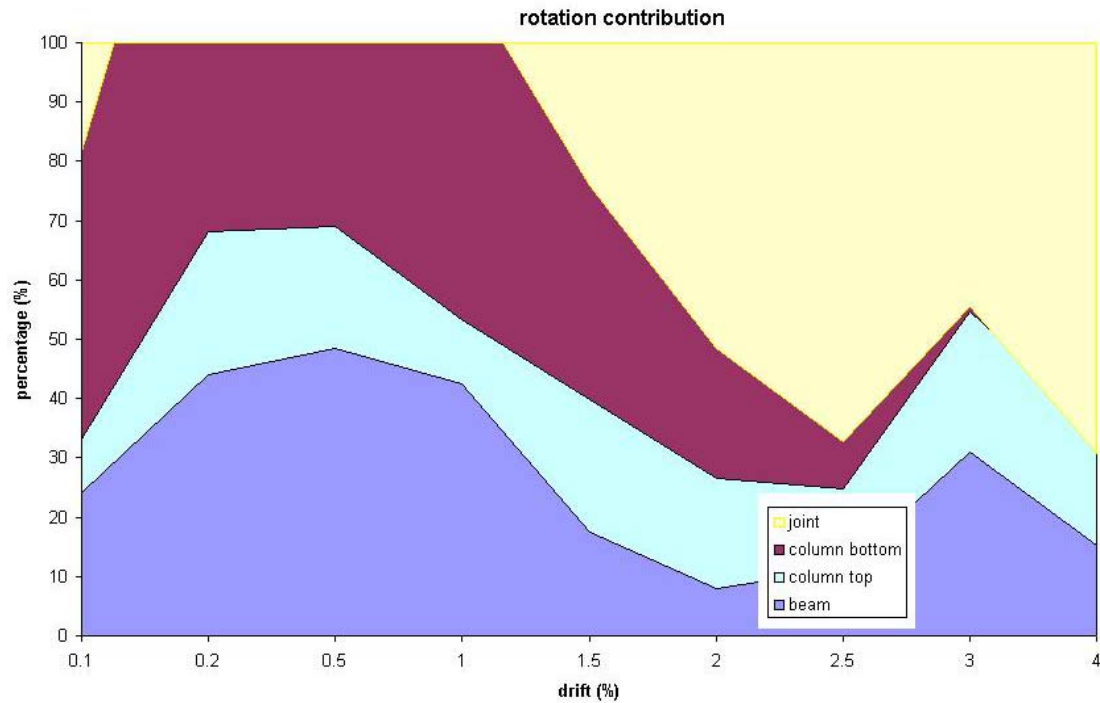
Figure 4.16 Lateral force versus Top displacement of Unit TDD-2

4.2.4.3 Displacement Components

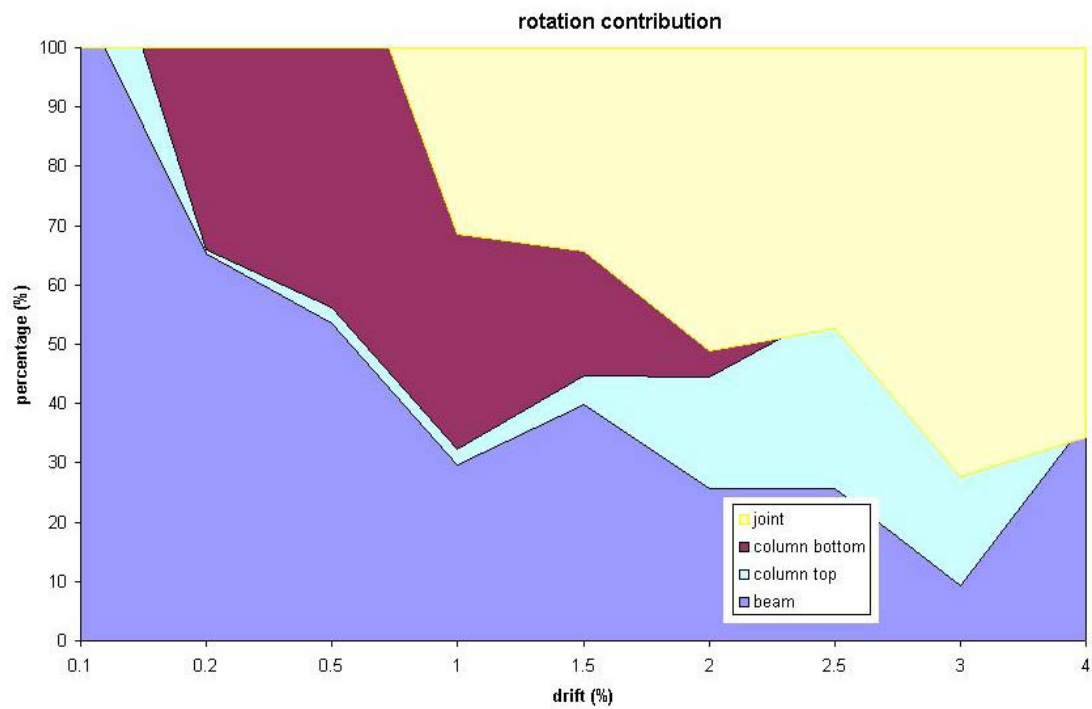
The same difficulties in measuring the actual displacement also happened for this unit. The data recorded from the potentiometers had to be observed in test of Unit TDD-2 to approximate the actual displacement as close as possible. In the negative loading direction, the data recorded from the potentiometer located at the column at the small drift was not really clear therefore the chart showed that the beam was fully governing.

At the start of the test, the column governed the displacement of Unit TDD-2, until the first joint crack and the joint started to increase its contribution. The maximum column displacement contribution was about 65%, the maximum beam displacement

contribution was up to 65% and the maximum joint displacement contribution was up to 70%. Figure 4.17 shows the members contribution of Unit TDD-2 total displacement.



(a) positive loading direction



(b) negative loading direction

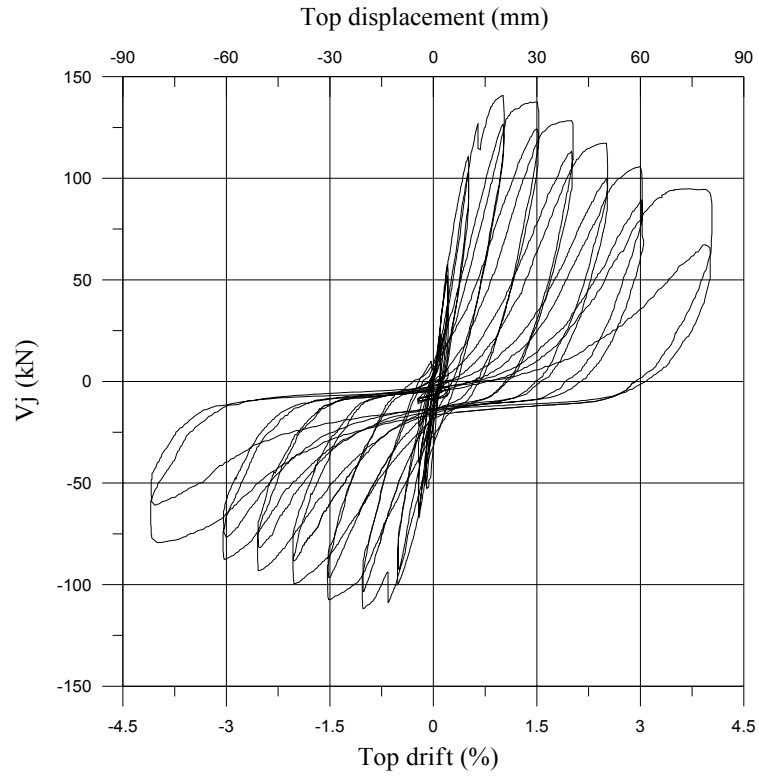
Figure 4.17 Members displacement contribution of Unit TDD-2

4.2.4.4 Force and Stress in the Joint

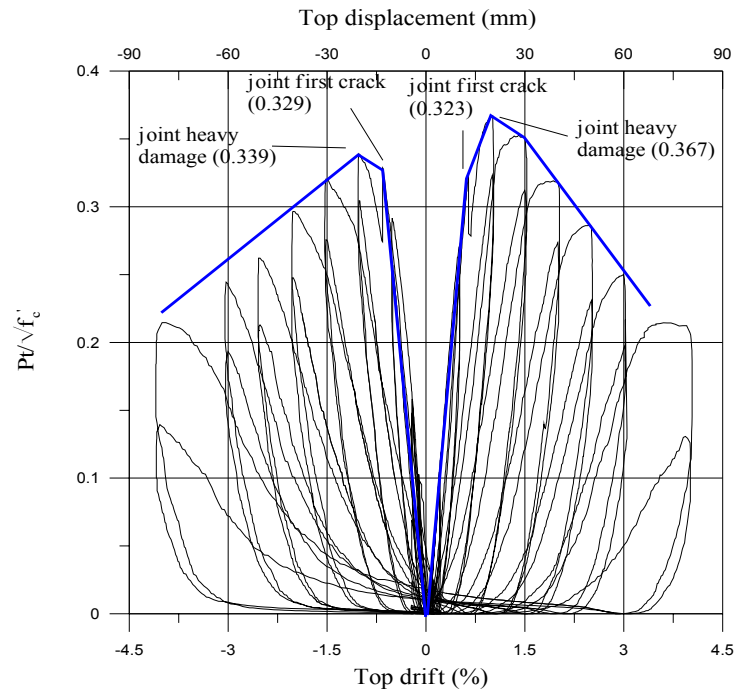
The assessment in Chapter 2 shows that the joint was the critical member for Unit TDD-2. The joint will crack both in positive and negative directions and preventing the plastic hinge occurring in the beam.

In the positive loading direction, the principal tensile stress in the joint was increasing up to $0.323\sqrt{f'_c}$ when the first joint diagonal cracking occurred. At that point, the principal tensile stress in the joint reduced suddenly and began to pick up again until $0.367\sqrt{f'_c}$ when the joint suffered heavy damage and the strength of the unit was reducing significantly. In the negative loading direction, the principal tensile stress in the joint was increasing up to $0.329\sqrt{f'_c}$ when the first joint diagonal cracking occurred. At that point, the principal tensile stress in the joint reduced suddenly and began to pick up again until $0.339\sqrt{f'_c}$ when the joint suffered heavy damage and the strength of the unit was reduced significantly.

The horizontal shear in the joint area reached 141 kN and -112 kN in the positive and negative loading directions respectively. The principal tensile stress reached $0.516\sqrt{f'_c}$ and $0.347\sqrt{f'_c}$ in the positive and negative loading directions respectively. The axial load applied to the top of column was varied from $0.13\sqrt{f'_c}$ to $0.43\sqrt{f'_c}$. Figure 4.18 shows the joint horizontal shear force versus top drift (a) and the joint horizontal principal tensile stress versus top drift (b).



(a) Horizontal shear (V_j) versus Top drift of Unit TDD-2



(b) Principal tensile stress (P_t)/ $\sqrt{f'_c}$ versus Top drift of Unit TDD-2

Figure 4.18 Force and stress in the joint core of Unit TDD-2

4.2.4.5 Summary

Unit TDD-2, an as-built two third scale beam-column joint unit was tested under a simulated seismic loading with varying axial load. Initial axial load of 75 kN was applied representing the gravity load on the column. The deficiency of Unit TDD-2 is the lack of transverse reinforcement in the joint core.

From this test we can conclude:

1. Poor seismic behaviour

The overall performance of the unit was poor. After the joint cracked at 1% of drift, the strength started to reduce significantly. The shear hinge formed in the joint core rather than the desirable plastic hinge in the beam.

2. Lack of transverse reinforcement in the joint

Diagonal cracks occurred in the joint area due to the shear forces working in the joint could not be resist by the single transverse reinforcement in the joint. The concrete cover of the column outer steel layer was not spalling due to better bond strength of the deformed bars. The joint first cracking occurred when the principal tensile stress in the joint reached $0.33\sqrt{f'_c}$, which is slightly higher than $0.29\sqrt{f'_c}$ proposed by Pampanin. The joint transverse reinforcement helps the concrete confinement so it makes the joint stronger than the unit tested by Pampanin, which did not use any transverse reinforcement in the joint core.

3. Contribution of varying axial load

Refer to Section 4.2.2.6.

4.3 SHALLOW BEAM

Two geometrically identical exterior beam-column joint units with shallow beams, each different in reinforcement details, were constructed. The units are referred to as Units TSP and TSD. Unit TSP used plain round longitudinal reinforcement, while units TSD used deformed longitudinal reinforcement. Grade 300 plain round steel was used for the longitudinal and transverse reinforcement. The joint cores contained one transverse reinforcement, typical in pre-1970's building construction and one additional stirrup was used to confine the joint longitudinal reinforcement.

4.3.1 Unit TSP

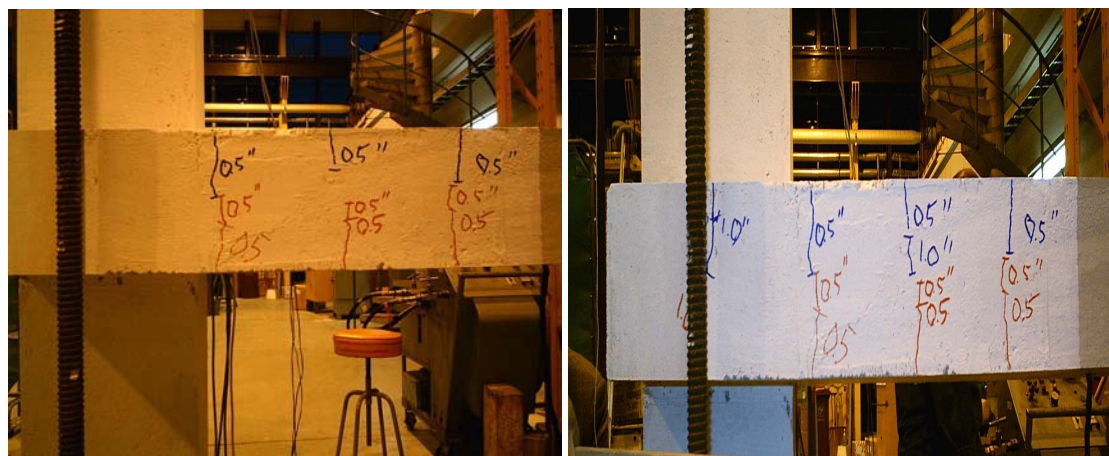
Unit TSP used plain round bars as the longitudinal reinforcement in the column and beam. The beam bars were hooked in the joint core area. The aim of this test is to investigate the behaviour of the unit with different beam geometry and the behaviour of the shallow beam under seismic loading. Initial axial load of 75 kN was applied on the top of the column to represent the gravity load.

4.3.1.1 Crack Development and Damage

Minor cracks started to occur at the location of the beam stirrups at 0.5% of drift. The cracks were spreading on the beam's top and bottom surface rather than the side of the beam. Diagonal cracks started to occur in the beam side anchored outside the column due to absence of reinforcement to resist the diagonal tension in that area. The existing cracks were extending and widening with the increase of the drift.

The beam was so shallow, giving no critical problem in the joint area from the tension force. The shallow beam behaved like a slab with flexural cracks occurring along the surface. The unit was loaded until 4% of drift as planned and was still performing well up to 4.5% of drift. Due to limited range of the instrumentation used, no information was recorded after 4% of drift.

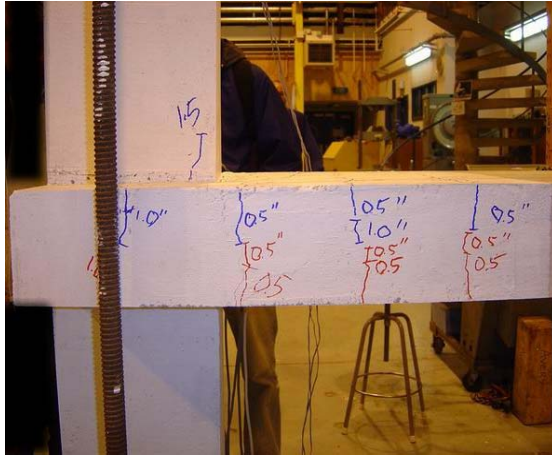
Figure 4.19 shows the crack development and the final appearance of Unit TSP.



(a) At 0.5% of drift

(b) At 1% of drift

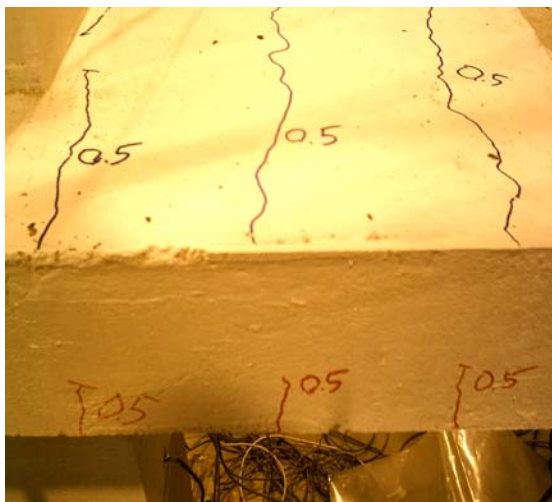
Figure 4.19 Cracks development of Unit TSP



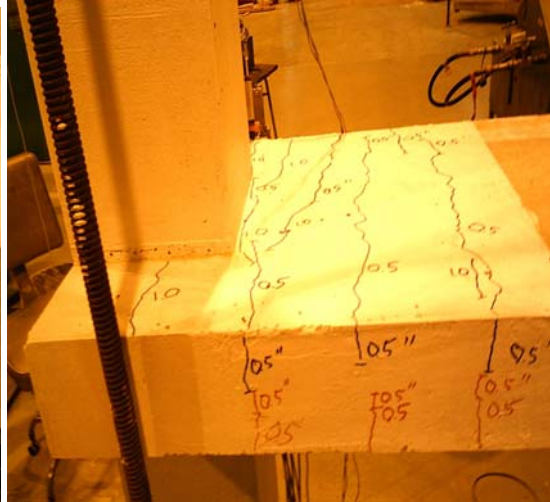
(c) At 1.5% of drift



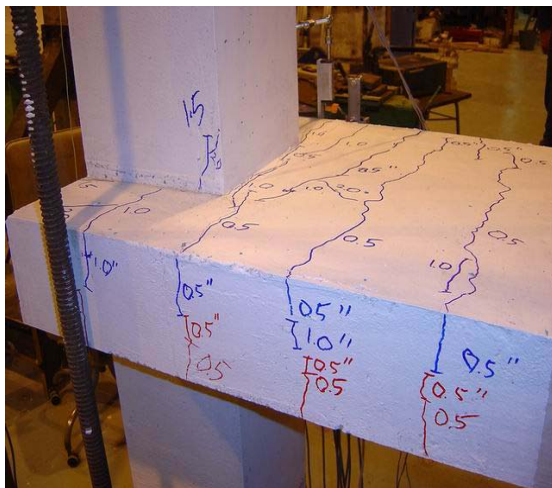
(d) At 3% of drift



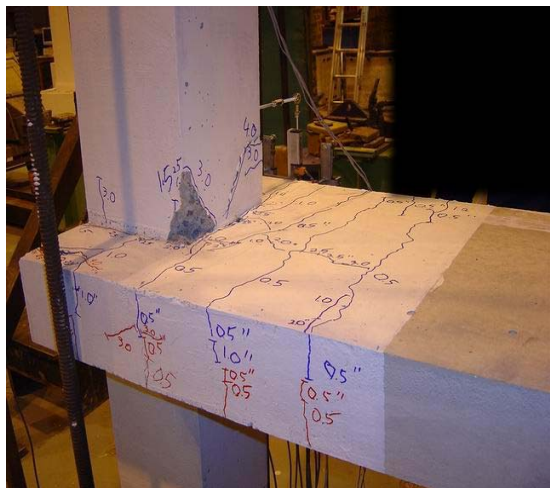
(e) Beam crack at 0.5% of drift



(f) Beam crack at 1% of drift

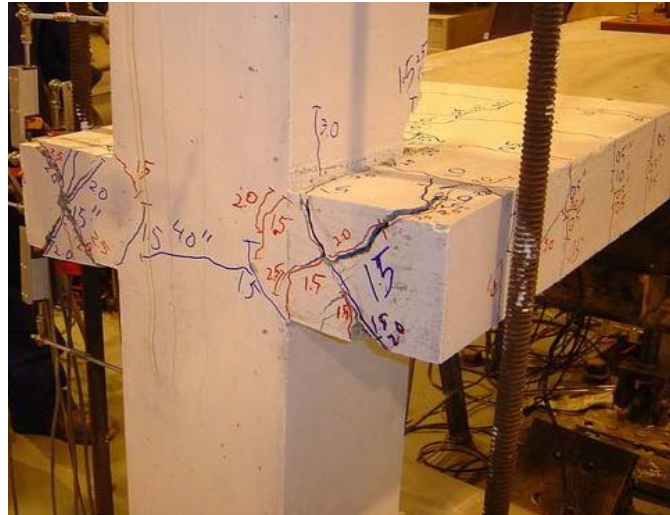


(g) Beam crack at 1.5% of drift



(h) Beam crack at the end of the test

Figure 4.19 Cracks development of Unit TSP (continued)



(i) Column crack at the end of the test

Figure 4.19 Cracks development of Unit TSP (continued)

4.3.1.2 Hysteretic Response

The lateral force versus the top column displacement of Unit TSP is shown in Fig. 4.20. The beam longitudinal reinforcement started to yield at 1.5% of drift both in positive and negative loading direction respectively. The maximum lateral force that can be resisted by Unit TSP was 10.7 kN and 7.5 kN for positive and negative loading direction respectively.

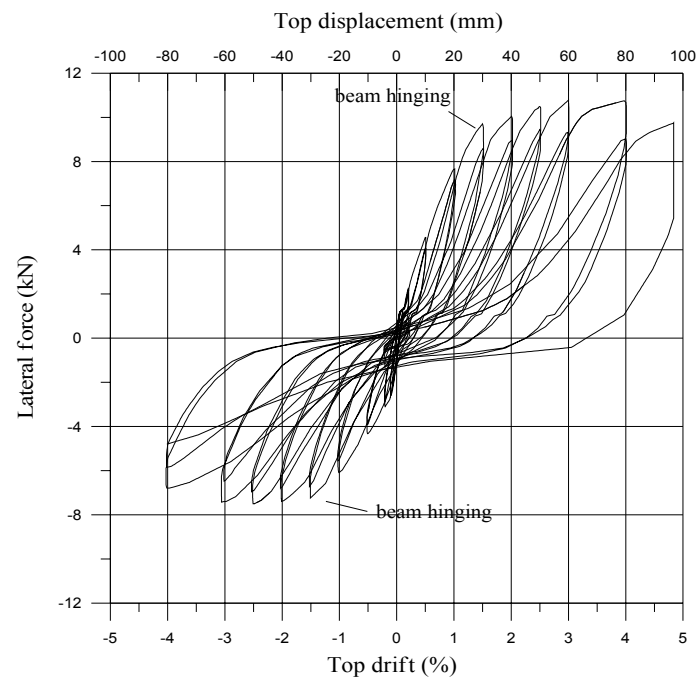
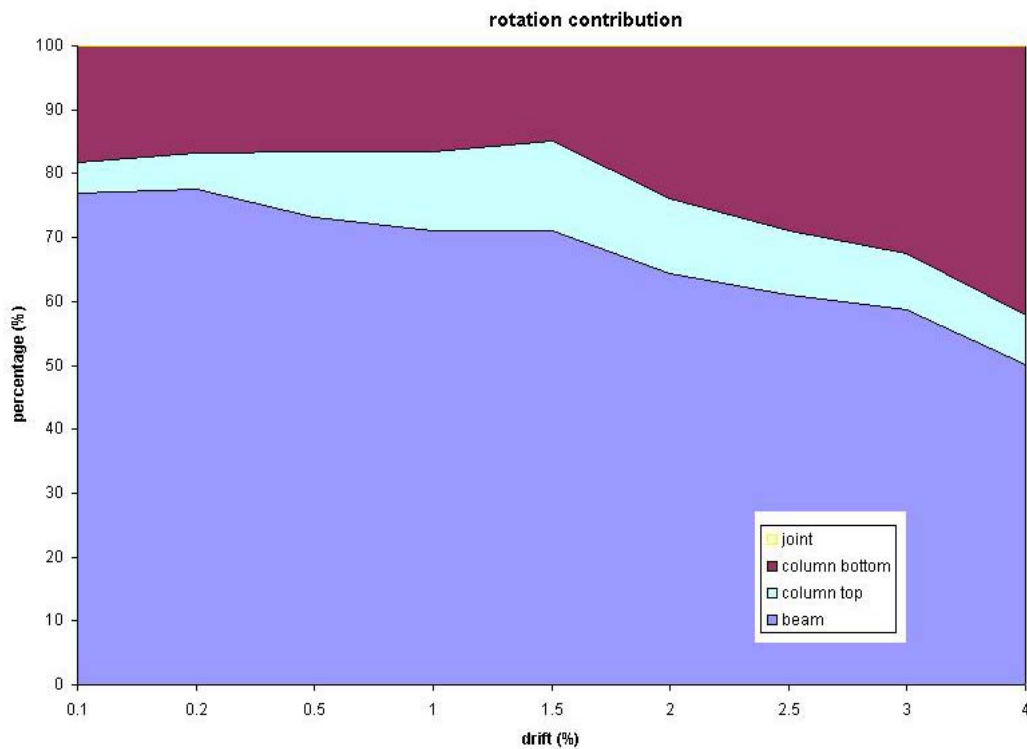


Figure 4.20 Lateral force versus Top displacement of Unit TSP

4.3.1.3 Displacement Components

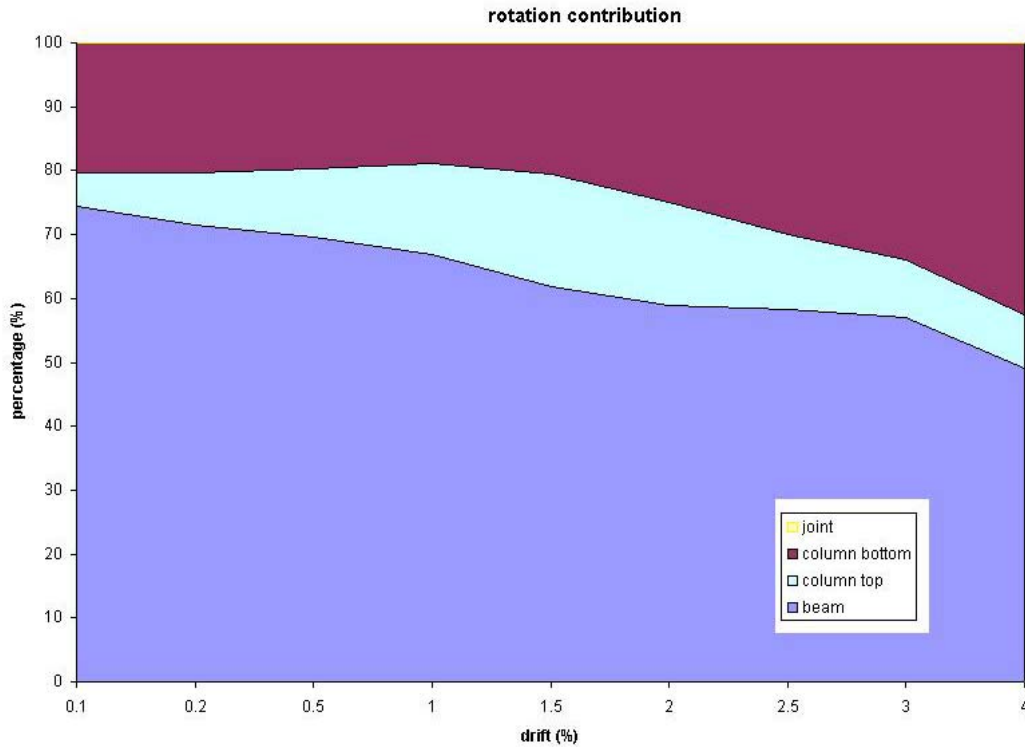
The joint core in this unit was in the beam section therefore no instrumentation could be located in the joint core. The potentiometer was placed on the beam side and the displacement data recorded did not reflect the actual joint deformation. The joint was assumed to have not moved since the cracks occurred in the beam rather than joint area.

The beam governed the displacement of Unit TSP from the start of the test. After the crack occurred in the beam and column interface, the column displacement contribution started to increase. The maximum column displacement contribution was about 50% and the maximum beam displacement contribution was up to 50% as well. Figure 4.21 shows the members contribution of Unit TSP total displacement.



(a) positive loading direction

Figure 4.21 Members displacement contribution of Unit TSP



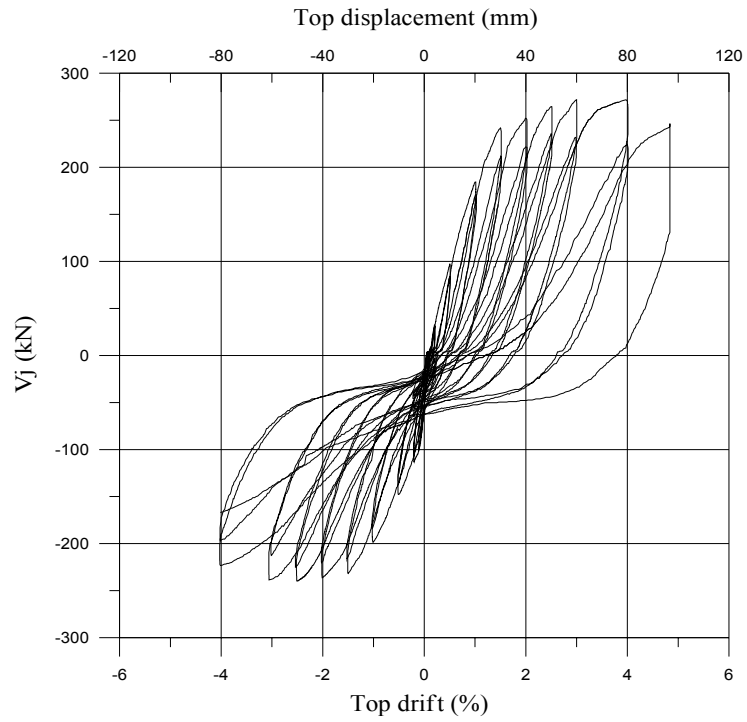
(b) negative loading direction

Figure 4.21 Members displacement contribution of Unit TSP (continued)

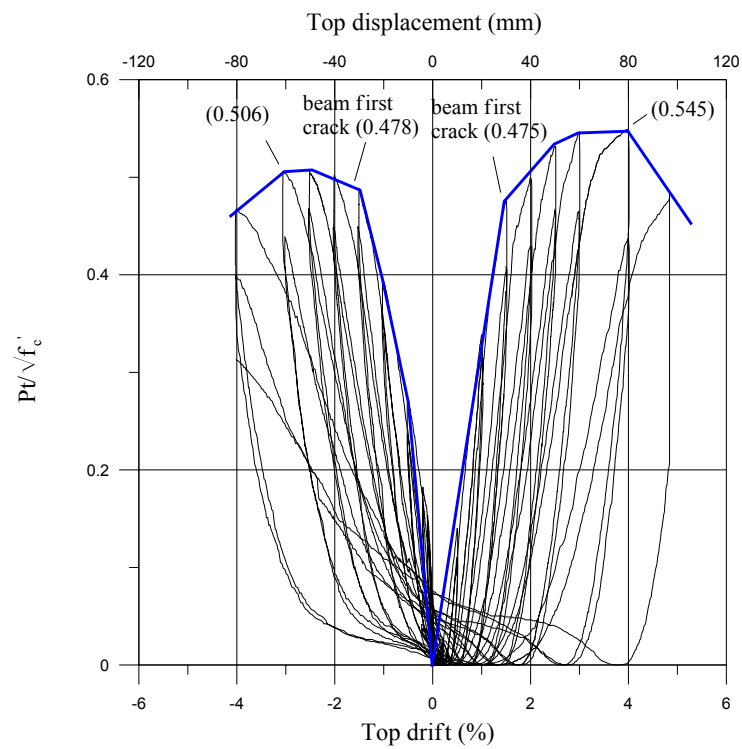
4.3.1.4 Forces and Stress in the Joint

The assessment in Chapter 2 shows that the beam was the critical member for Unit TSP; therefore there is no damage in the joint core. The forces in the joint were increasing up to the level when Unit TSP suffered heavy damage and lost its strength. From that point, the forces in the joint started to degrade as the beam steel tension was reducing as well.

The horizontal shear in the joint area reached 272 kN and -240 kN in the positive and negative loading direction respectively. The principal tensile stress reached $0.545\sqrt{f'_c}$ and $0.506\sqrt{f'_c}$ in the positive and negative loading direction respectively. The axial load applied to the top of column was varied from $0.25\sqrt{f'_c}$ to $0.37\sqrt{f'_c}$. Figure 4.22 shows the joint horizontal shear force versus top drift (a) and the joint horizontal principal tensile stress versus top drift (b).



(a) Horizontal shear (V_j) versus Top drift of Unit TSP



(b) Principal tensile stress (P_t)/ $\sqrt{f'_c}$ versus Top drift of Unit TSP

Figure 4.22 Force and stress in the joint core of Unit TSP

4.3.1.5 Summary

Unit TSP, an as-built two third scale beam-column joint unit was tested under a simulated seismic loading with varying axial load. Initial axial load of 75 kN was applied representing the gravity load on the column. The deficiency of Unit TSP is the shallowness of the beam geometry, which reduces the beam flexural lever arm significantly and the use of plain round longitudinal reinforcement and the hook anchorage of the beam longitudinal reinforcement in the joint core.

From this test we can conclude:

1. Poor seismic behaviour

The overall performance of the unit was poor. The unit can only resist the lateral force of 10 kN before failing in the beam, which is about half of the moment capacity. The reason is that only half of the amount of beam reinforcement anchored to the column, and the ones anchored outside the column did not totally contribute. The use of plain round longitudinal reinforcement caused loss in bond strength and the bar slipping which can be seen in the pinching of the hysteresis loop of the unit. Hook anchorage worsen the behaviour of the unit because the tension forces from the beam longitudinal reinforcement were not transferred properly to the joint core but concentrated in the hooks.

2. Adequate confinement in the joint

Due to the number of beam longitudinal reinforcement anchored in the column, the joint area was fully congested. This prevents the joint from concrete tension failure which is not a desirable mechanism under seismic loading.

3. Contribution of varying axial load

Refer to Section 4.2.2.6.

4.3.2 Unit TSD

Unit TSD used deformed bars as the longitudinal reinforcement in the column and beam. The beam bars were bent 90 degrees into the joint core area. The aim of this test is to investigate the behaviour of the unit with different beam geometry, the different reinforcement detailing and the behaviour of the shallow beam under seismic loading. Initial axial load of 75 kN was applied on the top of the column to represent the gravity load.

4.3.2.1 Crack Development and Damage

Minor cracks started to occur at the location of the beam stirrups at 0.5% of drift. The cracks were spreading on the beam's top and bottom surface rather than the side of the beam. Diagonal cracks started to occur in the beam side anchored outside the column due to absence of reinforcement to resist the diagonal tension in that area. The existing cracks were extending and widening along with the increase of the drift percentage.

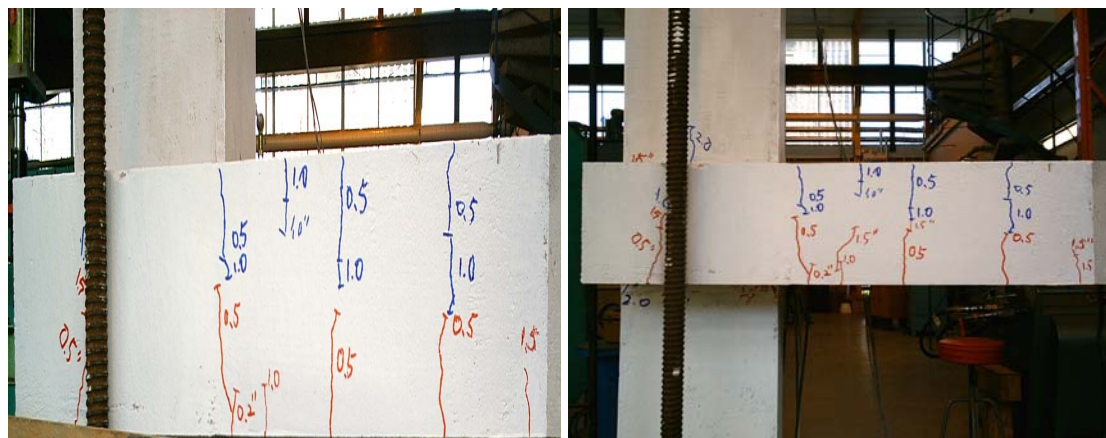
The beam was so shallow that no critical problem in the joint area from the tension force. The shallow beam behaved like a slab with flexural cracks occurring along the surface. The unit was loaded until 4% of drift as planned and was still performing well up to 5% of drift. Due to limited range of the instrumentation used, no information was recorded after 4% of drift.

Figure 4.23 shows the crack development and the final appearance of Unit TSD.



(a) At 0.5% of drift

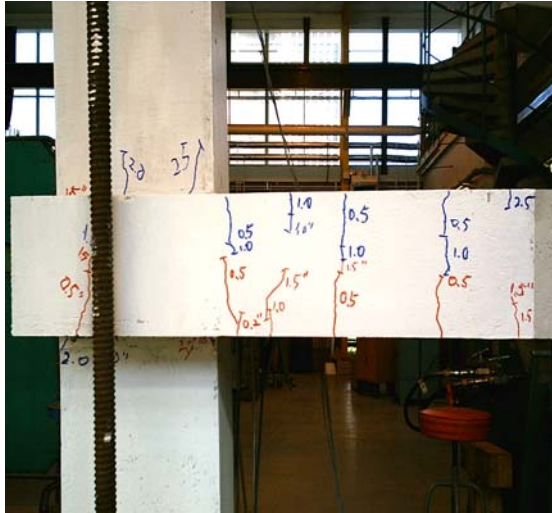
(b) At 1% of drift



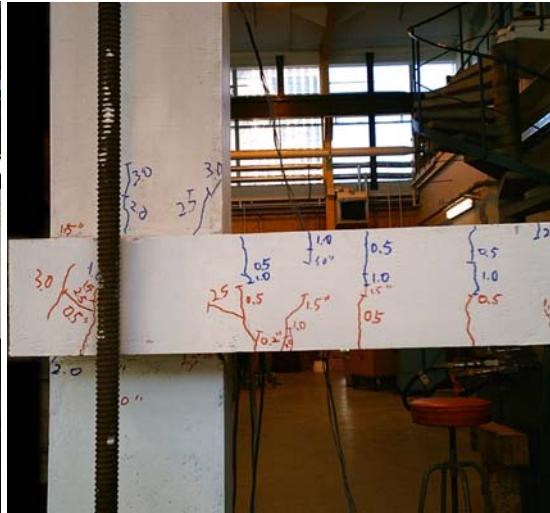
(c) At 1.5% of drift

(d) At 2% of drift

Figure 4.23 Cracks development of Unit TSD



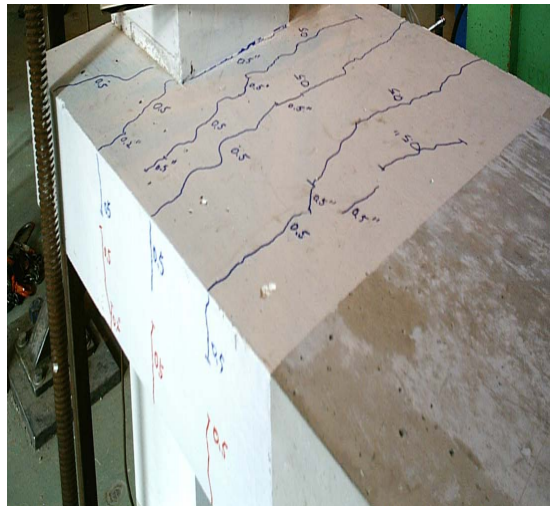
(e) At 2.5% of drift



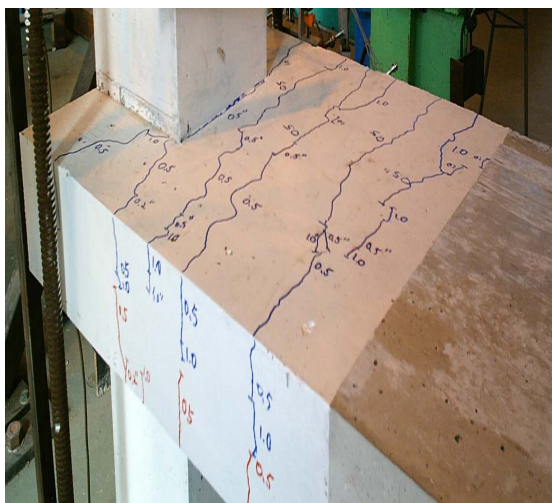
(f) At 3% of drift



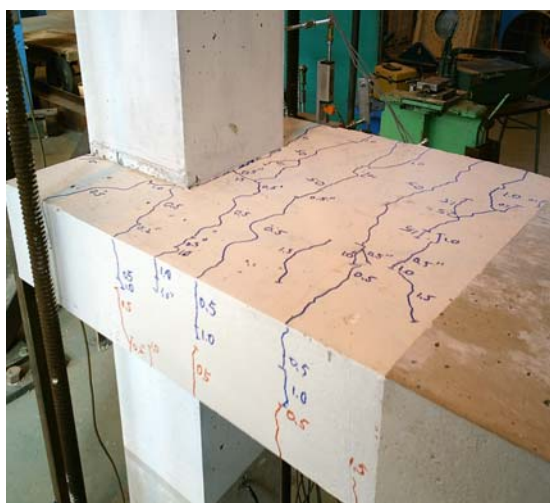
(g) At the end of the test



(h) Beam surface at 0.5% of drift

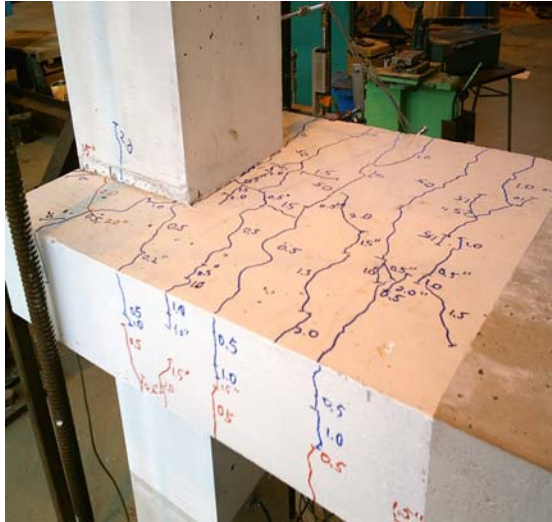


(i) Beam surface at 1% of drift

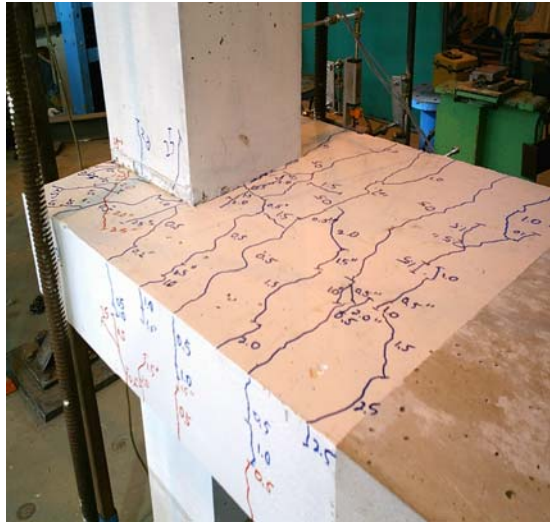


(j) Beam surface at 1.5% of drift

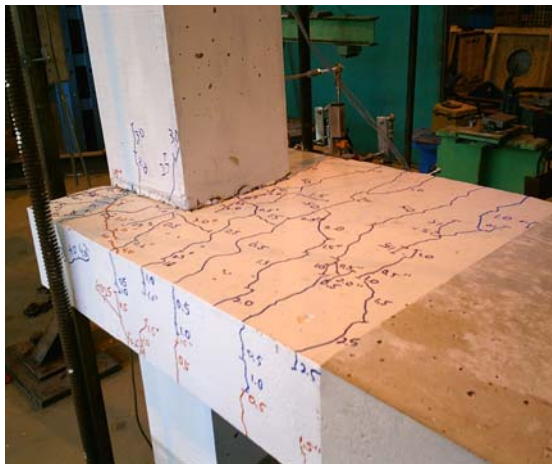
Figure 4.23 Cracks development of Unit TSD (continued)



(k) Beam surface at 2% of drift



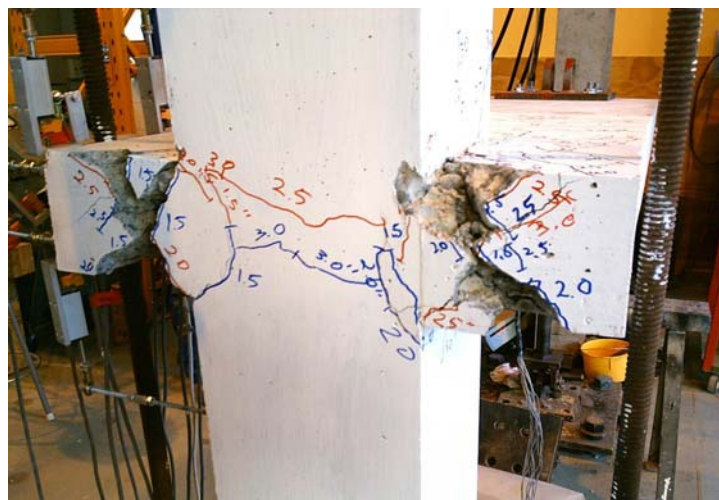
(l) Beam surface at 2.5% of drift



(m) Beam surface at 3% of drift



(n) Beam surface at the end of the test



(o) Column crack at the end of the test

Figure 4.23 Cracks development of Unit TSD (continued)

4.3.2.2 Hysteretic Response

The lateral force versus the top column displacement of Unit TSD is shown in Fig. 4.24. The beam longitudinal reinforcement started to yield at 2% and 1.5% of drift for positive and negative loading directions respectively. The maximum lateral force that can be resisted by Unit TSD was 12 kN and 8 kN for positive and negative loading directions respectively.

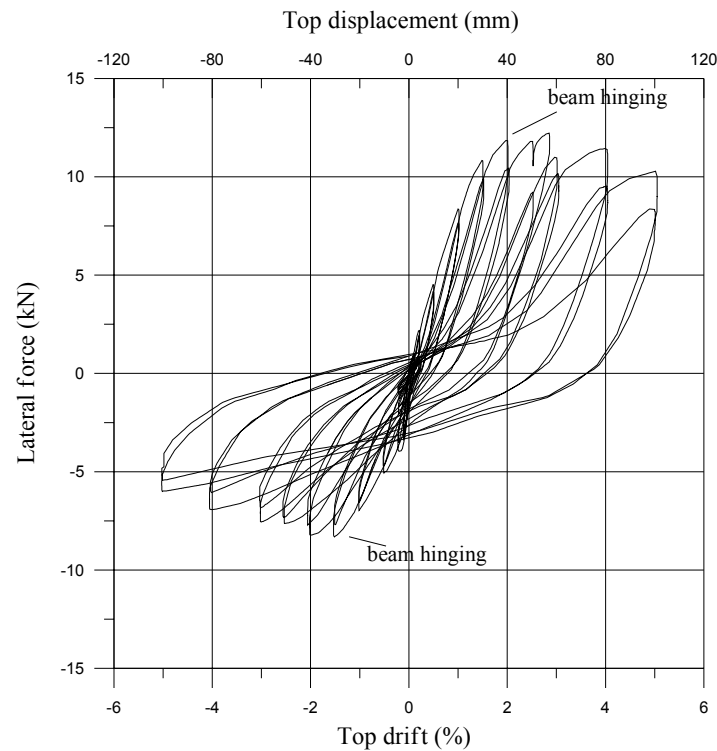


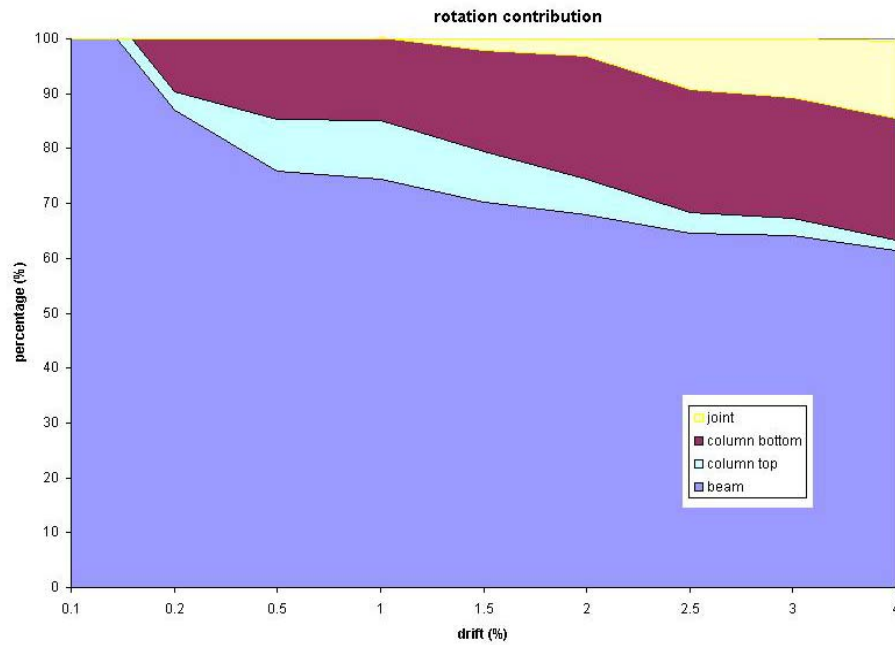
Figure 4.24 Lateral force versus Top displacement of Unit TSD

4.3.2.3 Displacement Components

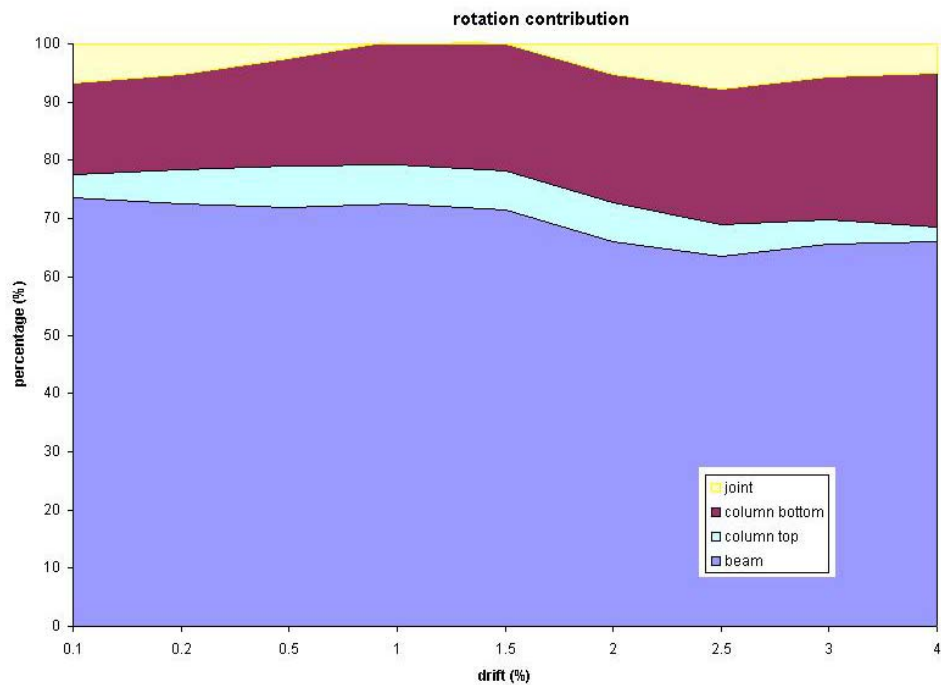
The joint core in this unit was in the beam section therefore no instrumentation could be located in the joint core. The potentiometer was placed on the beam side and the displacement data recorded did not reflect the actual joint deformation. The joint was assumed to have not moved since the cracks occurred in the beam rather than joint area. The data recorded from the potentiometers had to be observed in test of Unit TSD to approximate the actual displacement as close as possible.

The beam governed the displacement of Unit TSD from the start of the test. After the crack occurred in the beam and column interface, the column displacement contribution started to increase. The maximum column displacement contribution

was about 30% and the maximum beam displacement contribution was up to 75% as well, with a small contribution from joint, which is 15% maximum. Figure 4.25 shows the members contribution of Unit TSD total displacement.



(a) positive loading direction



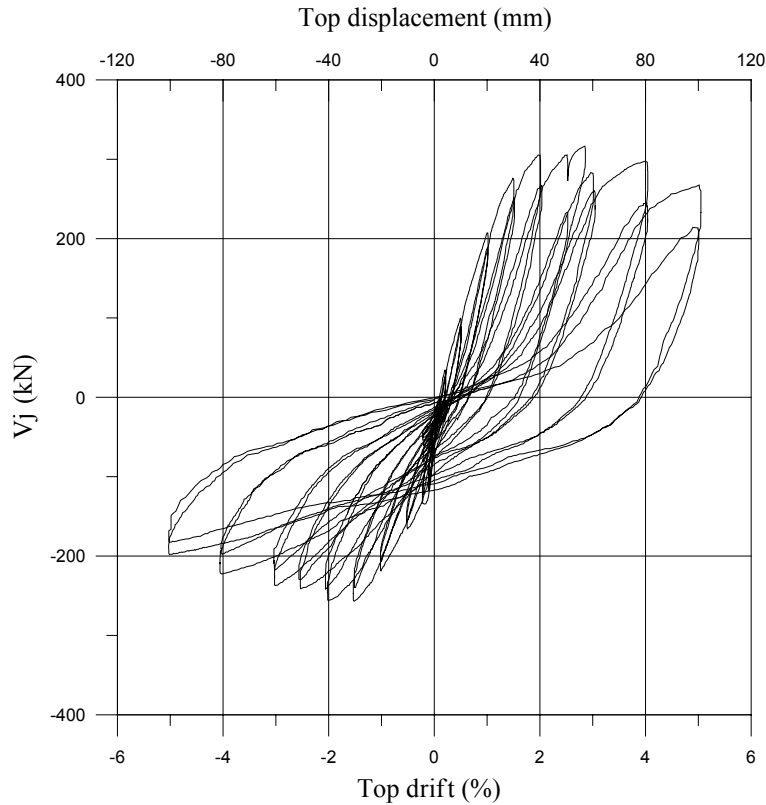
(b) negative loading direction

Figure 4.25 Members displacement contribution of Unit TSD

4.3.2.4 Force and Stress in the Joint

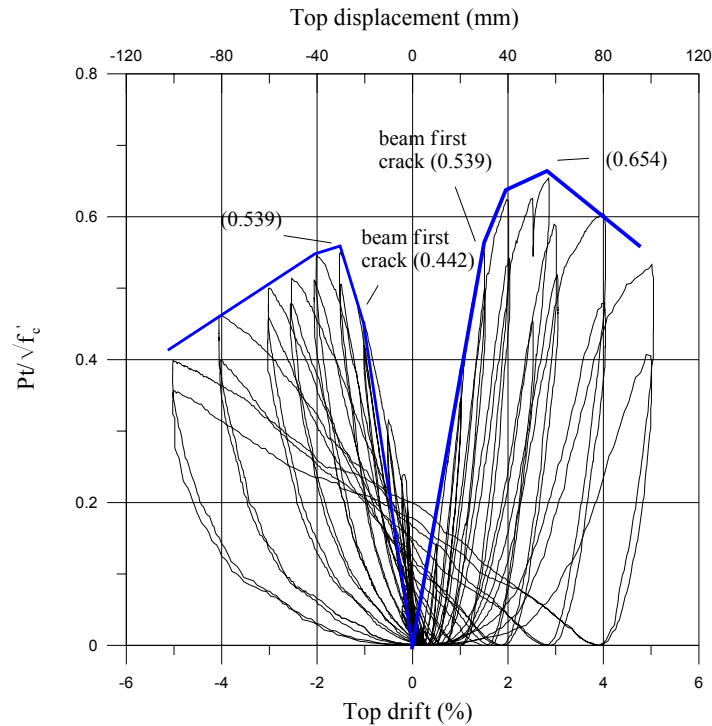
The assessment in Chapter 2 shows that the beam was the critical member for Unit TSD, therefore there is no damage in the joint core. The forces in the joint were increasing up to the level when Unit TSD suffered heavy damage and lost its strength. From that point, the forces in the joint started to degrade as the beam steel tension was reducing as well.

The horizontal shear in the joint area reached 317 kN and -257 kN in the positive and negative loading directions respectively. The principal tensile stress reached $0.654\sqrt{f'_c}$ and $0.539\sqrt{f'_c}$ in the positive and negative loading directions respectively. The axial load applied to the top of column was varied from $0.24\sqrt{f'_c}$ to $0.38\sqrt{f'_c}$. Figure 4.26 shows the joint horizontal shear force versus top drift (a) and the joint horizontal principal tensile stress versus top drift (b).



(a) Horizontal shear (V_j) versus Top drift of Unit TSD

Figure 4.26 Force and stress in the joint core of Unit TSD



(b) Principal tensile stress $(Pt)/\sqrt{f'_c}$ versus Top drift of Unit TSD

Figure 4.26 Force and stress in the joint core of Unit TSD (continued)

4.3.2.5 Summary

Unit TSD, an as-built two third scale beam-column joint unit was tested under a simulated seismic loading with varying axial load. Initial axial load of 75 kN was applied representing the gravity load on the column. The deficiency of Unit TSD is the shallowness of the beam geometry, which reduces the beam flexural lever arm significantly.

From this test we can conclude:

1. Poor seismic behaviour

The overall performance of the unit was poor. The unit can only resist the lateral force of 12 kN before failing in the beam, which is about half of the moment capacity. The reason is that only half of the amount of beam reinforcement anchored to the column, and the ones anchored outside the column did not totally contribute.

2. Adequate confinement in the joint

Due to the number of beam longitudinal reinforcement anchored in the column, the joint area was fully congested. This prevents the joint from concrete tension failure, which is not a desirable mechanism under seismic loading.

3. Contribution of varying axial load

Refer to Section 4.2.2.6.

4.4 TESTS SUMMARY

Six two-third scaled as-built reinforced concrete beam-column joint units, tested under simulated seismic loading with varying axial load on the column, using 75 kN as the initial axial load. The units were divided into two main categories according to the beam geometry, deep beams and shallow beams. The joint cores of all units contained single shear reinforcement, typical in pre-1970s construction.

The test results are shown in Table 4.3.

4.4.1 Results Comparison

The test results from all six exterior beam-column joints are summarized in this section. Comparisons are made to investigate the difference in two aspects, longitudinal reinforcement type and beam dimension. The main objective is to determine the difference in term of global strength and the joint strength.

4.4.1.1 Hysteresis Response

The force versus displacement hysteretic response from all units are being compared to each other for the units with similar flexural moment capacity but using different reinforcement type and/or beam dimension.

Test Unit	Max. Lateral Force (kN)		f'c (MPa)	Failure type		Joint horizontal shear (kN)		Principal tensile stress/ $\sqrt{f'_c}$			
	(+) loading	(-) loading		(+) loading	(-) loading	(+) loading	(-) loading	(+) loading		(-) loading	
								1st crack	Maximum	1st crack	Maximum
Unit TDP-1	16.4	9.2	22.9	Joint failure	Beam failure	97	67	0.233	0.233	0.149	0.17
Unit TDD-1	16.8	10.2	23.1	Beam failure	Beam failure	100	77	0.211	0.238	0.183	0.209
Unit TDP-2	16.2	14.7	25	Joint failure	Joint failure	117	94	0.28	0.3	0.228	0.272
Unit TDD-2	23.1	16.3	24.7	Joint failure	Joint failure	141	112	0.323	0.367	0.329	0.339
Unit TSP	10.8	7.5	23.4	Beam failure	Beam failure	272	240	0.475	0.545	0.478	0.506
Unit TSD	12.2	8.3	23.6	Beam failure	Beam failure	317	257	0.539	0.654	0.442	0.539

Table 4.3 Plane frame test result

4.4.1.1.1 Unit TDP-1 and TDD-1

Unit TDP-1 (deep-plain-4 top-2 bottom) and TDD-1 (deep-deformed-4 top-2 bottom) have the same moment capacity, beam and column dimension, and reinforcement detailing. The differences are the type of reinforcement and anchorage. Unit TDP-1 used plain round bars for the beam and column longitudinal reinforcement with hook-ends for beam bars while Unit TDD-1 used deformed bars with the beam bars bent into the joint core. The maximum lateral force is the same for both units, with Unit TDP-1 reaching up to 16.4 kN and 9.2 kN, while Unit TDD-1 reaching a little bit higher, up to 16.8 kN and 10.2 kN for positive and negative direction respectively. The difference is due to the slipping phenomena of the plain round bar for Unit TDP-1.

There is a little difference in the initial stiffness of the two units. This is due to the accident that happened with Unit TDP-1 before the test, which resulted in a crack on the beam; therefore the stiffness is not purely the initial stiffness.

The difference in the strength degradation for the units is due to the different types of failure that occurred on the units. Unit TDP-1 has severe strength degradation in the positive loading direction caused by joint shear failure while Unit TDD-1 has flat curve caused by beam flexural failure. In the negative loading direction, it is similar for both units since they have the same type of failure, which is beam flexural failure.

Fig. 4.27 shows the envelope of force displacement hysteresis loop for both Unit TDP-1 and TDD-1.

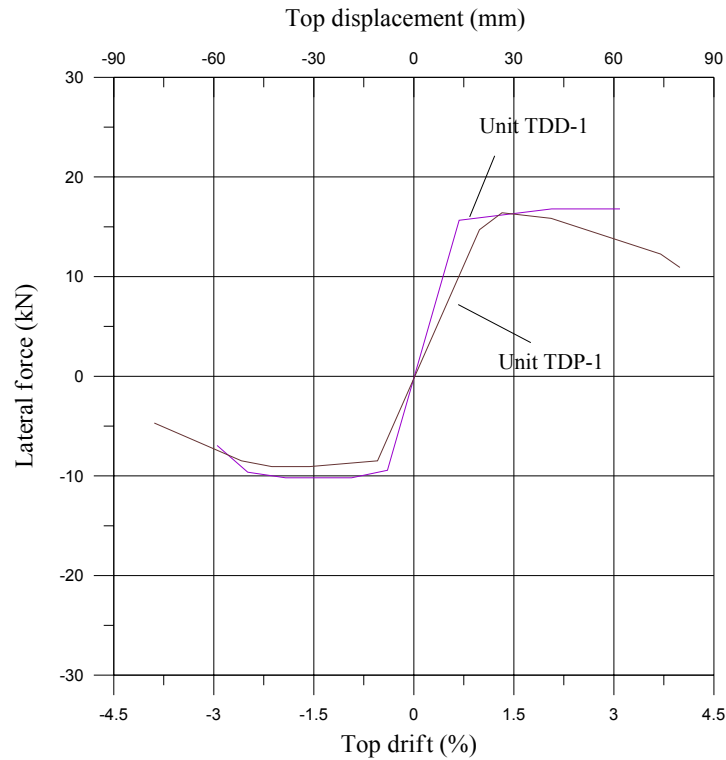


Figure 4.27 Hysteresis envelopes of Units TDP-1 (deep-plain) and TDD-1 (deep-deformed)

4.4.1.1.2 Unit TSP and TSD

Unit TSP (shallow-plain-12 top-6 bottom) and TSD (shallow-deformed-12 top-6 bottom) have the same moment capacity, beam and column dimension, and reinforcement detailing. The differences are the type of reinforcement and anchorage. Unit TSP used plain round bars with for the beam and column longitudinal reinforcement with hook-ends for the beam bars while Unit TSD used deformed bars with the beam bars bent into the joint core. The maximum lateral force is the same for both units, with Unit TSP reaching up to 10.7 kN and 7.5 kN, while Unit TSD reaching a little higher, up to 12 kN and 8 kN for positive and negative directions respectively. The difference is due to the slipping phenomena of the plain round bars for Unit TSP.

Both units suffered the same type of failure, beam flexural failure. Therefore the stiffness and the strength degradation are similar one to another.

Fig. 4.28 shows the envelope of force displacement hysteresis loop for both Unit TSP and TSD.

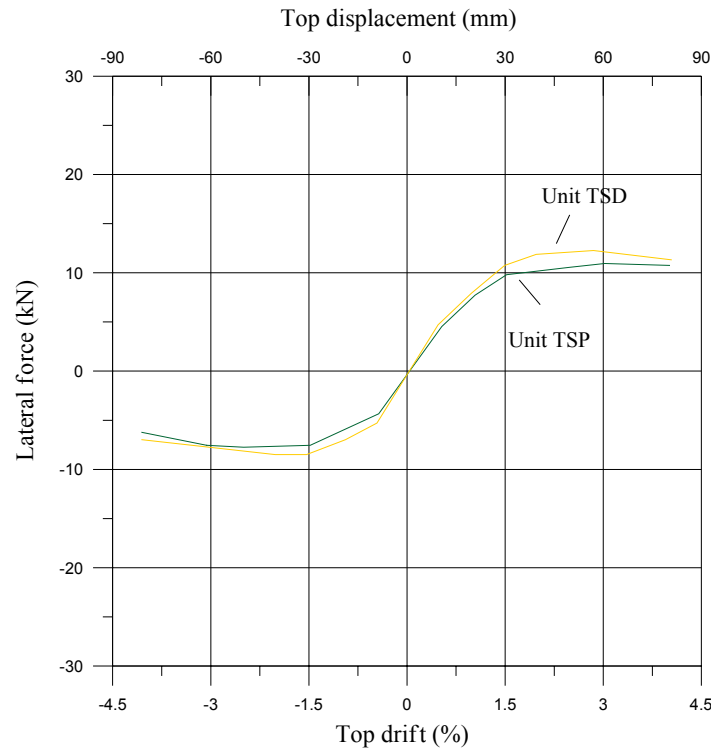


Figure 4.28 Hysteresis envelopes of Units TSP (shallow-plain) and TSD (shallow-deformed)

4.4.1.1.3 Unit TDP-1 and TSP

Unit TDP-1 (deep-plain-4 top-2 bottom) and TSP (shallow-plain-12 top-6 bottom) have the same moment capacity, reinforcement type and anchorage. The only difference is the beam dimension. Unit TDP-1 has a 200mm x 330 mm beam while the beam dimension for Unit TSP is 130mm x 535mm. The maximum lateral force for Unit TDP-1 is 16.4 kN and 9.2 kN, while Unit TSP only reached 10.7 kN and 7.5 kN for positive and negative directions respectively. The capacity of Unit TSP is 65% of Unit TDP-1 in the positive direction and 81% in the negative direction. This is due to the distribution of beam reinforcement with only 33% anchored to the column and the rest outside the column reinforcement. This is a common mistake in the design process of the shallow beam when the designer did not consider about the amount of reinforcement anchored in the column. The strain distribution of the beam longitudinal reinforcement from Unit TSP is shown in Fig. 4.29. The further the position of the beam longitudinal reinforcement from the joint core, the smaller contribution given.

The initial stiffness of Unit TSD is only about 50% of Unit TDP-1 due to different *Moment of Inertia Area*.

The difference in the strength degradation for the units is due to different type of failure occurred on the units. Unit TDP-1 has severe strength degradation in the positive loading direction caused by joint shear failure while Unit TSP has flat curve caused by beam flexural failure. In the negative loading direction, it is similar for both units since they have the same type of failure, which is beam flexural failure.

Fig. 4.30 shows the envelope of force displacement hysteresis loop for both Unit TDP-1 and TSP.



Figure 4.29 Strain distribution on beam reinforcement for Unit TSP (shallow-plain)

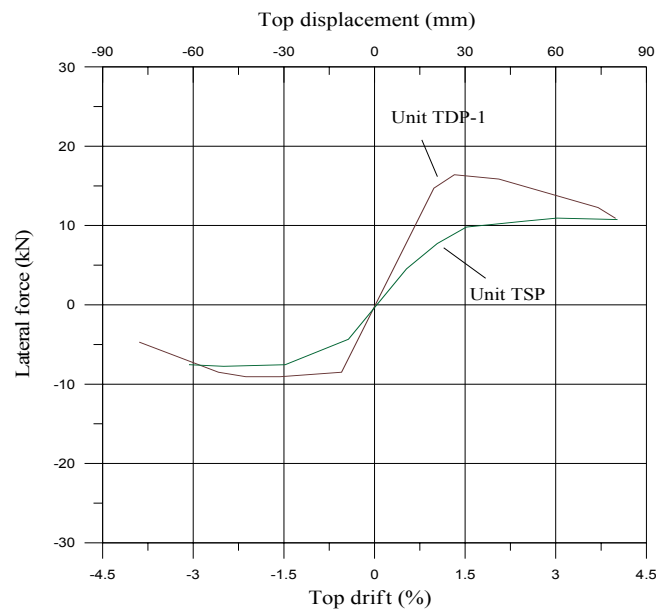


Figure 4.30 Hysteresis envelopes of Units TDP-1 (deep-plain) and TSP (shallow-plain)

4.4.1.1.4 Unit TDD-1 and TSD

Unit TDD-1 (deep-deformed-4 top-2 bottom) and TSD (shallow-deformed-12 top-6 bottom) have the same moment capacity, reinforcement type and anchorage. The only difference is the beam dimension. Unit TDD-1 has a 200mm x 330 mm beam while the beam dimension for Unit TSD is 130mm x 535mm. The maximum lateral force for Unit TDD-1 is 16.8 kN and 10.2 kN, while Unit TSD only reached 12 kN and 8 kN for positive and negative directions respectively. The capacity of Unit TSD is 71% of Unit TDD-1 in the positive direction and 78% in the negative direction. This is due to the distribution of beam reinforcement with only 33% anchored to the column and the rest outside the column reinforcement. The strain distribution of the beam longitudinal reinforcement from Unit TSD is similar with Unit TSP as shown in Fig. 4.29. The further the position of the beam longitudinal reinforcement from the joint core, the smaller contribution given.

The initial stiffness of Unit TSD is only about 35% to 50% of Unit TDD-1 due to different *Moment of Inertia Area*.

Both units suffered the same type of failure, beam flexural failure. Therefore the stiffness and the strength degradation are similar one another.

Fig. 4.31 shows the envelope of force displacement hysteresis loop for both Unit TDD-1 and TSD.

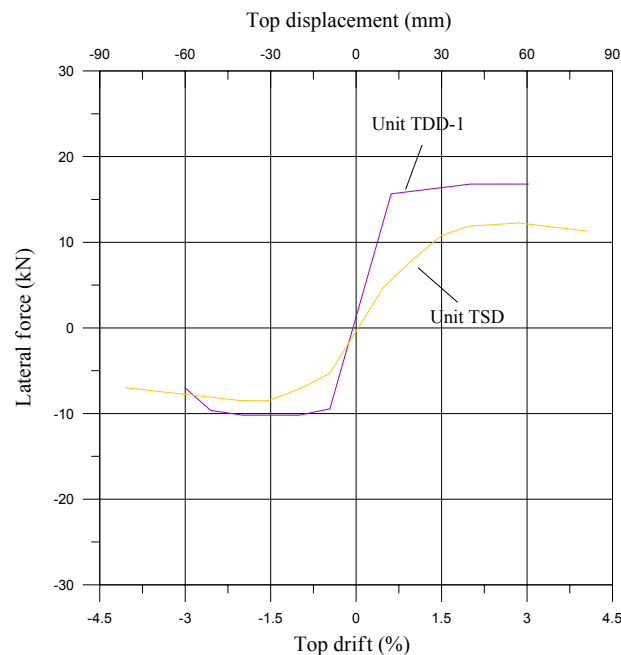


Figure 4.31 Hysteresis envelopes of Units TDD-1 (deep-deformed) and TSD (shallow-deformed)

4.4.1.2 Joint Principal Tensile Stress

From six exterior beam-column joints tested, only three specimens suffered joint shear failure. Unit TDP-1 has a joint shear failure in the positive loading direction only while Units TDP-2 and TDD-2 have joint shear failure in both directions.

Fig. 4.32 shows the strength degradation curve for Units TDP-1, TDP-2 and TDD-2.

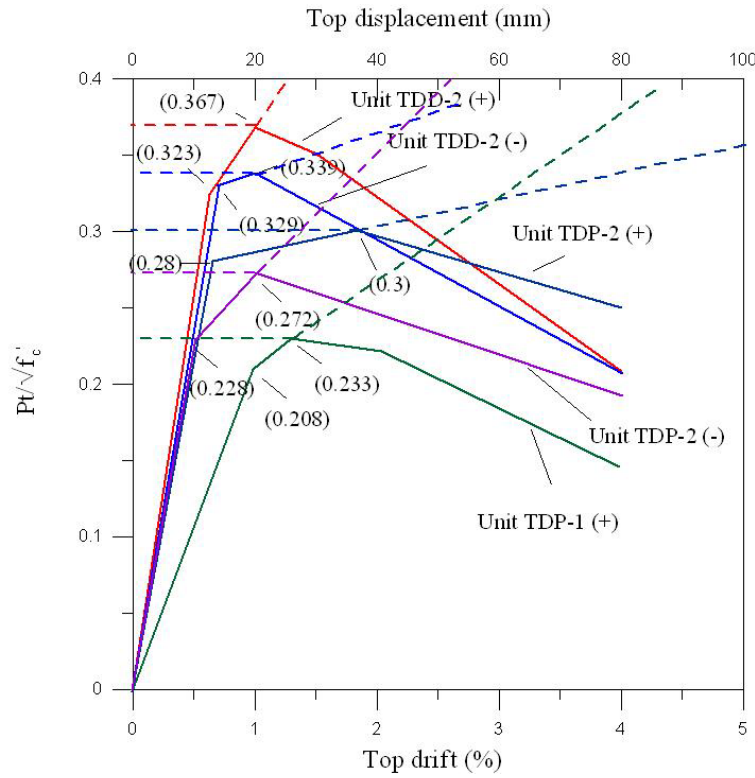


Fig. 4.32 Strength degradation curve for Units TDP-1 (deep-plain-4-2), TDP-2 (deep-plain-4-4) and TDD-2 (deep-deformed-6-4)

From the results, two strength degradation curves, one for deformed bars bent into joint with one stirrup in the joint core and one for smooth beam bars with end hooks and one stirrup in the joint core is proposed as shown in Fig. 4.33.

For deformed beam bars bent into the joint with one stirrup in the joint core, joint failure is expected to occur at a principal tensile stress $P_t = 0.33 \sqrt{f'_c}$ and increasing up to $P_t = 0.37 \sqrt{f'_c}$ before degrading quite significantly.

For smooth beam bars with end hooks and one stirrup in the joint core, joint failure is expected to occur at a principal tensile stress $P_t = 0.28 \sqrt{f'_c}$ and increasing up to $P_t =$

$0.3\sqrt{f'_c}$ before degrading quite significantly. The ability to maintain and increase the strength after the first joint crack is due to the stirrup contribution in confining the concrete so that even with the joint crack, the strength will not drop suddenly.

The newly proposed strength degradation curves are compared with the previous model proposed by Priestley and Pampanin and shown in Fig. 4.34.

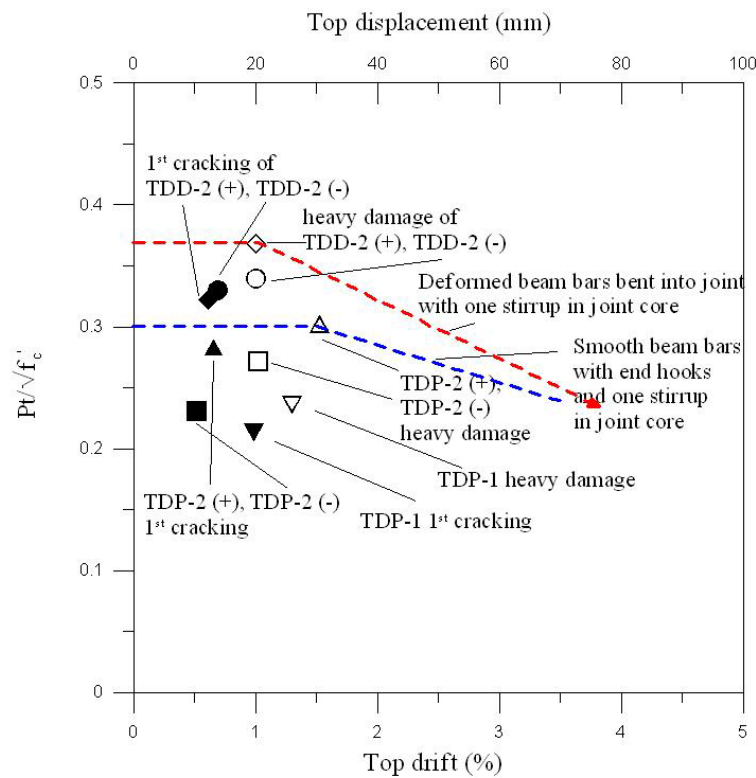


Figure 4.33 Strength degradation curve for Units TDP-1, TDP-2 and TDD-2

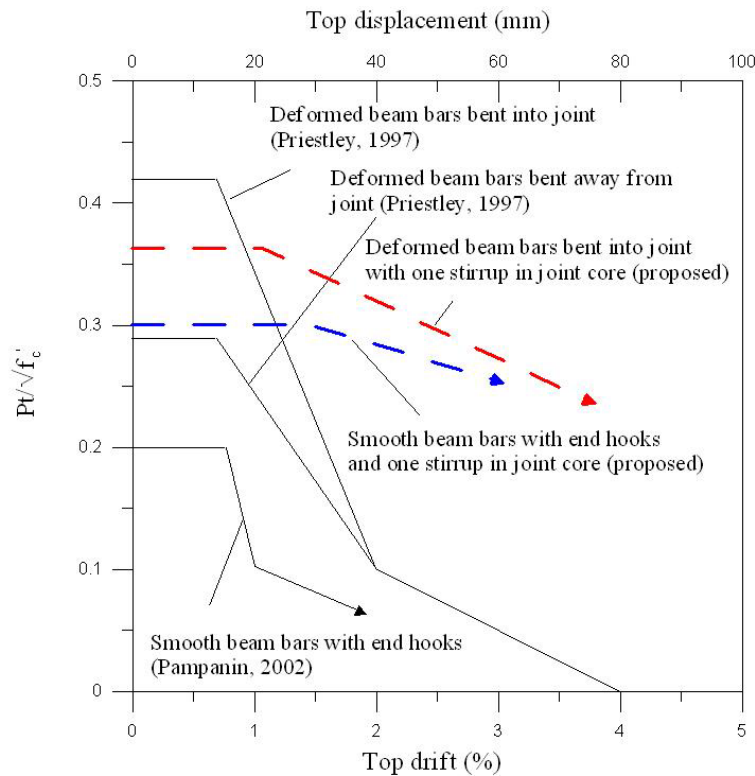


Figure 4.34 Strength degradation curve for exterior joints

4.5 CONCLUSION

This chapter presents the test results and proposes two strength degradation curves for as-built reinforced beam-column joint members under seismic loading with specific reinforcement details. The conclusions are:

1. The type of bar used for the longitudinal reinforcement has a major role in determining the type of failure that may occur in the beam-column joint subassembly. The use of plain round bars can lead to joint shear failure, which will result in severe strength degradation. The use of deformed bars will have a bigger possibility of having a beam flexural failure as desired in seismic design. Plain round bars were widely used in the pre-1970s buildings; therefore they have to be assessed referring to the seismic design code at present so that a most suitable retrofit strategy can be applied to prevent the building from collapse under seismic excitation.
2. A beam-column joint subassembly with beam width to depth ratio more than one has bigger ductility than conventional beams (width to depth ratio less than one). The inertia area of the beam contributes to the ability of the subassembly to allow

bigger displacement. A common mistake made by the designers using shallow beams is that they did not consider the amount of the beam longitudinal reinforcement anchored to the column, which can result to the beam not providing the theoretical moment capacity since the reinforcement anchored outside the column will only have a small contribution.

A joint shear failure is really unlikely for the shallow beam due to the large area working as the joint core. The congestion in the joint core caused by the number of reinforcement inside also contributes to provide sufficient strut and tie mechanism.

3. Contribution of transverse reinforcement in the joint area is really important to help the confinement. A single transverse reinforcement can make a big difference and alter the failure mechanism for the beam-column joint subassembly.
4. Based on experimental results, two strength degradation curves for exterior joint are proposed. One is for a beam-column joint subassembly using deformed bars bent into the joint with one stirrup in the joint core and the other is for a beam-column joint subassembly using smooth bars with end hooks and one stirrup in the joint core.
5. From the damage observed in during the test, a limit state for exterior joints with substandard details based on joint shear deformation is proposed to justify the limit state proposed by Pampanin et al. (2003)

Limit State	Proposed in this work	Proposed by Pampanin et al. (2003)
Undamaged	$\gamma < 0.0007$	$\gamma < 0.0002$
Limited Damage	$0.0007 \leq \gamma < 0.006$	$0.0002 \leq \gamma < 0.005$
Extensive Damage	$0.006 \leq \gamma < 0.01$	$0.005 \leq \gamma < 0.01$
Critical Damage	$0.01 \leq \gamma < 0.016$	$0.01 \leq \gamma < 0.015$
Collapse	$\gamma \geq 0.016$	$\gamma \geq 0.015$

Table 4.4 Limit state based on joint shear deformation

CHAPTER 5

SPACE FRAME TEST RESULTS

5.1 INTRODUCTION

The space frame test consists of three two-third scaled as-built reinforced concrete beam-column joint units, tested under simulated seismic loading with varying axial load on the column, using 75 kN as the initial axial load. The units were corner joints and divided into two main categories according to the beam geometry, deep-deep beams and deep-shallow beams. The joint cores of all units contained single shear reinforcement, except for Unit DD-2, which doesn't have shear reinforcement in its joint core, typical in pre-1970s construction. Tables 5.1 and 5.2 show the reinforcing details and material strength of the space frame specimens.

This chapter reports the results of the series of test conducted on the space frame units.

To clarify the signs and directions of the loading and the displacement, Fig. 5.1 shows the sign convention.

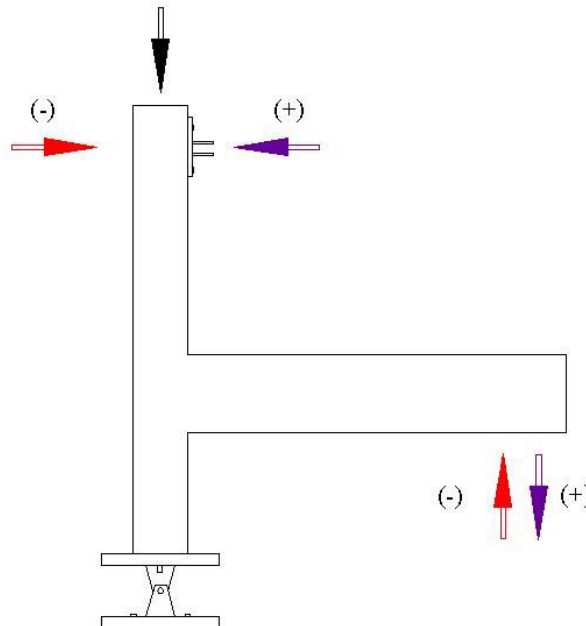


Figure 5.1 Positive loading and displacement

Test Unit	Bars type	Column			Axis	Beam			Joint's stirrup	
		Dimension	Reinforcement			Dimension	Reinforcement			
			bars number	Stirrups			bars number			Stirrups
							(mm ²)	(mm)		
Unit DD-1	Plain	230x230	6Φ10	Φ6-100	X	200x330	4Φ10 top - 4Φ10 bottom	Φ6-133	1	
					Y	200x330	4Φ10 top - 4Φ10 bottom	Φ6-133		
Unit DD-2	Plain	230x230	6Φ10	Φ6-100	X	200x330	4Φ10 top - 4Φ10 bottom	Φ6-133	none	
					Y	200x330	4Φ10 top - 4Φ10 bottom	Φ6-133		
Unit DS	Plain	230x230	6Φ10	Φ6-100	X	200x330	4Φ10 top - 4Φ10 bottom	Φ6-133	1	
					Y	130x535	12Φ10 top - 12Φ10 bottom	Φ6-133		

Table 5.1 Reinforcement details of space frame test units

Test Unit	Concrete strength (fc')		Age at test	Reinforcing bars strength (fy)	
	(MPa)			MPa	
	28 days	at test day	(days)	Plain Φ10	Plain Φ6
Unit DD-1	24.8	24.2	153	387.9	343.9
Unit DD-2	28.9	27.4	40	341	388
Unit DS	21.1	23.8	136	387.9	343.9

Table 5.2 Material properties of space frame test units

5.2 DEEP-DEEP BEAMS

Two geometrically identical corner beam-column joint units with deep beams were constructed. The units are referred to as Units DD-1 and DD-2. Unit DD-1 used single shear reinforcement in the joint area, while unit DD-2 used no shear reinforcement in the joint area. Grade 300 plain round steel was used for the longitudinal and transverse reinforcement. The units used plain round longitudinal bars for beams and column reinforcement.

5.2.1 Unit DD-1

Unit DD-1 consists of two deep beams and one column. The beam bars were hooked in the joint core area. A single transverse reinforcement was used in the joint core. The aim of this test is to investigate the behaviour of the unit in the biaxial manner and compare it with the uniaxial manner from the test done for plane frame units. Initial axial load of 75 kN was applied on the top of the column to represent the gravity load.

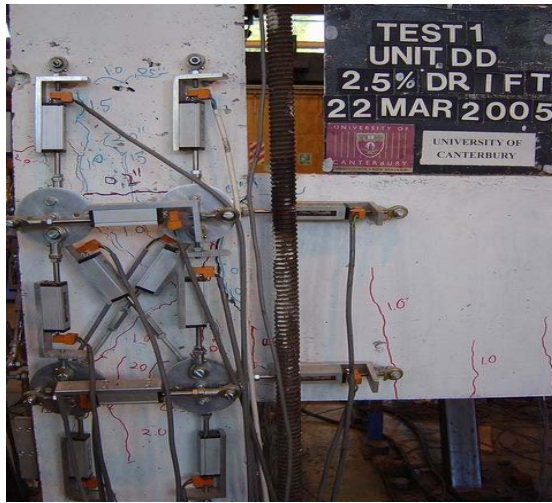
A mistake in sign convention was made during the test; therefore the test result is equal to the situation when the lateral load is applied at the base of the column, instead of the top of the column. Since the beam is symmetrically reinforced, there is no major difference than if the lateral load was applied at the top of the column.

5.2.1.1 Crack Development and Damage

Minor cracks started to occur at the location of the beam stirrups at 0.2% of drift. The diagonal joint crack occurred at 1% of drift for both positive and negative loading directions for X excitation. In the Y excitation, the diagonal joint crack occurred at 1% and 1.5% of drift for positive and negative loading directions respectively. Minor diagonal cracks were spread in the joint core area due to the lack of transverse reinforcement in the joint. The existing cracks were extending and widening with the increase of the drift.

The concrete in the outer layer of the column was not spalling at the end of test and still quite well united since the beams are helping one another in terms of confining the concrete and preventing it from falling down. The unit was loaded until 4% of drift when the unit strength reduced significantly due to the damage in the beam and joint area.

Figure 5.2 shows the cracks and the final appearance of Unit DD-1. Since the instrumentations were attached on the joint area are covering the cracks in there, only pictures with major cracks which are visible, is shown.



(a) At 2.5% of drift (X)



(b) At 2.5% of drift (Y)



(c) At 3% of drift (X)

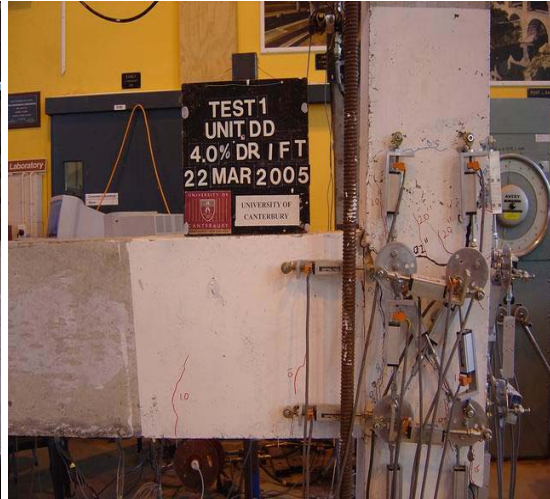


(d) At 3% of drift (Y)

Figure 5.2 Cracks of Unit DD-1



(e) At 4% of drift (X)



(f) At 4% of drift (Y)



(g) At the end of the test (X)



(h) At the end of the test (Y)



(i) At the end of the test (diagonal angle)

Figure 5.2 Cracks of Unit DD-1 (continued)

5.2.1.2 Hysteretic Response

The lateral force versus the top column displacement of Unit DD-1 is shown in Fig. 5.3. The first cracking in the joint occurred at 1% of drift both in positive and negative loading directions respectively for X and Y excitation.

The extra confinement provided by the other beam in the transverse direction help to hold the concrete together even after the joint first crack has occurred so the strength can still pick up for about one level of drift higher before starting to degrade. The strength degradation was more severe than the plane frame unit. The maximum lateral force that can be resisted by Unit DD-1 was 10.9 kN and 12.6 kN for positive and negative loading directions respectively for X excitation. And for Y excitation, the maximum lateral force was 10.6 kN and 12.4 kN for positive and negative loading directions respectively.

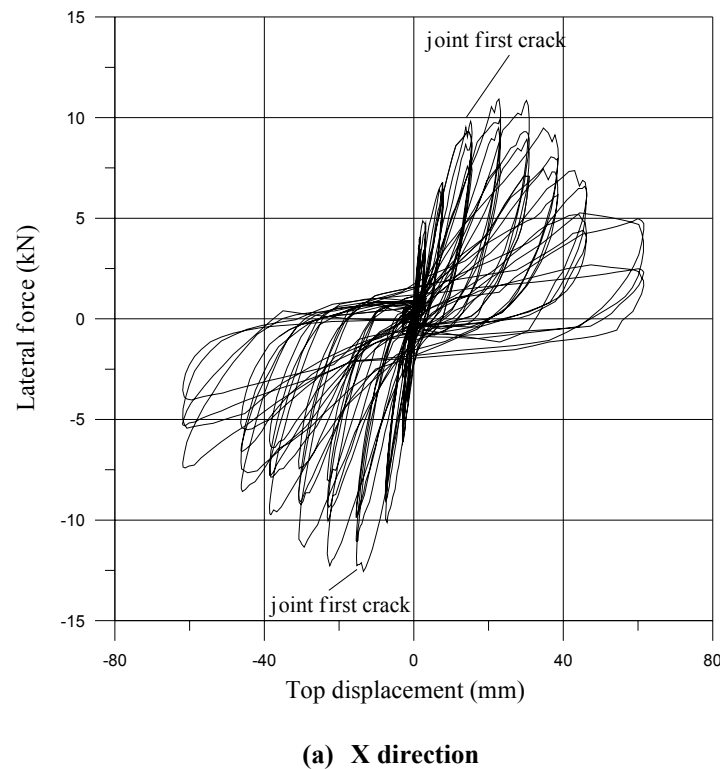
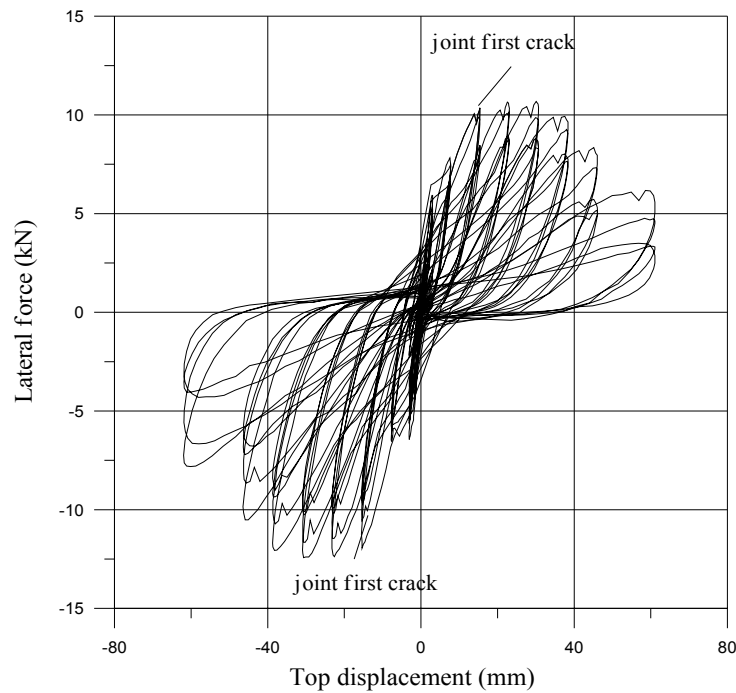


Figure 5.3 Lateral force versus Top displacement of Unit DD-1



(b) Y direction

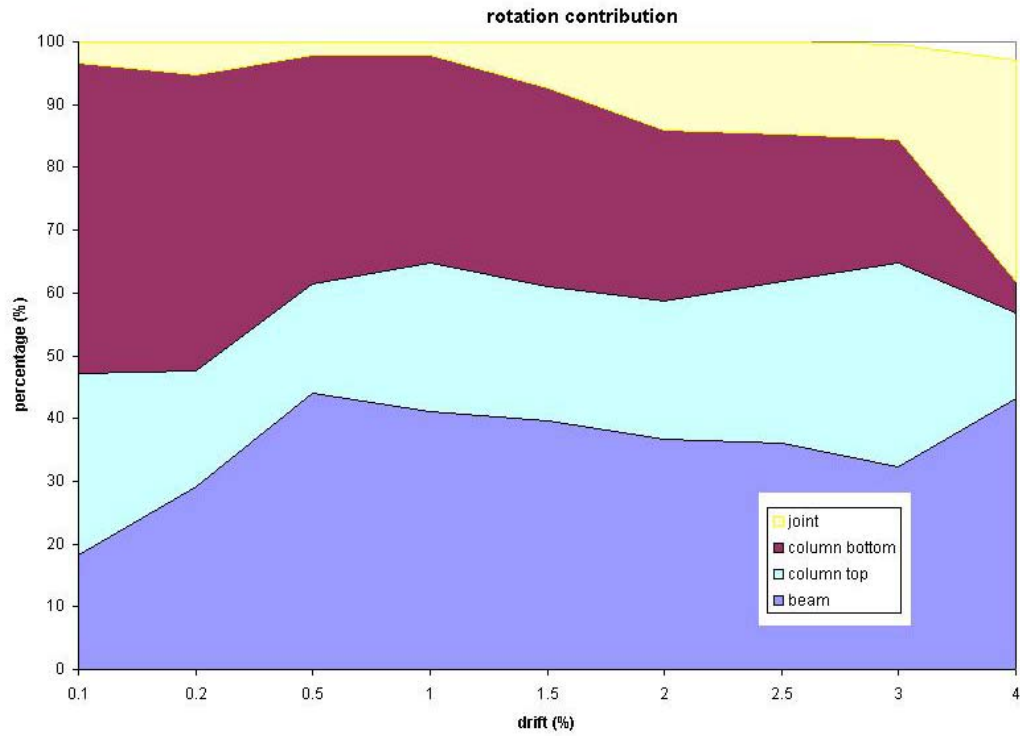
Figure 5.3 Lateral force versus Top displacement of Unit DD-1 (continued)

5.2.1.3 Displacement Components

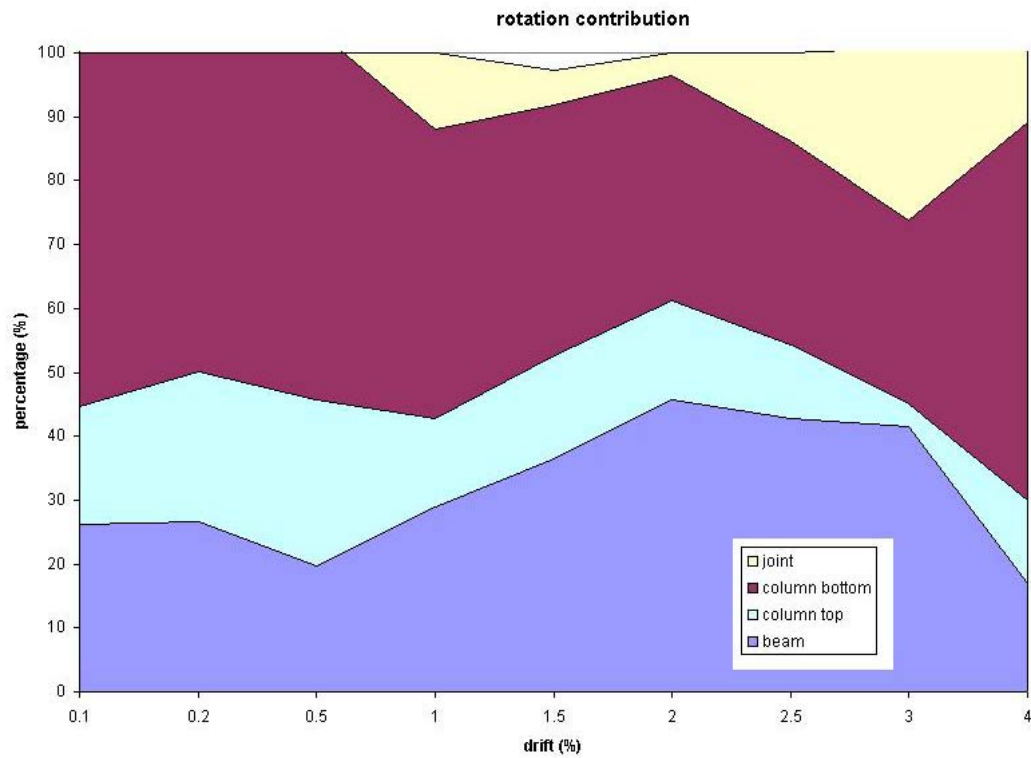
The same difficulties in measuring the actual displacement also occurred for this unit. The data recorded from the potentiometers had to be observed in test of Unit DD-1 to approximate the actual displacement as close as possible.

At the start of the test, the column governed the displacement of Unit DD-1, until the joint first crack and the joint started to increase its contribution. For X excitation, the maximum column displacement contribution was about 80%, the maximum beam displacement contribution was up to 40% and the maximum joint displacement contribution was up to 40%. For Y excitation, the maximum column displacement contribution was about 75%, the maximum beam displacement contribution was up to 50% and the maximum joint displacement contribution was up to 40%.

Note that the value here had been modified so it is not very accurate. Figure 5.4 shows the members contribution of Unit DD-1 total displacement.

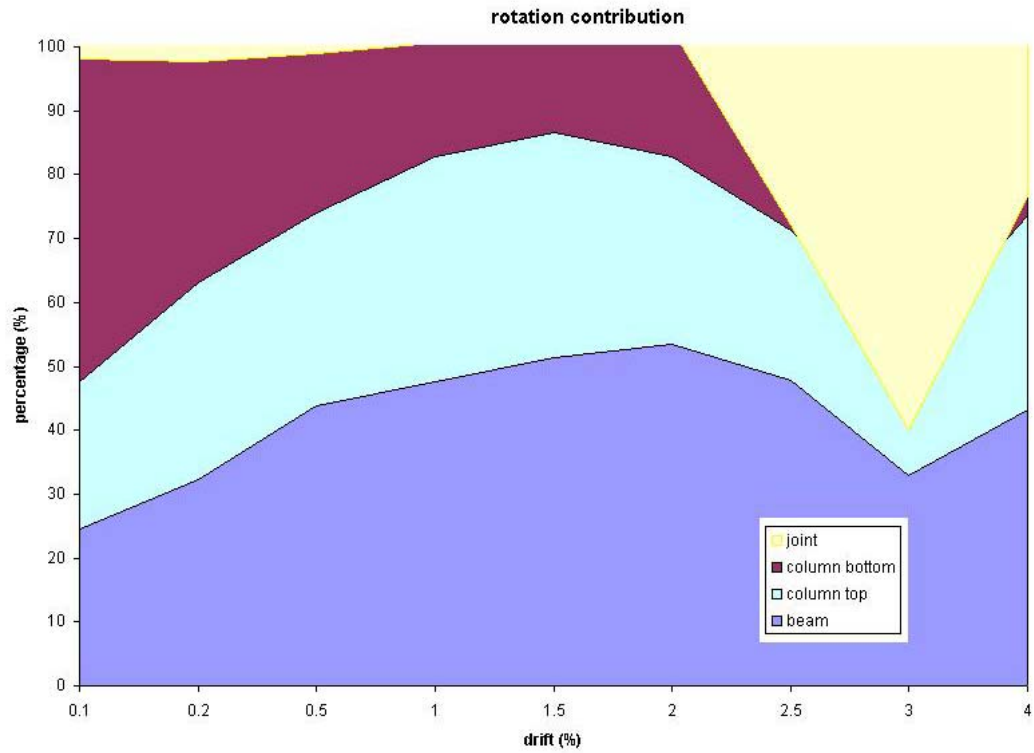


(a) positive loading direction (X)

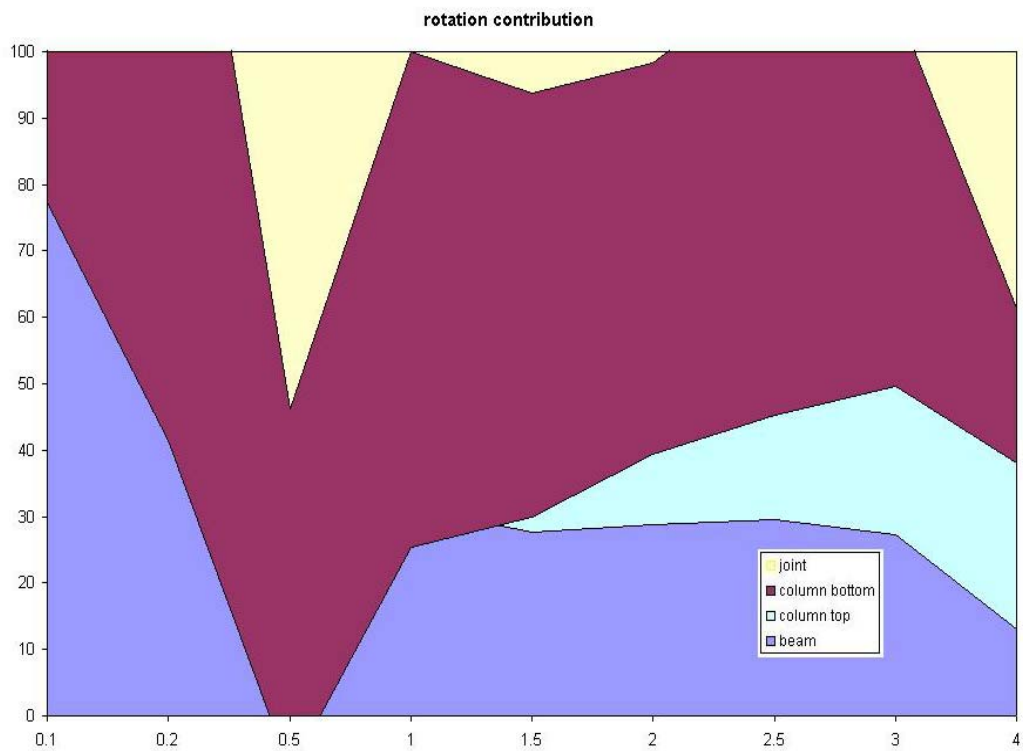


(b) negative loading direction (X)

Figure 5.4 Members displacement contribution of Unit DD-1



(c) positive loading direction (Y)



(d) negative loading direction (Y)

Figure 5.4 Members displacement contribution of Unit DD-1 (continued)

5.2.1.4 Force and Stress in the Joint

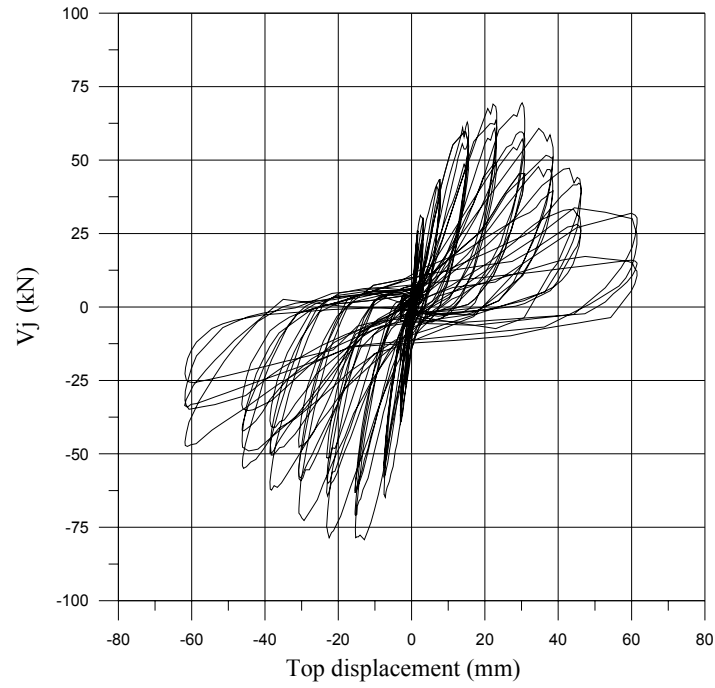
From the assessment in Chapter 2 and the results from the experiments on the plane frame units, it is known that the joint was the critical member for Unit DD-1. The joint will crack both in the positive and negative directions and thus preventing the plastic hinges occurring in the beams.

For the X excitation, in the positive loading direction, the principal tensile stress in the joint was increasing up to $0.151\sqrt{f'_c}$ when the first joint diagonal cracking occurred. From that point, the principal tensile stress in the joint can still increase up to $0.168\sqrt{f'_c}$ before degrading significantly. In the negative loading direction, the maximum joint principal tensile stress was $0.171\sqrt{f'_c}$ before degrading significantly. The horizontal shear in the joint area reached 70 kN and -80 kN in the positive and negative loading directions respectively.

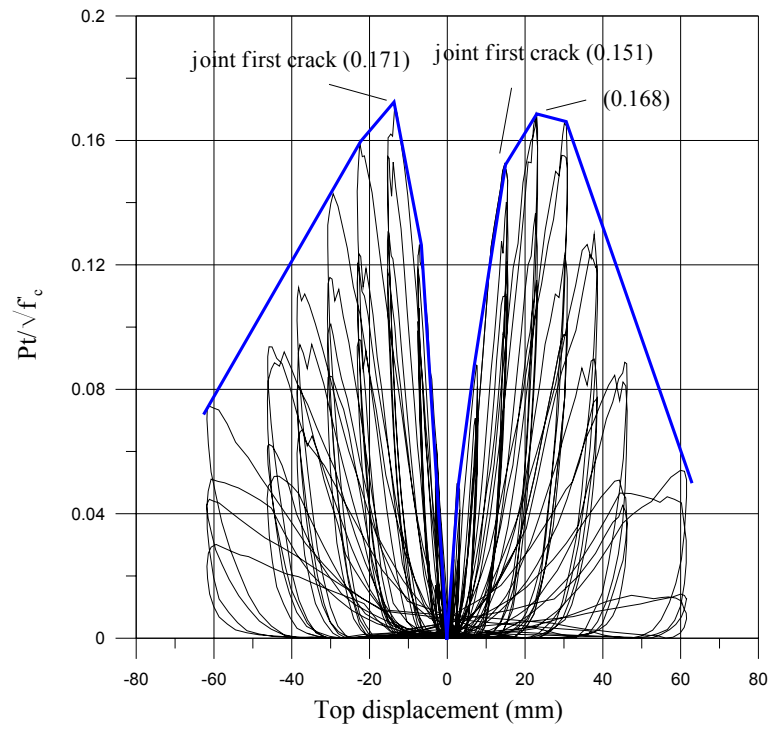
For the Y excitation, in the positive loading direction, the principal tensile stress in the joint was increasing up to $0.179\sqrt{f'_c}$ when the first joint diagonal cracking occurred. From that point, the principal tensile stress in the joint can still increase up to $0.186\sqrt{f'_c}$ before degrading significantly. In the negative loading direction, the joint diagonal cracking occurred when the principal tensile stress was $0.166\sqrt{f'_c}$. From that point, the principal tensile stress in the joint can still increase up to $0.182\sqrt{f'_c}$ before degrading significantly. The horizontal shear in the joint area reached 68 kN and -80 kN in the positive and negative loading directions respectively.

The axial load applied to the top of column was varied from $0.17\sqrt{f'_c}$ to $0.44\sqrt{f'_c}$.

Figure 5.5 shows the joint horizontal shear force versus top displacement and the joint horizontal principal tensile stress versus top displacement for both X and Y directions.

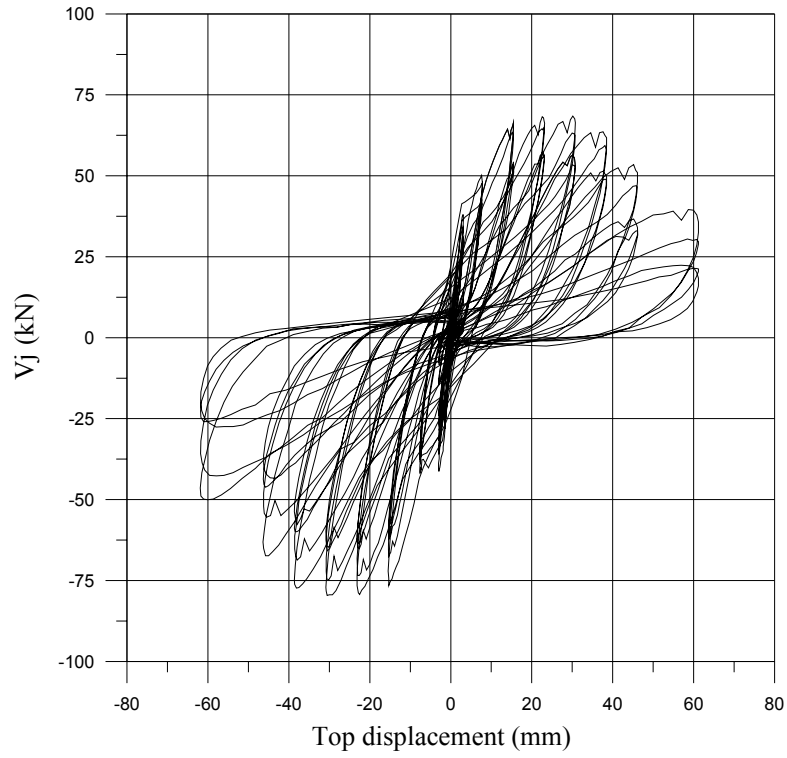


(a) X Horizontal joint shear (V_j) versus Top displacement of Unit DD-1

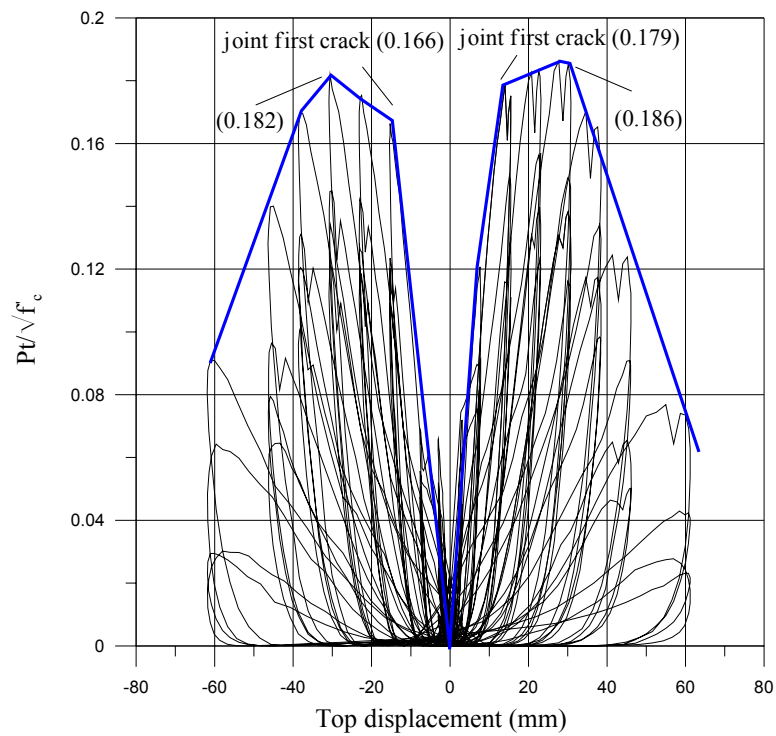


(b) X Joint principal tensile stress (P_t)/ $\sqrt{f'_c}$ versus Top displacement of Unit DD-1

Figure 5.5 Force and stress in the joint core of Unit DD-1



(c) Y Horizontal joint shear (V_j) versus Top displacement of Unit DD-1



(d) Y Joint principal tensile stress ($P_t/\sqrt{f'_c}$) versus Top displacement of Unit DD-1

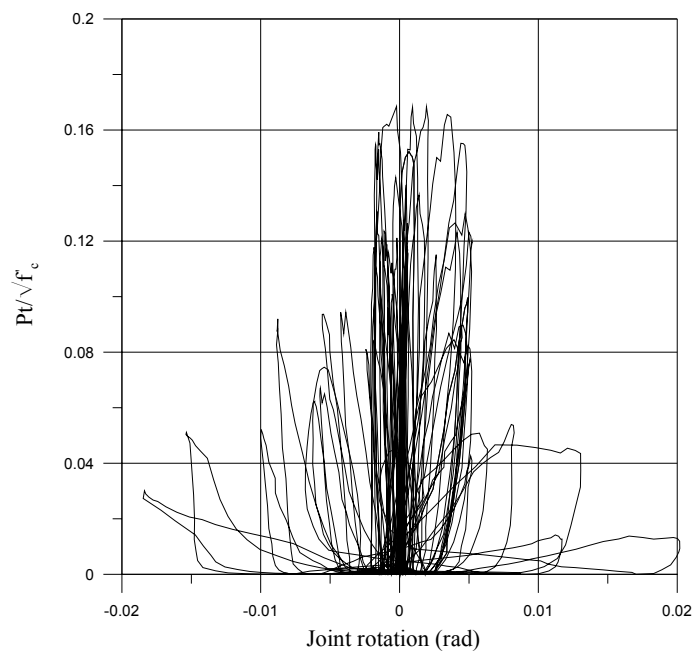
Figure 5.5 Force and stress in the joint core of Unit DD-1 (continued)

5.2.1.5 Joint Shear Deformation

From the damage in the unit observed during the test, the limit state in term of joint rotation (γ) is proposed as follow:

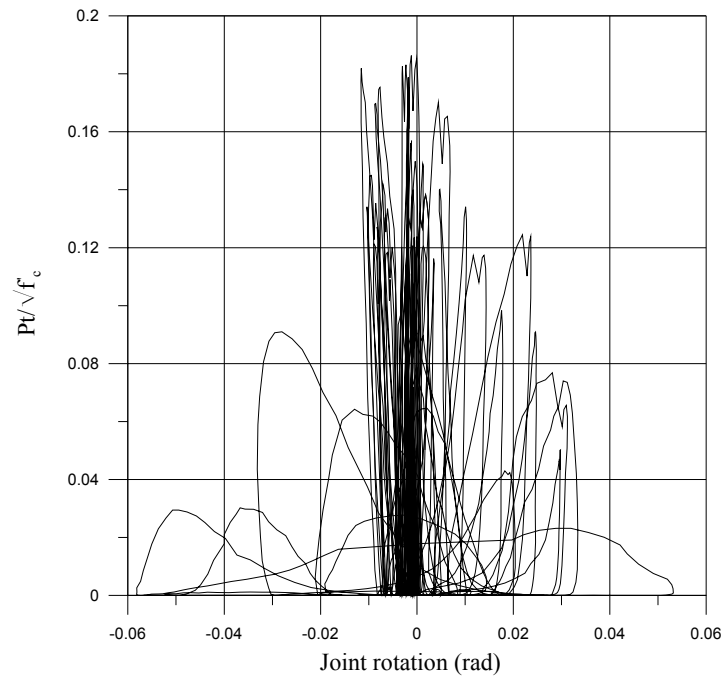
- Undamaged: $\gamma < 0.0007$
- Limited damage: $0.0007 \leq \gamma < 0.002$
- Extensive damage: $0.002 \leq \gamma < 0.005$
- Critical damage: $0.005 \leq \gamma < 0.02$
- Collapse: $\gamma \geq 0.02$

Figure 5.6 shows the plot of joint horizontal principal tensile stress versus joint rotation for both X and Y excitations.



(a) X excitation

Figure 5.6 Joint principal tensile stress (Pt)/ $\sqrt{f'_c}$ versus Joint rotation of Unit DD-1



(b) Y excitation

Figure 5.6 Joint principal tensile stress $(Pt)/\sqrt{f_c}$ versus Joint rotation of Unit DD-1 (continued)

5.2.1.6 Summary

Unit DD-1, an as-built two third scale beam-column joint unit was tested under a simulated seismic loading with varying axial load. Initial axial load of 75 kN was applied representing the gravity load on the column. The deficiencies of Unit DD-1 are the lack of transverse reinforcement in the joint core, the used of plain round longitudinal reinforcement and the hook anchorage of the beam longitudinal reinforcement in the joint core.

From this test we can conclude:

1. Poor seismic behaviour

The overall performance of the unit was poor. After the joint cracked at 1% of drift, the strength started to degrade. The use of plain round longitudinal reinforcement caused a loss in bond strength and the bar slipping which can be seen in the pinching of the hysteresis loop of the unit. Hook anchorage worsen the behaviour of the unit because the tension forces from the beam longitudinal reinforcement were not transferred properly to the joint core but concentrated in the hooks and initiated the concrete wedge phenomena.

2. Lack of transverse reinforcement in the joint

Diagonal cracks occurred in the joint area due to the shear forces working in the joint could not be resist by the single transverse reinforcement in the joint. The concrete cover of column outer layer was spalling when the high level of drift was applied on the unit. However, the joint first cracking occurred when the principal tensile stress in the joint reached $0.17\sqrt{f'_c}$ to $0.18\sqrt{f'_c}$, which is lower than $0.28\sqrt{f'_c}$ observed in the plane frame test. The joint transverse reinforcement and the beams help to confine the concrete so that the spalling of the concrete did not occur until high level of drift.

3. Contribution of varying axial load

Refer to Section 6.2.2.6.

4. Limit state in term of joint rotation (γ)

Proposed limit state

- Undamaged: $\gamma < 0.0007$
- Limited damage: $0.0007 \leq \gamma < 0.002$
- Extensive damage: $0.002 \leq \gamma < 0.005$
- Critical damage: $0.005 \leq \gamma < 0.02$
- Collapse: $\gamma \geq 0.02$

5.2.2 Unit DD-2

Unit DD-2 consists of two deep beams and one column. The beam bars were hooked in the joint core area. No shear reinforcement was used in the joint core. The aim of this test is to investigate the behaviour of the unit in the biaxial manner and compare it with Unit DD-1 to investigate the contribution of the shear reinforcement in the joint area. Initial axial load of 75 kN was applied on the top of the column to represent the gravity load.

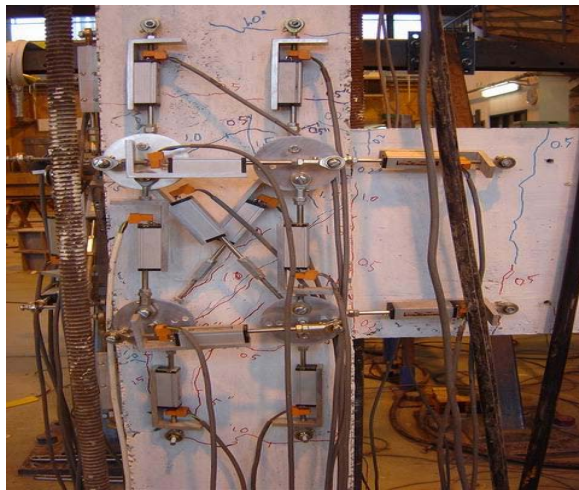
5.2.2.1 Crack Development and Damage

Minor cracks started to occur at the location of the beam stirrups at 0.2% of drift. The diagonal joint crack occurred at 1% of drift for both positive and negative loading directions for X and Y excitations. Minor diagonal cracks were spread in the joint

core area due to the lack of transverse reinforcement in the joint. The existing cracks were extending and widening with the increase of the drift.

The concrete in the outer layer of the column was not spalling at the end of test and still quite well united since the beams are helping one another in terms of confining the concrete and preventing it from falling down. The unit was loaded until 3% of drift when the unit strength reduced significantly due to the damage in the beam and joint area. The beams were hardly damaged with only minor cracks occurring at the stirrup locations.

Figure 5.7 shows the cracks and the final appearance of Unit DD-2. Since the instrumentations were attached on the joint area are covering the cracks in there, only pictures with major cracks which are visible, is shown.



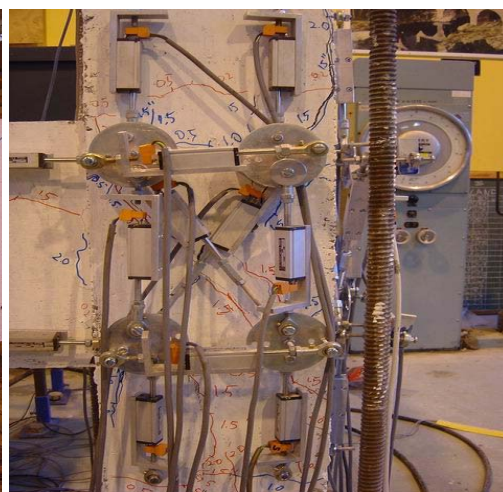
(a) At 1.5% of drift (X)



(b) At 1.5% of drift (Y)

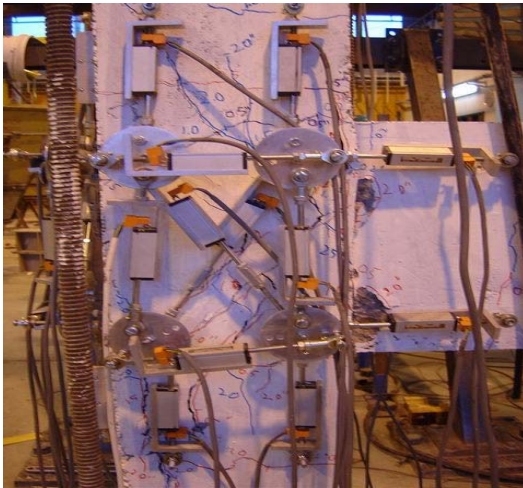


(c) At 2% of drift (X)

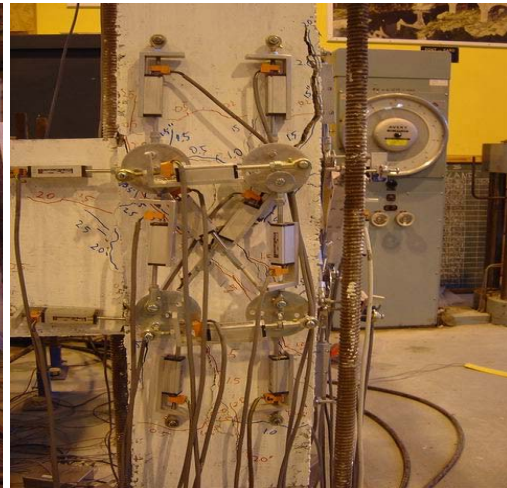


(d) At 2% of drift (Y)

Figure 5.7 Cracks of Unit DD-2



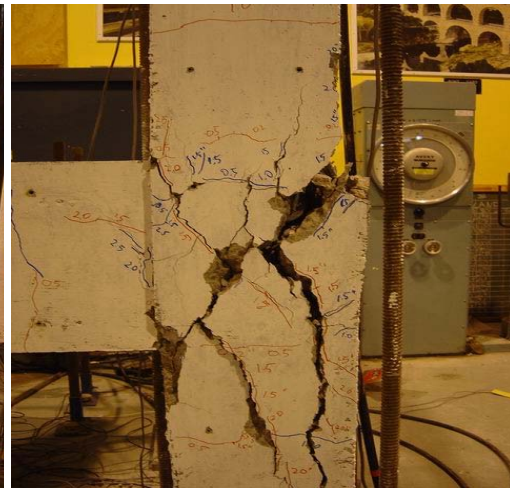
(e) At 2.5% of drift (X)



(f) At 2.5% of drift (Y)



(g) At 3% of drift (X)



(h) At 3% of drift (Y)



(i) At the end of the test (X)



(j) At the end of the test (Y)

Figure 5.7 Cracks of Unit DD-2 (continued)



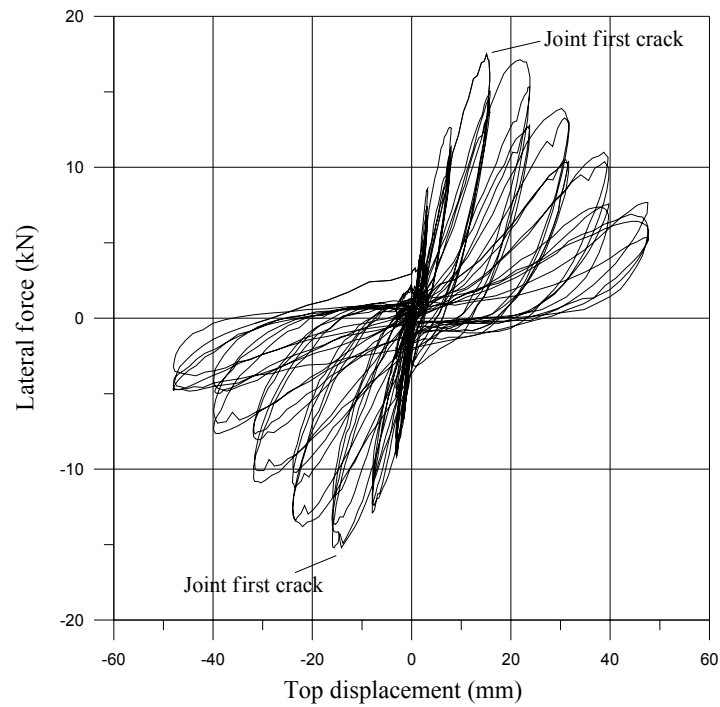
(k) At the end of the test (diagonal angle)

Figure 5.7 Cracks of Unit DD-2 (continued)

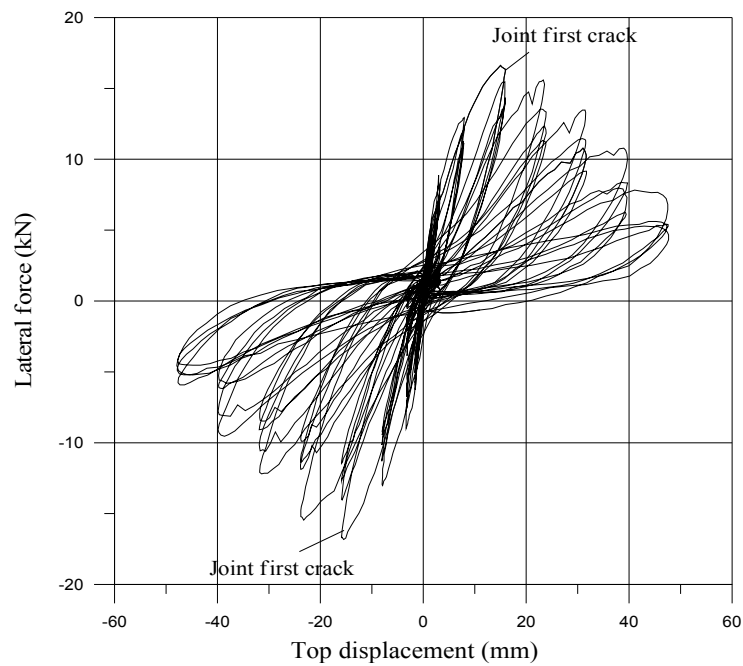
5.2.2.2 Hysteretic Response

The lateral force versus the top column displacement of Unit DD-2 is shown in Fig. 5.8. The first cracking in the joint occurred at 1% of drift both in positive and negative loading directions respectively for X and Y excitations.

The extra confinement provided by the other beam in transverse direction help to hold the concrete together even after the joint first crack has occurred so the strength can still pick up for about one level of drift higher before starting to degrade. The strength degradation was more severe than Unit DD-1 due to the absence of shear reinforcement in the joint core. The maximum lateral force that can be resisted by Unit DD-2 was 17.5 kN and 15.2 kN for the positive and negative loading directions respectively for the X excitation. For the Y excitation, the maximum lateral force was 16.6 kN and 16.8 kN for the positive and negative loading directions respectively.



(a) X direction



(b) Y direction

Figure 5.8 Lateral force versus Top displacement of Unit DD-2

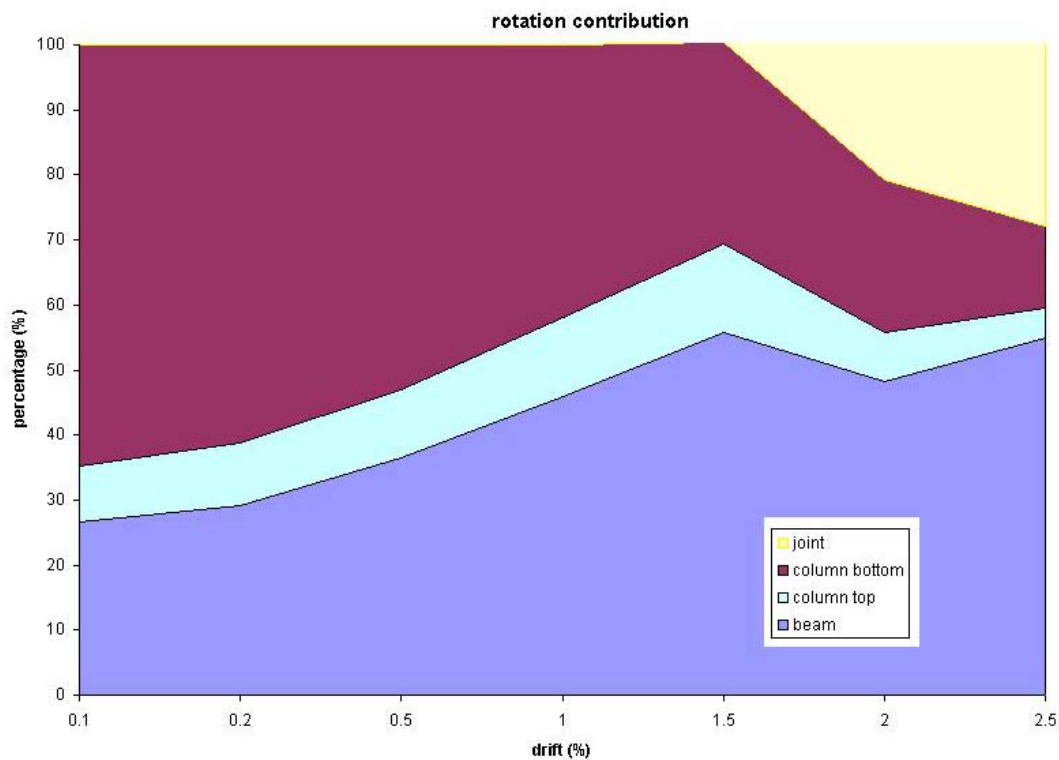
5.2.2.3 Displacement Components

The same difficulties in measuring the actual displacement also happened for this unit. The data recorded from the potentiometers had to be observed in test of Unit

DD-2 to approximate the actual displacement as close as possible. All the potentiometers were taken off after 2.5% of drift to prevent the instrumentation from being damaged due to the severe concrete spalling of the specimen.

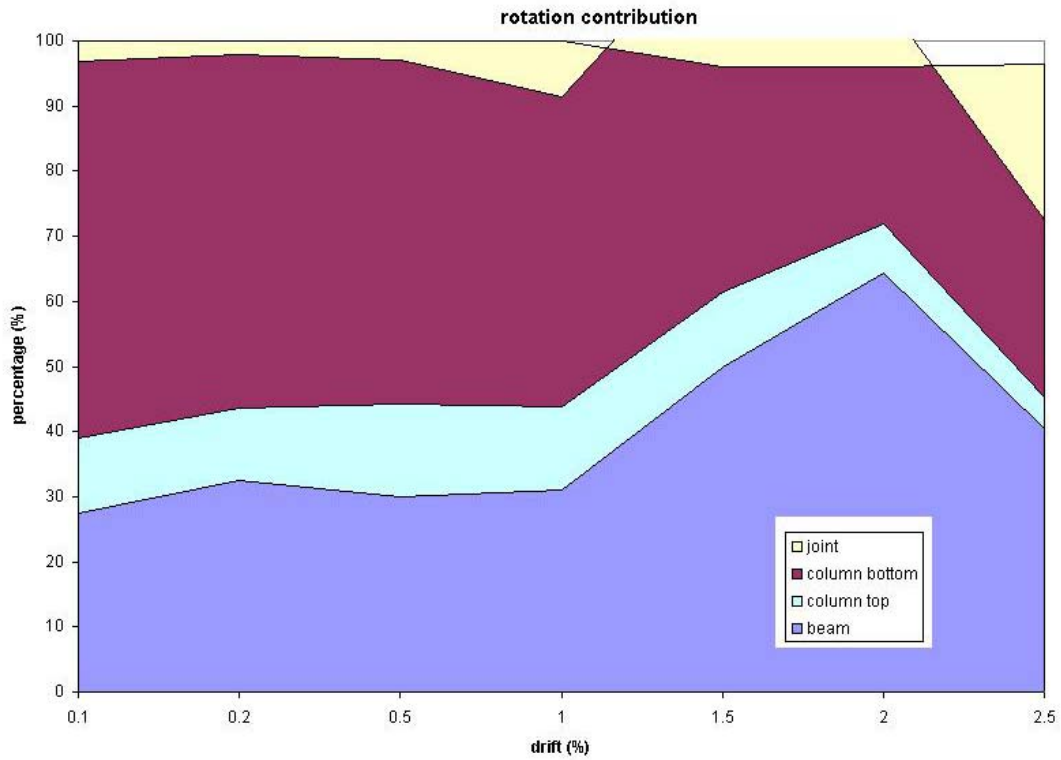
At the start of the test, the column governed the displacement of Unit DD-2, until the joint first crack and the joint started to increase its contribution. For the X excitation, the maximum column displacement contribution was about 65%, the maximum beam displacement contribution was up to 50% and the maximum joint displacement contribution was up to 40%. For Y excitation, the maximum column displacement contribution was about 80%, the maximum beam displacement contribution was up to 55% and the maximum joint displacement contribution was up to 40%.

Note that the value here had been modified so it is not very accurate. Figure 5.9 shows the members contribution of Unit DD-2 total displacement.

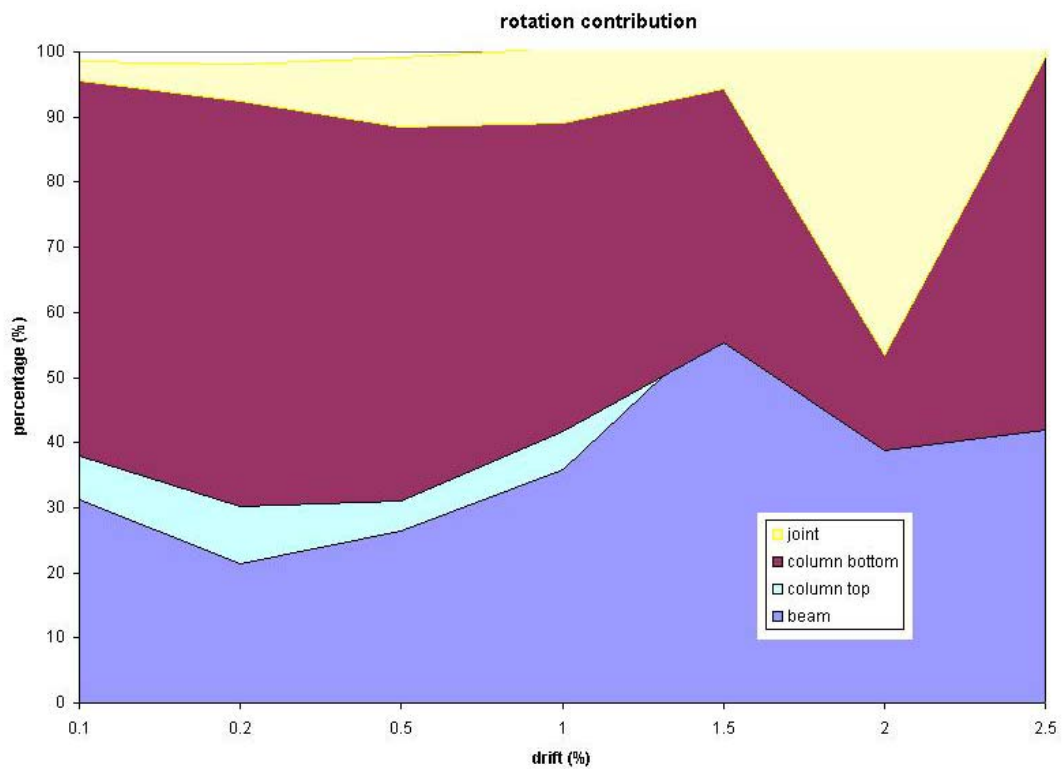


(a) positive loading direction (X)

Figure 5.9 Members displacement contribution of Unit DD-2

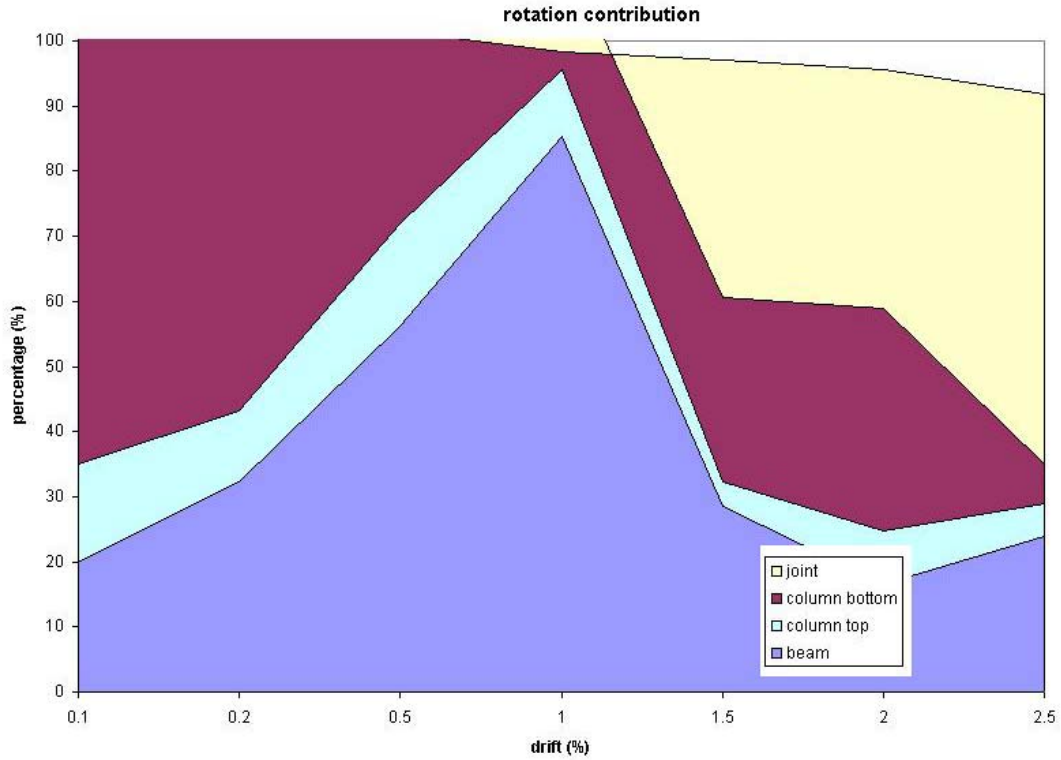


(b) negative loading direction (X)



(c) positive loading direction (Y)

Figure 5.9 Members displacement contribution of Unit DD-2 (continued)



(d) negative loading direction (Y)

Figure 5.9 Members displacement contribution of Unit DD-2

5.2.2.4 Force and Stress in the Joint

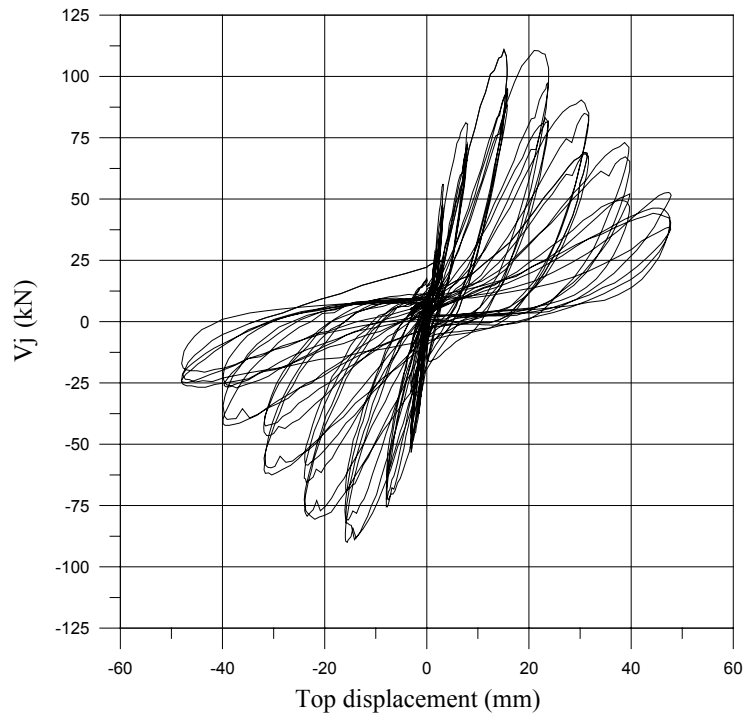
From the assessment in Chapter 2 and the results from the experiments on the plane frame units, it is known that the joint was the critical member for Unit DD-2. The joint will crack both in the positive and negative directions and thus preventing the plastic hinges occurring in the beams.

For the X excitation, in the positive loading direction, the principal tensile stress in the joint was increasing up to $0.232\sqrt{f'_c}$ when the first joint diagonal cracking occurred. From that point, the principal tensile stress in the joint can still increase up to $0.24\sqrt{f'_c}$ before degrading significantly. In the negative loading direction, the maximum joint principal tensile stress was $0.266\sqrt{f'_c}$ before degrading significantly. The horizontal shear in the joint area reached 111 kN and -90 kN in the positive and negative loading directions respectively.

For the Y excitation, in the positive loading direction, the principal tensile stress in the joint was increasing up to $0.205\sqrt{f'_c}$ when the first joint diagonal cracking occurred before degrading significantly. In the negative loading direction, the joint diagonal cracking occurred when the principal tensile stress was $0.32\sqrt{f'_c}$ before degrading significantly. The horizontal shear in the joint area reached 98 kN and -114 kN in the positive and negative loading directions respectively.

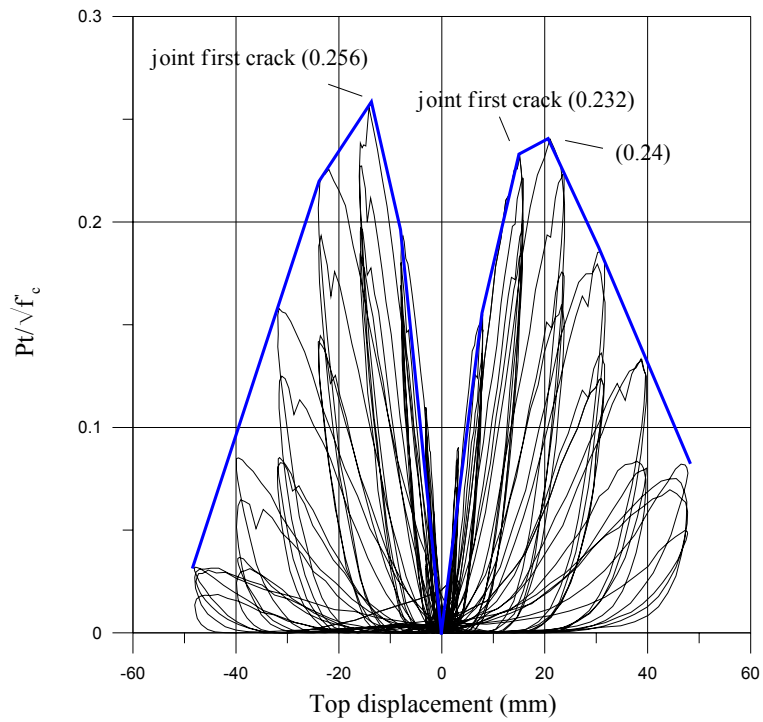
The axial load applied to the top of column was varied from $0.12\sqrt{f'_c}$ to $0.48\sqrt{f'_c}$.

Figure 5.10 shows the joint horizontal shear force versus top displacement and the joint horizontal principal tensile stress versus top displacement for both X and Y directions.

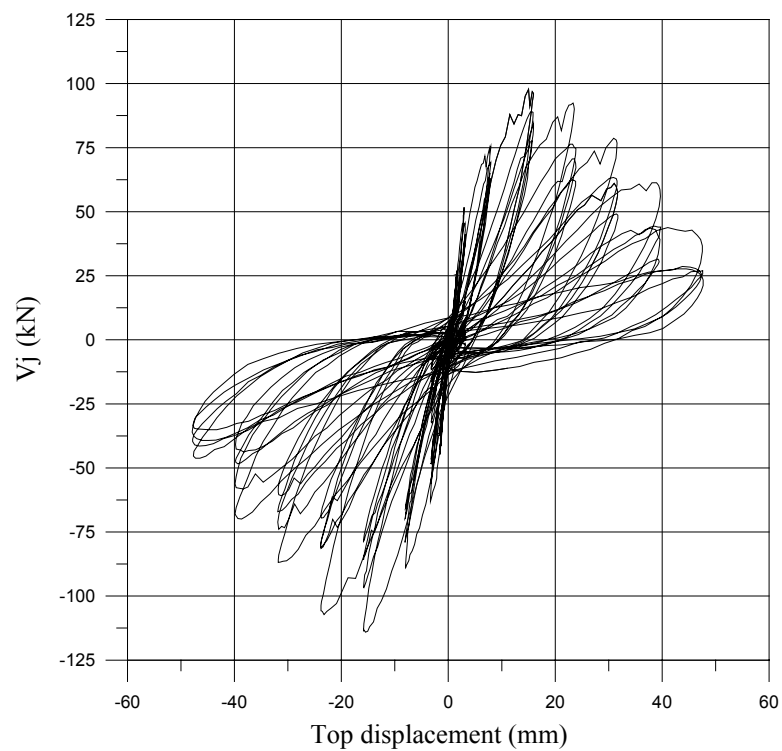


(a) X Horizontal joint shear (V_j) versus Top displacement of Unit DD-2

Figure 5.10 Force and stress in the joint core of Unit DD-2

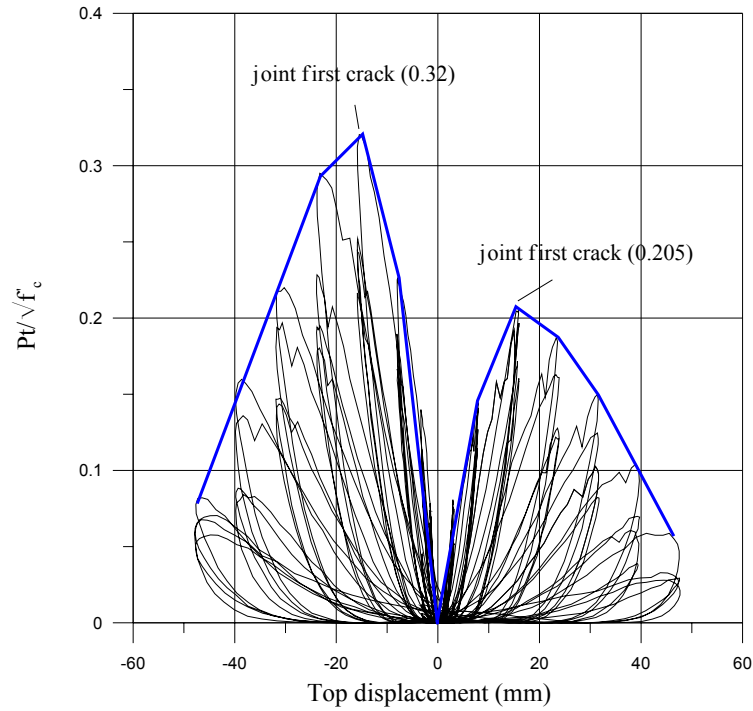


(b) X Joint principal tensile stress ($Pt/\sqrt{f_c}$) versus Top displacement of Unit DD-2



(c) Y Horizontal joint shear (V_j) versus Top displacement of Unit DD-2

Figure 5.10 Force and stress in the joint core of Unit DD-2 (continued)



(d) Y Joint principal tensile stress ($P_t/\sqrt{f_c}$) versus Top displacement of Unit DD-2

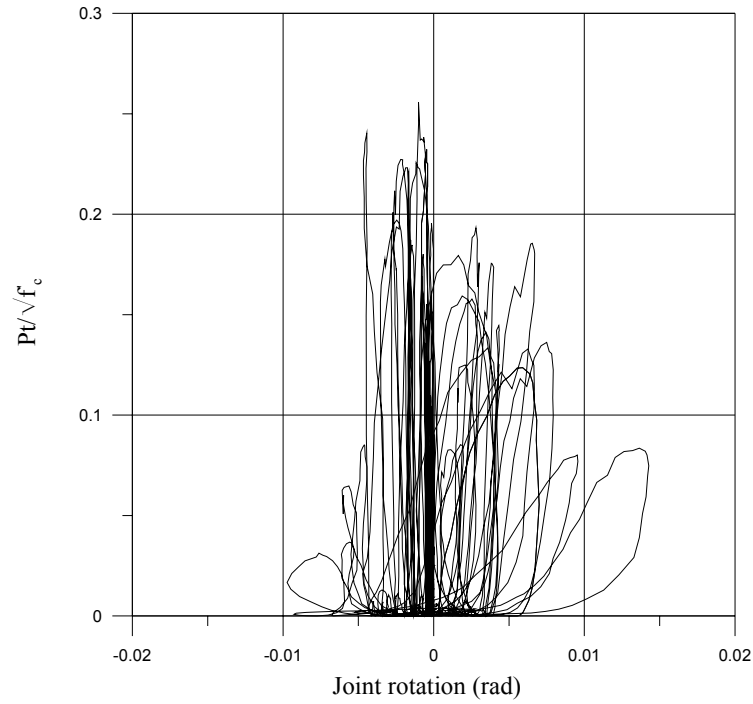
Figure 5.10 Force and stress in the joint core of Unit DD-2 (continued)

5.2.2.5 Joint Shear Deformation

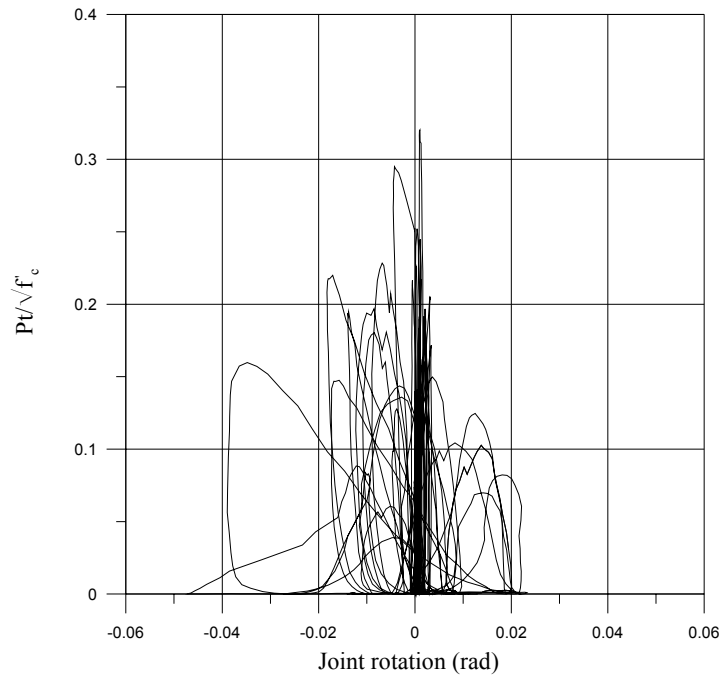
From the damage in the unit observed during the test, the limit state in term of joint rotation (γ) is proposed as follow:

- Undamaged: $\gamma < 0.0007$
- Limited damage: $0.0007 \leq \gamma < 0.004$
- Extensive damage: $0.004 \leq \gamma < 0.008$
- Critical damage: $0.008 \leq \gamma < 0.015$
- Collapse: $\gamma \geq 0.015$

Figure 5.11 shows the plot of joint horizontal principal tensile stress versus joint rotation for both X and Y excitations.



(a) X excitation



(b) Y excitation

Figure 5.11 Joint principal tensile stress $(Pt)/\sqrt{f_c}$ versus Joint rotation of Unit DD-2

5.2.2.6 Summary

Unit DD-2, an as-built two third scale beam-column joint unit was tested under a simulated seismic loading with varying axial load. Initial axial load of 75 kN was

applied representing the gravity load on the column. The deficiencies of Unit DD-2 are the absence of transverse reinforcement in the joint core, the use of plain round longitudinal reinforcement and the hook anchorage of the beam longitudinal reinforcement in the joint core.

From this test we can conclude:

1. Poor seismic behaviour

The overall performance of the unit was poor. After the joint cracked at 1% of drift, the strength started to degrade. The use of plain round longitudinal reinforcement caused loss in bond strength and the bar slipping which can be seen in the pinching of the hysteresis loop of the unit. Hook anchorages worsen the behaviour of the unit because the tension forces from the beam longitudinal reinforcement were not transferred properly to the joint core but concentrated in the hooks and initiated the concrete wedge phenomena.

2. Lack of transverse reinforcement in the joint

Diagonal cracks occurred in the joint area due to the shear forces working in the joint could not be resist by the single transverse reinforcement in the joint. The concrete cover of column outer layer was spalling when the high level of drift was applied to the unit. The column longitudinal bars were buckled badly as shown at the end of the test. However, the joint first cracking occurred when the principal tensile stress in the joint reached $0.2 \sqrt{f'_c}$ up to $0.3 \sqrt{f'_c}$, higher than $0.18 \sqrt{f'_c}$ observed in Unit DD-1. This is due to the concrete strength of Unit DD-2, which is higher than Unit DD-1.

3. Contribution of varying axial load

Refer to Section 6.2.2.6.

4. Limit state in term of joint rotation (γ)

Proposed limit state:

- Undamaged: $\gamma < 0.0007$
- Limited damage: $0.0007 \leq \gamma < 0.004$
- Extensive damage: $0.004 \leq \gamma < 0.008$
- Critical damage: $0.008 \leq \gamma < 0.015$

- Collapse: $\gamma \geq 0.015$

5.3 DEEP-SHALLOW BEAMS

One corner beam-column joint units with combination of deep beam and shallow beam was constructed. The unit is referred to as Units DS. Unit DS used one vertical and one horizontal shear reinforcement in the joint area. Grade 300 plain round steel was used for the longitudinal and transverse reinforcement. The units used plain round longitudinal bars for beams and column reinforcement.

5.3.1 Unit DS

Unit DS consists of one deep beam, one shallow beam and one column. The beam bars were hooked in the joint core area. One vertical and one horizontal shear reinforcement was used in the joint core, placed to confine the column bars and beam bars respectively. The aim of this test is to investigate the behaviour of the unit in the biaxial manner and compare it with the uniaxial manner from the test done for plane frame units. Initial axial load of 75 kN was applied on the top of the column to represent the gravity load.

A mistake in sign convention was made during the test; therefore the test result is equal to the situation when the lateral load is applied at the base of the column, instead of the top of the column. Since the beam is symmetrically reinforced, there is no major difference than if the lateral load was applied at the top of the column.

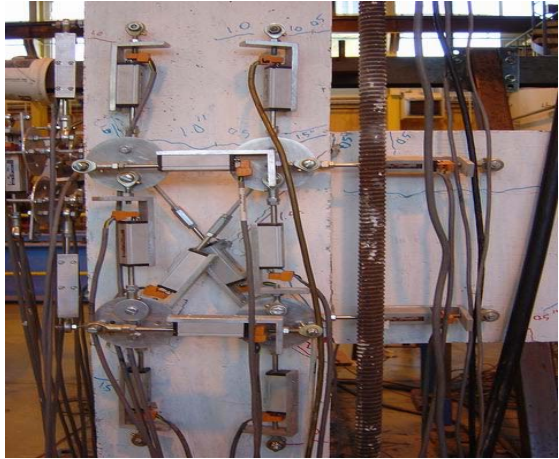
5.3.1.1 Crack Development and Damage

Minor cracks started to occur at the beam-column interface at 0.5% of drift. The diagonal joint crack occurred at 1% of drift for both positive and negative loading directions in X excitation. There was no diagonal joint crack in the Y beam since the beam was really shallow so it acted like a slab. Minor diagonal cracks were spread in the joint core area due to the lack of transverse reinforcement in the joint. Horizontal cracks occurred in the shallow beam while there was a large crack on the deep beam at the location where the edge of the shallow beam was attached. The existing cracks were extending and widening along with the increase of the drift percentage.

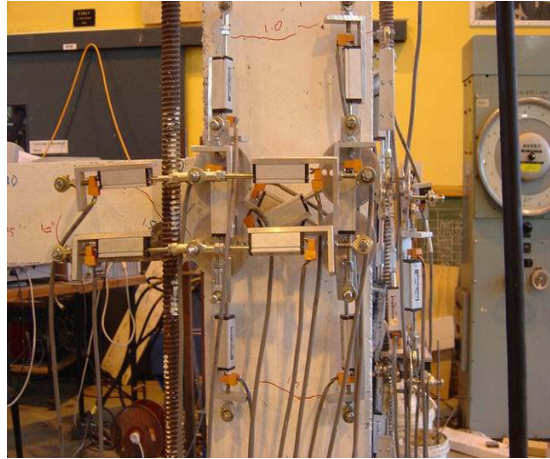
The concrete in the outer layer of the column was not spalling at the end of the test and still quite well united since the beams are helping one another in terms of

confining the concrete and preventing it from falling down. The unit was loaded until 4% of drift when the unit strength reduced significantly due to the damage in the beam and joint area.

Figure 5.12 shows the cracks and the final appearance of Unit DS. Since the instrumentations were attached on the joint area are covering the cracks in there, only pictures with major cracks which are visible, is shown.



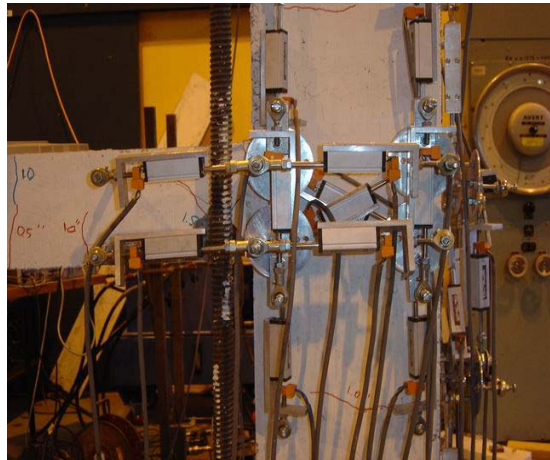
(a) At 2.5% of drift (X)



(b) At 2.5% of drift (Y)

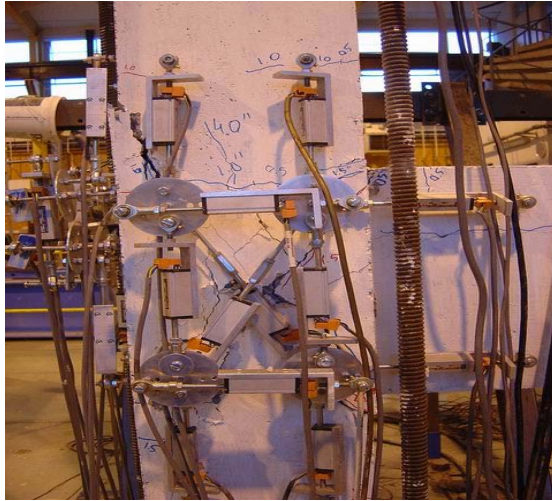


(c) At 3% of drift (X)

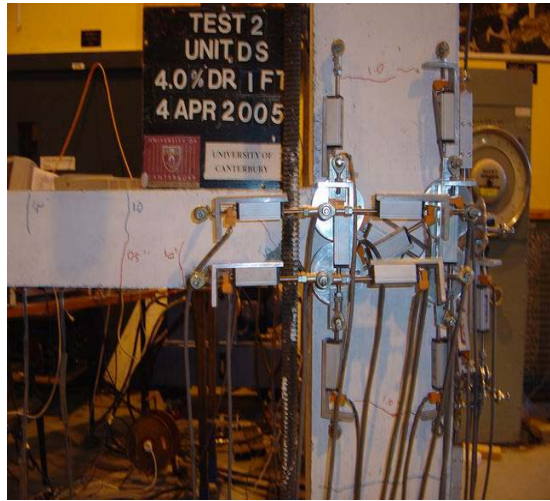


(d) At 3% of drift (Y)

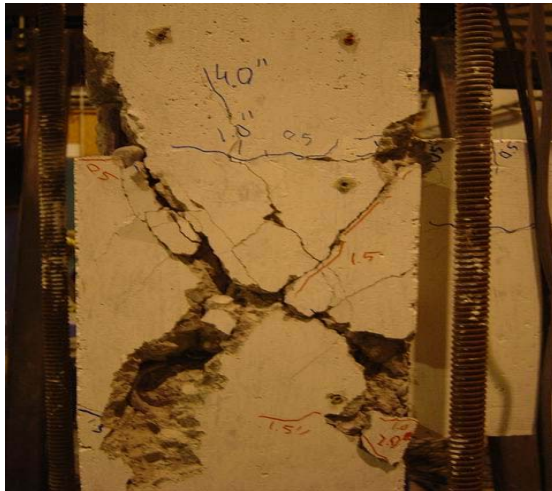
Figure 5.12 Cracks of Unit DS



(e) At 4% of drift (X)



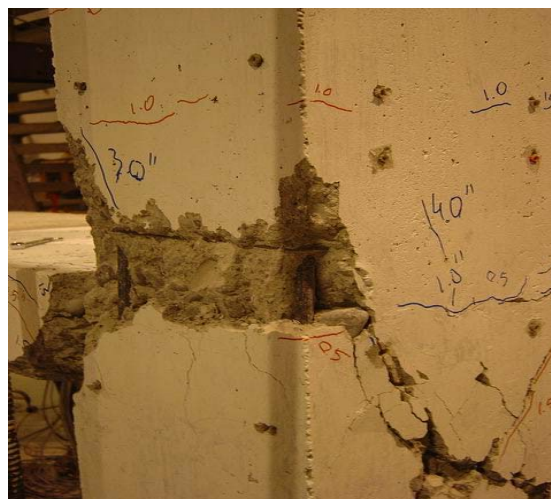
(f) At 4% of drift (Y)



(g) Final appearance (X)



(h) Final appearance (Y)



(i) Final appearance (diagonal angle)

Figure 5.12 Cracks of Unit DS (continued)

5.3.1.2 Hysteretic Response

The lateral force versus the top column displacement of Unit DS is shown in Fig. 5.13. The first cracking in the joint occurred at 1% and 1.5% of drift in positive and negative loading directions respectively in the X excitation. In the Y excitation, no joint crack occurred due to the shallowness of the beam.

The extra confinement provided by the shallow beam in the transverse direction of the deep beam helps to hold the concrete together even after the first joint crack has occurred so the strength can still pick up for about one level of drift higher before starting to degrade. The strength degradation was not as severe as Unit DD-1 or DD-2. The maximum lateral force that can be resisted by Unit DS was 15.5 kN and 17.1 kN for positive and negative loading directions respectively for X excitation. For the Y excitation, the maximum lateral force was 7.4 kN and 7.8 kN for positive and negative loading directions respectively.

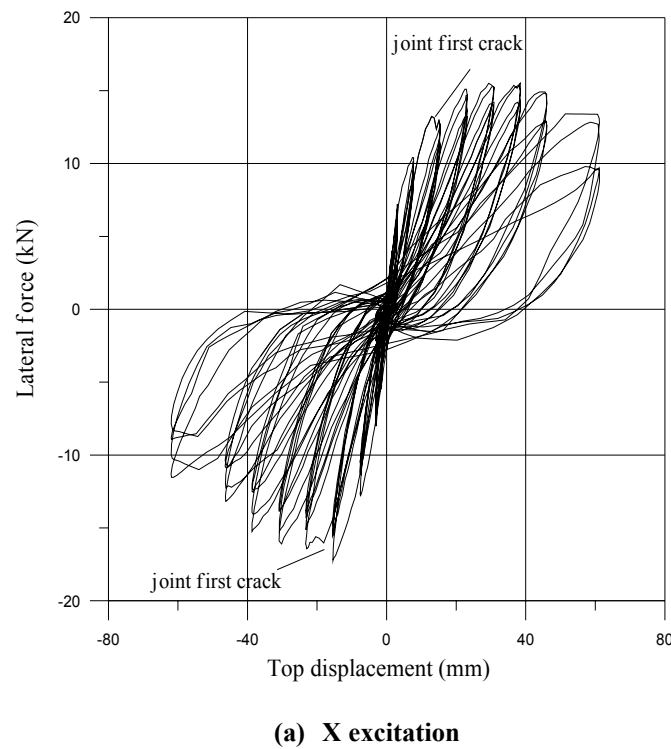
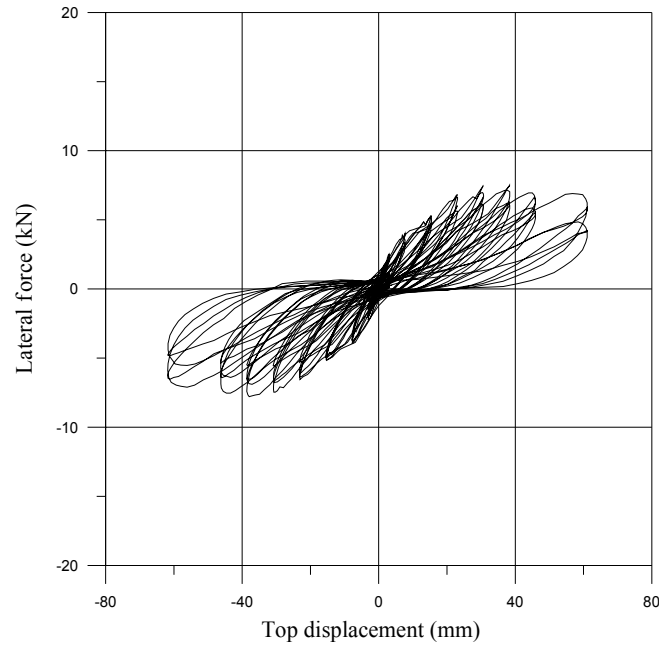


Figure 5.13 Lateral force versus Top displacement of Unit DS



(b) Y excitation

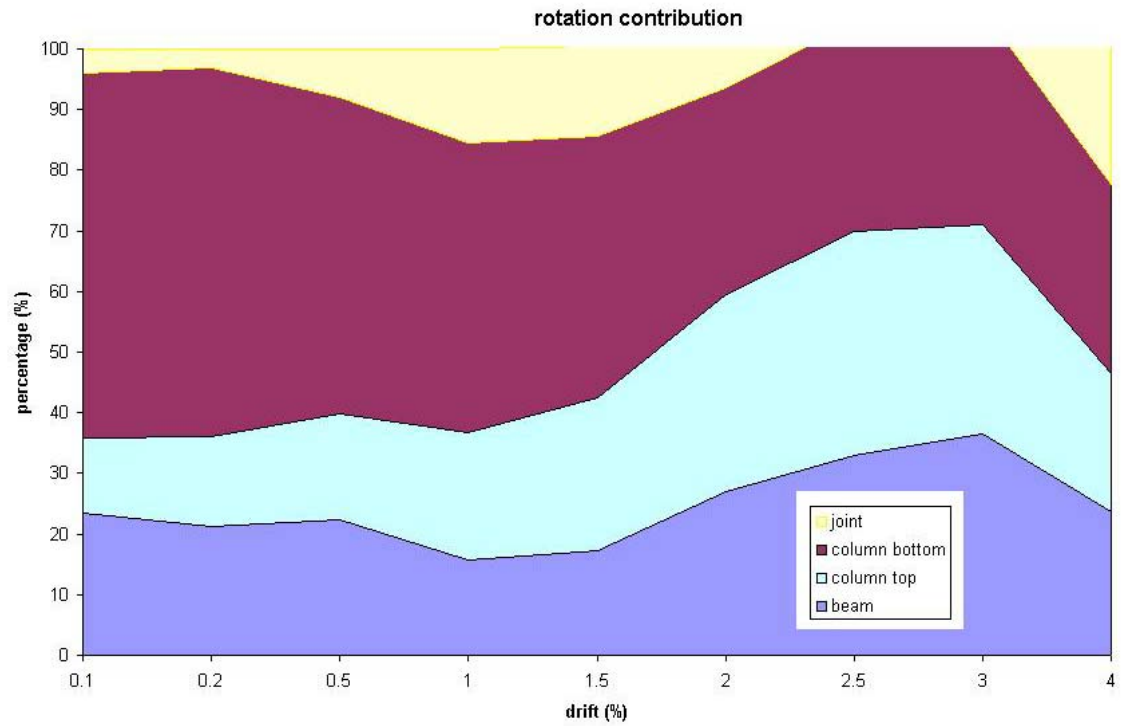
Figure 5.13 Lateral force versus Top displacement of Unit DS (continued)

5.3.1.3 Displacement Components

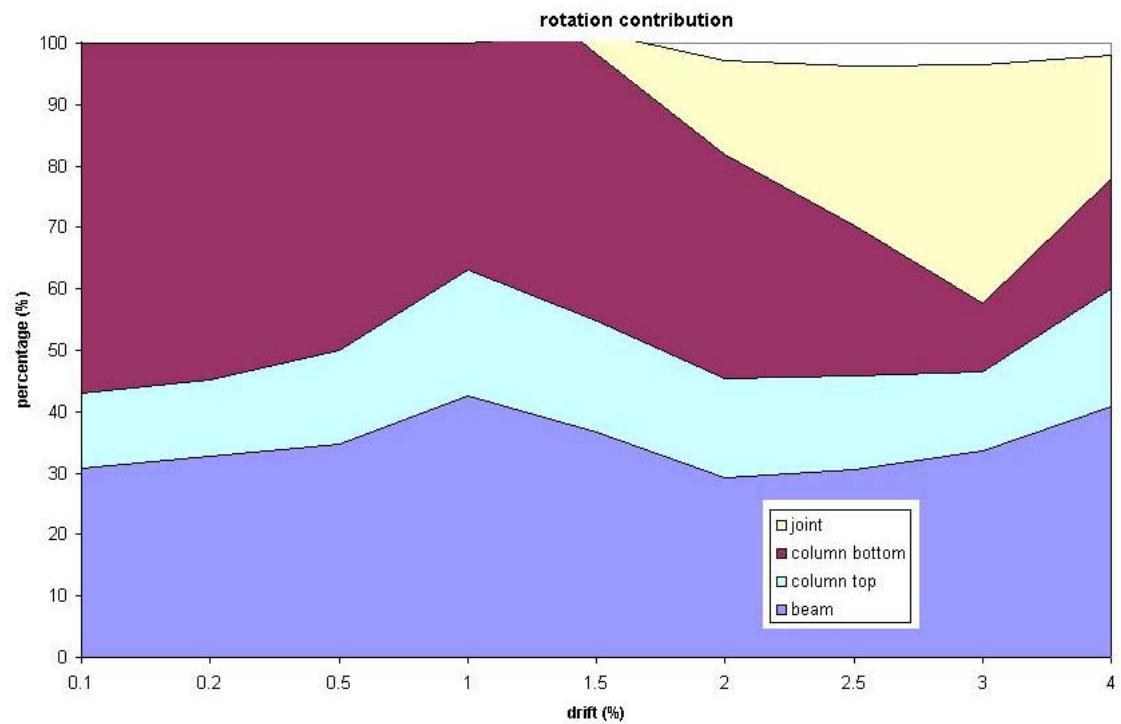
The same difficulties in measuring the actual displacement also occurred for this unit. The data recorded from the potentiometers had to be observed in test of Unit DS to approximate the actual displacement as closely as possible.

At the start of the test, the column governed the displacement of Unit DS, until the first joint crack and the joint started to increase its contribution. For the X excitation, the maximum column displacement contribution was about 70%, the maximum beam displacement contribution was up to 40% and the maximum joint displacement contribution was up to 50%. For Y excitation, the maximum column displacement contribution was about 50%, the maximum beam displacement contribution was up to 100% and there was no joint displacement contribution since the joint displacement was really small, it can be ignored.

Note that the value here had been modified so it is not very accurate. Figure 5.14 shows the members contribution of Unit DS total displacement.

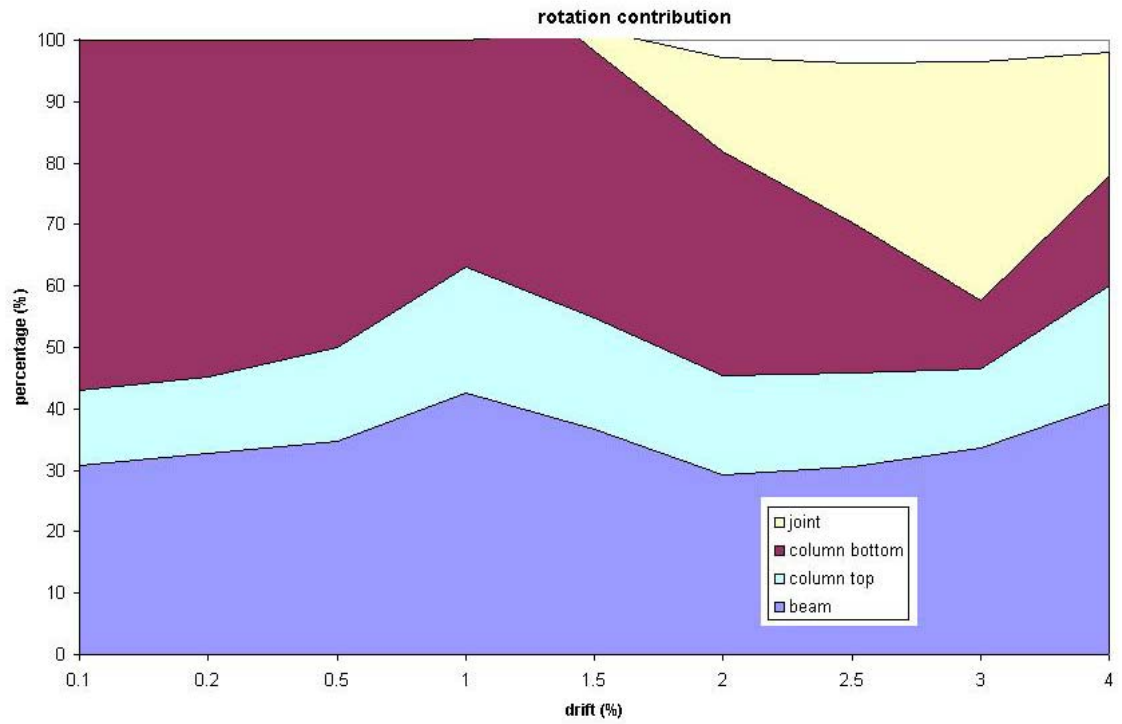


(a) positive loading direction (X)

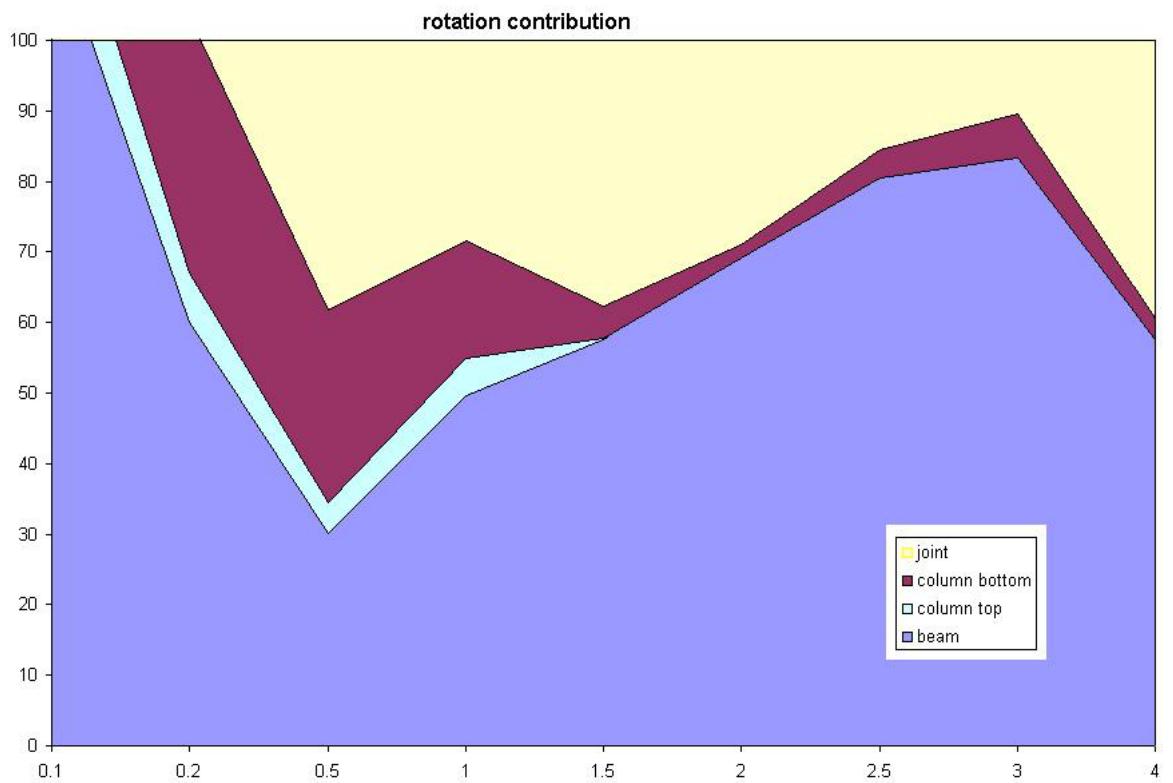


(b) negative loading direction (X)

Figure 5.14 Members displacement contribution of Unit DS



(c) positive loading direction (Y)



(d) negative loading direction (Y)

Figure 5.14 Members displacement contribution of Unit DS (continued)

5.3.1.4 Force and Stress in the Joint

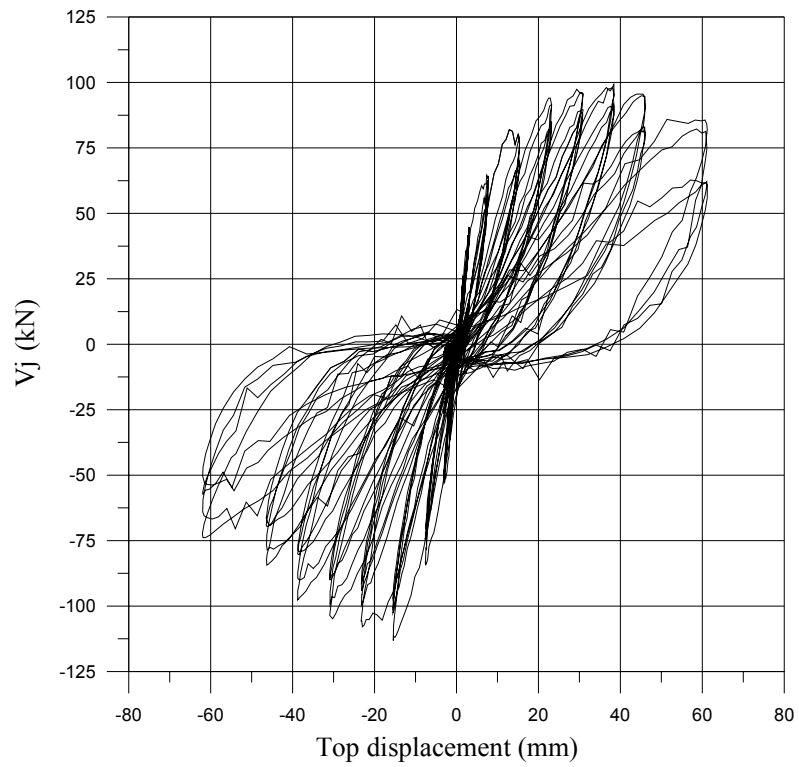
From the assessment in Chapter 2 and the results from the experiments on plane frame units, it is known that the joint was the critical member for the deep beam, while the beam was the critical member for the shallow beam of Unit DS. The joint will crack both in positive and negative directions of the deep beam and the beam will crack for the shallow beam.

For the X excitation, in the positive loading direction, the principal tensile stress in the joint was increasing up to $0.236\sqrt{f'_c}$ when the first joint diagonal cracking occurred. From that point, the principal tensile stress in the joint can still increase up to $0.31\sqrt{f'_c}$ before degrading significantly. In the negative loading direction, the maximum joint principal tensile stress was $0.269\sqrt{f'_c}$ before degrading significantly. The horizontal shear in the joint area reached 99 kN and -113 kN in the positive and negative loading directions respectively.

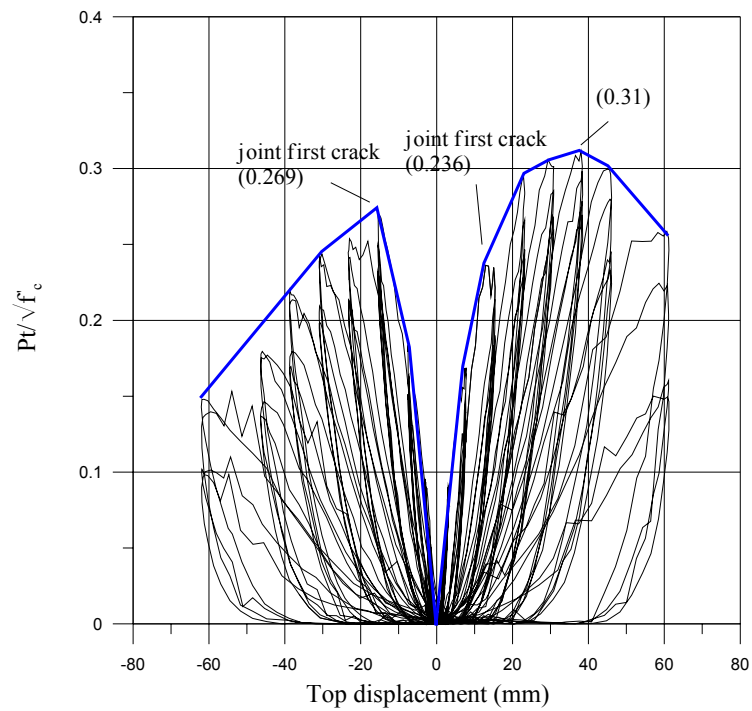
For the Y excitation, in the positive loading direction, the principal tensile stress in the joint was increasing up to $0.364\sqrt{f'_c}$ and in the negative loading direction; the maximum joint principal tensile stress was $0.323\sqrt{f'_c}$. The horizontal shear in the joint area reached 120 kN and -125 kN in the positive and negative loading directions respectively.

The axial load applied to the top of column was varied from $0.15\sqrt{f'_c}$ to $0.45\sqrt{f'_c}$.

Figure 5.15 shows the joint horizontal shear force versus top displacement and the joint horizontal principal tensile stress versus top displacement for both X and Y excitations.

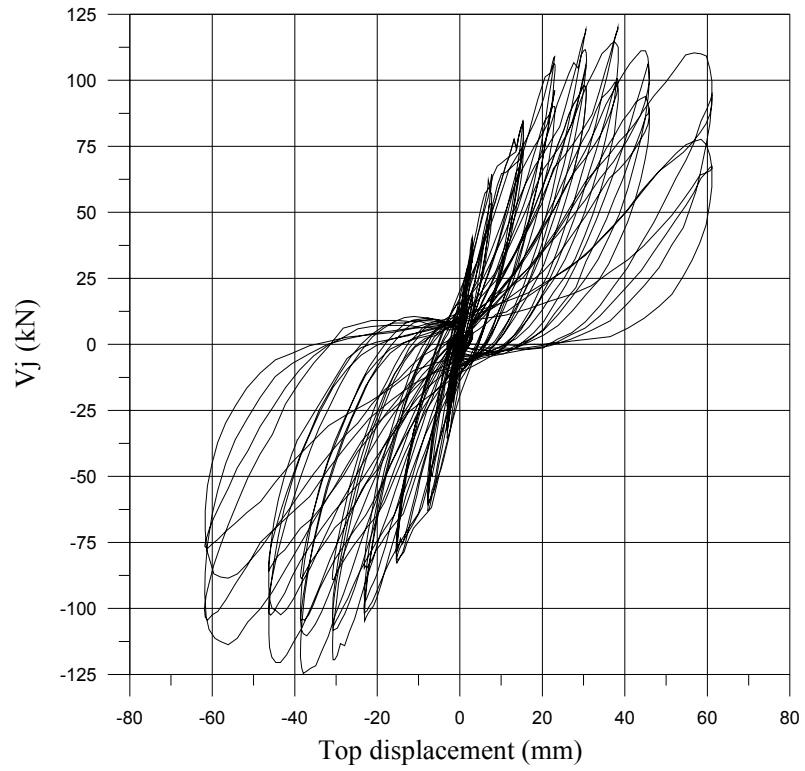


(a) X Horizontal joint shear (V_j) versus Top displacement of Unit DS

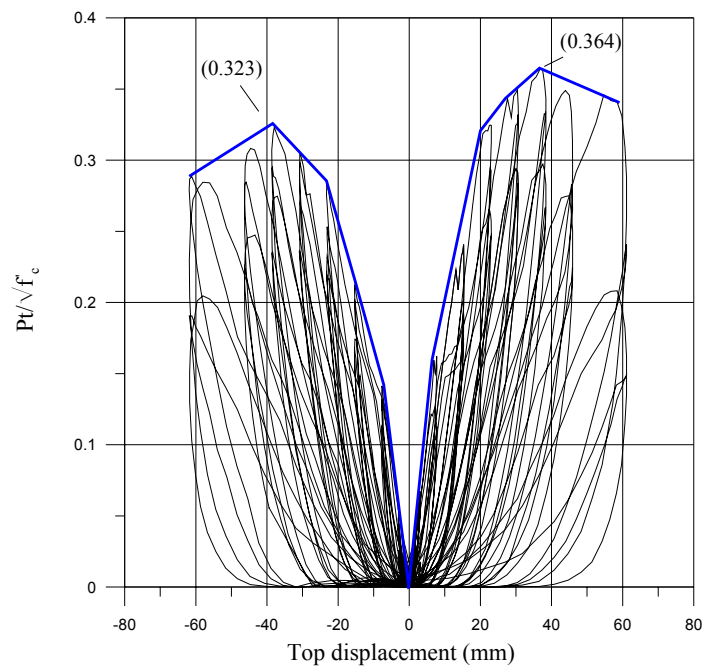


(b) X Joint principal tensile stress (P_t)/ $\sqrt{f_c}$ versus Top displacement of Unit DS

Figure 5.15 Force and stress in the joint core of Unit DS



(c) Y Horizontal joint shear (V_j) versus Top displacement of Unit DS



(d) Y Joint principal tensile stress (P_t)/ $\sqrt{f_c}$ versus Top displacement of Unit DS

Figure 5.15 Force and stress in the joint core of Unit DS (continued)

5.3.1.5 Joint Shear Deformation

From the damage in the unit observed during the test, the limit state in terms of joint rotation (γ) is proposed as follow:

- Undamaged: $\gamma < 0.0015$
- Limited damage: $0.0015 \leq \gamma < 0.004$
- Extensive damage: $0.004 \leq \gamma < 0.008$
- Critical damage: $0.008 \leq \gamma < 0.012$
- Collapse: $\gamma \geq 0.012$

Figure 5.16 shows the plot of joint horizontal principal tensile stress versus joint rotation for the X excitation.

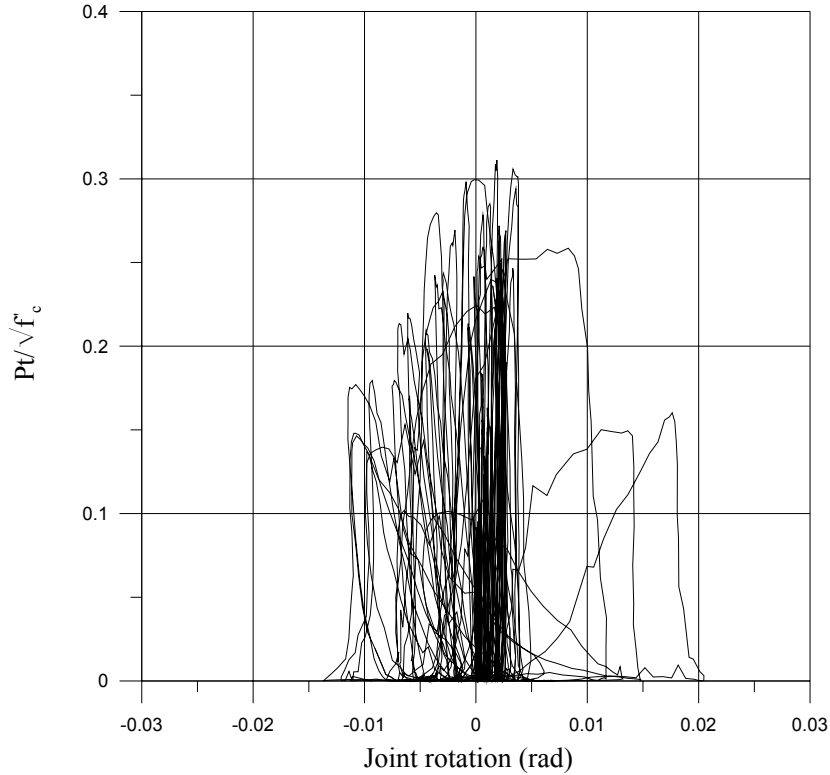


Figure 5.16 Joint principal tensile stress $(Pt)/\sqrt{f'_c}$ versus Joint rotation (X) of Unit DS

5.3.1.6 Summary

Unit DS, an as-built two third scale beam-column joint unit was tested under a simulated seismic loading with varying axial load. Initial axial load of 75 kN was applied representing the gravity load on the column. The deficiencies of Unit DS are

the use of shallow beam, the lack of transverse reinforcement in the joint core, the used of plain round longitudinal reinforcement and the hook anchorage of the beam longitudinal reinforcement in the joint core.

From this test we can conclude:

1. Poor seismic behaviour

The overall performance of the unit was poor. The shallow beam can only resist about 50% of the lateral load from the deep beam. The use of plain round longitudinal reinforcement caused loss in bond strength and the bar slipping which can be seen in the pinching of the hysteresis loop of the unit. Hook anchorages worsen the behaviour of the unit because the tension forces from the beam longitudinal reinforcement were not transferred properly to the joint core but concentrated in the hooks.

2. Adequate confinement in the joint

Due to the number of beam longitudinal reinforcement anchored in the column, the joint area was very congested. This prevents the joint from concrete tension failure in the direction, which has the shallow beam. While in the direction with deep beam, the joint cracked but there was no severe spalling of the concrete due to confinement provided by the shallow beam in the transverse direction.

3. Contribution of varying axial load

Refer to Section 6.2.2.6.

4. Limit state in terms of joint rotation (γ)

Proposed limit state:

- Undamaged: $\gamma < 0.0015$
- Limited damage: $0.0015 \leq \gamma < 0.004$
- Extensive damage: $0.004 \leq \gamma < 0.008$
- Critical damage: $0.008 \leq \gamma < 0.012$
- Collapse: $\gamma \geq 0.012$

5.4 TESTS SUMMARY

Three two-third scaled as-built reinforced concrete corner beam-column joint units, tested under simulated seismic loading with varying axial load on the column, using 75 kN as the initial axial load. The units were divided into two main categories according to the beam geometry, deep beams and shallow beams. The joint cores of all units contained single shear reinforcement, except for Unit DD-2, typical in pre-1970s construction.

The test results are shown in Table 5.3. Summary of force and stress in the joint for all units are shown in Table 5.4.

5.4.1 Result Comparison

The test results from all three corner beam-column joints are summarized in this section. Comparisons are made to investigate the difference in two aspects, the contribution of joint transverse reinforcement and beam dimension. The main objective is to determine the difference in term of global strength and the joint strength.

5.4.1.1 Hysteresis Response

The force versus displacement hysteretic response from all units is being compared to each other to investigate the effect of different reinforcement detailing and beam dimension. Figure 5.17 shows the plot of hysteresis envelope of all the units in both directions.

It is clear that the dimension of the transverse beam has an important contribution in determining the global behaviour of the beam-column joint subassembly. Unit DD-1 and Unit DD-2 which were using deep beams have more severe strength degradation compared to Unit DS which used the combination of deep beam and shallow beam. It shows that the shallow beam in the Y excitation for Unit DS was contributing only on the positive side of the X excitation. On the negative side, the strength degradation is quite similar with Unit DD-1 since the shallow beam was only attached on the top half of the deep beam. The behaviour of Unit DS is basically the same with a beam-column joint subassembly with one way slab attached to it.

Test Unit	Max. Lateral Force (kN)				f'c (MPa)	Failure type			
	X		Y			X		Y	
	(+)	(-)	(+)	(-)		(+)	(-)	(+)	(-)
Unit DD-1	10.9	12.6	10.6	12.4	24.2	Joint failure	Joint failure	Joint failure	Joint failure
Unit DD-2	17.5	15.2	16.6	16.8	27.4	Joint failure	Joint failure	Joint failure	Joint failure
Unit DS	15.5	17.1	7.4	7.8	23.8	Joint failure	Joint failure	Beam failure	Beam failure

Table 5.3 Summary of space frame units global behaviour

Test Unit	Joint horizontal shear (kN)				Principal tensile stress/ $\sqrt{f_c}$							
					X				Y			
	X		Y		(+ loading)		(- loading)		(+ loading)		(- loading)	
	(+)	(-)	(+)	(-)	1st crack	Maximum	1st crack	Maximum	1st crack	Maximum	1st crack	Maximum
Unit DD-1	70	80	60	80	0.151	0.168	0.171	0.171	0.179	0.186	0.166	0.182
Unit DD-2	111	90	98	114	0.232	0.24	0.266	0.266	0.205	0.205	0.32	0.32
Unit DS	99	113	120	125	0.236	0.31	0.269	0.269	n/a	0.364	n/a	0.323

Table 5.4 Summary of force and stress in joint of space frame units

To know the effect of joint transverse reinforcement, the hysteresis envelope of Unit DD-1 and DD-2 is compared. Unit DD-1 was picking up the force quite constantly with constant change of the stiffness until the peak point when the joint first cracking occurred before the strength was reducing. Unit DD-2 was picking up the force rapidly, maintaining the initial stiffness, up to the peak when the joint crack before the strength was reducing significantly. The strength degradation of Unit DD-2 is more severe than Unit DD-1, losing about 70% of the maximum strength at 3% of drift while only about 50% of the maximum strength was lost for Unit DD-1 at 4% of drift. The transverse reinforcement placed in the joint area helped Unit DD-1 to maintain the strength and confine the concrete so the strength was reducing slowly.

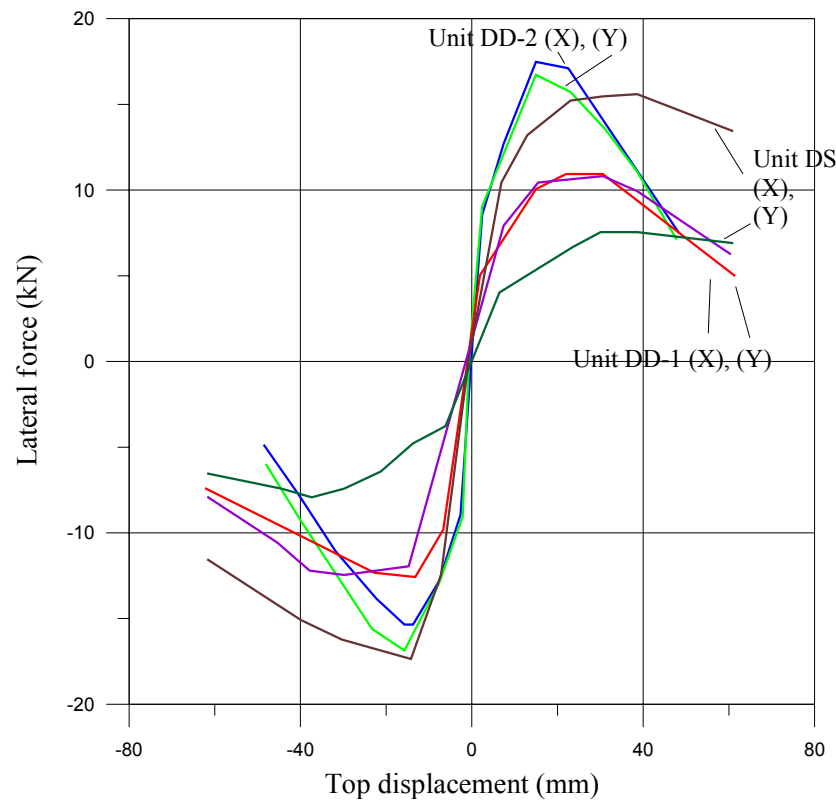


Figure 5.17 Hysteresis envelopes of Units DD-1 (deep-deep-one joint stirrup), DD-2 (deep-deep-no joint stirrup), DS (deep-shallow)

5.4.1.2 Joint Principal Tensile Stress

Units DD-1 and DD-2 have joint failure in both the X and Y excitations, while Unit DS only has joint failure in the X excitation. The joint principal tensile stress envelope of the failed joint only will be compared to each other in Figure 5.18.

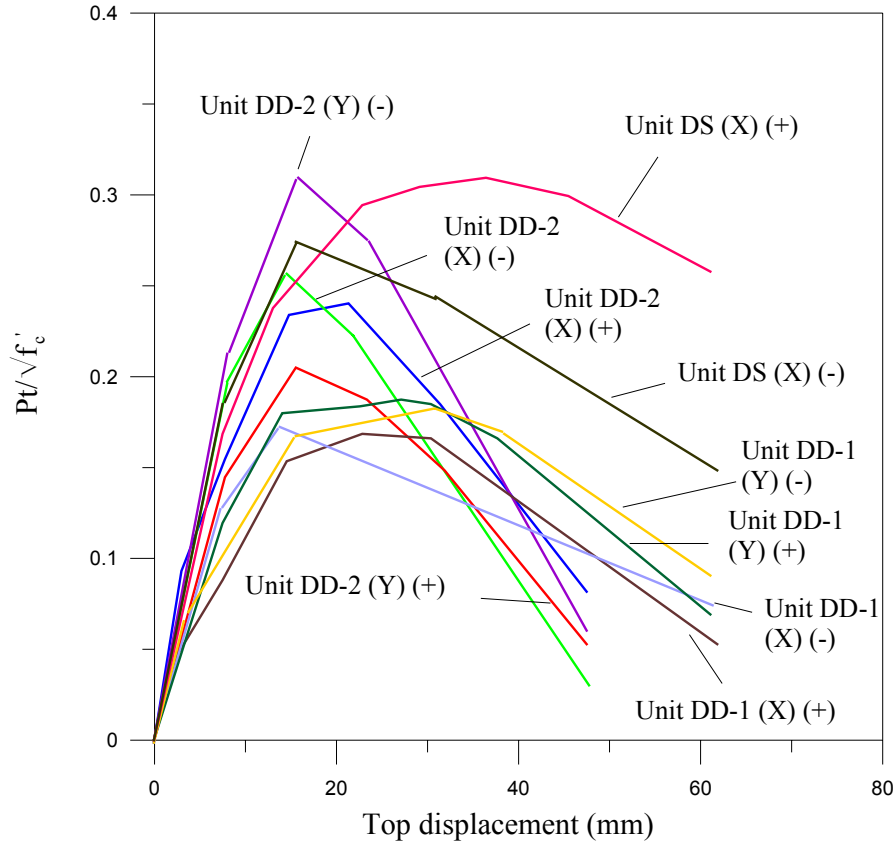


Figure 5.18 Joint principal tensile stress envelopes of Units DD-1 (deep-deep-one joint stirrup), DD-2 (deep-deep-no joint stirrup), DS (deep-shallow)

From that, two strength degradation curves, one for smooth beam bars with end hooks and one for smooth beam bars with end hooks and one stirrup in the joint core is proposed as shown in Fig. 5.19 to 5.20.

For smooth beam bars with end hooks, joint failure is expected to occur at a principal tensile stress $P_t = 0.27\sqrt{f'_c}$ before degrading significantly.

For smooth beam bars with end hooks and one stirrup in the joint core, joint failure is expected to occur at a principal tensile stress $P_t = 0.17\sqrt{f'_c}$ and increasing up to $P_t = 0.19\sqrt{f'_c}$ before degrading quite significantly. The ability to maintain and increase the strength after the first joint crack is due to the stirrup contribution in confining the concrete so that even the joint crack, the strength did not drop suddenly.

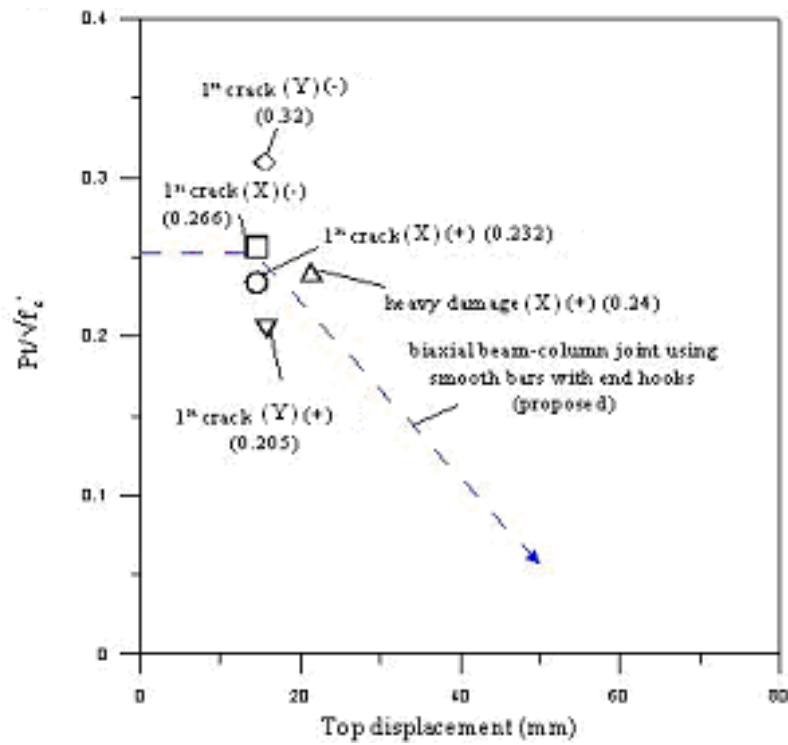


Figure 5.19 Proposed strength degradation for smooth bars without joint stirrup

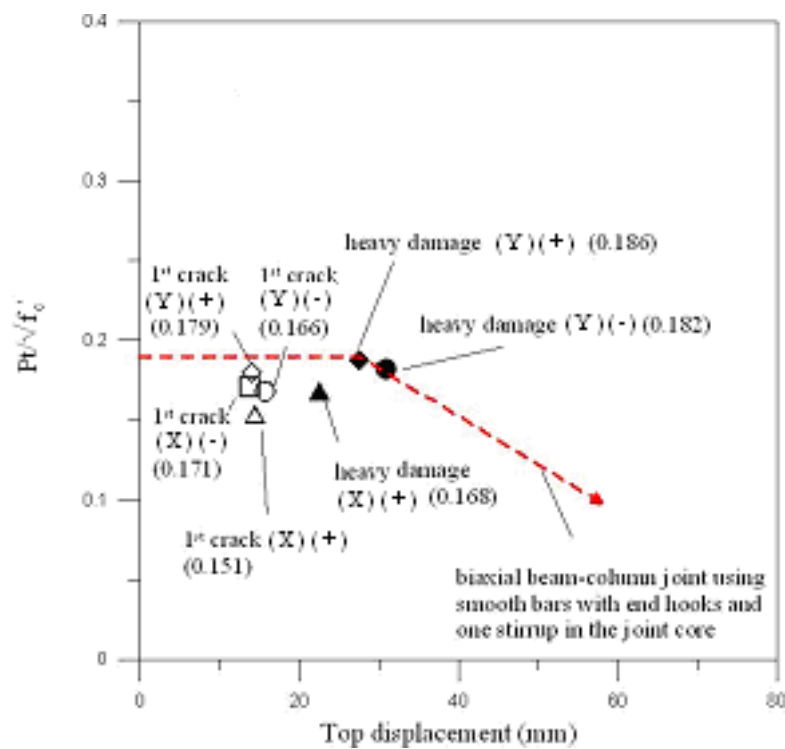


Figure 5.20 Proposed strength degradation curves for smooth bars with joint stirrup

5.5 BIAXIAL EFFECT

The result from Unit DD-1 will be compared with Unit TDD-2 to investigate the effect of biaxial loading on beam-column joint unit since both units have the same reinforcement details and reasonably similar material properties. The objective is to find the strength reduction in terms of global and joint strength.

5.5.1 Hysteresis Response

The envelope of hysteresis response from Unit DD-1 for both X and Y excitations are compared with Unit TDD-2 in Fig. 5.21. It is clear to see that a significant amount of reduction occurred as the result of biaxial loading.

It is important to remember that the loading path used for the plane frame test is different with the space frame test. The drift target used for the space frame is the displacement of the top column at a 45 degrees angle. Therefore the displacement of the top column in both directions individually for the space frame is less than the displacement of the top column for the plane frame. The amount of strength reduction will be made assuming that the issue mentioned above will not have a major effect. In positive direction, the strength reduction is up to 33% and in negative direction, the strength reduction is 15%. Considering the effect of varying axial load, the average of the two numbers, 25% is proposed as a strength reduction factor if a beam-column joint subassembly is to be loaded biaxially.

5.5.2 Joint Principal Tensile Stress

Joint principal tensile stress reduction under biaxial loading is also investigated. The two proposed strength degradation curves for plane frame and space frame beam-column joint subassemblies using smooth bars with end hooks are shown in Fig. 5.22.

The principal tensile stress for the biaxially loaded joint is only about 61% of the uniaxially loaded joint. The reason for this is that the biaxial joint was loaded from two directions at the same time, so the force coming into the joint is higher than the uniaxial joint. The proposed value for joint principal stress reduction for biaxial joint is 40%. The value is really conservative considering it comes from only a few test results.

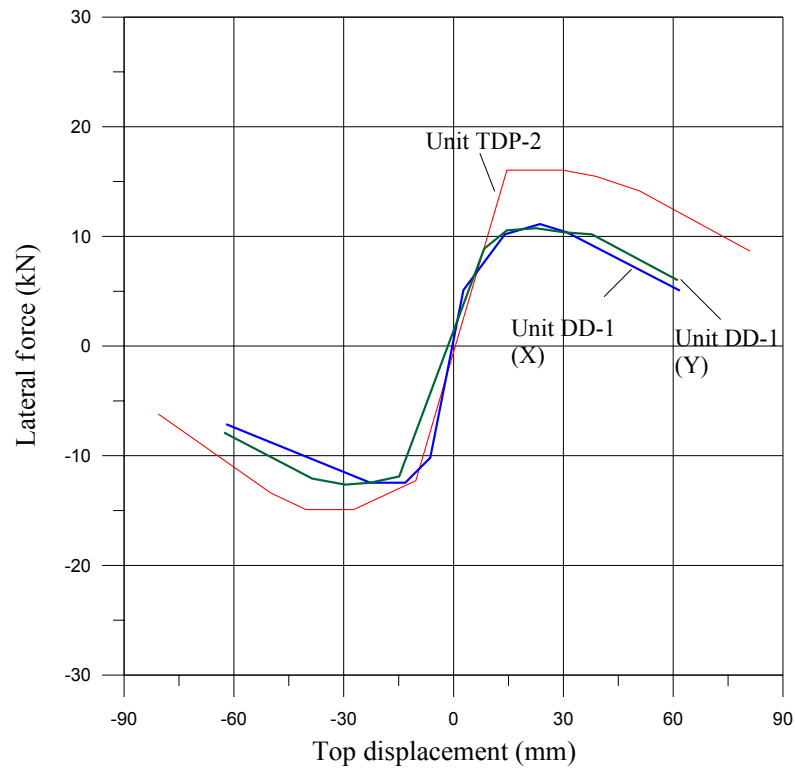


Figure 5.21 Hysteresis envelopes of Units DD-1 (deep-deep) and TDP-2 (deep-plain)

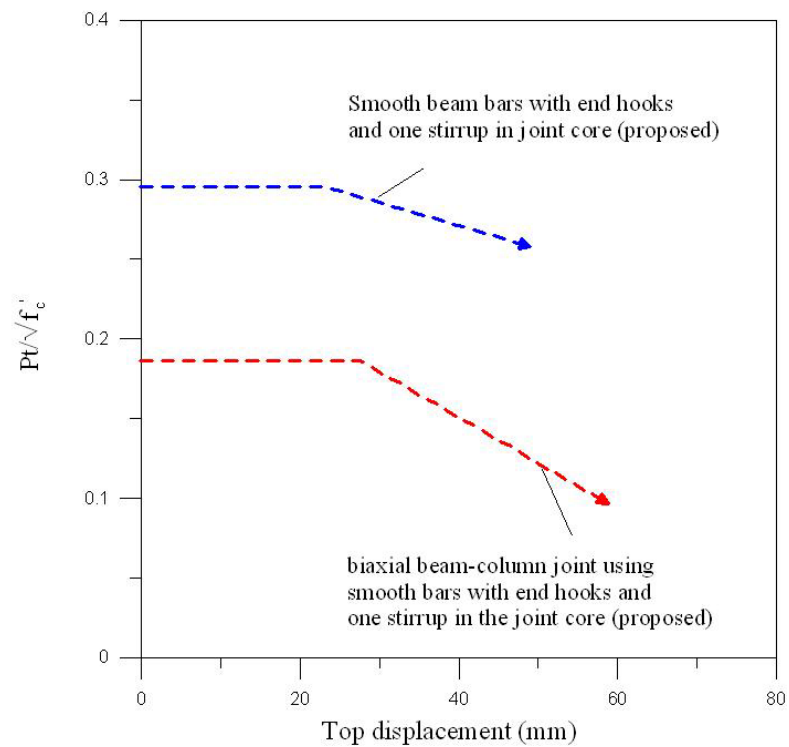


Figure 5.22 Proposed strength degradation curves for corner joints

5.6 CONCLUSION

1. Beam dimension has an important effect on the behaviour of a corner beam-column joint. There are advantages and disadvantages that have to be considered in designing the beam. Beam depth can provide an additional confinement for the joint to resist the force coming from the other beam in the transverse direction. In the other side, the bigger the beam depth, the higher the moment capacity, which will result in larger forces from the beam coming into the joint and thus has more chance to destroy the joint.
2. As in the plane frame beam-column joint subassembly, the transverse reinforcement in the joint area gives a major contribution in confining the concrete and maintaining the strength of the unit. Although joint shear failure occurs, the strength can be maintained and the severity of the strength degradation can be reduced. From the results, it is clear that even a single transverse reinforcement can improve the joint quite significantly.
3. Two strength degradation curves are proposed for space frame beam-column joint subassemblies. One is for smooth bars with hooked ends and without stirrup in the joint and the other is for smooth bars with hook ends and one stirrup in the joint.
4. A certain amount of strength reduction has to be considered when assessing space frame beam-column joints. For global strength, a 25% reduction is proposed as a reasonable value from the experimental results, while a 40% reduction is proposed for joint principal tensile stress. The numbers are considered conservatively since they come from limited experimental results.
5. From the damage observed in during the test, a limit state for corner joints with substandard details based on joint shear deformation is proposed:
 - Undamaged: $\gamma < 0.0007$
 - Limited damage: $0.0007 \leq \gamma < 0.002$
 - Extensive damage: $0.002 \leq \gamma < 0.005$
 - Critical damage: $0.005 \leq \gamma < 0.012$
 - Collapse: $\gamma \geq 0.012$

CHAPTER 6

ANALYTICAL-EXPERIMENTAL COMPARISONS

6.1 INTRODUCTION

The model proposed and described in Chapter 2 is used to simulate the behaviour of all the beam-column joint subassemblies which have been tested. Takeda hysteresis rule was assigned to the beam and column elements plastic hinge and newly proposed hysteresis with appropriate pinching, Pampanin hysteresis, was assigned to the joint shear hinge (except for Unit TDP-1), to model the bar slips. Strength degradation was also included in this analysis program to fit the experimental data better. The main purpose of this comparison is to justify that the model used is capable to model the behaviour of substandard exterior beam-column joint taking into account the effect of the column axial load to the joint and to further calibrate the parameters needed for Pampanin hysteresis.

6.2 PLANE FRAME BEAM-COLUMN JOINTS

Six plane frame beam-column joint subassemblies with typical detailing of pre-1970s reinforced concrete structure were tested under quasi static cyclic loading at the University of Canterbury. The results were presented more specifically in Chapter 4. This section will show the comparison of the global behaviour between the analytical and experimental results.

6.2.1 Unit TDD-1

Unit TDD-1 had deformed bars for the column and the beam longitudinal reinforcement. Plastic hinges occurred on the beam both in positive and negative directions. The use of Pampanin hysteresis to model the joint shear are has no effect since the joint is still in its elastic range and the global behaviour is governed by the beam plastic behaviour (Fig. 6.1). The Pampanin hysteresis parameters used in Ruaumoko analysis of Unit TDD-1 is shown in Table 6.1.

IOP (Option)	α_{s1}	α_{s2}	α_{u1}	α_{u2}	Delta F	β
1	0.8	0.5	0	1.2	20	0

Table 6.1 Pampanin hysteresis parameter for Unit TDD-1

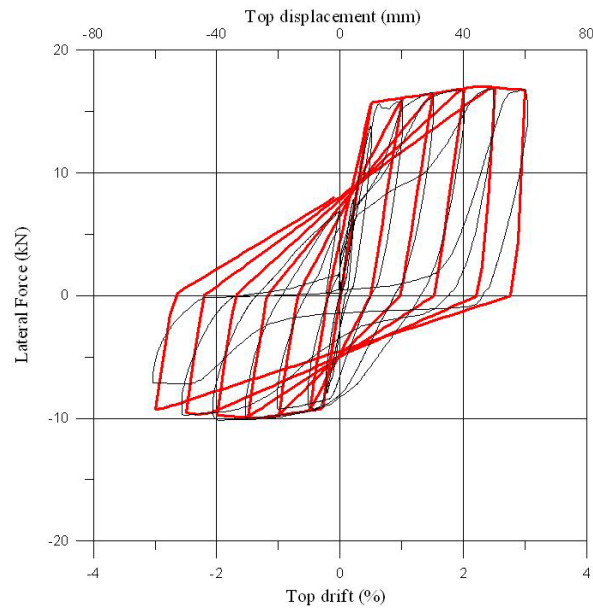


Figure 6.1 Analytical-experimental comparison of Unit TDD-1

6.2.2 Unit TDP-1

Unit TDP-1 had plain round bars for the column and the beam longitudinal reinforcement. Plastic hinge formed on the beam in the negative direction and joint shear hinge formed in the positive direction. Since the global behaviour is governed by the combination of joint shear hinge behaviour and beam plastic behaviour, Pampanin hysteresis is not applicable to model the joint shear hinge and Takeda hysteresis was chosen instead. The comparison is shown in Fig. 6.2.

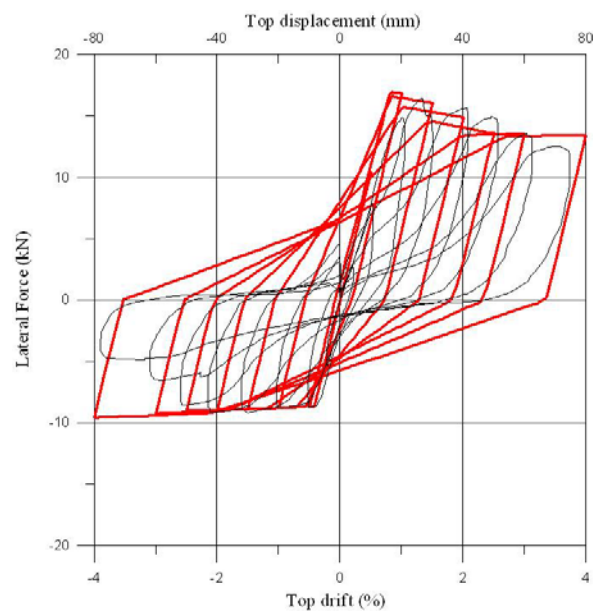


Figure 6.2 Analytical-experimental comparison of Unit TDP-1

6.2.3 Unit TDP-2

Unit TDP-2 had plain round bars for the column and the beam longitudinal reinforcement. Joint shear hinge formed both in the negative and positive directions while the beam and column were still in elastic range. Pampanin hysteresis with proper pinching behaviour was used to model the joint taking into account the bars slips. Fig. 6.3 shows that the use of Pampanin hysteresis to model the joint shear hinge allows the satisfactory reproduction of the global behaviour from the experimental results and Table 6.2 shows the Pampanin hysteresis parameters used in Ruaumoko analysis of Unit TDP-2

IOP (Option)	α_{s1}	α_{s2}	α_{u1}	α_{u2}	Delta F	β
1	1.25	0.9	-1	0.9	20	-0.1

Table 6.2 Pampanin hysteresis parameter for Unit TDP-2

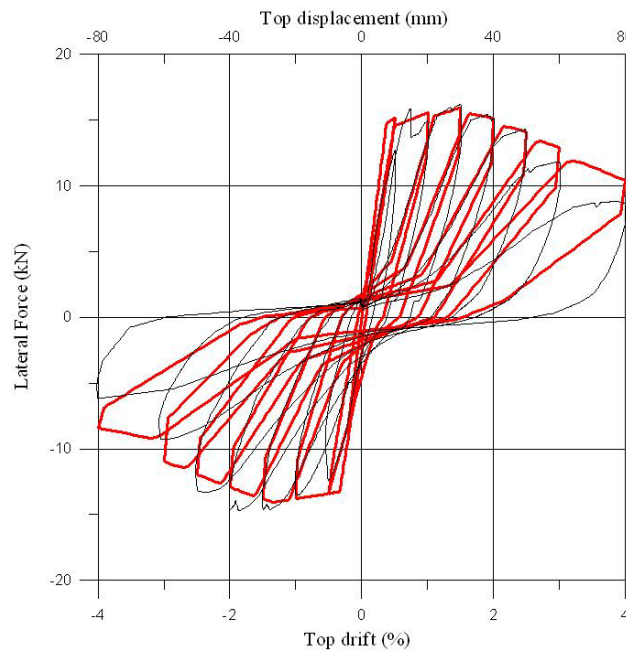


Figure 6.3 Analytical-experimental comparison of Unit TDP-2

6.2.4 Unit TDD-2

Unit TDD-2 had deformed bars for the column and the beam longitudinal reinforcement. Joint shear hinge formed both in the negative and positive directions while the beam and column were still in elastic range. As for Unit TDP-2, Pampanin hysteresis was used to model the joint taking into account the bars slips. However,

due to the unbalanced lateral strength of the subassembly, the reproduction of the global behaviour from experimental results is not accurate as shown in Fig. 6.4. Table 6.3 shows the Pampanin hysteresis parameters used in Ruaumoko analysis of Unit TDD-2.

IOP (Option)	α_{s1}	α_{s2}	α_{u1}	α_{u2}	Delta F	β
1	1.2	0.9	-1	0.85	20	-0.1

Table 6.3 Pampanin hysteresis parameter for Unit TDD-2

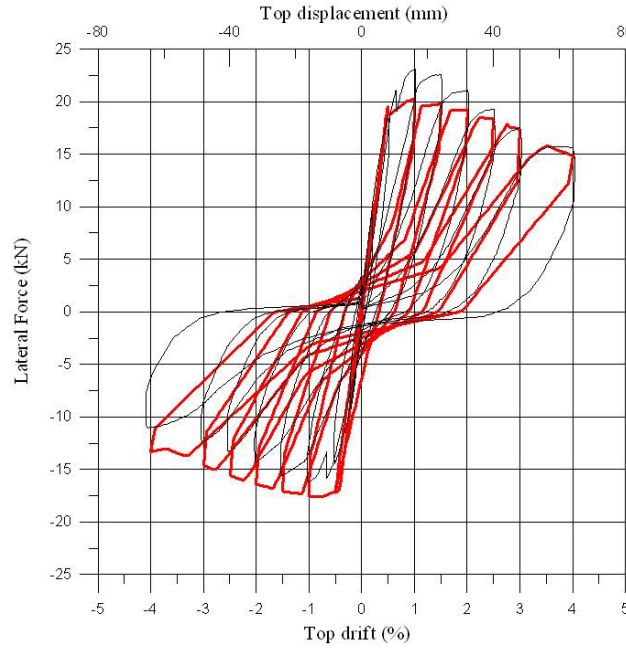


Figure 6.4 Analytical-experimental comparison of Unit TDD-2

6.2.5 Unit TSP

Unit TSP had shallow (wide) beam and were using plain round bars for the column and the beam longitudinal reinforcement. There was no damage in the joint area due to the small demand of shear force as the result of high flexibility of the subassembly. Beam plastic behaviour governed the global behaviour of the subassembly (Fig. 6.5) therefore the choice of hysteresis to model the joint shear hinge is not critical. Pampanin hysteresis parameters used in Ruaumoko analysis for Unit TSP is shown in Table 6.4.

IOP (Option)	α_{s1}	α_{s2}	α_{u1}	α_{u2}	Delta F	β
1	0.8	0.5	0	1.2	20	0

Table 6.4 Pampanin hysteresis parameter for Unit TSP

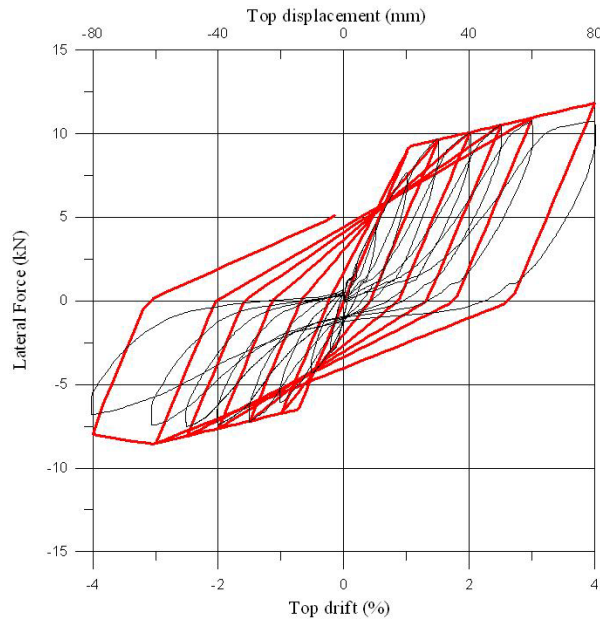


Figure 6.5 Analytical-experimental comparison of Unit TSP

6.2.6 Unit TSD

Unit TSD had shallow (wide) beam and were using deformed bars for the column and the beam longitudinal reinforcement. As for Unit TSD, there was no damage in the joint area due to the small demand of shear force as the result of high flexibility of the subassembly. Since the beam plastic behaviour governed the global behaviour of the subassembly (Fig. 6.6), the choice of hysteresis to model the joint shear hinge is not critical. Table 6.5 shows the Pampanin hysteresis parameters used in Ruaumoko analysis for Unit TSD.

IOP (Option)	α_{s1}	α_{s2}	α_{u1}	α_{u2}	Delta F	β
1	0.8	0.5	0	1.2	20	0

Table 6.5 Pampanin hysteresis parameter for Unit TSD

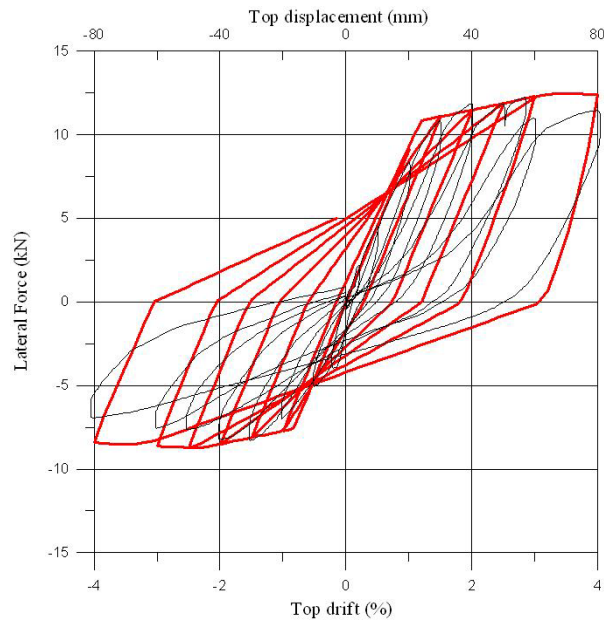


Figure 6.6 Analytical-experimental comparison of Unit TSD

6.3 SPACE FRAME BEAM-COLUMN JOINTS

The proposed model showed reasonably well results in simulating the behaviour of substandard plane frame exterior beam-column joint subassemblies. However, the model could not operate in space frame under biaxial loading yet. Further investigations and improvements are currently in progress. Furthermore, the calibration of the test results to find the joint shear relation in the two directions is currently underway.

CHAPTER 7

CONCLUSIONS AND RECOMMENDATION FOR FUTURE RESEARCH

7.1 GENERAL

Reinforced concrete structures designed in pre-1970s are vulnerable under severe earthquakes due to lack of seismic detailing to provide adequate ductility. To reduce the seismic risk (combination of hazard and vulnerability), the suitable retrofit strategy must be applied to the structure. Seismic assessment is the first step of retrofit strategy and requires a good understanding of the weak point of a structure under seismic loading.

In this study, simulated seismic loading tests were conducted on plane frame and space frame beam-column joint units to study the cyclic loading behaviour of reinforced concrete of the structures designed with older code provisions and investigate the effect of bi-axial loading in space frame on the behaviour of the exterior beam-column joints. The information of the behaviour of the units is then used to develop a further refined existing analytical procedure and numerical models to predict the seismic behaviour of pre-1970s reinforced concrete structures. This study emphasizes on the behaviour of beam-column joints with different detailing and the effect of bi-axial loading in space frame on the behaviour of the exterior beam-column joints.

The units consist of six as-built two third scale plane frame exterior beam-column joint subassemblies and three as-built two third scale space frame corner beam-column joint subassemblies. All the units had reinforcing details typical of an existing reinforced concrete structure designed before 1970s. The plane frame units contained:

1. Two exterior beam-column joint units with normal (deep) beams using plain round longitudinal reinforcement and the beam bars end were hooked into the joint. These units were referred to as Unit TDP-1 and Unit TDP-2.

2. Two exterior beam-column joint units with normal (deep) beams using deformed longitudinal reinforcement and the beam bars bent into the joint. These units were referred to as Unit TDD-1 and Unit TDD-2.
3. One exterior beam-column joint units with shallow (wide) beam using plain round longitudinal reinforcement and the beam bars end were hooked into the joint. This unit was referred to as Unit TSP.
4. One exterior beam-column joint units with shallow (wide) beam using deformed longitudinal reinforcement and the beam bars bent into the joint. This unit was referred to as Unit TSD

The space frame units used plain round longitudinal reinforcement and the beam bars end were hooked into the joint. They contained:

1. Two corner beam-column joint units with combination of normal (deep) beams. These units were referred to as Unit DD-1 and Unit DD-2.
2. One corner beam-column joint units with combination of normal (deep) beam and shallow (wide) beam. This unit was referred to as Unit DS.

All units were tested under varying axial load to simulate the column behaviour in the real structure under earthquake loading. From the test results, four strength degradation curves for different reinforcement detailing were proposed.

Analytical models used were developed from the information on the behaviour of existing reinforced concrete members obtained from previous and current test programme. Non-linear static analyses were conducted using the program RUAUMOKO developed at the University of Canterbury (Carr, 2004).

Conclusions from this study and recommendations for future research are presented below.

7.2 CONCLUSIONS FROM SIMULATED QUASI STATIC CYCLIC LOADING TESTS

7.2.1 Plane Frame Beam-Column Joint Subassemblies

1. The type of bar used for the longitudinal reinforcement has a major role in determining the type of failure that may occur in the beam-column joint

subassembly. The use of plain round bars can lead to joint shear failure, which will result in severe strength degradation. The use of deformed bars will have a bigger possibility of having a beam flexural failure as desired in seismic design. Plain round bars were widely used in the pre-1970s buildings; therefore they have to be assessed referring to the seismic design code at present so that a most suitable retrofit strategy can be applied to prevent the building from collapse under seismic excitation.

2. A beam-column joint subassembly with beam width to depth ratio more than one has bigger ductility than conventional beams (width to depth ratio less than one). The inertia area of the beam contributes to the ability of the subassembly to allow bigger displacement. A common mistake made by the designers using shallow beams is that they did not consider the amount of the beam longitudinal reinforcement anchored to the column, which can result to the beam not providing the theoretical moment capacity since the reinforcement anchored outside the column will only have a small contribution.

A joint shear failure is really unlikely for the shallow beam due to the large area working as the joint core. The congestion in the joint core caused by the number of reinforcement inside also contributes to provide sufficient strut and tie mechanism.

3. Contribution of transverse reinforcement in the joint area is really important to help the confinement. A single transverse reinforcement can make a big difference and alter the failure mechanism for the beam-column joint subassembly.
4. The variation of axial load can both strengthens and weakens the joint core. In the positive loading direction, the joint strength is slightly higher than the negative one due to the different axial load applied on the column. The axial load applied in the positive loading direction can be up to double the axial load applied in the negative loading direction, although the difference in terms of joint principal tensile stress is not that high.
5. Based on experimental results, two strength degradation curves for exterior joint are proposed. One is for a beam-column joint subassembly using

deformed bars bent into the joint with one stirrup in the joint core and the other is for a beam-column joint subassembly using smooth bars with end hooks and one stirrup in the joint core.

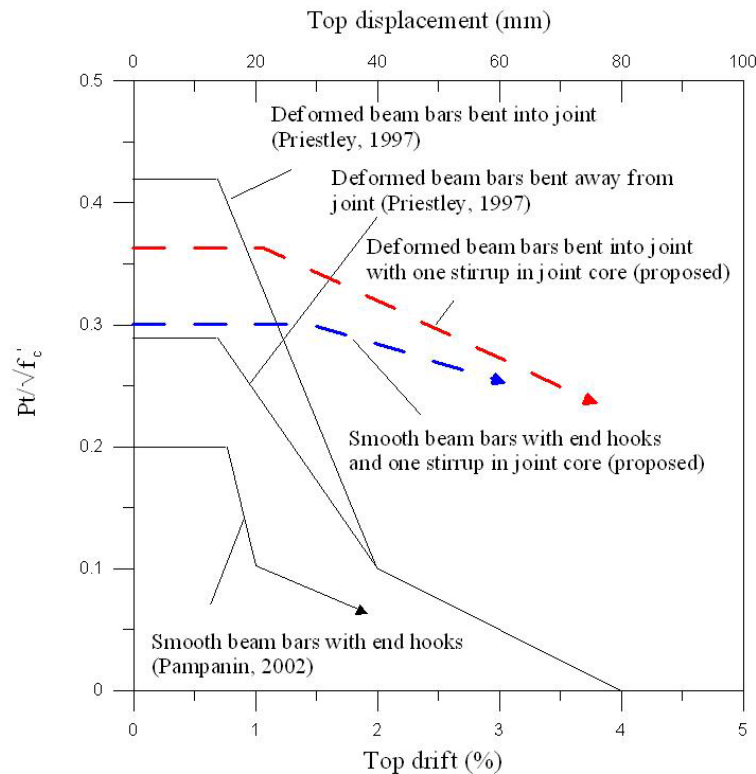


Figure 7.1 Strength degradation curve for exterior joints

7.2.2 Space Frame Beam-Column Joint Subassemblies

1. Beam dimension has an important effect on the behaviour of a corner beam-column joint. There are advantages and disadvantages that have to be considered in designing the beam. Beam depth can provide an additional confinement for the joint to resist the force coming from the other beam in the transverse direction. In the other side, the bigger the beam depth, the higher the moment capacity, which will result in larger forces from the beam coming into the joint and thus has more chance to destroy the joint.
2. As in the plane frame beam-column joint subassembly, the transverse reinforcement in the joint area gives a major contribution in confining the concrete and maintaining the strength of the unit. Although joint shear failure occurs, the strength can be maintained and the severity of the strength

degradation can be reduced. From the results, it is clear that even a single transverse reinforcement can improve the joint quite significantly.

3. Two strength degradation curves are proposed for space frame beam-column joint subassemblies. One is for smooth bars with hooked ends and without stirrup in the joint and the other is for smooth bars with hook ends and one stirrup in the joint.

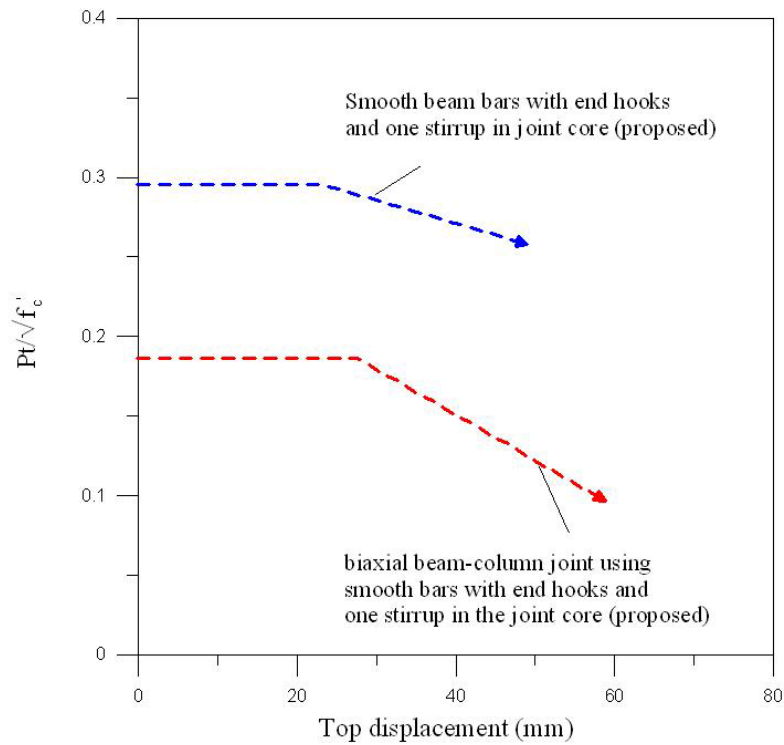


Figure 7.2 Proposed strength degradation curves for corner joints

4. A certain amount of strength reduction has to be considered when assessing space frame beam-column joints. For global strength, a 25% reduction is proposed as a reasonable value from the experimental results, while a 40% reduction is proposed for joint principal tensile stress. The numbers are considered conservatively since they come from limited experimental results.

7.3 RECOMMENDATIONS AND SUGGESTIONS FOR FUTURE RESEARCH

1. Tests on corner beam-column joints designed using current seismic codes must be performed to gather the information on the seismic behaviour to obtain the benchmark of the good behaviour.
2. The effects of slab on the corner beam-column joint behaviour under bi-axial loading need to be investigated.
3. Tests on existing beam-column joints with other typical deficiencies of the pre 1970s reinforced concrete structure such as lapped splice and use of infills should be done to gather more information on the seismic behaviour of existing reinforced concrete structure.
4. A further calibration on the newly proposed hysteresis (Pampanin hysteresis) needs to be done to obtain the range or limitation of the control parameters.
5. A dynamic analysis on a typical pre 1970s reinforced concrete structure needs to be carried out using the proposed analytical model and hysteresis.
6. The effect of infills typically used in pre 1970s reinforced concrete structures has to be investigated and taken into account for future analysis.

REFERENCES

Abdouka, K., (2003) “The Seismic Performance of Reinforced Concrete Wide Band Beam Frames: Exterior Connections”, PhD Thesis, The Department of Civil and Environmental Engineering, University of Melbourne

ACI Committee 318, (1989) “Building Code Requirements for Reinforced Concrete and Commentary (ACI 318-89/ACI 318R-89)”, American Concrete Institute, Detroit, 353 pp.

Anderson, J. C., Townsend, W. H., (1977) “Models for RC Frames with Degrading Stiffness”, Journal of the Structural Division, Vol. 103, No. ST12, 2361-2376

Aycardi, L. E., Mander, J. B., Reinhom, A. M., (1994) “Seismic Resistance of Reinforced Concrete Frame Structures Designed Only for Gravity Loads: Experimental Performance of Subassemblages”, ACI Structural Journal, Vol. 91, No. 5, pp.552-563

Beckingsale, C.H., (1990) “Post Elastic Behaviour of Reinforced Concrete Beam-Column Joints”, PhD Thesis, Department of Civil Engineering, University of Canterbury, New Zealand

Beres, A., Pessiki, S. P., White, R. N., Gergely, P., (1996) “Implications of Experiments on the Seismic Behaviour of Gravity Load Designed RC Beam-to-Column Connections”, Earthquake Spectra, Vol. 12, No. 12, 185-198

Bing, L., Yiming, W., Tso-Chien, P., (2003) “Seismic Behaviour of Nonseismically Detailed Interior Beam-Wides Column Joints-Part II: Theoretical Comparisons and Analytical Studies”, ACI Journal, V. 100, No. 1, January-February

Bolong, Z., Yuzhou, C., (1991) “Behaviour of Exterior Reinforced Concrete Beam-Column Joints Subjected to Bi-Directional Cyclic Loading”, Design of Beam-Column Joints for Seismic Resistance, Special Publication, SP-123-3, 69-96

Bracci, J. M., Reinhorn, A. M., Mander, J. B., (1995) “Seismic Resistance of Reinforced Concrete Frame Structures Designed for Gravity Loads: Performance of Structural System”, ACI Structural Journal, Vol. 92, No. 5, pp. 597-609

Bracci, J. M., Reinhorn, A. M., Mander, J. B., (1995) “Seismic Retrofit of Reinforced Concrete Buildings Designed for Gravity Loads: Performance of Structural Model”, ACI Structural Journal, Vol. 92, No. 5, pp. 711-723

Bresler, B., (1960) “Design Criteria for Reinforced Columns under Axial Load and Biaxial Bending”, Journal of the American Concrete Institute, November

Calvi, G. M., (1999) “A Displacement-Based Approach for Vulnerability Evaluation of Classes of Buildings”, Journal of Earthquake Engineering, Vol. 3 No. 3

Carr, A., (2004) “RUAUMOKO – Inelastic Dynamic Analysis”, Department of Civil Engineering, University of Canterbury

Cheung, P.C., (1991) “Seismic Design of Reinforced Concrete Beam-Column Joints with Floor Slab”, PhD Thesis, Department of Civil Engineering, University of Canterbury, New Zealand

Crisafulli, F. J., (1997) “Seismic Behaviour of Reinforced Concrete Structures with Masonry Infills”, PhD Thesis, Department of Civil Engineering, University of Canterbury, New Zealand

EERI, (2000) “Koaceli, Turkey, Earthquake of August 17, 1999 Reconnaissance Report”, Earthquake Spectra, Vol. 16 Sup. A

EERI, (2001) “Chi-Chi, Taiwan, Earthquake of September 21, 1999 Reconnaissance Report”, Earthquake Spectra, Vol. 17 Sup. A

EERI, (2003) "Preliminary Observations on the May 1, 2003, Bingol, Turkey, Earthquake", EERI Special Earthquake Report

Elmorsi, M., Kianoush, M. R., Tso, W. K., (2000) "Modeling bond-slip deformations in reinforced concrete beam-column joints", Canadian Journal of Civil Engineering, Vol. 27, 490-505

NEHRP, (2000) "Prestandard and commentary for the Seismic Rehabilitation of Buildings", FEMA 356, prepared by American Society for Civil Engineers (ASCE) Reston, Virginia for Federal Emergency Management Agency, Washington D. C.

Furlong, R., (1961) "Ultimate Strength of Square Columns Under Biaxially Eccentric Loads", Journal of the American Concrete Institute, March

Glaister S., Pinho, R. (2003) "Development of a Simplified Deformation-Based Method for Seismic Vulnerability Assessment", Journal of Earthquake Engineering, Vol. 7, Special Issue No. 1

Gentry, T. R., Wight, J.K., (1994) "Wide Beam-Column Connections under Earthquake-Type Loading", Earthquake Spectra, Vol. 10, No. 4, 675-703

Hakuto, S., Park, R., Tanaka, H., (2000) "Seismic Load Tests on Interior and Exterior Beam Column Joints with Substandard Reinforcing Details", ACI Structural Journal, V.97, No.1, January-February

Hoehler, M., Ozbolt, J., (2001) "Three-Dimensional Reversed-Cyclic Analysis of Reinforced Concrete Members Using the Microplane Model", Otto Graf Journal, Vol. 12, pp. 93-113

Johnston, J. A. R., (1960) "A Brief History of Damaging Earthquakes in Wellington City and Developments in Multi-Storey Building Construction in New Zealand", Proceedings of the Second World Conference on Earthquake Engineering, Japan

Kaba, S., Mahin, S. A., (1984) “Refined Modeling of Reinforced Concrete Columns for Seismic Analysis”, EERC Report 84-03, Earthquake Engineering Research Center, University of California, Berkeley

Kunnath, S. K., Hoffmann, G., Reinhorn, A. M., Mander, J. B., (1995) “Gravity-Load-Designed Reinforced Concrete Buildings-Part I: Seismic Evaluation of Existing Construction”, ACI Structural Journal, Vol. 92, No. 3, pp. 343-354

Kunnath, S. K., Hoffmann, G., Reinhorn, A. M., Mander, J. B., (1995) “Gravity-Load-Designed Reinforced Concrete Buildings-Part II: Evaluation of Detailing Enhancements”, ACI Structural Journal, Vol. 92, No. 4, pp. 470-478

Kurose, Y., Guimaraes, G. N., Zuhua, L., Kreger, M. E., Jirsa, J. O., “Evaluation of Slab-Beam-Column Connections Subjected to Bidirectional Loading”, Design of Beam-Column Joints for Seismic Resistance, Special Publication, SP-123-3, 39-67

Kwak, H. G., Filippou, F. C., (1990) “Finite Element Analysis of Reinforced Concrete Structures under Monotonic Loading”, Report No. UCB/SEMM-90/14, Structural Engineering, Mechanics and Materials, Department of Civil Engineering, University of California, Berkeley

Leon, R., Jirsa, O., (1986) “Bidirectional Loading of R.C Beam Column Joints”, Earthquake Spectra, Vol. 2, No. 3, 537-564

Lettow, S., Mayer, U., Ozbolt, J., Eligehausen, R., (2004) “Bond of RC Members Using 3D FE Analysis”, Proceedings of the Fifth International Conference on Fracture Mechanics of Concrete and Concrete Structures, 12-16 April, Colorado, USA, pp. 861-868

Liu, A., (2001) “Seismic Assessment and Retrofit of Pre-1970’s Reinforced Concrete Frame Structures”, PhD Thesis, Department of Civil Engineering, University of Canterbury, New Zealand

Lowes, L., Altoontash, A., (2003) “Modeling Reinforced-Concrete Beam-Column Joints Subjected to Cyclic Loading”, *Journal of Structural Engineering*, Vol. 129, No. 12, 1686-1697

Lupoi, G., Lupoi, A., Pinto, P. E., (2002) “Seismic Risk Assessment of RC Structures with the ‘2000 SAC / FEMA’ Method”, *Journal of Earthquake Engineering*, Vol. 6, No.4

Magenes, G., Pampanin, S., (2004) “Seismic Response of Gravity-Load Design Frames with Masonry Infills”, 13th World Conference on Earthquake Engineering, Vancouver, Canada, August 1-6, Paper No. 4004

Monti, G., Spacone, E., Filippou, F. C., (1993) “Model for Anchored Reinforcing Bars Under Seismic Excitations”, EERC Report 93-08, Earthquake Engineering Research Center, University of California, Berkeley

Nagai, T., Kashiwazaki, T., Noguchi, H., (1996) “Three Dimensional Nonlinear Finite Element Analysis of RC Interior Beam-Column Joints with Ultra High-Strength Materials Under Bi-directional Load”, *Transactions of the Japan Concrete Institute*, Vol. 18

Ngo, D., Scordelis, A. C., (1967) “Finite Element Analysis for Reinforced Concrete Beams”, *Journal of ACI*, Vol. 64, No. 3, pp. 152-163

NZS3101 (1995), “The Design of Concrete Structures, NZS3101: 1995”, *Standards New Zealand*

Owada, Y., (2000) “Three-dimensional Behaviour of Reinforced Concrete Beam-Column Joint Under Seismic Load”, 12th World Conference of Earthquake Engineering, New Zealand

Pampanin, S., (2005) “Vulnerability Assessment and Retrofit Strategies for Existing Under-Designed R. C. Frame Buildings”, NZSEE Conference, Auckland

Pampanin, S., Christopoulos, C., (2003) “Non-Invasive Retrofit of Existing RC Frames Designed for Gravity Loads Only”, Proceedings of the fib2003 Symposium – Concrete Structure in Seismic Regions, Athens

Pampanin, S., Calvi, G.M., Moratti, M., (2003) “Seismic Response of Reinforced Concrete Buildings Designed for Gravity Loads. Part 1: Experimental Test on Beam-Column Subassemblies”, ASCE Journal of Structural Engineering

Pampanin, S., Magenes G., Calvi, G.M, (2003) “Seismic Response of Reinforced Concrete Buildings Designed for Gravity Loads. Part 2: Experimental Test on a Three Storey Frame”, ASCE Journal of Structural Engineering

Pampanin, S., Magenes, G., Carr, A., (2003) “Modeling of Shear Hinge Mechanism in Poorly Detailed RC Beam Column Joints” FIB Symposium “Concrete Structures in Seismic Regions”, Athens 2003

Park, R., Paulay, T., (1975) “Reinforced Concrete Structures”, Wiley, New York

Paulay, T., Priestley, M.N.J., (1992) “Seismic Design of Reinforced Concrete and Masonry Buildings”, Wiley, New York

Popov, E. P., Cohen, J. M., Koso-Thomas, K., Kasai, K., (1992) “Behaviour of Interior Narrow and Wide Beams”, ACI Structural Journal, Vol. 89, No. 6, 607-616

Priestley, M. N. J., (1997) “Displacement-Based Seismic Assessment of Reinforced Concrete Buildings”, Journal of Earthquake Engineering, Vol. 1, No. 1, 157-192

Priestley, M. N. J., (1995) “Displacement-Based Seismic Assessment of Existing Reinforced Concrete Buildings”, Pacific Conference on Earthquake Engineering, Australia, 20-22 November

Priestley, M. N. J., Calvi, G. M., (1991) “Towards a Capacity-Design Assessment Procedure for Reinforced Concrete Frames”, Earthquake Spectra, Vol. 7 No. 3

Rodriguez, M., Diaz C., (1989) "The Mexico Earthquake of September 19, 1985: Analysis of the Seismic Performance of a Medium Rise, Waffle Flat Plate Building", *Earthquake Spectra*, Vol. 5, No. 1

Rodriguez, M., Santiago, S., Meli, R., (1995) "Seismic Load Tests on Two-Storey Waffle Flat-Plate Structure", *Journal of Structural Engineering*, Vol. 121, No. 9

Saunders, D. B., (2004) "Seismic Performance of the Pre 1970's Non-Ductile Reinforced Concrete Waffle Slab Frame Structures Constructed with Plain Round Reinforcing Steel", PhD Thesis, Department of Civil Engineering, University of Canterbury, New Zealand

Tauser, F. F., Spacone, E., Filippou, F. C., (1991) "A Fiber Beam-Column Element for Seismic Response Analysis of Reinforced Concrete Structure", EERC Report 91-17, Earthquake Engineering Research Center, University of California, Berkeley

Trowland, M., (2004) "Modeling the Shear Hinge in Beam-Column Joints", Report, University of Canterbury, New Zealand

Uang, C. M., Elgamal, A., Li, W. S., Chou, C. C., (1999) "Ji-Ji, Taiwan Earthquake of September 21, 1999: A Brief Reconnaissance Report", PEER Program, Department of Structural Engineering, University of California, San Diego

Youssef, M., Ghobarah, A., (2001) "Modelling of RC Beam-Column Joints and Structural Walls", *Journal of Earthquake Engineering*, Vol. 5, No. 1

Zeris, C. A., Mahin, S. A., (1991) "Behavior of Reinforced Concrete Structures Subjected to Biaxial Excitation", *Journal of Structural Engineering*, ASCE, 117(ST9), pp. 2657-2673